

University of Alberta

Drosophila melanogaster hephaestus (heph) encodes a polypyrimidine-tract binding protein that represses *Notch* activity in the developing wing disc.

by



David A. Dansereau

A thesis submitted to the Faculty of Graduate Studies and Research in partial fulfillment of the requirements for the degree of Doctor of Philosophy

in

Molecular Biology and Genetics

Department of Biological Sciences

Edmonton, Alberta

Fall 2002



National Library
of Canada

Acquisitions and
Bibliographic Services

395 Wellington Street
Ottawa ON K1A 0N4
Canada

Bibliothèque nationale
du Canada

Acquisitions et
services bibliographiques

395, rue Wellington
Ottawa ON K1A 0N4
Canada

Your file Votre référence

Our file Notre référence

The author has granted a non-exclusive licence allowing the National Library of Canada to reproduce, loan, distribute or sell copies of this thesis in microform, paper or electronic formats.

The author retains ownership of the copyright in this thesis. Neither the thesis nor substantial extracts from it may be printed or otherwise reproduced without the author's permission.

L'auteur a accordé une licence non exclusive permettant à la Bibliothèque nationale du Canada de reproduire, prêter, distribuer ou vendre des copies de cette thèse sous la forme de microfiche/film, de reproduction sur papier ou sur format électronique.

L'auteur conserve la propriété du droit d'auteur qui protège cette thèse. Ni la thèse ni des extraits substantiels de celle-ci ne doivent être imprimés ou autrement reproduits sans son autorisation.

0-612-81176-X

Canada

University of Alberta

Library Release Form

Name of Author: David Arthur Dansereau

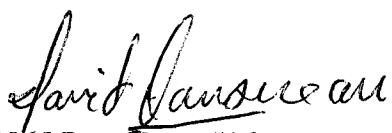
Title of Thesis: *Drosophila melanogaster hephaestus (heph)* encodes a polypyrimidine-tract binding protein that represses *Notch* activity in the developing wing disc.

Degree: Doctor of Philosophy

Year this Degree Granted: 2002

Permission is hereby granted to the University of Alberta Library to reproduce single copies of this thesis and to lend or sell such copies for private, scholarly or scientific research purposes only.

The author reserves all other publication and other rights in association with the copyright in the thesis, and except as herein before provided, neither the thesis nor any substantial portion thereof may be printed or otherwise reproduced in any material form whatever without the author's prior written permission.


2865 Rue Goyer #16

Montreal, PQ, H3S-1H2

24 June 2002

"The heart of the matter is not so much the molecules involved, but more the flow of information and the logic of the system they participate in."

Peter Lawrence

University of Alberta

Faculty of Graduate Studies and Research

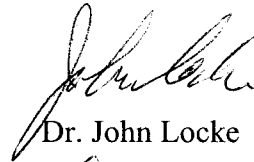
The undersigned certify that they have read, and recommend to the Faculty of Graduate Studies and Research for acceptance, a thesis entitled "*Drosophila melanogaster hephaestus (heph)* encodes a polypyrimidine-tract binding protein that represses *Notch* activity in the developing wing disc", submitted by David Arthur Dansereau in partial fulfillment of the requirements for the degree of Doctor of Philosophy in Molecular Biology and Genetics.



Dr. Michael Russell (supervisor)



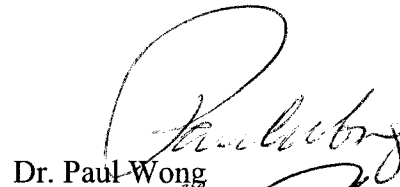
Dr. William Brook (co-supervisor)



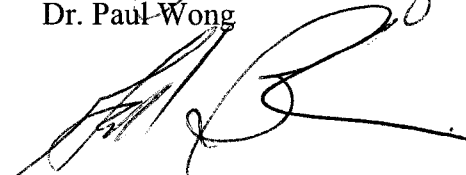
Dr. John Locke



Dr. Michael Walter



Dr. Paul Wong



Dr. Gabrielle Boulianne

24 June 2002

ABSTRACT

Pattern formation is the fundamental process by which cells organize into highly ordered spatial arrangements of diverse cell types. A central molecular component of the pattern formation mechanism in metazoans is the Notch signalling pathway. The *Notch* gene encodes a transmembrane receptor that functions in an evolutionarily conserved cell interaction pathway controlling fate determination. For example, *Notch* is required in the *Drosophila* wing to induce wing margin fate and to restrict wing vein fate within vein competent regions. In this thesis, I will describe a genetic and molecular characterization of *hephaestus* (*heph*), and will present evidence that *heph* is required to repress Notch activity in the wing imaginal disc. The *heph* complementation group is defined by four lethal alleles that fail to complement the previously identified *heph* allele, *ms(3)heph²*. All five *heph* alleles map to a single transcription unit encoding a putative RNA binding protein homologous to vertebrate polypyrimidine-tract binding protein (PTB). This is the first genetic analysis of PTB in any organism and the first evidence that it plays a role in the Notch signalling pathway. The phenotypes of *heph* in genetic mosaics, where patches of *heph* mutant tissue (clones) are surrounded by wildtype tissue, were analyzed to study the normal role of *heph* during development. Near the normal wing margin, *heph* clones in any of the four distal wing compartments induce ectopic wing margin bristles that retain their normal compartmental identities. *heph* clones in the wing blade autonomously disrupt the differentiation of veins, and this depends on the Notch ligand Delta. These phenotypes suggest that *heph* normally represses activity of the Notch signalling

pathway. In support of this hypothesis, *heph* clones near the presumptive wing margin autonomously express the Notch target genes *wingless* and *cut*, and induce expression of the WG target gene *achaete* (and thus wing margin fate) in surrounding tissue. *heph* clones anywhere in the wing disc have higher levels of activated Notch compared to surrounding tissue, indicating a general role for *heph* in down-regulating Notch activity.

ACKNOWLEDGEMENTS

I thank those teachers who inspired my interest in genetics, development, and science in general:

Robert Lanman for spurring my interest in genetics and evolution. Without your influence, I might be an accountant.

Pliny Hayes for presenting the elegance of phage genetics with rare enthusiasm. You demonstrated that science provides "evidence of things unseen".

R.C. von Borstel for discussions on mutation and the power of selection*.

Michael Russell for clearly presenting theories of pattern formation and how they developed in the literature. I thoroughly enjoyed our discussions on the evolution of *Hox* genes, limbs and butterfly eyespot patterns.

I thank William Brook for providing the guidance and opportunity necessary to advance this project. I also thank Michael Russell, William Brook, John Locke and Mike Walter for their guidance as members of my supervisory committee. Finally, I thank Martine Lunke for sequencing the EMS-derived alleles of *heph* presented here, Cordula Schulz for sharing unpublished reagents, and Ariel Finkielsztejn for the initial analysis of *Df(3R)G45* genetic mosaics.

* And perhaps more importantly, for teaching me about good chocolate and good coffee.

TABLE OF CONTENTS

1 INTRODUCTION	1
1.1 The <i>Drosophila</i> wing as a model system for studying pattern formation	2
1.2 Regional identity	9
1.3 Short range communication	12
1.4 Long range patterning	15
1.5 D/V boundary formation.....	18
1.6 Pattern refinement.....	19
1.7 Summary of objectives	25
2 MATERIALS AND METHODS.....	27
2.1 <i>Drosophila</i> culture.....	27
2.2 Conventional <i>Drosophila</i> nomenclature	27
2.3 Genes and alleles	28
2.4 Induction of mitotic recombination	33
2.5 Summary of chromosomes and clone markers	33
2.6 Induction of <i>Df(3R)G45</i> clones in a <i>mod⁺ krz⁺</i> genetic background.....	37
2.7 Induction of <i>hephaestus</i> clones in a <i>Su(H)</i> mutant background.....	37
2.8 <i>hephaestus</i> genetic interaction screen.....	41
2.9.1 Screen for EMS-induced alleles that fail to complement <i>Df(3R)G45</i>	41
2.9.2 P-element hybrid dysgenesis at polytene region 100E-F.....	43
2.9.3 P-element induced male recombination at polytene region 100E-F.....	44
2.10 Characterization of the terminal phenotype of lethal <i>hephaestus</i> alleles.....	48

2.11 Targeted mis-expression of PTB	48
2.12 Rescue of the ectopic margin phenotype in <i>hephaestus</i> genetic mosaics	49
2.13 Molecular techniques and DNA manipulation	53
2.13.1 Cosmid and P1 DNA isolation	53
2.13.2 Radioactive labeling of DNA	53
2.13.3 Determining P-element insertion points with inverse PCR.....	53
2.13.4 Identification, sequencing and mapping of <i>hephaestus</i> cDNAs	54
2.13.5 PCR-based sequencing of EMS-derived <i>hephaestus</i> alleles	56
2.14 Histology and light microscopy.....	56
2.15 Antibody staining and laser scanning microscopy	56
3 RESULTS	59
3.1 Summary of genetic and molecular analysis of the <i>hephaestus</i> locus.....	59
3.1.1 Mobilization of viable P-insertions mapping to polytene region 100E-F by hybrid dysgenesis.	60
3.1.2 EMS-induced mutations that fail to complement <i>Df(3R)G45</i>	61
3.1.3 P-element insertions that fail to complement <i>Df(3R)G45</i>	62
3.1.4 Complexities in the <i>hephaestus</i> complementation pattern.....	69
3.1.5 Identification of the <i>hephaestus</i> transcription unit	71
3.1.6 Male recombination-induced mutations at polytene region 100E-F	79
3.1.7 Sequencing EMS-induced alleles of <i>hephaestus</i>	81
3.1.8 Rescue of the <i>hephaestus</i> genetic mosaic phenotype	84
3.2 Analysis of <i>hephaestus</i> in genetic mosaics	88

3.2.1	<i>Df(3R)G45</i> mitotic clones marked with <i>yellow</i>	89
3.2.2	<i>Df(3R)G45</i> mitotic clones marked with <i>forked</i>	92
3.2.3	<i>Minute</i> ⁺ <i>Df(3R)G45</i> mitotic clones marked with <i>forked</i>	99
3.2.4	<i>hephaestus</i> mitotic clones disrupt the pattern of the wing margin, wing veins, and ommatidia.	99
3.2.5	Thoracic bristle pattern in <i>hephaestus</i> genetic mosaics.	105
3.3	Epistasis	111
3.3.1	Genetic epistasis between <i>Delta</i> and <i>hephaestus</i>	111
3.3.2	<i>heph</i> ⁰³⁴²⁹ partially rescues the <i>fng</i> ^{D4} margin loss phenotype	112
3.3.3	<i>wingless</i> protein expression in <i>hephaestus</i> genetic mosaic wing discs.....	117
3.3.4	<i>achaete</i> protein expression in <i>hephaestus</i> genetic mosaic wing discs.....	123
3.3.5	<i>Delta</i> , <i>Serrate</i> and <i>Distal-less</i> protein expression in <i>hephaestus</i> genetic mosaic wing discs.....	123
3.3.6	<i>cut</i> protein expression in <i>hephaestus</i> genetic mosaic wing discs	130
3.3.7	Molecular nature of Notch signalling	133
3.3.8	NICD protein expression in <i>hephaestus</i> genetic mosaic wing discs.	134
3.3.9	<i>Delta</i> and NICD protein expression in <i>Su(H)</i> mutant <i>hephaestus</i> genetic mosaic wing discs.	139
4	DISCUSSION	142
4.1	Logic identifying <i>ectopic margin</i> with <i>hephaestus</i>	142
4.2	The <i>hephaestus</i> ectopic margin clonal phenotype is consistent with ectopic <i>wingless</i> expression	143
4.3	The <i>hephaestus</i> ectopic margin and vein loss phenotypes suggest ectopic Notch activation.....	145

4.4	<i>Delta hephaestus</i> epistasis	151
4.5	<i>hephaestus</i> is required where <i>Notch</i> activity must be reduced	151
4.6	Model of Notch-Ligand interactions	152
4.7	NICD degradation.....	157
4.8	Future directions: Targets of <i>hephaestus</i> , molecular and genetic approaches...	159
4.9	Summary	164
5	BIBLIOGRAPHY	166

LIST OF TABLES

Table 1. Abbreviations and genetic designations of P-elements	29
Table 2. <i>Drosophila</i> strains used in this study.....	30
Table 3. PCR primers used for DNA sequencing.....	55
Table 4. Complementation test results between lethal P-element excisions and alleles mapping to 100F.....	64
Table 5. Complementation test results between alleles mapping to 100E-F.....	65
Table 6. Complementation test results between alleles that fail to complement <i>Df(3R)G45</i>	66
Table 7. Summary of allele names and synonyms.....	67
Table 8. Summary of the effects of <i>PTB</i> expression on the <i>hephaestus</i> ectopic margin phenotype.....	87
Table 9. The effect of timing of <i>heph</i> clone induction on the range of adult phenotypes observed.....	101
Table 10. Summary of genetic interactions.....	115
Table 11. Characterized targets of <i>PTB/hnRNPI</i>	163

LIST OF FIGURES

Figure 1. The wing imaginal disc.....	4
Figure 2. Morphology of a <i>Drosophila</i> wing.....	5
Figure 3. Wing disc fate map.....	7
Figure 4. Schematic representation of inductive intercellular interactions along the D/V boundary.....	14
Figure 5. Summary of interactions between <i>Delta</i> and <i>Notch</i>	22
Figure 6. Summary of chromosomes constructed for this study.	34
Figure 7. Crossing scheme used to generate <i>Df(3R)G45</i> clones in a <i>mod⁺ krz⁺</i> background.....	38
Figure 8. Crossing scheme used to generate Stock I (<i>heph</i> clones in <i>Su(H)</i> mutant background).....	39
Figure 9. Crossing scheme used to generate <i>hephaestus</i> clones in a <i>Su(H)</i> mutant background.....	40
Figure 10. Crossing scheme used to isolate EMS-induced alleles that fail to complement <i>Df(3R)G45</i>	42
Figure 11. Crossing scheme used to isolate lethal excision derivatives of <i>P{PZ}G45</i>	45
Figure 12. Crossing scheme used to isolate lethal excision derivatives of <i>P{LacW}L1022</i> and <i>P{wA}4-4</i>	46
Figure 13. Crossing scheme to generate new deletions at 100E-F using male recombination.....	47
Figure 14. Crossing scheme used to generate Stock II (<i>heph</i> rescue).....	50
Figure 15. Crossing scheme used to generate Stock III (<i>heph</i> rescue).	51
Figure 16. Crossing scheme used to rescue the ectopic margin phenotype of <i>hephaestus</i> in genetic mosaics.....	52

Figure 17. Diagrammatic summary of the genetic analysis of <i>hephaestus</i>	68
Figure 18. Model of transcripts complementary to the <i>P{PZ}G45</i> genomic flanking DNA.....	72
Figure 19. Schematic representation of overlapping Cosmid and P1 clones including sequences from <i>P{PZ}G45</i> , <i>heph</i> , and <i>mod</i>	74
Figure 20. Physical map of the <i>hephaestus</i> transcription unit.	77
Figure 21. Examples of detached posterior crossveins from <i>mr55</i> and <i>hephaestus</i> mutant flies.	80
Figure 22. Breakpoint map of the <i>heph^{e2}</i> deletion.....	82
Figure 23. Ectopic expression of <i>PTB</i> is associated with wing margin loss.	85
Figure 24. Examples of mitotic clones of <i>Df(3R)G45</i> marked by <i>yellow</i>	90
Figure 25. An example of a of <i>Df(3R)G45</i> mitotic clone marked by <i>forked</i>	93
Figure 26. Summary of <i>Df(3R)G45</i> genetic mosaic analyses.....	95
Figure 27. Examples of <i>Minute⁺</i> mitotic clones of <i>Df(3R)G45</i> marked by <i>forked</i>	97
Figure 28. The timing of <i>heph⁰³⁴²⁹</i> clone induction affects the ratio of WM nicks to ectopic margin.	102
Figure 29. <i>hephaestus</i> genetic mosaic wing phenotypes.....	104
Figure 30. <i>hephaestus</i> mitotic clones disrupt ommatidial pattern.	107
Figure 31. Thoracic phenotypes of <i>hephaestus</i> genetic mosaics.	109
Figure 32. <i>Delta</i> is epistatic to <i>hephaestus</i>	113
Figure 33. <i>heph⁰³⁴²⁹</i> partially rescues the <i>fng^{D4}</i> margin loss phenotype.	116
Figure 34. Green Fluorescent Protein as a cell marker for analysis of genetic mosaic wing discs.....	118
Figure 35. Ectopic <i>wingless</i> expression is induced within <i>hephaestus</i> mitotic clones that are near the D/V boundary.	119

Figure 36. Ectopic <i>achaete</i> expression is induced around anterior <i>hephaestus</i> mitotic clones that are near the D/V boundary.....	121
Figure 37. <i>Delta</i> expression is low in <i>hephaestus</i> mutant tissue.	125
Figure 38. <i>Serrate</i> expression is low in <i>hephaestus</i> mutant tissue.	127
Figure 39. Expression of <i>Distal-less</i> is not altered by loss of <i>hephaestus</i>	129
Figure 40. Ectopic <i>cut</i> expression is induced within <i>hephaestus</i> mitotic clones that are near the D/V boundary.....	131
Figure 41. The amount of NICD is higher in <i>hephaestus</i> clones relative to normal surrounding tissue.....	135
Figure 42. The intracellular localization of NICD is altered in <i>hephaestus</i> clones.	137
Figure 43. The effects of <i>hephaestus</i> clones on Delta and NICD staining depends on <i>Su(H)</i>	140
Figure 44. Comparison of genetic mosaic phenotypes among <i>heph</i> , <i>Dl</i> , <i>Ser</i> , <i>Notch</i> ⁺ and <i>N^{4x}</i>	146
Figure 45. Schematic representation of Notch feedback mechanisms in the wing disc.	155
Figure 46. Amino acid sequence comparison among <i>D. melanogaster</i> HEPH, <i>X. laevis</i> VgRBP60, and <i>H. sapiens</i> PTB1.....	160

LIST OF ABBREVIATIONS

α	anti- (antibody)
a.a.	amino acid
AEL	after egg lay (hr)
bp	base pair
BDGP	Berkeley <i>Drosophila</i> Genome project
BSA	bovine serum albumin
cDNA	cloned DNA copy of an <i>mRNA</i>
<i>CyO</i>	<i>Curly of Oster</i> (balancer chromosome)
<i>Df</i>	Deficiency (deletion)
DNA	deoxyribonucleic acid
dpi	dots per inch (image resolution)
EDGP	European <i>Drosophila</i> Genome project
EM	electron microscopy
EMS	ethyl methanesulfonate
EST	expressed sequence tag
FLN	full-length Notch protein
FLP	yeast <i>Flip recombinase</i>
FRT	FLP recombination target
<i>gf</i>	gain-of-function allele

GFP	green fluorescent protein
<i>Hsp70</i>	gene encoding the 70kDa heat shock protein
kb	kilobase pairs (1000 bp)
kDa	kilo-Dalton (unit of molecular weight)
<i>lf</i>	loss-of-function allele
mr	male recombination
<i>mRNA</i>	messenger RNA
NECD	extracellular domain of the Notch protein
NICD	intracellular domain of the Notch protein
PBS	phosphate buffered saline
PCR	polymerase chain reaction
RNA	ribonucleic acid
RT	room temperature (~20°C)
STS	sequence tagged site
<i>TM</i>	<i>Third Multiple</i> (balancer chromosome)
ts	temperature sensitive
UAS	upstream activating sequence
UTR	untranslated region of an <i>mRNA</i>
WM	wing margin
wt	wildtype
X-gal	5-bromo-4-chloro-3-indolyl- β -D-galactoside

1 INTRODUCTION

Pattern formation is the mechanism by which initially equipotent embryonic cells proliferate and organize into an intricate spatial arrangement of diverse cell types. In theoretical terms, pattern formation is accomplished by individual cells responding appropriately to some form of relative positional information (Wolpert, 1969). In this model, positional information is globally specified in relation to an arbitrary set of points in the system. Individual cells are able to interpret the local positional value within the global positional coordinate system and respond by differentiating appropriately. In this context, those cells whose positional information is specified with respect to the same set of points belong to the same single field of cells. The mechanism by which positional information might be specified and interpreted is an intriguing problem. The strict reproduction of pattern within a species indicates that positional information is genetically coordinated. Therefore, understanding positional information depends on understanding how genetic information is interpreted into a reliable spatial pattern.

Developmental geneticists have established *Drosophila melanogaster* as a premiere model for the study of pattern formation. *Drosophila* makes an ideal organism in which to isolate and study new mutations that affect development because of its well-developed genetic system. In addition, *Drosophila* are relatively complex organisms compared to other genetic model systems, and use a regulative mode of development that resembles our own. Large numbers of mutations that affect *Drosophila* pattern specification have been isolated and characterized. The convergent application of molecular biology and *Drosophila* developmental genetics to the problem of pattern formation has defined some important molecular mechanisms of fate specification. Many mutations that affect pattern formation disrupt the function of genes involved in intercellular communication. These have been studied in detail and ordered into several important signal transduction pathways used repeatedly throughout development. By extension, intercellular communication is a necessary component of the pattern formation mechanism.

In this thesis, I will present the identification and characterization of some novel pattern mutants of *hephaestus* (*heph*), including evidence that *heph* affects pattern formation by regulating the Notch signal transduction pathway in the wing disc. The mutant phenotypes of *heph* described here emphasize the importance of refining positional information during development.

1.1 The *Drosophila* wing as a model system for studying pattern formation

This study utilizes *Drosophila* wing development as an example of pattern formation. The following is an outline of *Drosophila* development designed to summarize the early biology of wing development, and the morphology of the adult wing. A more general account of imaginal disc development and its relationship to adult morphology can be found in "The Development of *Drosophila melanogaster*" (Cohen 1993; Fristrom and Fristrom 1993) and "Biology of *Drosophila*" (Bodenstein, 1984).

Adult wings develop from imaginal wing discs. Fertilized *Drosophila* eggs (embryos) hatch into feeding larvae that will grow through three larval stages (instars) separated by moults (ecdysis). During early embryonic development, the precursors of each adult appendage are first determined as small groups of ectodermal cells from within the appropriate embryonic segments. Once established, these imaginal* structures follow a developmental program distinct from that of their larval "host". While larval cells replicate their DNA repeatedly in the absence of cell divisions, the cells determined for the adult legs, wings, eyes, antennae, head capsule, halteres and genital organs proliferate mitotically and invaginate to form sac-like structures called imaginal discs. The abdominal epidermis of the adult derives from similar segmental clusters of precursor cells called abdominal histoblast nests, which instead only begin to proliferate during pupal stages. In addition, while larval epidermal cells secrete a differentiated cuticle at each larval moult, the imaginal cells remain undifferentiated and do not secrete cuticle during larval life.

An imaginal disc is thus a single layer of undifferentiated cells comprising the columnar epithelium of the "disc proper" and the squamous epithelium of the peripodial membrane (Fig. 1). At the onset of pupariation, the larval cuticle becomes the pupal case (puparium) that surrounds the fly during metamorphosis. Within the puparium, imaginal precursors undergo a complex process of morphogenesis into the shape of the adult fly. Imaginal discs evert so that the apical, cuticle-secreting surface is on the outside of the animal, and elongate by limited cell rearrangement to convert the radial dimension into a proximal-distal axis. The discs then spread and fuse to create a continuous adult epidermis. After the secretion of a thin, featureless pupal cuticle, the secretion of adult cuticle in stereotypic patterns of sensory bristles (macro- and microchaetae), non-sensory epidermal hairs (trichomes), and "naked" epidermis, completes epidermal development.

Wing morphology. The wings, much of the dorsal thorax (notum, scutellum), and parts of the lateral thorax (notopleura) develop from a pair of wing discs, which begin as epithelial pouches of about 10-20 cells determined during embryogenesis (reviewed in Cohen 1993). During larval stages, the wing disc cells proliferate to number about

* Structures formed during embryonic and larval stages that persist into adulthood. Although not commonly used, the term "imago" refers to a sexually mature adult insect.

50,000. Within the single epithelial layer that will form the wing, dorsal and ventral cells are side by side and are separated by a cell-lineage restriction called the dorsal/ventral (D/V) compartment boundary (see below). During metamorphosis, cells of the dorsal and ventral compartments of the wing disc become apposed to create the dorsal and ventral cell layers of the wing (Fig. 1B). Cells of the pupal wing disc secrete cuticle in the form of hairs, sensory bristles, trichomes or naked cuticle, the sum of which form the wing blade with wing margin, hinge, and most of the dorsal thorax.

Cells along the border between the dorsal and ventral cell layers secrete the bristles of the wing margin (Fig. 2). The anterior wing margin consists of a proximal triple row of bristles (two distinguishable dorsal and one ventral) and a distal double row of bristles (one dorsal and one ventral). The posterior wing margin consists of an alternating dorsal and ventral row of non-innervated hairs. In the wing blade, each cell produces a trichome and builds part of a characteristic pattern of veins and interveins. The wing has five major longitudinal veins (L1-L5) and two crossveins—one anterior and one posterior (aCV and pCV). The major contribution to the corrugation of vein L2 is ventral, L3 and L5 are dorsal, and L4 is dorsal distally and ventral proximally.

Virtually every cell of the wing disc forms a hair or gives rise to an external sensory structure (Dobzhansky, 1929; Simpson, 1990; Waddington, 1941). The adult wing disc is an excellent model system for a study of pattern formation because changes in the stereotypical placement of thoracic chaetae, and the normal wing vein and wing margin pattern, can be easily scored with light microscopy. In addition, unfixed wings can be viewed as whole mounts without any special treatment. Thus, the pattern of cell differentiation of the *Drosophila* wing is an ideal model for a high-resolution study of fate specification in a complex tissue.

Disc cell fate and developmental potential. The first experimental method employed in the elucidation of *Drosophila* disc pattern specification was fate mapping. Imaginal discs transplanted from donor third instar larvae into the abdominal cavity of host larvae of the same age can metamorphose with the host. Each transplanted disc differentiated an invariant set of adult structures corresponding to the structures missing if the same disc was extirpated (Schubiger 1971 and references therein). Specific disc fragments transplanted in the same way differentiated only a particular contiguous subset of the adult structures that the whole disc can differentiate. The topographic correlation between the part of the disc used, and the specific fraction of the disc's territory differentiated, was used to construct fate maps, for example, of the leg disc (Schubiger 1968) and the wing disc (Fig. 3; Bryant and Schneiderman 1969; Bryant 1975).

Fate mapping experiments indicate that discs for appendages like the leg or wing are organized like collapsed telescopes, with distal structures of the adult cuticle derived from the center of the imaginal disc and proximal structures from the periphery. The fact

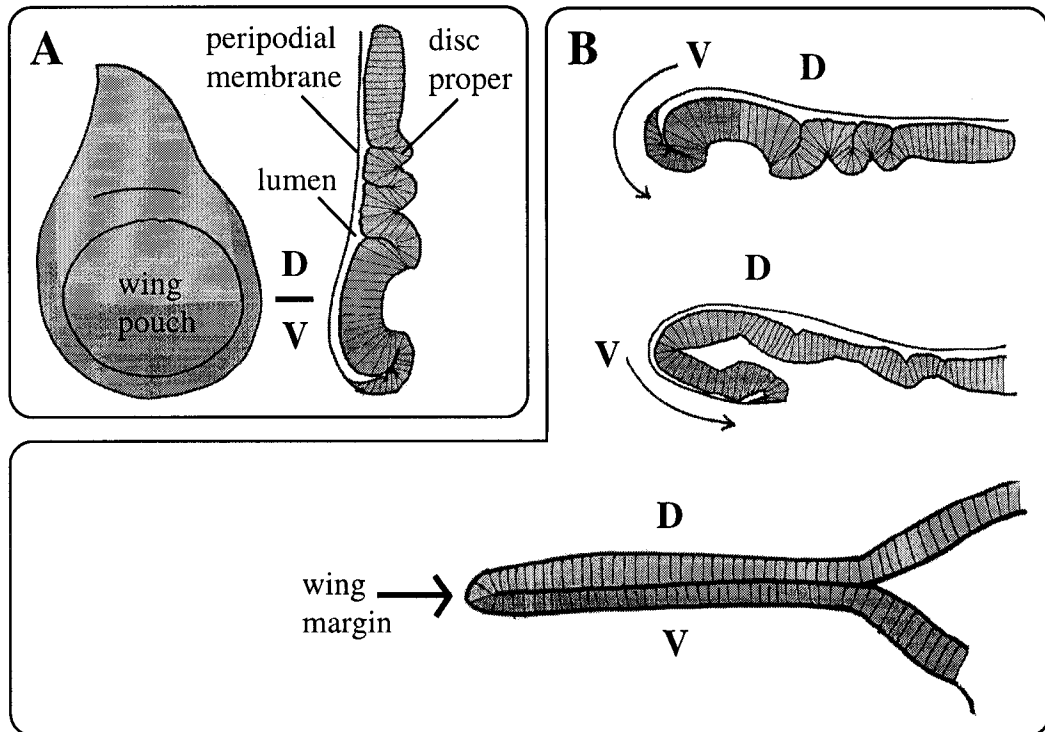


Figure 1. The wing imaginal disc.

(A) A simplified face view diagram of a wing disc (left) and a longitudinal section through the center of a wing disc (right). Dorsal (D; green) and ventral (V; blue) cells are side-by-side along the D/V boundary. The wing pouch will form the adult wing blade. The disc sac is comprised of two epithelial layers, the disc proper and the peripodial membrane, which enclose the disc lumen. The apical surface of the epithelium faces the disc lumen, while the basement membrane forms the outside of the disc. (B) Schematic diagrams of longitudinal sections through pupal wing discs. During metamorphosis, the D and V cells become apposed to create a double cell-layered wing, and the wing margin is differentiated by cells at the newly formed edge. The peripodial membrane retracts during this process (not shown) and may contribute cells to the ventral thorax. These drawings were adapted from Fristrom and Fristrom (1993).

Figure 2. Morphology of a *Drosophila* wing.

The adult wing consists of a proximal hinge and distal wing blade produced by the apposition of dorsal (D) and ventral (V) cell layers. In the wing blade, each cell secretes a single trichome. Along the wing margin (WM), cells produce larger bristles and hairs. The anterior wing margin is made up of a proximal triple row (TR) and distal double row (DR) of mechanosensory and chemosensory bristles. The anterior component of the TR is made up of a medial row of wide mechanosensory bristles (mTR) and a dorsal row of thin mechanosensory and chemosensory bristles (dTR). The ventral triple row (vTR) is a single row of mechanosensory and chemosensory bristles. The posterior row of margin bristles consists of an alternating dorsal and ventral row of non-innervated hairs (PR). Veins give the wing blade mechanical support and also act as vessels for hemolymph. Each vein includes both dorsal and ventral components, with the major contribution to the vein's corrugation from cells of either the dorsal (blue) or ventral (red) wing blade surface. L1-L6, longitudinal veins 1-6; aCV, anterior cross-vein; pCV, posterior cross-vein.

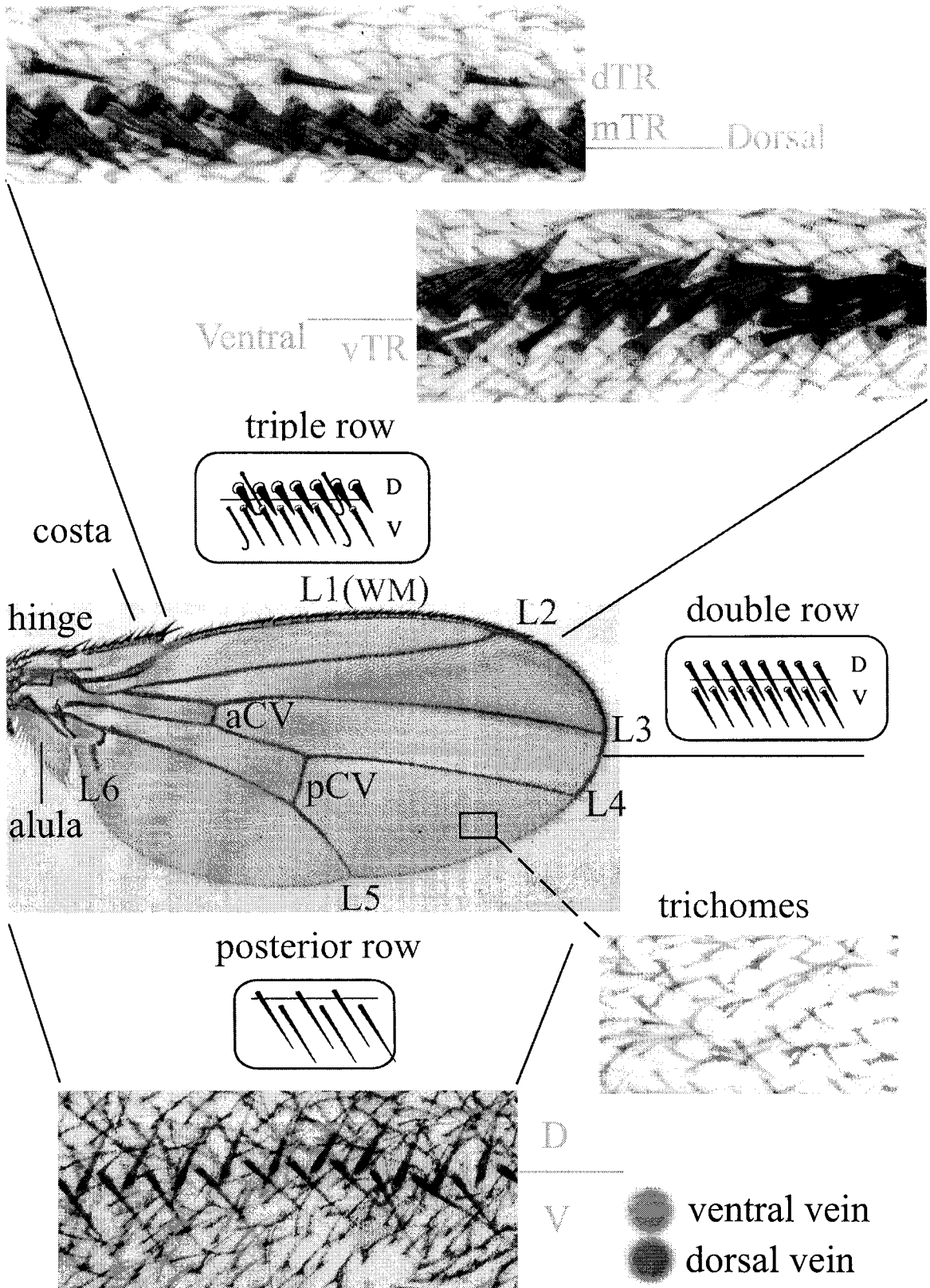
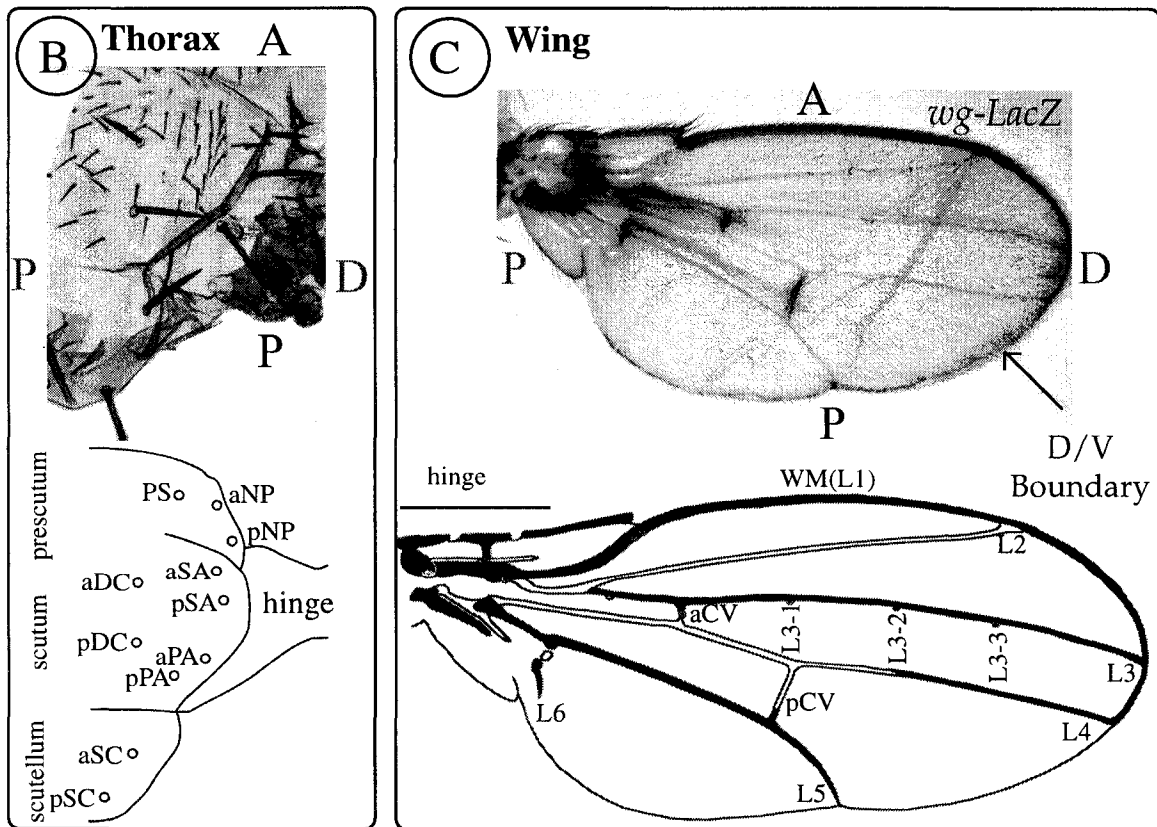
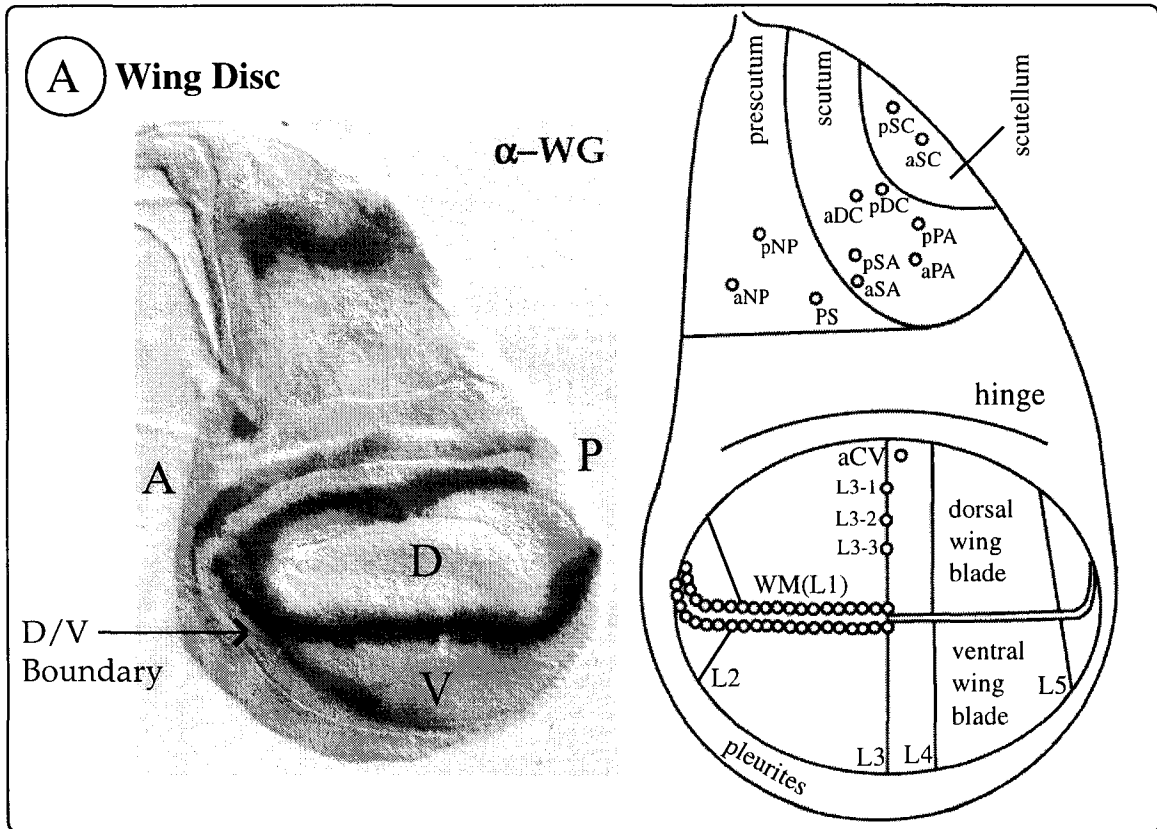


Figure 3. Wing disc fate map.

(A) Wing disc with a representative fate map including the location of the developing sensory organ precursors (SOPs; modified from de Celis, et al. 1996). The adult thorax (B, modified from Heitzler and Simpson 1991) and wing (C) with illustrations of the macrochaete and sensilla that develop from the SOPs illustrated in (A). The larval wing disc everts and flattens during pupariation to form most of the dorsal thorax and the wing. Expression of *wingless* (*wg*) along the D/V boundary of the wing disc in (A) and its final position in the adult wing in (C) are marked with arrows. Notice that the D/V boundary separates dorsal from ventral cells of the developing wing disc and is present along the margin of the adult wing. The orientations used in this figure have been used throughout this thesis: wing discs are oriented dorsal up, anterior left, (proximal center), while wings and thoraces are oriented anterior up, proximal left (dorsal facing).

Axis labels: P, proximal; D, distal; A, anterior; P, posterior; D, dorsal; V, ventral. Vein labels: WM(L1), wing margin (the anterior WM is longitudinal vein L1); L2-6, longitudinal veins 2-6; aCV and L3-1 to L3-3, campaniform sensilla of the anterior crossvein and longitudinal vein 3, respectively. Thoracic macrochaetae: a, anterior; p, posterior; NP, notopleural; PS, presutural; DC, dorsocentral; PA, postalar, SA, supraalar; SC, scutellar.

(A,C) Photographs courtesy of Fernando Diaz-Benjumea.



that fate maps of imaginal discs can be made in this way implies that disc cell fates must have been specified in normal development before fragmentation and transplantation. The simple topographical projection of the adult pattern of markers onto the fate map of the disc suggests that a cell's fate is precisely coordinated according to its position within the disc as a whole. This finding led to the interest in using this system to ask the question of how cells acquire information about their relative positions in a tissue.

Schubiger also found that although cells in the mature disc had a highly detailed pattern of developmental fates, their fates were not cell-heritably restricted (Schubiger, 1971). He found that imaginal disc fragments are able to regenerate missing parts when cultured *in vivo*. Imaginal disc fragments cultured in the abdomen of an adult female, then transplanted into third instar larvae, will metamorphose with the larvae. In contrast to late (mature) larval culture, the period of culture in the adult host permits cell proliferation in the disc fragments (Bodenstein 1940, Wildermuth 1968; in Schubiger 1971). Careful analysis of the differentiated cuticle showed that any two parts of a single disc either duplicate, or regenerate the other missing part of the disc (Bryant, 1971; Bryant, 1975). During disc fragment culture, cells along the edge of the cut become apposed at a wound heal (Reinhardt et al., 1977). Analysis of genetic mosaics (Abbott et al., 1981) and distribution maps of S-phase cells (O'Brochta and Bryant, 1987) show that the majority of dividing cells originate from, and are localized to, a small area close to the wound heal. These results support a model of blastema formation in which cells next to a free edge created by surgical removal are respecified to form a regenerate or duplicate (Bryant 1971; Haynie and Bryant 1976). It seems probable that disc cells apposed at a wound heal recognize and respond to the disparate positional information of their neighbors (French et al. 1976, for example).

These results indicate that, although the fate of disc cells is patterned and can be mapped, their fate is not cell-heritably restricted until differentiation is initiated. That is, disc cells have the developmental potential to exceed their normal fates. This pattern re-formation phenomenon provides evidence of a coordinated pattern formation mechanism in discs. In the next sections, a model for coordinated fate specification in the wing disc will be presented based on intercellular communication.

1.2 Regional identity

Compartment boundaries. A series of clonal restrictions occurs during larval development to subdivide the wing disc into successively smaller compartments. This characteristic of disc patterning was identified when the relationship between cell fate and cell lineage was studied in genetic mosaic wings (Bryant, 1970; Garcia-Bellido and Merriam, 1971; Garcia-Bellido et al., 1973).

A genetic mosaic tissue includes a group of cells of clonal origin with a different genotype from the surrounding tissue. Genetic mosaic discs can be created by inducing somatic crossing over using x-rays, which induce chromosome breaks. Thus, the timing of x-ray treatment can be used to regulate the timing of clone induction. Induction of crossing over in animals heterozygous for a cell marker allows the identification of mutant cells in the mosaic tissue.

In general, cell lineage in the wing disc is highly irregular. The descendants of different marked cells often assume irregular shapes and differentiate overlapping sets of pattern elements (Bryant, 1970). Clones induced even very late in development were often able to straddle several distinct cell types, indicating that cell lineage is not generally related to specific cell types. Cell fate depends instead on position in the wing disc. Nevertheless, most clones were restricted to either the dorsal or ventral wing surface as if the wing margin represented a boundary that clones were unable to cross (Bryant 1970; Garcia-Bellido and Merriam 1971).

Early irradiation produces larger marked patches of cells since the descendants of a cell in a young imaginal disc make up a larger proportion of the disc than those of a cell in an older disc (Bryant, 1970). Thus, clones induced very late in development were very small, making it difficult to confirm the existence of cell lineage restrictions at late stages. To overcome this limitation, Garcia-Bellido et al. (1973) induced recombination in animals heterozygous for a dominant *Minute* mutation *in trans* to a recessive visible cell marker. Since the *Minute* mutation dominantly slows the rate of cell division (Morata and Ripoll 1975), the marked mitotic clone was given a growth advantage over surrounding *Minute* tissue.

In spite of their very large size, the clones of marked cells analyzed by Garcia-Bellido et al. were never observed to label both anterior (A) and posterior (P) wing structures. A and P clones defined two separate and spatially contiguous groups of cells; the straight line separating A and P clones defined a cell lineage restriction. Other lineage restrictions appeared successively at different times during development. For example, early clones were observed to label both dorsal and ventral wing structures but clones induced just after the end of the first larval instar were restricted to either dorsal or ventral structures, defining a new D/V lineage restriction (Bryant 1970; Garcia-Bellido and Merriam 1971; Garcia-Bellido et al. 1973). Garcia-Bellido et al. called these lineage restrictions "compartment boundaries" because they subdivided the wing disc into successively smaller compartments. Disc cell fate within a compartment is not clonally restricted until a new compartment boundary subdivides an earlier compartment. Therefore, compartmental restrictions are assigned according to position, then clonally transmitted.

Although the A/P lineage restriction does not correspond to any obvious morphological feature of the wing, compartmentalization can be related to the acquisition of a final cell fate (Garcia-Bellido et al., 1973). The A/P compartment boundary separates cells of anterior or posterior fates. During larval development successive boundaries seem to separate thorax from wing, wing hinge from wing blade, and dorsal wing from ventral wing. Thus, compartmentalization might involve binary subdivisions that progressively restrict normal fate.

Selector genes. Evidence of a genetic basis for this phenomenon began with the analysis of the *engrailed* (*en*) mutant. The original *en*¹ mutant has only posterior wing defects, partially transforming the posterior wing to a mirror-image duplication of anterior structures (Garcia-Bellido and Santamaria, 1972). This effect is general for the posterior compartments of leg, eye-antennal and wing discs. The *en* wing phenotype is very interesting: in the absence of *en* function, the positional information of the wing disc appears to be symmetrical on either side of the A/P compartment boundary. One of the normal functions of *en* seems to change the way posterior wing cells interpret this positional information within the posterior compartment. In addition, while anterior *Minute*⁺ *en* mutant clones delineate the A/P compartment boundary, posterior clones form irregular borders and no longer respect the A/P lineage restriction (Morata and Lawrence, 1975).

From such results, it was suggested that *en* activity is required in the posterior compartment to promote the posterior fate and to maintain the A/P lineage restriction. This led to the concept of the selector gene (Crick and Lawrence, 1975; Garcia-Bellido, 1975). In this model, each new lineage restriction represents a binary separation of cells into discrete compartments. This could be controlled by setting the cell-heritable binary state of a different selector gene activity at each compartmentalization event, which would be the controlling difference between the two new compartments. The acquisition of a final cell fate could be controlled by the progressive compartmentalization of a field, encoded in a binary combinatorial code by the activity of a series of selector genes. Different combinations of a number of selector genes (*n*) would determine an exponentially greater number of distinct developmental fates (2^n) if new compartments bisected old ones. Therefore, the selector gene hypothesis provides a testable model for the genetic control of pattern formation mechanisms.

***apterous* acts as the dorsal selector gene.** The most convincing evidence for the role of *apterous* (*ap*) as the dorsal selector gene is the phenotype of *ap* in genetic mosaic wings (Diaz-Benjumea and Cohen 1993). Ectopic wing margin is induced at the boundary between *ap* mutant clones in the wing blade and neighboring wildtype tissue. This effect is only seen when *ap* clones are in the dorsal compartment where they create an ectopic boundary between *ap*-expressing cells (wildtype dorsal tissue) and non-expressing cells (*ap* mutant clone). The ectopic margin is differentiated by cells on both sides of the clone border. Within the clone, only ventral cell types are differentiated, and outside the

clone, only dorsal cell types are differentiated. The *ap* mosaic phenotype is most easily explained if *ap* mutant cells transform into cells of ventral fate and a new border with pattern reorganizing capabilities forms at the new D/V boundary.

ap and *en* encode homeobox transcription factors (Cohen et al., 1992; Poole et al., 1985) responsible for controlling unique patterns of cell-differentiation for each of the four distal wing compartments (reviewed in Blair 1995; Mann and Morata 2000). Compartmentalization of the wing thus seems to involve binary subdivisions that progressively restrict developmental potential. However, strong evidence exists today for only these two selector genes in the wing: *ap* and *en*. A combinatorial code of two selector genes acting simply as described above is not sufficient to account for the complex organization of pattern within each compartment. As presented below, pattern within compartments is not generated by further subdivision. Instead, it is controlled by *ap* and *en* which act to regulate both short-range and long-range intercellular communication in the compartments they specify.

1.3 Short range communication

Wing margin induction. Recent work has shown that specification of the *Drosophila* wing margin and growth of the wing pouch requires spatially restricted short range inductive signalling between dorsal and ventral cells of the wing disc. Early asymmetric signalling between dorsal and ventral cells induces a band of activated Notch signalling that defines the lineage restriction and wing margin organizing properties of the D/V boundary (see below). The Notch-activated boundary cells express *wingless* (*wg*), a WNT (Wingless/Int-1)-family secreted signalling molecule that is required to induce the wing margin fate in adjacent tissue.

Notch and the genes for its ligands *Serrate* (*Ser*) and *Delta* (*Dl*) encode large transmembrane proteins with extracellular Epidermal Growth Factor (EGF)-like repeats (reviewed in Artavanis-Tsakonas et al. 1995). In its extracellular domain (NECD), Notch has 36 EGF repeats and 3 LIN-12/Notch repeats (LNR) required for association with its ligands. The Notch intracellular domain (NICD) includes a RAM domain* and 6 Ankyrin repeats that are required for signal transduction, and a PEST domain thought to limit protein stability. NOTCH activation involves a series of proteolytic steps that are required for the eventual release of NICD in response to ligand binding (Blaumueller et al. 1997; Parks et al. 2000). Notch signal transduction is thought to operate by a direct mechanism in which NICD is transported into the nucleus where it interacts with the DNA binding protein encoded by *Suppressor of Hairless* (*Su(H)*) to activate target gene expression. Genes of the *Enhancer of split Complex* (*E(spl)-C*) are direct targets for binding by SU(H) and are transcriptionally activated in response to Notch signalling

* Named after the mRAM23 domain of mouse Notch1, identified as an RBP-jκ (mouse Su(H)) interacting fragment in a yeast 2-hybrid screen (Roehl et al., 1996; Tamura et al., 1995).

(Bailey and Posakony, 1995; Fortini and Artavanis-Tsakonas, 1994; Lecourtois and Schweisguth, 1995). Although a direct role has not been shown for SU(H) in *wg* transcriptional activation, both *Notch* and *Su(H)* are required for *wg* expression along the dorsal-ventral (D/V) boundary of the wing disc (de Celis and Bray, 1997; Klein et al., 2000; Neumann and Cohen, 1996).

Notch receptor activation is required for and sufficient to direct *wg* expression at the presumptive margin (Diaz-Benjumea and Cohen 1995; Rulifson and Blair 1995; de Celis and Bray 1997). Mitotic clones of cells mutant for *Notch* that meet the D/V boundary from either side cause gaps in the expression domain of *wg*, causing "notches" in the adult wing margin. Ectopic expression of the active intracellular domain of Notch is sufficient to induce ectopic expression of *wg*, and induce the formation of ectopic bristles and outgrowths from the wing surface. These Notch-activated cells do not form margin structures but signal adjacent tissue, through WG, to become margin bristles.

Ser encodes a transmembrane Notch ligand which is expressed throughout the dorsal compartment of the wing disc. *Ser* is required in cells immediately ventral to the D/V boundary where it activates the Notch receptor (de Celis et al., 1996b; Diaz-Benjumea and Cohen, 1995; Kim et al., 1995). Only dorsal *Ser* mitotic clones have effects on pattern. When a dorsal *Ser* mitotic clone meets the D/V boundary, the endogenous margin is disrupted. Ectopic expression of *Ser* has effects only in the ventral compartment where it induces ectopic *wg* expression and ectopic margin in the adult. This is consistent with a role for SER as a signal from dorsal to ventral cells (Fig. 4).

Dl, also encoding a Notch ligand, is required for normal wing margin formation in both dorsal and ventral cells at the D/V boundary (de Celis and Bray, 1997; de Celis et al., 1996b; Doherty et al., 1996). All cells in the wing disc express *Dl*, with highest *Dl* expression in dorsal and ventral cells centered along the D/V boundary. Several lines of evidence support a role for DL as a signal from ventral to dorsal cells. Ventral clones that abut the D/V boundary cause non-autonomous wing margin loss, while dorsal clones that abut the D/V boundary cause only autonomous loss of bristle differentiation (de Celis et al. 1996b). Ectopic *Dl* expression in the dorsal compartment but not the ventral compartment can induce expression of the Notch target genes *wg* and *cut*, leading to dorsal ectopic margin and wing outgrowths in the adult (Doherty et al. 1996). These results indicate that DL acts as a ventral to dorsal signal that, together with SER, activates the Notch receptor in cells on either side of the D/V boundary (Fig. 4). Notch activation at the boundary is sufficient to induce *wg* expression in the boundary cells, and to induce the wing margin fate in neighboring tissue.

Localized Notch activation along the D/V boundary is specified through the interaction of *ap*-expressing cells of the dorsal compartment and non-expressing cells of the ventral compartment (Blair et al., 1994; Diaz-Benjumea and Cohen, 1993; Williams et al., 1994).

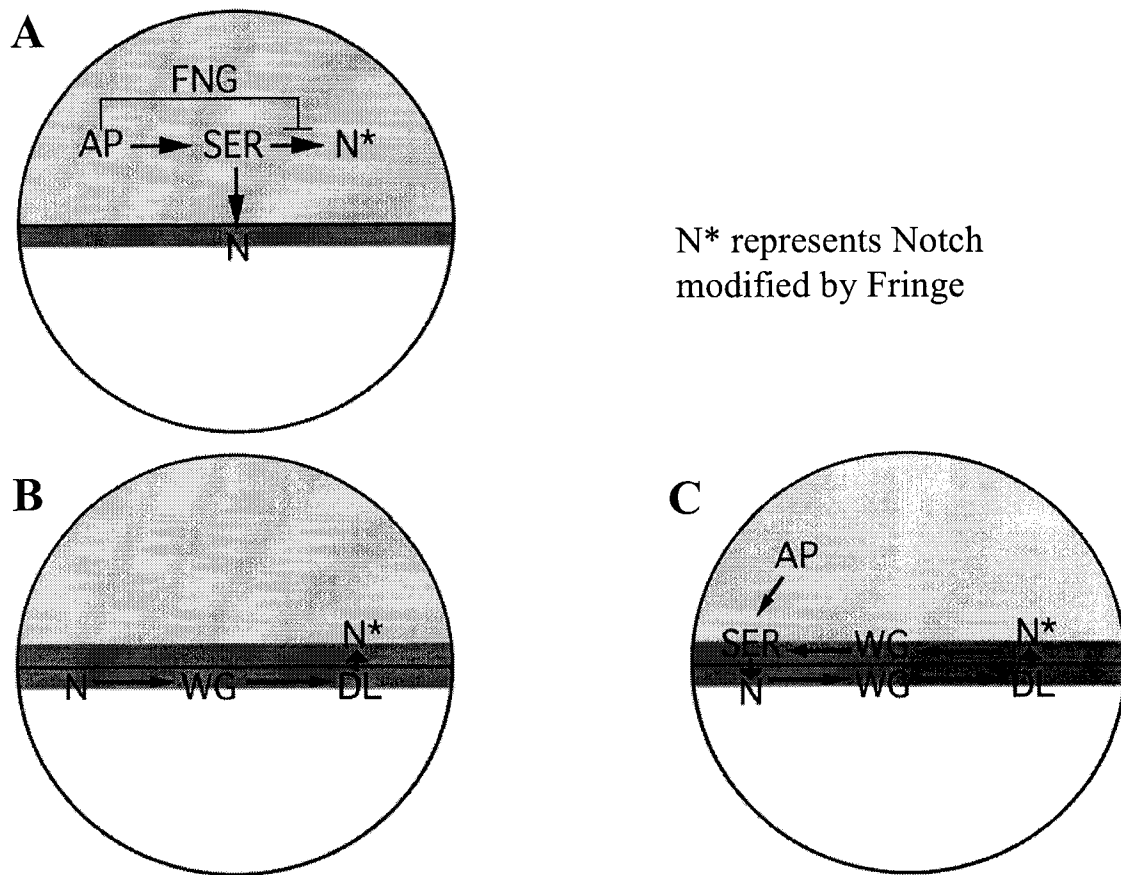


Figure 4. Schematic representation of inductive intercellular interactions along the D/V boundary.

The D/V boundary is represented by a black line between dorsal (green, upper) and ventral (white, lower) areas of each circle, representing wing disc pouches. Activated Notch is represented in red. (A) AP induces expression of *fng* and *Ser* in each dorsal cell of the wing disc. FNG inhibits the ability of SER to signal to Notch while potentiating the ability of DL to signal to N. SER thus activates N in ventral cells along the D/V boundary. (B) Ventral N activation (leading to WG signalling, see below) increases *Dl* expression on both sides of the D/V boundary but *Dl* is only required in ventral cells to activate N in dorsal cells across the D/V boundary. This may be due to the dorsal redundancy of DL and SER. (C) Together, DL and SER activate N signal transduction in cells on either side of the D/V boundary. N activation in the boundary cells induces the expression of *wg*, which is required to induce the wing margin fate in cells flanking the boundary cells.

As previously described, ectopic wing margin is differentiated by both mutant and wildtype cells along the border of a dorsal *ap* mutant clone. This phenotype is due to the requirement for *ap* to induce expression of *fng* and *Ser* in all dorsal cells of the wing disc (Irvine and Wieschaus 1994; Kim et al. 1995). *fng* encodes a glycosyltransferase that modifies the Notch receptor (Bruckner et al., 2000; Ju et al., 2000; Moloney et al., 2000; Munro and Freeman, 2000), autonomously inhibiting the ability of SER to activate Notch, and potentiating the ability of DL to activate Notch (Fleming et al., 1997; Panin et al., 1997). Co-expression of *fng* and *Ser* in cells of the dorsal compartment thus restricts the domain of SER activation of Notch to ventral cells along the D/V boundary (Panin et al. 1997). A dorsal *fng* mitotic clone has an effect similar to that of a dorsal *ap* mitotic clone: ectopic wing margin is induced at the boundary between *fng*-expressing and non-expressing cells. However, all of the ectopic bristles, both within the *fng* mutant clone and in neighboring wildtype tissue have a dorsal fate because they still express *ap*, the dorsal selector gene.

ap mutant flies have no wings because of failure of distalization, which is dependent on signalling across both the A/P and D/V boundaries. Yet this phenotype can be rescued with dorsal expression of *fng* to restore short-range signalling between dorsal and ventral cells (O'Keefe and Thomas, 2001). Differentiation of a normally shaped wing also requires dorsal expression of α PS1, a dorsally expressed integrin subunit, so the two wing surfaces can stick together. The resulting wing looks nearly normal in shape except it consists entirely of ventral cell types. In the absence of *ap*, the positional information of the wing disc appears to be symmetrical on either side of the D/V boundary. *ap* specifies the genetic address "dorsal" by activating expression of the *muscle segment homeobox* (*msh*) transcription factor, which is affected by *Dorsal wing* (*msh^{Dhw}*) mutations (Tiong et al. 1995; Milan et al. 2001). This evidence indicates that the requirement for *ap* to select dorsal fate and organize wing pattern is accomplished by activating expression of a small number of effectors with distinct functions.

1.4 Long range patterning

Early work on imaginal disc regeneration indicated that disc cells have a developmental potential exceeding their normal fates. The necessary conclusion from these results is that cell fate is regulated within the disc as a whole. That is, each disc cell belongs to a common field of cells in which cell fate is globally regulated. Wolpert (1969) suggested that the regulative properties of a field could be most easily explained if a field is a group of cells which all have their positional values specified with respect to a single coordinate system. As a possible explanation of how positional values within a field are specified, Wolpert suggested the existence of concentration gradients of some chemical fate-controlling factor that each cell can measure. High and low points in these hypothetical form-generating or "morphogen" gradients would generally define the boundaries of such fields. Concentration gradients of different morphogens could theoretically define the orthogonal axes of a 2-dimensional field in a sheet of cells (epithelium). In this

"Positional Information" model, a wing might act as a regulative unit if it is a group of cells whose fates are all specified with respect to position relative to a single such set of high and low points of positional information (field boundaries).

Although the three axes of the adult *Drosophila* limb imply three dimensions of positional information in the developing disc, the epithelium of a disc is a single cell layer and can be represented in two physical dimensions. For the wing disc, these field dimensions have been described in a simple 2-dimensional Cartesian coordinate system, in which each cell senses positional information along an x- and y-axis. Hypothetically, this could occur by each cell responding to the local concentration of diffusible substances originating at orthogonal field boundaries. This conceptual view of pattern formation fits quite nicely with the loss of function phenotypes of *ap* and *en* if the D/V and A/P compartment boundaries act as sources or high points of positional information (an idea first presented in Crick and Lawrence 1975). Positional information would thus be symmetrical about the boundaries, leading to mirror image fate duplications in the absence of selector gene function.

Wing disc morphogens. Within each compartment, pattern is organized over a long-range by two secreted signalling molecules: WG and Decapentaplegic (DPP). *wg* is expressed in dorsal and ventral cells along the D/V boundary, while *dpp* is expressed in cells along the anterior edge of the A/P boundary. As described above, expression of *wg* is controlled by the dorsal selector gene *ap* (reviewed in Blair 1995; Brook et al. 1996). AP directs expression of a transmembrane signal (*Ser*) in all dorsal cells while making dorsal cells insensitive to this signal by inducing *fng* expression. Thus, SER only activates expression of *wg* in ventral cells along the *ap* expression boundary. *ap* also represses dorsal expression of a second transmembrane signal (*Dl*) while making dorsal cells more responsive to DL via *fng*. Together, DL and SER induce *wg* expression in a limited domain spanning the *ap* expression boundary (the D/V lineage restriction). Expression of *dpp* along the A/P boundary can be explained in similar terms (reviewed in Blair 1995; Brook et al. 1996). Expression of *dpp* is controlled by the posterior selector gene *en*. EN directs expression of a short range signal encoded by *hedgehog* (*hh*) in all posterior cells while making posterior cells insensitive to this signal by repressing *cubitus interruptus* expression. Thus, the *hh* signal activates expression of *dpp* only in anterior cells along the *en* expression boundary (the A/P lineage restriction).

Activation of *wg* expression in cells along the D/V boundary appears to be sufficient to mediate the cell fate specification and growth control activities of the D/V boundary (Couso et al., 1994; Diaz-Benjumea and Cohen, 1995). These studies found that clones of wing disc cells over-expressing *wg* in either the dorsal or ventral compartment can differentiate ectopic margin and induce ectopic margin from neighboring tissue without affecting the compartmental identity of those cells. Clones of cells expressing *wg* also are also associated with non-autonomous outgrowths from the surface of the wing blade, supporting a role for WG in organizing growth in surrounding cells at a distance. This

experiment is analogous to amphibian organizer transplantation experiments (Spemann and Mangold, 1923) and suggests that WG is the long-range D/V morphogen in the wing. Only recently was the concentration gradient of the WG protein visualized in the wing disc (Strigini and Cohen, 2000). However, dose-dependent responses to WG at a distance were inferred earlier by the induction of different genes at distinct distances from the WG source. For example, WG induces expression of *achaete (ac)* only next to the WG source, while it induces *Distal-less (Dll)* expression in most of the wing pouch (Neumann and Cohen 1997; Zecca et al. 1996). It has also been inferred that WG acts directly on distant cells based on the following observations. Firstly, all disc cells must be able to transduce the WG signal for normal gene expression patterning, e.g. *disheveled* mutant cells do not express WG target genes. Secondly, ectopic autonomous activation of the WG pathway (e.g. activated Armadillo clones) causes ectopic WG target gene expression only autonomously. Thus, WG seems to organize wing disc pattern by directly inducing distinct gene expression outputs at different concentrations along the D/V axis.

WG and DPP are each secreted by expressing cells, leading to orthogonal "mirror gradients" of protein concentration that have been directly observed (Strigini and Cohen 2000; Teleman and Cohen 2000). In the absence of *wg* or *dpp*, discs do not grow and cell fates are not specified. When they are ectopically expressed, *wg* or *dpp* is sufficient to induce ectopic growth and patterning, indicating their expression is necessary and sufficient to organize a pattern of cell fates (Struhl and Basler 1993; Zecca et al. 1995; Diaz-Benjumea and Cohen 1995; Capdevila and Guerrero 1994). Different concentrations of WG and DPP have specific effects on gene expression patterns that affect cell fate (Neumann and Cohen 1997; Nellen et al. 1996; Lecuit et al. 1996; Zecca et al. 1996). WG and DPP therefore each satisfy the required properties of a morphogen: it should act directly on target cells at a distance and in a concentration-dependent manner to specify different cell fates.

The positional information in a wing can thus be described as a 2-dimensional Cartesian coordinate system where the D/V boundary functions as the x-axis, and the A/P boundary as the y-axis. Each wing disc cell seems to measure its relative position along the x and y axis by sensing its exposure level to WG and DPP. This may be solely accomplished through the concentration-dependent activation of different combinations of WG and DPP target gene expression throughout the future wing. In this model, the combinatorial code of *ap* and *en* expression would specify regional identity by differentially affecting the interpretation of this 2-dimensional mirror-image positional information system in each quadrant. Because expression of *dpp* and *wg* are also controlled by the selector genes *ap* and *en*, compartmentalization is the pre-eminent organizational feature of wing disc patterning.

1.5 D/V boundary formation

In the *Drosophila* wing, cell fate depends on position (rather than cell-lineage) until very late in development, as small clones even late in development often straddle several distinct cell types. There is one exception: compartment boundaries are strict lineage restrictions that divide cells into sub-populations with restricted compartmental fates. The mechanism of boundary formation is an active area of research. Several mechanisms have been proposed to account for boundary properties including localized cell death, zones of non-proliferation, and preferentially oriented cell proliferation. None of them appears important to A/P or D/V lineage restriction in *Drosophila* (Blair 1993).

The boundary between *ap* expressing cells and non-expressing cells corresponds exactly to the D/V lineage restriction, suggesting a direct relationship (Blair 1993; Diaz-Benjumea and Cohen 1993). *ap* expression appears near the time that the restriction is thought to be established, and loss of *ap* function from dorsal cells after the formation of the boundary causes them to cross into the ventral compartment, suggesting that *ap* is required for the lineage restriction (Blair et al., 1994).

Garcia-Bellido (1975) suggested that selector genes may indirectly specify compartment-specific cell affinities. This remains an attractive hypothesis but there is little direct evidence for differences in cell adhesion between compartments. Recently, some characteristics of two dorsally expressed putative cell adhesion molecules encoded by *capricious* and *tartan* suggest they play a role in compartment-specific cell adhesion regulated by *ap* (Milan et al., 2001a). Although *capricious* and *tartan* over-expression causes some very interesting cell sorting behaviors, loss of function data consistent with either gene being required to establish or maintain a functional D/V lineage restriction is not yet available.

Several recent papers implicate inter-compartmental signalling in the maintenance of the D/V lineage restriction. As previously presented, *ap* controls local intercellular interactions between dorsal and ventral disc cells. In the absence of *ap*, D/V compartmentalization (and Notch activation) can be rescued with *fng* expression, leading to an all-ventral but morphologically normal wing (O'Keefe and Thomas, 2001). The *fng* expression boundary is normally required to define a line of Notch activation spanning the D/V boundary. The rescue of *ap* mutant wings with *fng* expression suggests that it is signalling between compartments, mediated by Notch, and not the acquisition of compartment specific affinity, which plays the crucial role in D/V compartmentalization. In support of this hypothesis, disrupting Notch activation at the D/V margin disrupts the lineage restriction (Micchelli and Blair, 1999; Rauskolb et al., 1999). This has been accomplished by disrupting *ap* or *fng* expression in dorsal cells at the D/V boundary, by ectopically expressing *fng* in ventral cells, or by losing *Notch* expression in clones or in a restrictive temperature shifts in a *N^{ts}* background. Although Notch has properties of a cell adhesion molecule, clones of cells expressing signalling deficient Notch proteins in

which the extracellular domain of Notch is intact (N^{Co} ; Brennan et al. 1997) disrupt the D/V lineage restriction. Thus, it seems that the lineage restriction is a property of cells with activated Notch, not a characteristic of Notch itself. However, the domain of Notch activated cells includes cells on both sides of the *ap* expression boundary, which marks the D/V lineage restriction. To account for this discrepancy, it has been proposed that *ap* regulates compartment-specific cell affinity, but only in cells along the D/V boundary that are Notch activated (Micchelli and Blair, 1999).

Since Notch activation plays a role in maintaining the D/V lineage restriction, and is necessary and sufficient for the expression of *wg*, the D/V morphogen, these results define a molecular link between compartmentalization and organizer properties of the boundary.

1.6 Pattern refinement

The global positional information derived from gradients is coarse. Refinement of gene expression patterns during development, and mutant phenotypes such as the wide veins of *Delta* mutant flies, indicate that cells communicate to refine their positional information. Lateral inhibition describes the intercellular interactions that subdivide initially equivalent cell populations through competitive cell signalling. An early lateral inhibition model explained the differentiation of a regularly spaced heterogeneous pattern by proposing that once a cell adopts a certain fate, it can inhibit its neighbors from adopting that same fate (Wigglesworth, 1940). A current model for lateral inhibition originates in a study of pattern formation among multipotent vulval precursor cells (VPCs) in *C. elegans* (Sternberg, 1988). This study indicated that the *C. elegans* Notch-like gene (*lin-12*) is required for the decision between primary and secondary vulval cell fates, and implicated it as a receptor in this process. The following is a summary of the archetypical lateral inhibition model arising from this work.

In this model, a single VPC selects a dominant cell fate through assessment of relative *lin-12* activity among VPCs. The dominant cell, stochastically biased as a signal-producing cell, promotes *lin-12* activity in other members of the group. Activated *lin-12* leads to a cell-autonomous reduction in signal production, potentiating and maintaining the initial signal-producing bias toward the dominant cell. Finally, primary cell fate is inhibited by high *lin-12* activity in receiving cells, which then adopt the secondary (inhibited) fate. This sequence of events leads to the prediction of two classes of genes: one necessary to establish the equivalence group and the second to ensure only one cell per group adopts the primary fate.

A large body of evidence supports a role for DL-Notch signalling in analogous lateral inhibition processes in *Drosophila*. Some of the evidence is summarized here in order to describe the regulative interactions between *Dl* and *Notch* during pattern refinement.

Neurogenic and proneural genes. During embryonic development, about 25% of the ventral neuroectodermal cells become neuroblasts in a regularly spaced pattern (reviewed in Campos-Ortega 1993). Neuroblasts segregate from surrounding ectodermal cells and give rise to the central nervous system. Once the neuroblast fate is adopted by a cell, it appears to inhibit its neighbors from becoming neuroblasts. The most direct evidence for this "lateral inhibition" is the replacement of an ablated neuroblast by a neighboring epidermal cell in the grasshopper embryo (Doe and Goodman, 1985). This result suggests the existence of a cell signalling process by which cells negotiate their fates during neurogenesis.

In *Drosophila*, mutations that cause excessive neuroblast differentiation at the expense of the epidermal cell fate define a class of "neurogenic" genes (Lehmann et al., 1981; Lehmann et al., 1983). In contrast, mutations leading to a reduction in the number of neuroblasts define a set of "proneural" genes (see below). The mutant phenotype and subsequent molecular characterization of the neurogenic genes *Notch* and *Dl* suggests that they define an intercellular communication mechanism affecting lateral inhibition during neuroblast segregation. Both *Notch* and *Dl* encode large transmembrane proteins with epidermal growth factor (EGF)-like repeats in their extracellular domains (Kidd et al., 1986; Kopczynski et al., 1988; Vässin et al., 1987; Wharton et al., 1985). Since EGF is a secreted growth factor, the sequence similarity between DL, Notch and EGF suggested that they might all be signalling molecules.

Another important class of neurogenic mutations were allelic to the previously identified *E(spl)* mutation. *spl* mutations are recessive viable *Notch* mutations and the original *E(spl)* mutation was identified as a dominant enhancer of the *spl* phenotype (Lindsley and Zimm, 1992). The original *E(spl)* affects one of a complex of related transcription units encoding DNA binding proteins collectively referred to as the *Enhancer of split-Complex (E(spl)-C)*. The genes of this complex are required during neurogenesis to limit neural fate, since deletions which remove the complex lead to neural hypertrophy (reviewed in Bray 1997).

Those genes necessary for neuroblast development define the proneural class. In both the embryo and the adult, development of neural tissue is initiated by proneural gene expression in small groups of cells, known as proneural clusters (Campuzano and Modolell, 1992). The first of these to be identified were those encoded by the *achaete-scute complex (AS-C)*; Campuzano et al. 1985; Ghysen and Dambly-Chaudiere 1989; Ghysen and Dambly-Chaudiere 1990), named after mutants affecting the pattern of thoracic bristles or chaetae (Lindsley and Zimm, 1992). Loss of function alleles of the *AS-C* suppress the formation of neuroblasts and suppress the loss-of-function neurogenic phenotype of *Dl*, *Notch* and *E(spl)* (Brand and Campos-Ortega, 1988). *AS-C* members are initially expressed in spaced clusters of cells, where they promote the neural fate. Later, one cell of each cluster accumulates *AS-C* transcripts at a high level and adopts the

neural fate (Cabrera, 1990; Cabrera et al., 1987; Ruiz-Gomez and Ghysen, 1993). In neurogenic mutants, this *AS-C* transcript restriction does not occur (Skeath and Carroll, 1992), suggesting that the neurogenic genes normally inhibit neural fate by turning off *AS-C* expression.

Genetic interactions were used to arrange the neurogenic genes and the proneural genes into an epistatic series (de la Concha et al., 1988; Vässin et al., 1985). Epistasis refers to a genetic interaction whereby a mutation at one locus masks the phenotypic expression of a mutation at a second locus. However, since all of the neurogenic alleles give similar neurogenic phenotypes (overgrown CNS and reduced epidermis), gene dosage interactions were used. For example, while the phenotype of an *E(spl)* mutant is not affected by an increase in the *Notch* gene dose, the phenotypic severity of a *Notch* mutant is reduced by a duplication of the *E(spl)* loci. This indicates that *E(spl)* is epistatic to *Notch*, and that *Notch* activates *E(spl)* function. Results such as these were interpreted in a formal genetic pathway as presented in Fig. 5A. In this model, *Notch* can positively regulate *E(spl)* and negatively regulate *Dl*. The net positive influence on *E(spl)* results in negative regulation of *AS-C*, relieving inhibition of the epidermal fate. In other words, the genetic evidence suggests that the neurogenic genes inhibit the function of proneural genes in cells that become epidermal.

Thoracic microchaetae patterning. Studies of *Dl* and *Notch* in thoracic bristle development provided the first convincing evidence for the role of *Dl* and *Notch* in lateral inhibition (Heitzler and Simpson, 1991; Heitzler and Simpson, 1993). The bristles of the adult are divided into the macrochaetae, those that are particularly large and characteristically positioned, and the microchaetae, which are smaller and more uniformly arranged. For this discussion, I will focus on the microchaetae.

The normal pattern of bristle differentiation depends on Notch signalling, since in the absence of *Dl* or *Notch*, a uniform field of densely packed adjacent microchaetae is formed (Heitzler and Simpson, 1991). Heitzler and Simpson found that differentiation of bristles along the border of a genetically marked and otherwise wildtype clone, microchaetae differentiation is random. However, at the border of a clone with reduced *Notch* activity or reduced *Notch* gene dose, cells autonomously tend to adopt the neural fate (in spite of the presence of neighboring wildtype cells). Compatible results were obtained in mosaic embryos, where *Notch* mutant cells are not rescued by neighboring wildtype tissue (Hoppe and Greenspan, 1986). This cell-autonomous behavior of *Notch* is consistent with the proposed role for *Notch* as a receptor in a lateral feedback mechanism required to repress neural fate.

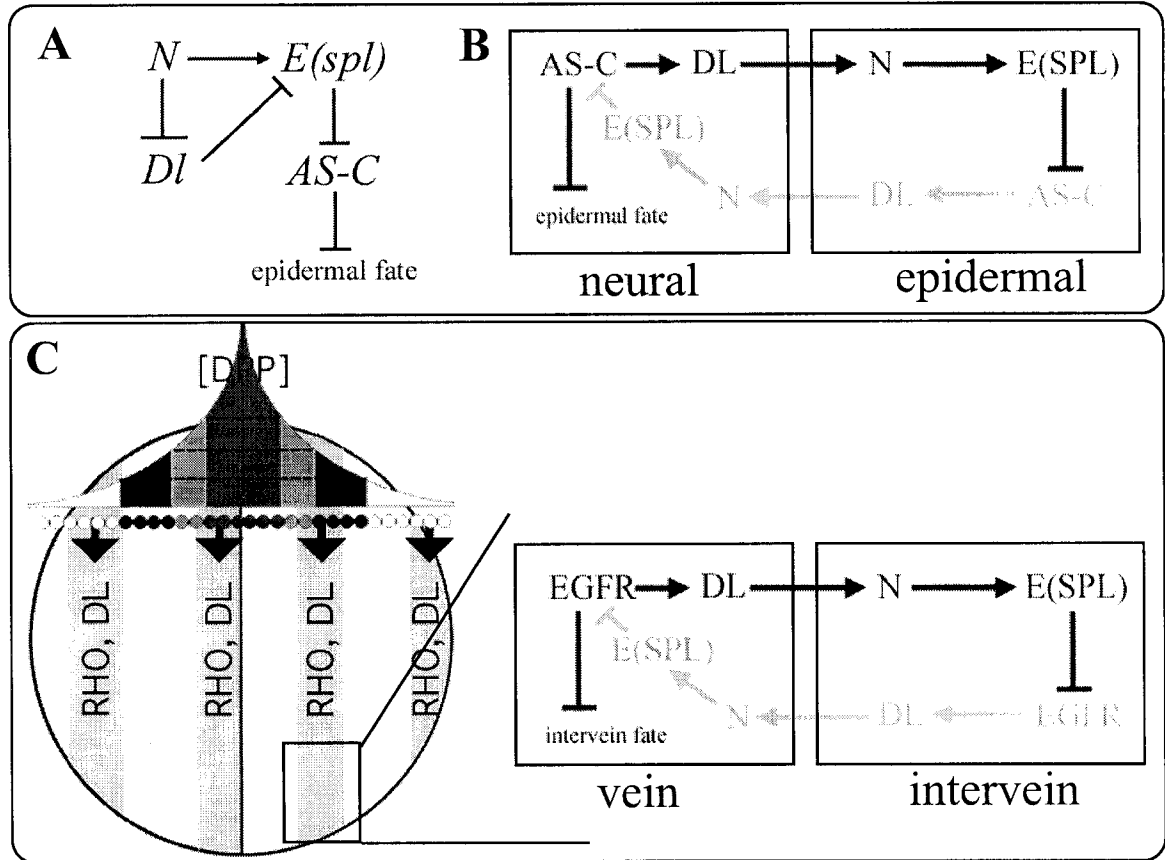


Figure 5. Schematic representation of Notch feedback mechanisms in the wing disc.

(A) Formal genetic pathway summarizing dosage interactions between *Notch*, *Delta*, *E(spl)* and *AS-C* during embryonic neurogenesis (de la Concha et al. 1988).

(B) Model of protein interactions regulating the choice between neural and epidermal fate in the developing thorax (Heitzler and Simpson 1991, 1993, 1996a). Each box represents a single cell of a proneural cluster.

(C) A model representing the DPP morphogen gradient inducing bands of vein competent cells by inducing *rhomboid* (*rho*) expression. During pupal development, a feedback loop illustrated to the right refines *rho* expression therefore refining EGFR activation and vein differentiation to a subset of the vein competent cells (de Celis et al. 1997). Each box represents a single provein cell. Notice the similarity between the models in B and C.

In contrast, at the border of clones with decreased *Dl* activity compared to surrounding tissue, cells outside of the clone preferentially adopt the neural fate and differentiate microchaetae. Thus, *Dl* mutant cells behave non-autonomously and produce epidermis when adjacent to wildtype cells. This result is consistent with a role for *Dl* as a signal in *Notch* mediated lateral inhibition. Since the choice of the precursor cell can be influenced by the relative levels or activity of *Notch* and *Dl* in mosaic animals, Heitzler and Simpson proposed that microchaetae precursors are chosen in a stochastic manner that relies on *Notch* mediated lateral inhibition.

All cells express *Notch* and *Dl* (Fehon et al., 1991; Kooh et al., 1993), therefore, all cells have the capacity to inhibit, or be inhibited by their neighbors. The question is this: how are cells that are able to inhibit their neighbors chosen from groups of initially equivalent cells? To explain how the system advances to a state where one dominant cell escapes from inhibition while its neighbors remain inhibited, it has been proposed that *Dl* expression is regulated by lateral inhibition (Heitzler et al., 1996a). In this model, cells that receive more inhibitory signal will in turn produce less inhibitory signal. This is likely coordinated through the *E(spl)-C* genes whose transcripts accumulate in response to *Notch* signalling, and are autonomously required for reception of the inhibitory signal (Heitzler et al., 1996a; Jennings et al., 1994; Lieber et al., 1993). In agreement with the results of genetic epistasis experiments, *E(spl)-C* expression can inhibit transcription of *AS-C* members, which are positive regulators of *Dl* transcription (Bailey and Posakony, 1995; Heitzler et al., 1996a; Seugnet et al., 1997). This relationship defines a possible mechanism to decrease production of signal (*Dl*) in response to signal reception (Fig. 5B).

In contrast to a stochastic lateral inhibition model, an extrinsic signal may bias cell fate choice by affecting ligand or receptor activity within an equivalence group. In *C. elegans*, the choice of primary vs secondary VPC fate is controlled by lateral inhibition, but is pre-determined by an Epidermal Growth Factor (EGF)-like signal from a neighboring cell (Horvitz and Sternberg, 1991). This may also be the case for *Drosophila* thoracic microchaetae and neuroblast precursors, which consistently differentiate in rows. An extreme form of this model has been proposed in which *Notch* signalling provides an inhibitory signal, but factors independent of *Notch* signalling are required to select the dominant precursor cell and to render it insensitive to *Notch* signalling so that it escapes inhibition (Muskavitch, 1994).

Wing veins. Cross-regulation of at least three signal transduction pathways—*Notch*, *DPP*, and *EGF*—are required for the differentiation of veins of correct width (reviewed in de Celis 1998). Loss of function of *Dl* or *Notch* leads to the differentiation of wider veins, indicating that *DL-Notch* signalling is an essential component of the system specifying vein width. The differentiation of wider veins in *Dl* or *Notch* mutant clones, or in viable hetero-allelic *Dl* or *Notch* combinations, occurs only in contiguity with normally positioned vein tissue and affects every vein (de Celis and Garcia-Bellido, 1994b; Garcia-

Bellido and de Celis, 1992). This implies the existence of a vein competent or "pro-vein" region in which cells will normally differentiate as vein unless instructed otherwise. *Dl* mutant clones allow non-autonomous ectopic differentiation of vein tissue, while *Notch* behaves autonomously in clones (de Celis and Garcia-Bellido, 1994b; Garcia-Bellido and de Celis, 1992). Again, this suggests that *Dl* functions as an inhibitory signal, and *Notch* functions as its receptor. Since loss of either *Notch* or *Dl* produces wide veins, it follows that *Dl* activates *Notch* to inhibit vein differentiation. Therefore, the restriction of vein width may be analogous to neurogenic lateral inhibition, with *Notch* activation restricting vein fate within a pro-vein region (Fig. 5C).

In contrast to *Notch(lf)* mutations, *Abruptex (Ax)* alleles of *Notch*, which have been characterized as exhibiting excessive neurogenic signalling (de Celis et al., 1993; de Celis et al., 1991; Heitzler and Simpson, 1993; Palka et al., 1990), lead to distal vein loss (Foster, 1975). Consistent with *Ax* mutations representing gain-of-function *Notch* alleles, a duplication of the *Dl* locus greatly enhances *Ax* vein loss, while *Ax* mutations suppress the *Dl* thick vein phenotype (de Celis and Garcia-Bellido, 1994a). The *Ax* phenotype thus confirms that *Notch* activation can inhibit vein differentiation.

However, the role of Notch signalling during vein differentiation is not consistent with a stochastic lateral inhibition model. Rather, the position of veins is prefigured by mid-third instar by the expression of *rhomboid** (*rho*) in stripes of cells oriented parallel to the A/P compartment boundary in the wing pouch (Sturtevant et al., 1993). RHO facilitates signalling through the Epidermal Growth Factor Receptor (EGFR) and EGFR activation is required for the vein fate (Diaz-Benjumea and Garcia-Bellido, 1990). Diaz-Benjumea and Garcia-Bellido found that in the absence of EGFR activity, all vein differentiation was absent. The phenotype of double mutants indicate that loss of EGFR activity completely masks (is epistatic to) the wide vein phenotype of *Notch* mutants, indicating that EGFR activation induces pro-vein regions, then *Notch* functions to restrict vein fate within these regions.

Localized activation of EGFR along the presumptive veins is not completely understood, and the exact mechanism may be different for each vein (reviewed in de Celis 1998). Common to all veins is the induction of *rho* expression in response to A/P positional information (DPP and Hedgehog). The role of Notch in this process is to refine the domain of *rho* expression by repressing it in the lateral pro-vein cells, on either side of presumptive vein (de Celis et al., 1997). Possibly, the position of the presumptive vein is biased by initial variations in the level of EGFR activation, then Notch signalling refines and maintains this early pattern.

* Also named *veinlet (ve)*.

As in neurogenic lateral inhibition, a feedback loop maintains the polarity of DL-Notch signalling and the restriction of vein fate (Fig. 5C; de Celis et al. 1997; de Celis 1998). As previously discussed, DL-dependent Notch activation restricts the vein fate by repressing EGFR activity in the lateral provein cells. The expression of *Dl* along the veins depends on EGFR activation, since abolishing EGFR activity also abolishes *Dl* expression along the veins. Likewise, maintenance of *rhomboid* expression in the presumptive vein requires EGFR function (de Celis, 1998). Therefore, Notch-mediated restriction of EGFR activity restricts *Dl* expression and EGFR activation to the future vein. In addition, Notch activation increases *Notch* expression in the lateral provein cells of pupal wing discs (de Celis, 1998; de Celis et al., 1997), leading to polarized signalling, and a stable separation of veins from interveins during pupal development.

1.7 Summary of objectives

Using imaginal disc regeneration as a model for the study of normal development, an enhancer-trap screen was undertaken in the lab of M. Russell to identify genes involved in pattern formation (Brook, *et al.* 1993). This screen resulted in the isolation of an enhancer trap line—*P{PZ}G45*—used here in the identification of *hephaestus*. *P{PZ}G45* is a non-lethal P-element transgene insertion that reports gene expression asymmetrically located to one side of the wound heal of regenerating wing or leg disc fragments. This was considered to be consistent with the hypothesis that *P{PZ}G45* reports expression of a gene involved in intercellular communication during *de novo* pattern formation at the wound heal.

Since *P{PZ}G45* is a viable insertion, recessive lethal derivatives of the line were obtained to disrupt vital genes close to the insertion site (100E; Brook 1994). *Df(3R)G45* is a lethal excision derivative of *P{PZ}G45* that fails to complement *Df(3R)faf-BP*, a deletion of the entire 100E-F region (Fischer-Vize et al., 1992). To study the normal function of any gene(s) disrupted by *Df(3R)G45*, Ariel Finkielsztein (1997) has analyzed *Df(3R)G45* in genetic mosaics. Consistent with the disruption of at least one gene with a role in pattern formation, patches of ectopic wing margin were observed in *Df(3R)G45* genetic mosaic wings within a narrow zone on either side of the normal wing margin. The ectopic margin bristles included both marked *Df(3R)G45* and unmarked wildtype cells, suggesting a non-autonomous effect on neighboring cells. Although many patches of ectopic margin were not associated with marked *Df(3R)G45* tissue, marked bristles were significantly more frequent among the ectopic margin bristles than among bristles at the normal margin of the same wings. Finkielsztein proposed that *Df(3R)G45* clones in a competent zone close to the normal wing margin are transformed to wing margin, and also non-autonomously induce neighboring cells to differentiate margin bristles. He also suggested that *Df(3R)G45* cells must divide slowly or die to explain the absence of marked tissue in some ectopic patches. To account for the non-autonomous effect, Finkielsztein hypothesized that *Df(3R)G45* clones ectopically mis-express the *wg* signal,

and that close to the normal margin *wg* protein levels can exceed a hypothetical threshold required for wing margin induction.

Because of its genetic mosaic phenotype, we originally named the hypothetical gene affected by *Df(3R)G45 ectopic margin (ema)*. This thesis describes the genetic and molecular evidence that *ema* is synonymous with the previously identified male sterile locus *hephaestus (heph)*, and the characterization of its newly discovered role in wing patterning. The original hypothesis was that *ema* normally acts to restrict wing margin fate to those cells that normally differentiate margin, possibly by restricting *wingless* expression to the D/V boundary.

The general goal of this project was to characterize the role of *ema* in wing patterning. Firstly, new alleles of *ema* were isolated. Results of complementation tests between *ema* alleles and alleles of previously characterized genes will indicate that *ema* is synonymous with *hephaestus (heph)*. Each of the new *ema* alleles and the sole *heph* allele map to a transcription unit predicted to encode an RNA binding protein homologous to vertebrate polypyrimidine tract binding protein (PTB). Because the name *hephaestus* was coined first, it will be adopted once the relevant data has been presented. Secondly, to characterize the role of *ema* in wing disc patterning, the phenotypic consequences of loss of *ema* in genetic mosaics were analyzed, and were compared to those of known pattern mutants. In addition, expression patterns of genes known to be involved in specifying positional information in the wing disc were studied in *ema* genetic mosaic wing discs. The results of this analysis support a model in which *ema* is required to repress the activity of *Notch*, a regulator of *wg* expression at the wing margin and a central component of intercellular communication during alternative cell fate decisions.

2 MATERIALS AND METHODS

2.1 *Drosophila* culture

Drosophila melanogaster were cultured on a cornmeal-molasses medium (7.2% cornmeal, 9.6% v/v molasses, 0.8% Bacto-agar, 0.288% *p*-hydroxy-benzoic acid methyl ester, and 0.288% propionic acid) or standard Caltech fly culture medium (10% cornmeal, 5% sucrose, 1.5% Torumel yeast, 1% Bacto-agar, and 2% propionic acid, Ashburner, 1989). Fly stocks were maintained at 18°C or at RT (20-22°C) and all crosses were kept at 25°C unless otherwise indicated.

2.2 Conventional *Drosophila* nomenclature

Generally, *Drosophila* gene names follow the nomenclature outlined in "The Genome of *Drosophila melanogaster*" (Lindsley and Zimm, 1992) with some recent modifications described on Flybase (<http://flybase.bio.indiana.edu>). The name of a gene is usually based on some aspect of its mutant phenotype, or its wildtype function (e.g. *wingless* (*wg*) mutant flies have no wings). The symbol for a gene is a unique combination of letters based on the gene's name and the name and symbol are always italicized. When a specific allele is referred to, it is designated by a superscript after the gene symbol (e.g. *wg*¹). When the first characterized mutant allele of a gene was dominant, the gene name and symbol are capitalized. When the first characterized mutant allele was recessive, the gene name and symbol are not capitalized. When a full gene name or symbol is used to indicate a mutant phenotype, rather than a genotype, then the name or symbol is not italicized. When a gene was first identified by protein sequence similarity, the gene is named after the protein and the gene's symbol is in italicized capitals regardless of whether mutant alleles of that gene are dominant or recessive (e.g. the symbol for *polypyrimidine tract binding protein* is *PTB*). When referring to protein products, the gene's symbol is used in roman capitals and is not italicized. Predicted genes have been assigned four-digit serial numbers after the *Computational Gene* (*CG*) designation (e.g. *CG2094*). To uncharacterized lethal alleles, the general term "lethal" (symbol: *l(n)m*, where *n* is the chromosome number and *m* is a serial number) is applied, until analysis of the gene allows a more informative name to be applied. Finally, symbols of genes on homologous chromosomes are separated by a slash (/), while symbols for genes on non-homologous chromosomes are separated by a semicolon (;).

Transgene nomenclature is in the form ends{genes=construct-symbol} where ends stands for the symbol of a given transposon, such as P for P-element, and H for *hobo*-element, and genes stands for included genes, such as different w^+ or ry^+ rescuing transgenes. Full genotypes of the different transgenes used in this study are defined in Table 1. A complete description of the origin and molecular nature of the different transgenes can be found at Flybase (<http://www.flybase.bio.indiana.edu/>). In the text and figures, this nomenclature has been shortened to ends{construct-symbol}. For example, $P\{w^{+11.7}ry^{+17.2}=wA\}$ will rescue both *rosy* and *white* eye color mutants as it carries both w^+ and ry^+ transgenes. It is referred to in the text and figures as $P\{wA\}$ and the important visible markers and expected phenotypes are presented as required in the accompanying text. Whenever appropriate, a serial insertion identifier or when known a chromosomal location identifier or allele identifier is included to denote a specific chromosomal insertion. For example, *G45* is a serial identifier for the $P\{PZ\}$ insertion $P\{PZ\}G45$.

2.3 Genes and alleles

Drosophila strains, genes and alleles are listed with their sources in Table 2. They are organized into groups based on allele type or on their main experimental use. A full description of markers and balancer chromosomes can be found in "The genome of *Drosophila melanogaster*" (Lindsley and Zimm, 1992) and at Flybase (<http://flybase.bio.indiana.edu/>; FlyBase 1999).

FlyBase is a database of genetic and molecular data for *Drosophila* available on the World Wide Web. It includes information on more than 13,000 genes, their published alleles and their functions, descriptions of available stocks as well as information on protein and RNA expression patterns. *Drosophila* genetic, cytological, and molecular map information is linked to cDNA (Rubin et al., 2000) and genomic sequence information from the Berkeley *Drosophila* Genome Project (BDGP; <http://www.fruitfly.org/index.html>; Adams et al. 2000), Celera Genomics, Inc. (Myers et al., 2000), and the European *Drosophila* Genome Project (<http://edgp.ebi.ac.uk/>; EDGP, unpublished).

P-insertion lines were made available through the work of several large scale mutagenesis projects undertaken with the goal of identifying and mutating every gene in *Drosophila* (reviewed in Spradling et al. 1999). Many of the P-elements and other strains used in this study were ordered from the Bloomington *Drosophila* Stock Center at Indiana University, or from the European Stock Center at the University of Umeå in Sweden (<http://flystocks.bio.indiana.edu>). Several P-element insertion lines were obtained from the Szeged P-insertion *Drosophila* Stock Center at the University of Szeged in Hungary (<http://gen.bio.u-szeged.hu/stock/>). The site of insertion in most of these P-element insertion lines has been mapped by *in situ* hybridization (Spradling et al. 1999).

Table 1. Abbreviations and genetic designations of P-elements

Abbreviation	Genotype
$H\{P\Delta 2-3\}$	$Hobo\{w^{+mC} P\backslash T^{hs.PR\Delta 2-3}=P\Delta 2-3\}$
$P\{\Delta 2-3\}$	$P\{P\backslash T^{\Delta 2-3} ry^{+17.2}=\Delta 2-3\}$
$P\{Act-GFP\}$	$P\{w^{+mC} GFP^{Act5C.PR}=Act-GFP\}$
$P\{f^+\}$	$P\{w^{+mC} f^{+113}=f^+ 13\}$
$P\{GawB\}$	$P\{GAL4^{vB} w^{+mW.hs} amp^R ori=GawB\}$
$P\{hsFLP\}$	$P\{FLP1^{hs.PG} ry^{+17.2}=hsFLP\}$
$P\{hsGFP\}$	$P\{w^{+mC} P\backslash T^{hs.T}:GFP=hsGFP\}$
$P\{lacW\}$	$P\{lacZ^{p\backslash T.W} w^{+mC} amp^R ori=lacW\}$
$P\{neoFRT\}$	$P\{ry^{+17.2} neo^{Hsp70Bb.PS} <FRT <FRT ori amp^R neo^{Hsp70Bb.PS}=neoFRT\}$
$P\{\pi M\}$	$P\{w^{+mC} P\backslash T^{hs.T}:Myc=\pi M\}$
$P\{PZ\}$	$P\{lacZ^{p\backslash T.PZ} kan^R ori ry^{+17.2}=PZ\}$
$P\{tubP-GAL80\}$	$P\{w^{+mC} Scer\backslash GAL80^{aTub84B.PL}=tubP-GAL80\}$
$P\{Ubi-GFP\}$	$P\{w^{+mC} Avic\backslash GFP^{S65T.Ubi-p63E.T:SV40\backslash nls2}=Ubi-GFP(S65T).nls\}$
$P\{wA\}$	$P\{w^{+11.7} ry^{+17.2}=wA\}$
$P\{y^+\}$	$P\{y^{+17.7} ry^{+17.2}=Car20y\}$

Table 2. *Drosophila* strains used in this study

Balancers and wildtype:

Genotype	Source
<i>Oregon-R</i> (wildtype)	Bloomington Stock Center, Indiana, US
<i>w</i> ; <i>Ly</i> / <i>TM3</i> , <i>Sb e</i>	Bloomington Stock Center, Indiana, US
<i>y w</i> ; <i>Ly</i> / <i>TM6B</i> , <i>Tb Hu e</i>	Bloomington Stock Center, Indiana, US
<i>y w</i> ; <i>TM3</i> , <i>Sb e</i> / <i>TM6B</i> , <i>Hu e</i>	Bloomington Stock Center, Indiana, US
<i>Ly</i> / <i>TM3</i> , <i>ry Sb e</i>	Bloomington Stock Center, Indiana, US
<i>Sb</i> / <i>TM3</i> , <i>P{Act-GFP}JMR1</i> , <i>Ser e</i>	Bloomington Stock Center, Indiana, US

Deficiencies:

Genotype	Cytology	Source
<i>Df(3R)A4-4L8</i>	<i>Df(3R)100F4-5</i>	J. Pradel, Centre Universitaire Marseille-Luminy, FR
<i>ry Df(3R)G45</i>	<i>Df(3R)100E-F</i>	M. Russell, University of Alberta, CA
<i>st Df(3R)faf-BP</i>	<i>Df(3R)100D1-3;100E-F</i>	J. Fischer, University of Texas, US
<i>Df(3R)04661</i>	<i>Df(3R)100D2;100F5</i>	G. Rubin, University of California, Berkeley, US
<i>Df(3R)awd-KRB</i>	<i>Df(3R)100D1;100D3-4</i>	Bloomington Stock Center, Indiana, US

Mutations mapping to 100E-F:

Allele name	<i>in situ</i>	Source
<i>P{wA}4-4</i>	100F5	J. Pradel, Centre Universitaire Marseille-Luminy, FR
<i>P{lacW}l(3)06497</i>	100F5	Bloomington Stock Center, Indiana, US
<i>P{lacW}l(3)06886</i>	100F4-5	Bloomington Stock Center, Indiana, US
<i>P{lacW}l(3)03847</i>	100F4-5	Bloomington Stock Center, Indiana, US
<i>P{LacW}l(3)rH304</i>	100F4-5	Bloomington Stock Center, Indiana, US
<i>P{lacW}l(3)j11B9</i>	100F1-5; 74D	A. Beaton, University of California, Berkeley, US
<i>P{PZ}l(3)03429</i>	100F1-2	Bloomington Stock Center, Indiana, US
<i>P{lacW}L1022</i>	100F1-2	Bloomington Stock Center, Indiana, US
<i>P{lacW}l(3)L7321</i>	100F1-2	Bloomington Stock Center, Indiana, US
<i>P{lacW}l(3)s095214</i>	100F	Szeged Mutant Stock Center, HU
<i>P{PZ}ms(3)07570</i>	100E-F	Bloomington Stock Center, Indiana, US
<i>l(3)nuhl²</i>	100E-F	S. Campbell, University of Alberta, CA
<i>P{PZ}ms(3)heph²</i>	100E1-3	Bloomington Stock Center, Indiana, US
<i>faf^{1:08}</i>	100E1-2	J. Fischer, University of Texas, US
<i>P{lacW}l(3)s1921</i>	100E1-2	Bloomington Stock Center, Indiana, US
<i>P{lacW}l(3)awd^{Δ8700}</i>	100E1-2	Bloomington Stock Center, Indiana, US
<i>P{LacW}j2A4</i>	100E1-2	Bloomington Stock Center, Indiana, US
<i>P{PZ}G45</i>	100E	M. Russell, University of Alberta, CA
<i>P{lacW}l(3)s008224</i>	100D-F	Szeged Mutant Stock Center, HU
<i>P{lacW}l(3)s118416</i>	100D-F	Szeged Mutant Stock Center, HU
<i>P{lacW}l(3)s128104</i>	100D-F	Szeged Mutant Stock Center, HU
<i>P{lacW}l(3)s041303</i>	100D-F	Szeged Mutant Stock Center, HU
<i>P{lacW}l(3)s125015</i>	100D3-4	Szeged Mutant Stock Center, HU
<i>Med^Δ</i>	100D1	Umeå <i>Drosophila</i> Stock Center, SE

Mutagenesis:

Genotype	Source
<i>C(1)RM, y w f / O ; C(1:Y)6, w / O</i> <i>e¹</i>	J. Locke, University of Alberta, CA Bloomington Stock Center, Indiana, US
<i>In(1)w^{m4} ; Sb e P{Δ2-3}99B / TM6, Ubx e</i> <i>w ; P{neoFRT}82B</i> <i>y w ; CyO, H{PΔ 2-3}Hop2.1 / Bc Egfr^{E1}</i>	J. Locke, University of Alberta, CA Bloomington Stock Center, Indiana, US W. Brook, University of Calgary, CA

Clonal analysis:

Genotype	Source
<i>f^{36a} ; mwh vin bld¹ P{f⁺}98B / TM3, Ser e</i>	S. Tiong, Harvard University, US
<i>f^{36a} ; mwh P{f⁺}87D M(3)RpS³² / TM1, mwh</i> <i>P{neoFRT}82B P{y⁺}96E</i>	S. Tiong, Harvard University, US A. Finkielsztejn, University of Alberta, CA
<i>P{neoFRT}82B P{tubP-Gal80}LL3</i> <i>y w ; P{neoFRT}82B P{πM}87E Sb^{63b} P{y⁺}96E /</i> <i>TM6B, Tb Hu e</i>	Bloomington Stock Center, Indiana, US Bloomington Stock Center, Indiana, US
<i>y w P{hsFLP }1 ; Dr^{Mio} / TM3, ry Sb e</i> <i>y w P{hsFLP }1 ; Sp / CyO ; P{neoFRT}82B P{hsGFP} /</i> <i>TM6B, Hu e</i>	Bloomington Stock Center, Indiana, US S. Blair, University of Wisconsin, US
<i>P{neoFRT}82B P{Ubi-GFP.nls}3R</i> <i>pr pwn¹ P{hsFLP}38 / CyO ; Ki kar ry</i> <i>pr pwn¹ ; P{neoFRT}82B kar ry Ubx^{bx-3^e},</i> <i>Dp(2;3)P32=pwn⁺ / P{neoFRT}82B kar ry</i>	Bloomington Stock Center, Indiana, US P. Heitzler, IGBMC, FR P. Heitzler, IGBMC, FR

Transgenes, GAL4 and UAS lines:

Genotype	Source
<i>w ; P{GawB}ap^{md544}=ap-GAL4 / CyO</i>	Bloomington Stock Center, Indiana, US
<i>P{Gal4}bi^{omb-Gal4}=omb-Gal4, y w / FM7a</i>	Bloomington Stock Center, Indiana, US
<i>w ; P{GawB}C96=C96-GAL4</i>	Bloomington Stock Center, Indiana, US
<i>w ; P{w⁺, UAS-PTB.S}3-6=UAS-PTB</i>	C. Schulz, Stanford University, US
<i>w ; P{w⁺, mod⁺ krz⁺}; Df(3R)A4-4L8</i>	A. Pereira, University of Massachusetts, US
<i>C(1)A, y / + ; cosP479BE[Notch⁺]86E5 / TM6B</i>	G. Doughty, Harvard University, US

DNA clones:

Name	Insert	Source
cosmid 73E10	100EF genomic DNA	Sidén-Kiamos, Genome Mapping Institute, GR
cosmid 129G12	100EF genomic DNA	Sidén-Kiamos, Genome Mapping Institute, GR
cosmid 12C5	100EF genomic DNA	Sidén-Kiamos, Genome Mapping Institute, GR
P1 DS00831	100F genomic DNA	P. Lasko, McGill University, CA
P1 DS02174	100F genomic DNA	P. Lasko, McGill University, CA
P1 DS04961	100F genomic DNA	P. Lasko, McGill University, CA
pOT2a-GH17441	adult head <i>PTB</i> cDNA	Research Genetics, Inc. Huntsville, US
pBS-LD04329	0-22hr embryo <i>PTB</i> cDNA	Research Genetics, Inc., Huntsville, US
pBS-CST01	adult testis <i>PTB</i> cDNA	C. Schulz, Stanford University, US

Genetic interactions:

Allele	Source
Bx^1	Bloomington Stock Center, Indiana, US
cl^6	Bloomington Stock Center, Indiana, US
Dl^3	Bloomington Stock Center, Indiana, US
dx^{sm}	S. Artavanis-Tsakonas, Yale University, US
$Dl^{rev1/10}$	K. Irvine, Rutgers, NJ State U, US
$Egfr^{E1}$	Bloomington Stock Center, Indiana, US
fng^2	K. Irvine, Rutgers, NJ State U, US
fng^{52}	K. Irvine, Rutgers, NJ State U, US
fng^{D4}	K. Irvine, Rutgers, NJ State U, US
H^1	Bloomington Stock Center, Indiana, US
N^{Ax-1}	Glenn Doughty, Harvard University, US
N^{Ax-9B2}	J. de Celis, Universidad Autónoma de Madrid, ES
N^{Co}	Bloomington Stock Center, Indiana, US
N^{nd-1}	Bloomington Stock Center, Indiana, US
N^{spl-1}	Bloomington Stock Center, Indiana, US
Ser^{Bd-3}	Bloomington Stock Center, Indiana, US
Ser^D	E. Knust, Heinrich-Heine-Universität Düsseldorf, DE
$Ser^{rev2-11}$	J. de Celis, Universidad Autónoma de Madrid, ES
Ser^{RX106}	K. Irvine, Rutgers, NJ State U, US
sno^{E1}	U. Baneryee, UCLA, US
$Su(H)^2$	G. Doughty, Harvard University, USA
$Su(H)^8$	Umeå <i>Drosophila</i> Stock Center, SE
$P\{sev-N^{act}\}$	S. Artavanis-Tsakonas, Yale University, US

2.4 Induction of mitotic recombination

Twenty or more females were mated to five males in a vial, then passaged to fresh food every 24hr at RT (unless indicated otherwise). Mitotic recombination was induced using the FLP/FRT system or γ -rays during early second larval instar (60-72hr after egg lay–AEL–at RT) unless otherwise stated.

The heat inducible FLP/FRT recombination system was used to obtain a high frequency of mitotic recombination (Golic and Lindquist 1989; Golic 1991; Xu and Rubin 1993). The *Saccharomyces cerevisiae* *Flip-recombinase* gene, under the control of an *Hsp70* promoter, produces a site-specific recombinase in response to 1hr, 37°C heat treatments. In this case, the *Flip-recombinase* protein catalyzes recombination between two *P{neoFRT}* transgenes that are inserted near the centromere on the right arm of chromosome 3 [82B]. Markers and mutations distal to recombination at these *P{neoFRT}* transgenes are subject to aberrant segregation during the subsequent mitosis.

To induce mitotic recombination with γ -rays, second instar larvae from the appropriate cross were irradiated with a 1000-rad dose of γ -rays from a GammaCell 220 ^{60}Co source (University of Alberta) or a GammaCell 1000 ^{237}Cs source (University of Calgary).

2.5 Summary of chromosomes and clone markers

A representation of chromosome 3 illustrating the relative positions of alleles and P-elements used for genetic mosaic analysis and for building new chromosomes is presented in Figure 6. Following is a short description of the different markers used:

P{neoFRT}: Flies carrying a *P{neoFRT}* transgene were selected by their resistance to Geneticin (G418; Gibco-BRL, Inc.) following the protocol described by Xu and Rubin (1993). G418 (25mg/mL in distilled water) was added to standard fly medium by poking 6-8 holes in the food with a P200 pipet tip, then adding 200 μL of the G418 solution per vial. The G418 solution was allowed to soak in overnight before flies were added.

bald (bld) homozygous cells secrete trichomes, hairs and bristles that are almost clear when compared to wildtype. *bld* is an excellent clone marker with only one disadvantage: it maps very close to the centromere of 3R, decreasing the frequency of useful recombinants.

Figure 6. Summary of chromosomes constructed for this study.

The relative position of the centromere (CEN) to the transgenes and mutations used as clone and chromosome markers are shown with their respective meiotic map positions (or estimated positions) and their cytological map positions. Below the box are new recombinants isolated for this study. e^* designates an unknown allele of *ebony*.

P{w^{+mC}}: *white* eye color mutants on the X-chromosome can be partially rescued by expressing the *white* gene product from a P-element carrying the mini-white (*w^{+mC}*) transgene (Table 1). The rescued eye color ranges from light yellow to light orange, depending on chromosomal position effect. A fly with one *P{w^{+mC}}* transgene can easily be distinguished from a fly with two transgenes by comparing eye color. This color difference holds true in eye clones when cells with zero, one or two copies of the *P{w^{+mC}}* transgene can be distinguished.

Stubble: *Sb^{63b}* is a homozygous cell viable and dominant *Sb* allele that reduces the length of all bristles including those on the thorax and wing. Wildtype bristles can be distinguished from *Sb^{63b} / +* which can be distinguished from homozygous *Sb^{63b} / Sb^{63b}*. *Sb^{63b}* does not mark the trichomes of the wing blade.

Delta (Dl): Chromosomes bearing a *Dl* allele were selected based on wide, meandering posterior crossveins and deltas at the tips of the veins.

P{y⁺}: The *yellow* locus maps to the X-chromosome and can be dominantly rescued by a *P{y⁺}* transgene on 3R. Mutant *yellow* bristles are a lighter color than wildtype or *P{y⁺}*-rescued bristles. *y* marks the macrochaetae of the thorax and the wing margin but is very difficult to unambiguously score in the posterior row bristles, and is impossible to score in trichomes.

Serrate (Ser): Because loss-of-function *Ser* alleles do not have dominant visible adult phenotypes, *Ser^{RX106}* was selected by screening for chromosomes that fail to complement the lethality of *Ser^{rev2-11}*.

Minute (M) is a class of cell-lethal mutations that dominantly cause slow cell proliferation, commonly affecting a cell's capacity to translate proteins. In this analysis of genetic mosaics, *M(3)Rps³²* was used to give *M⁺ Df(3R)G45* clones a growth advantage relative to surrounding *M / +* cells. *M* can be selected based on its dominant thin thoracic macrochaetae phenotype.

forked: *f^{36a}* is an X-linked mutation causing short, barbed chaetae and hooked trichomes. All macrochaetae, microchaete and trichomes on the fly are affected. This mutation can be partially rescued by a *P{f⁺}* transgene, enabling its use as an autosomal clone marker. In a *f* mutant background, *P{f⁺}* was selected based on its partial rescue of the *f* barbed thoracic macrochaetae phenotype.

hephaestus (heph): Recombinant chromosomes carrying alleles of *heph*, except *Df(3R)G45*, were selected by failure to complement *Df(3R)G45*. *Df(3R)G45* was selected by failure to complement *Df(3R)faf-BP*. This ensured no second-site lethal mutation on any one chromosome was being selected.

pawn (*pwn*) is cell viable in homozygous clones, which have truncated bristles with pale tips, pin-shaped trichomes with basal spurs, and thin, transparent hairs. Because *pwn* maps to the second chromosome, clones of alleles on 3R were marked using a *pwn*⁺ rescuing duplication (*Dp(2;3)P32*) on 3R that has been adapted for use with the FLP/FRT system (Heitzler et al., 1996b). To mark clones with *pwn*, males with an allele of interest (indicated by **) on a *P{neoFRT}82B* chromosome were crossed to *pr pwn P{hsFLP}38 / CyO ; Ki kar ry* virgin females. Straight winged F1 males with Kinked bristles of genotype *pr pwn P{hsFLP}38 / + ; P{neoFRT}82B ** / Ki kar ry* were crossed to *pr pwn ; P{neoFRT}82B kar ry bx^{34e} Dp(2;3)P32 / P{neoFRT}82B kar ry* virgin females. The F2 non-Kinked flies with purple eyes were scored for mitotic clones marked with *pwn*.

2.6 Induction of *Df(3R)G45* clones in a *mod*⁺ *krz*⁺ genetic background

A *modulo* (*mod*) and *kurtz-arrestin* (*krz*) genomic rescuing transgene (Garzino et al. 1992, Roman et al. 2000) on the second chromosome was combined with *P{hsFLP}* and *P{neoFRT}82B* chromosomes to make clones of *Df(3R)G45* in a *mod*⁺ *krz*⁺ background (Fig. 7). Since F1 males were capable of passing on either the *mod*⁺ *krz*⁺ transgene or the *CyO* balancer, the phenotype of *Df(3R)G45* clones in control Curly winged flies was compared to that in straight winged flies that carried the *mod*⁺ *krz*⁺ rescuing transgene. Only female flies were scored to ensure the presence of a *P{hsFLP}* transgene.

2.7 Induction of *hephaestus* clones in a *Su(H)* mutant background

Generation of *heph* genetic mosaic wing discs that lack *Su(H)* was a multi-step process. First, *Su(H)*⁸ and *P{neoFRT}82B P{hsGFP}* were balanced in a stock homozygous for a *P{hsFLP}* source on the X-chromosome (Stock I, Fig. 8). The presence of the *Su(H)*⁸-bearing chromosome was indirectly scored through the absence of *Sp* in the F2. *P{neoFRT}82B P{hsGFP}* was selected using the *P{w⁺}* transgene carried by *P{hsGFP}*.

Second, F1 males carrying *P{neoFRT} P{πM} Sb heph⁰³⁴²⁹* and *Su(H)*² balanced by *CyO* were crossed to Stock I virgin females (Fig. 9). Approximately 1/3 of the progeny from this cross should inherit both *Su(H)* alleles. These larvae were selected by scoring for under-developed wing disc pouches characteristic of the *Su(H)*⁸ / *Su(H)*² allele combination. *P{neoFRT}82B P{hsGFP}* was selected indirectly by selecting against the *Tubby* marker carried on *TM6B* in stock I. Of the non-*Tb* F2 larvae with under-developed wing disc pouches, two possible genotypes were present since *P{neoFRT}82B P{πM} Sb heph⁰³⁴²⁹* cannot be selected in larvae or discs. A high frequency of *GFP*⁻ clones confirmed the presence of both *P{neoFRT}82B*-bearing chromosomes.

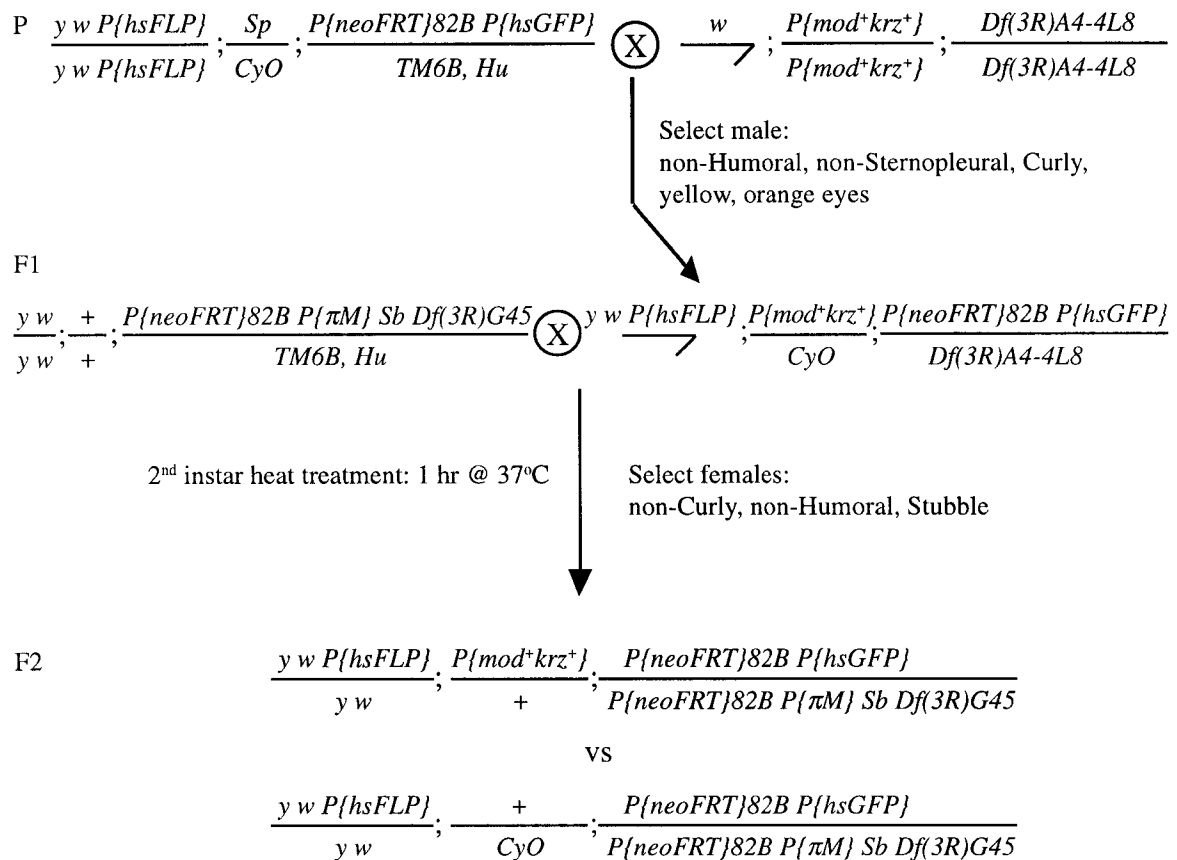


Figure 7. Crossing scheme used to generate *Df(3R)G45* clones in a *mod⁺ krz⁺* background.

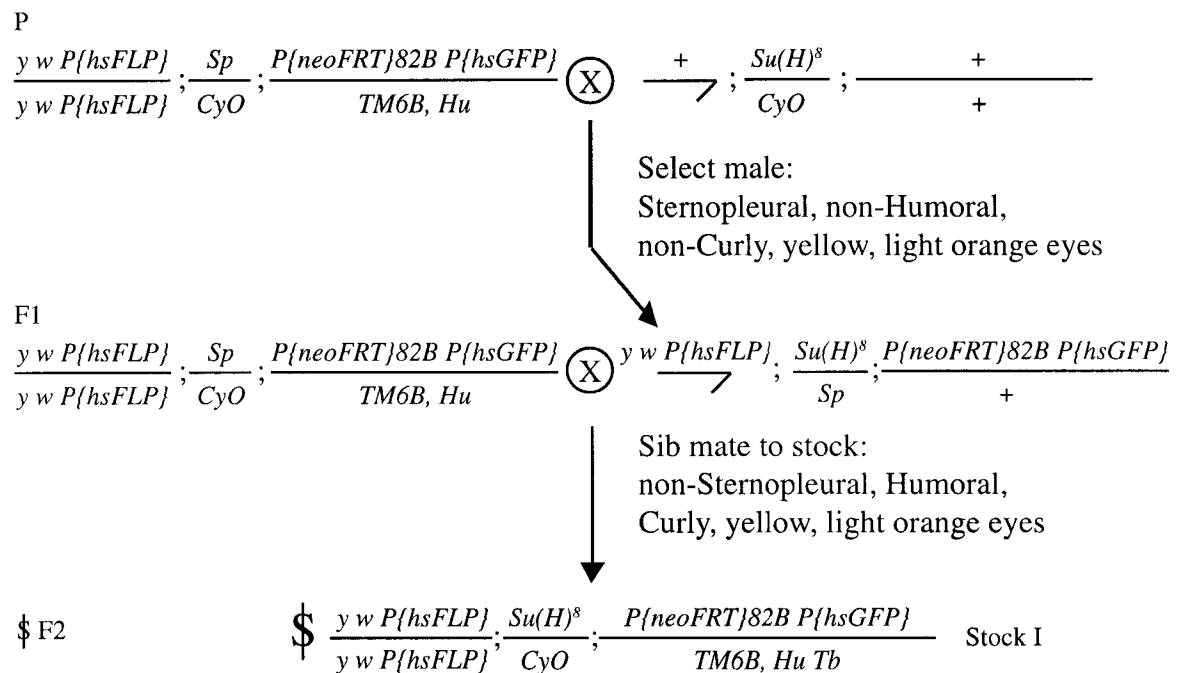


Figure 8. Crossing scheme used to generate Stock I (*heph* clones in *Su(H)* background).

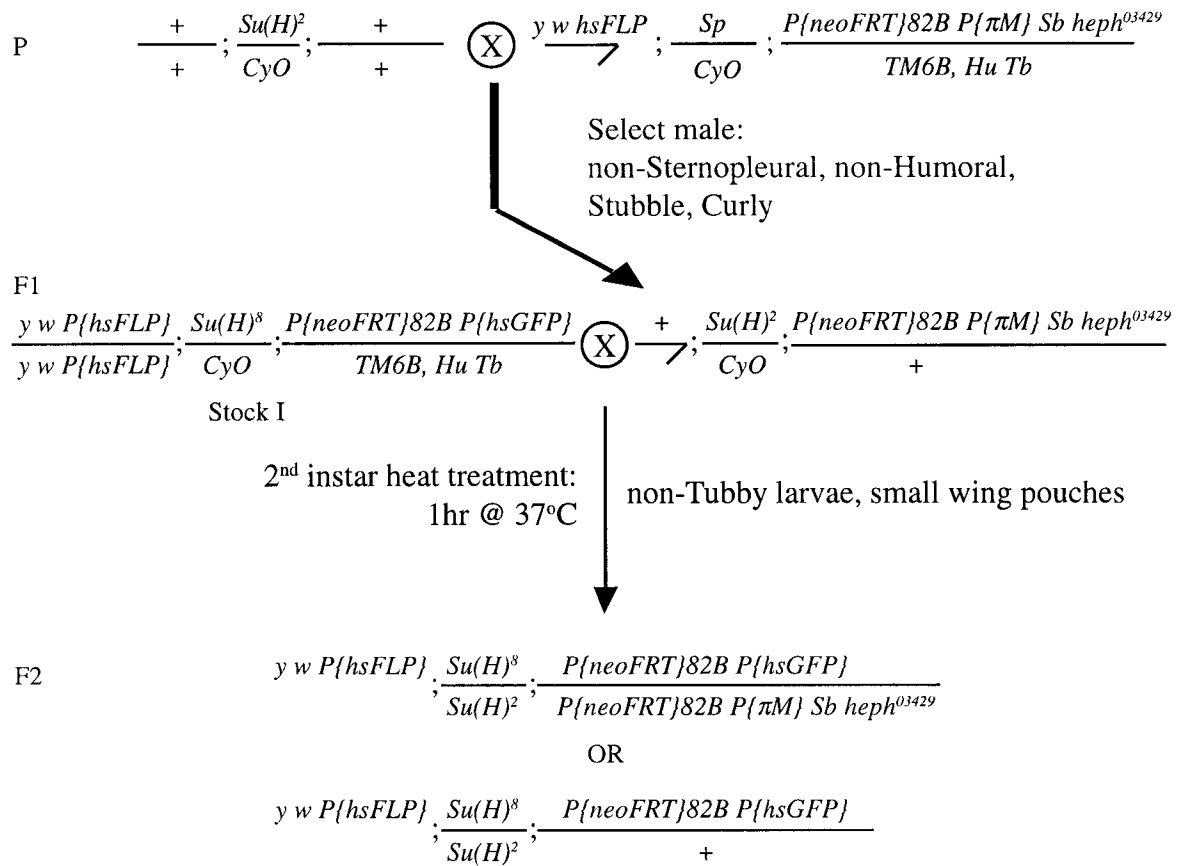


Figure 9. Crossing scheme to generate *hephaestus* clones in a *Su(H)* mutant background.

2.8 *hephaestus* genetic interaction screen

To study the possible role of *heph* in the wing margin pathway, I tested the ability of *Df(3R)G45* or *heph*⁰³⁴²⁹ to modify visible dominant adult phenotypes of mutations in characterized wing patterning genes. Possible genetic interactions were screened by comparing the phenotype of the visible allele crossed to *Oregon-R* and to *Df(3R)G45* or *heph*⁰³⁴²⁹. Recessive visible alleles on the X-chromosome (e.g. *ct*⁶) were scored in hemizygous males.

To test for a genetic interaction between *fng* hypomorphs and *heph*, a *fng*² *heph*⁰³⁴²⁹ recombinant was made. Because *fng*² could not be directly selected, it was combined with *heph*⁰³⁴²⁹ by selecting a recombinant between the dominant *fng*^{D4} allele and *P{neoFRT} heph*⁰³⁴²⁹, then selecting for maintenance of *P{neoFRT}* and loss of *fng*^{D4} in *trans*-heterozygotes with *fng*². The presence of *heph*⁰³⁴²⁹ was tested with a complementation test to *Df(3R)G45*. This recombinant was then crossed to *fng*⁵², and non-balancer progeny were compared to non-balancer progeny from a control cross between the original *fng*² and *fng*⁵² chromosomes.

2.9.1 Screen for EMS-induced alleles that fail to complement *Df(3R)G45*

The alkylating agent ethyl methanesulfonate (EMS, Sigma-Aldrich, Inc.) was used as a mutagen through feeding to adult males according to Lewis and Bacher (Lewis and Bacher, 1968). 30-50 young adult males (0-12hr after eclosion) were starved for 12hr in a bottle with wet Kleenex taped to the bottom. This preconditioning entices the flies to ingest the EMS-sucrose solution. The males were then fed EMS (1mL of 0.025M EMS in 5% sucrose) on Whatman paper for 12-16hr in a disposable culture vial. Males were allowed to recover for 12hr in a vial of standard fly medium before mating to an equal number of females. EMS waste and glassware were decontaminated by rinsing with an excess of 10% w/v anhydrous sodium thiosulfate in water.

The method used to screen for EMS-induced alleles that fail to complement *Df(3R)G45* is represented in Fig. 10. Mutagenized males were crossed *en masse* to *w ; Ly / TM3, Sb* females in order to isolate single mutagenized chromosomes in F1 males. Mutagenized *P{neoFRT}82B* chromosomes were isolated over a chromosome carrying the dominant marker *Lyra* so the segregation of the mutagenized chromosome could be followed in the next generation. To screen for lethal mutations that fail to complement *Df(3R)G45*, each of 9622 F1 *Lyra* males were crossed to 3-5 *Df(3R)G45 / TM3, ry Sb* virgin females in individual vials for a complementation test. F2 progeny were scored for absence of the non-Stubble, non-*Lyra* class which should have the genotype *P{neoFRT}82B ** / Df(3R)G45*, when ** represents a possible EMS-induced lethal mutation. Absence of this class was interpreted as failure to complement.

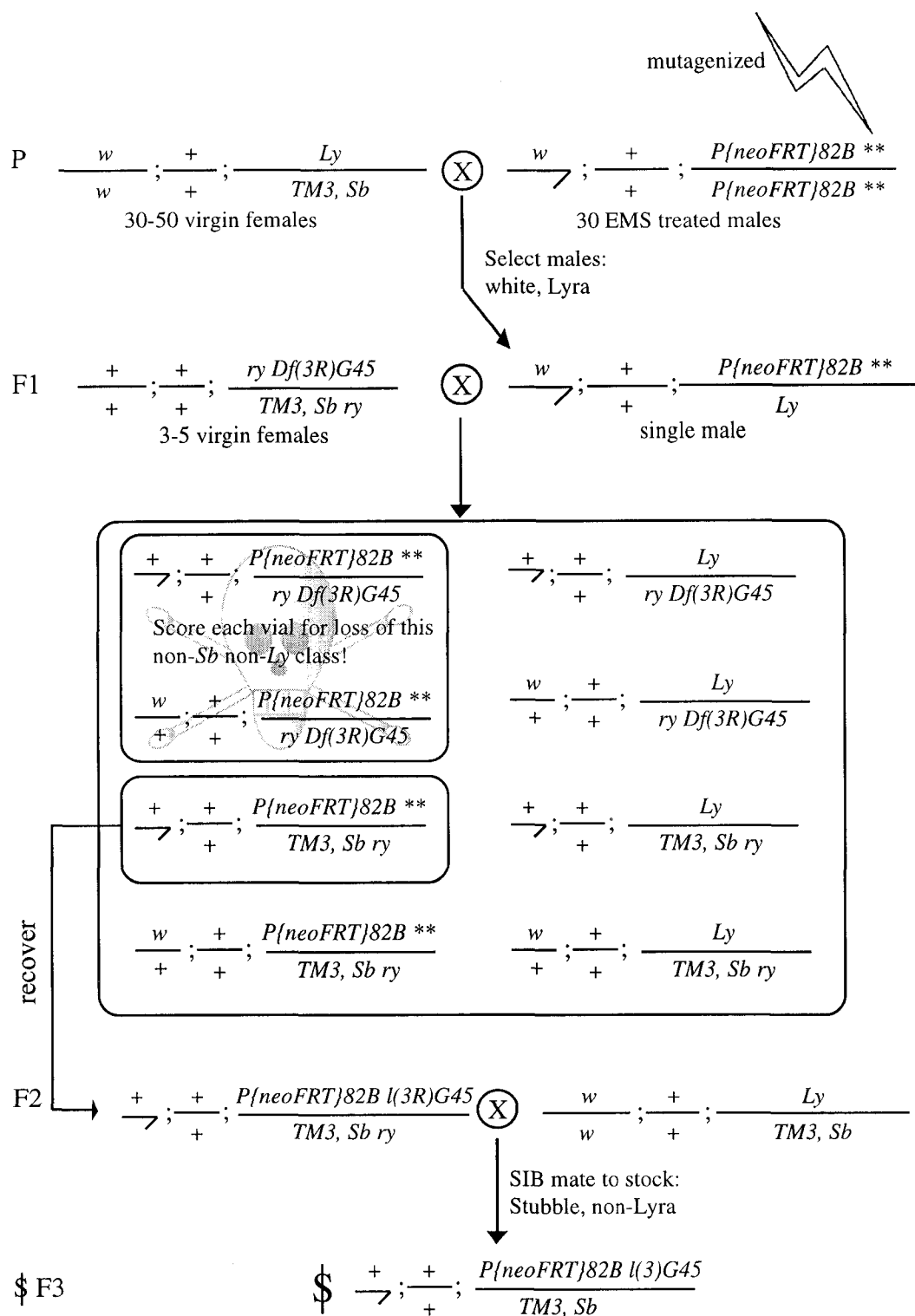


Figure 10. Crossing scheme used to isolate EMS-induced alleles that fail to complement $Df(3R)G45$.

From each of 5 independently isolated mutagenized chromosomes that failed to complement *Df(3R)G45*, a balanced *P{neoFRT}82B l(3)G45 / TM3, ry Sb* male was crossed to *w ; Ly / TM3, Sb* females to make a stock. *Df(3R)G45* was not re-isolated because any F2 progeny from non-virgin *Df(3R)G45* females had rosy eyes and were discarded.

The efficiency of EMS mutagenesis was tested in the sons of attached-X (*C(1)RM, y w f / O=X^X*) females, in which X-linked lethal alleles do not survive. There are two possible viable genotypes in the progeny of a cross between mutagenized males and attached-X virgin females. Females inherit an attached-X chromosome from the female parent and a Y chromosome from the mutagenized male (X[^]XY). Males inherit an X chromosome from the mutagenized male but no sex chromosome from the attached-X female (XO). These two classes are normally expected in equal proportions, but XO progeny inheriting an X chromosome with a lethal mutation will not survive. The ratio of males to females in the progeny of this cross, compared to the sex ratio in a control cross (no EMS) was used to estimate the efficiency of mutagenesis. In general, 12% of the EMS mutagenized X-chromosomes tested carried lethal mutations. The X-chromosome is approximately the same size as 3R, so about 12% of the mutagenized third chromosomes screened were likely to have carried at least one recessive lethal mutation on 3R. This low frequency should have limited the isolation of linked second-site mutations.

2.9.2 P-element hybrid dysgenesis at polytene region 100E-F

P-elements induce mutations directly through insertion into a gene, or by imprecise excision from their insertion within or near a gene. Three homozygous viable P-element insertions mapping to polytene region 100E-F were used to induce lethal P-element excision derivatives with the goal of collecting an overlapping series of deletions at 100E-F. These might then be used to map the genetic position of *ema* with reference to other lethal alleles. *P{PZ}G45* (Brook et al. 1993), *P{LacW}L1022* (Spradling et al., 1999), and *P{wA}4-4* (Hazelrigg et al., 1984), were mobilized with a *P-transposase* source that is incapable of transposition (*P{Δ2-3}*). To maximize the frequency of P-element excisions, these crosses were carried out at 25°C. To maintain the stability of any new alleles, *P{Δ2-3}* was selected against in the F2 by selecting non-ebony males (Fig. 11 and 12).

Excisions of *P{PZ}G45*, which carries a *rosy* rescuing transgene, were isolated from 240 F1 crosses by selecting single F2 males with rosy eyes (Fig. 11). A total of 110 independently isolated rosy-eyed F2 males were tested for failure to complement the lethality of *Df(3R)faf-BP=Df(3R)100D1-3;100E-F*. From each of 5 lines that failed to complement *Df(3R)faf-BP*, a single balanced male was selected and used to make a stock. *Df(3R)faf-BP* was not re-isolated because any progeny from non-virgin *Df(3R)faf-BP*

females had brown eyes (a second chromosomal recessive marker in the *Df(3R)faf-BP* stock, not shown) and were discarded.

Excisions of *P{LacW}L1022* and *P{wA}4-4* were isolated from 240 and 144 F1 crosses (respectively) by selecting single F2 males with white eyes (Fig. 12). 160 (*P{LacW}L1022*) and 112 (*P{wA}4-4*) independently isolated white-eyed F2 males were tested for allelism to *Df(3R)G45*. From each of 6 *P{LacW}L1022* and 1 *P{wA}4-4*-derived lines that failed to complement *Df(3R)G45*, a single balanced Stubble male was selected and used to make a stock. *Df(3R)G45* was not re-isolated because any progeny from non-virgin *Df(3R)G45* females had rosy eyes and were discarded.

The lethal excision derivatives of these 3 P-elements were named *l(3)p-#*, where *p* is the P-element from which the excision was derived, and # is a serial identifier (e.g. *L(3)G45-11* was the 11th rosy G45 excision). These new alleles were mapped using complementation tests to *Df(3R)G45*, *Df(3R)awd-KRB=Df(3R)100D1;100D3-4*, *Df(3R)faf-BP=Df(3R)100D1-3;100E-F* and alleles of *modulo (mod)* and *heph*. Each new allele was combined with *P{neoFRT}82B* and was tested for the ability to induce ectopic wing margin in genetic mosaics (the *ema* phenotype).

2.9.3 P-element induced male recombination at polytene region 100E-F

Recombination is normally suppressed in *Drosophila* males. However, with a *P-transposase* source, male recombination (mr) can be catalyzed at the site of a P-element insertion with a ~1% frequency (Preston and Engels, 1996; Preston et al., 1996). These P-element induced male recombination events are often associated with deletions or duplications of adjacent genomic DNA. Preston et al. (1996) reports that 1/3 of their male recombinants were deletions. To isolate mr-induced mutations at 100E-F, the distal *P{w⁺}* marker of *P{wA}4-4* and the proximal marker *e* were used to screen for putative male recombinants (Fig. 13). The parental *e P{wA}4-4* chromosome was isolated by selecting for an ebony-bodied and orange-eyed recombinant between *e* and *P{wA}4-4* chromosomes (not shown). The second chromosomal *P-transposase* source *H{PΔ2-3}* was used to mobilize *P{PZ}G45*. To maintain *P-transposase* expression at a low level to maintain the integrity of the *e P{wA}4-4* chromosome, P crosses were carried out at 18°C. Crosses were transferred to 25°C only once the *e P{wA}4-4 / ry P{PZ}G45* third chromosome combination was established.

Each of 200 curly-winged F2 males were crossed to *5 y w ; TM3, Sb e / TM6, Tb Hu e* virgin females. Notice that only ~1/2 of these F2 males were likely of the genotype shown since the *e P{wA}4-4* chromosome could not be selected in this *w⁺ e⁺* background. Putative recombinants between the *e P{wA}4-4* chromosome and a *ry P{PZ}G45* chromosome were isolated by selecting non-ebony orange-eyed balanced F3 males.

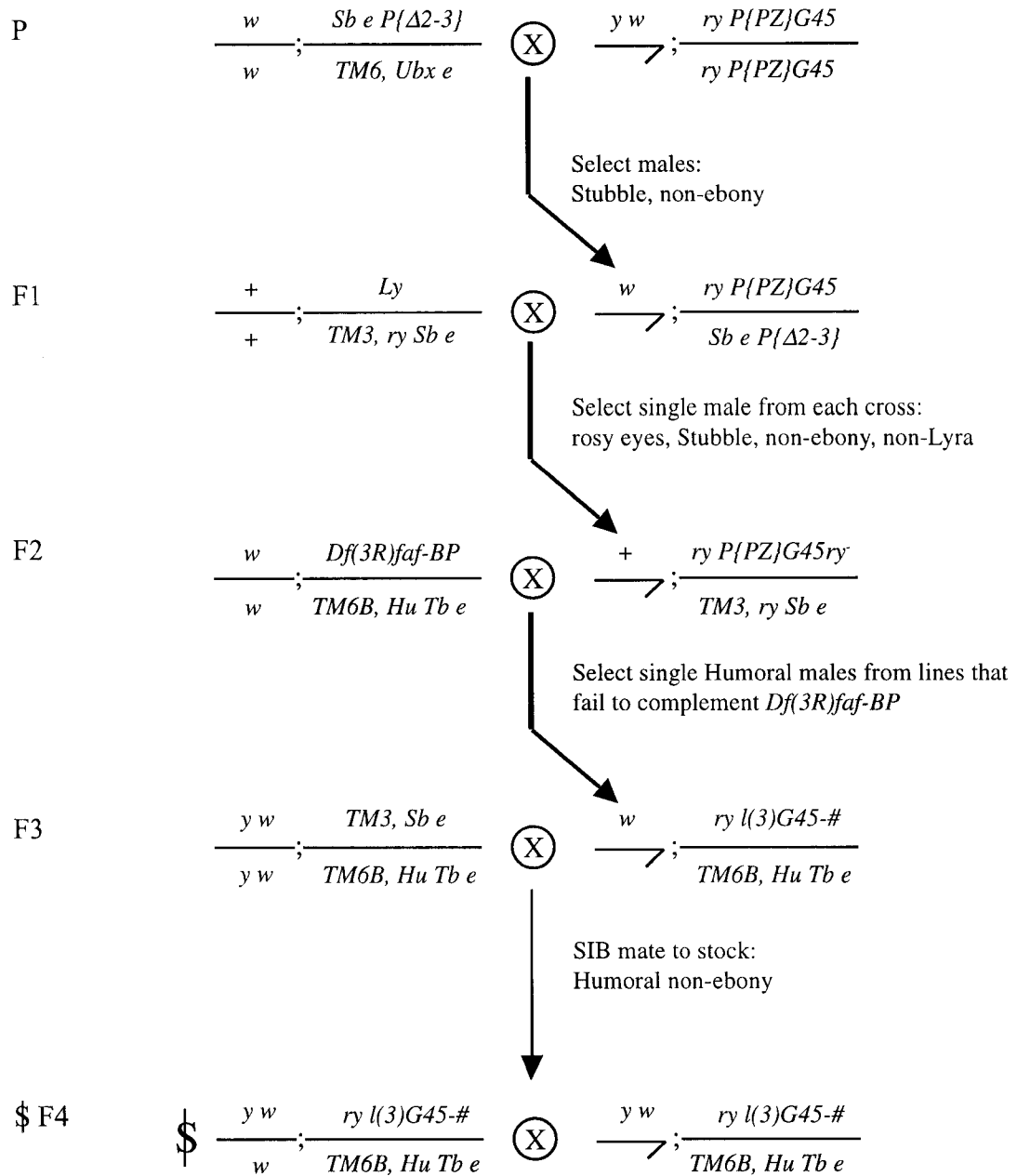


Figure 11. Crossing scheme used to isolate lethal excision derivatives of *P{PZ}G45*.

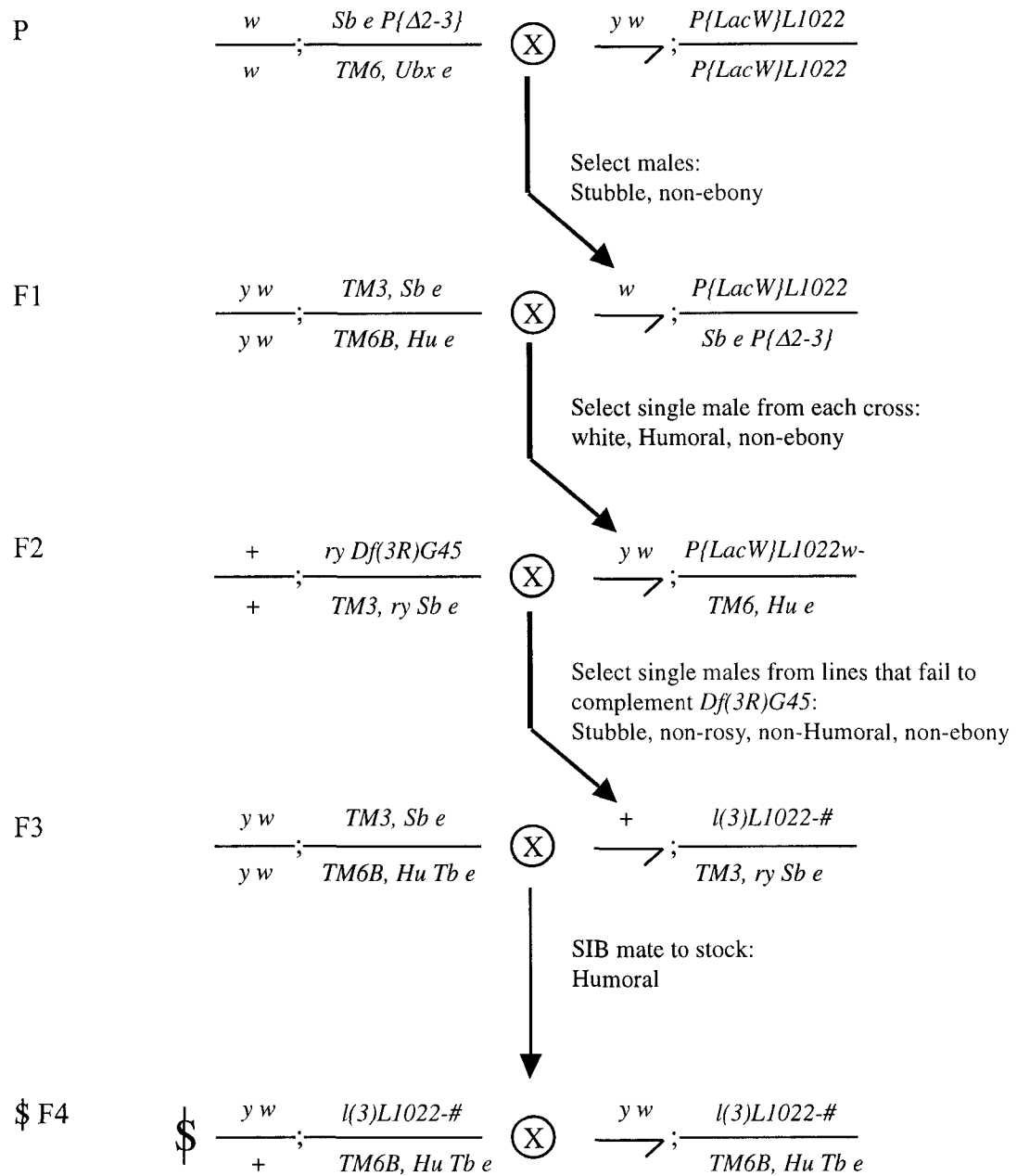


Figure 12. Crossing scheme used to isolate lethal excision derivatives of $P\{LacW\}L1022$ and $P\{wA\}4-4$.

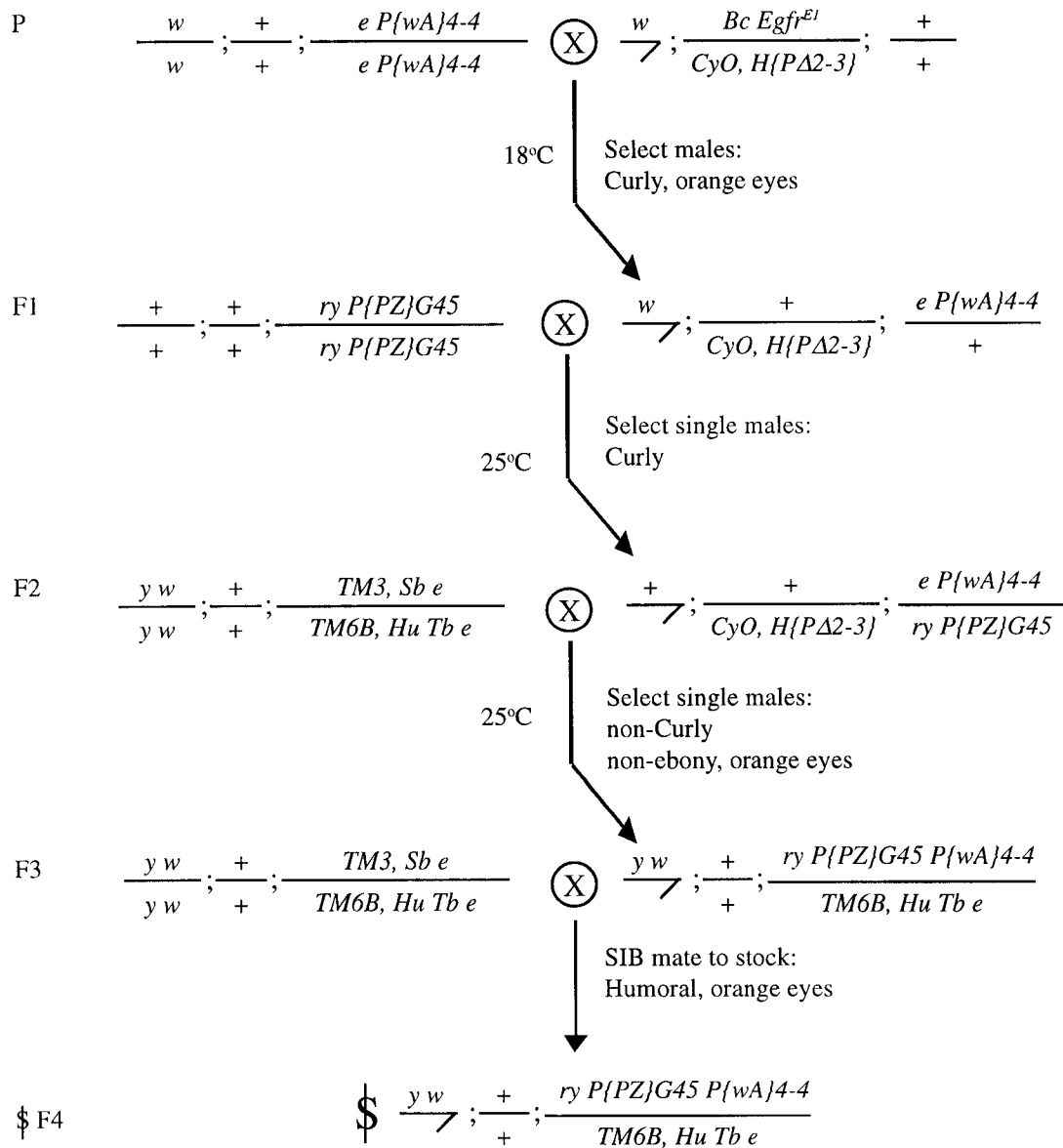


Figure 13. Crossing scheme to generate new deletions at 100E-F using male recombination.

P-element markers used: $P\{PZ\}$, ry^+ ; $P\{wA\}$, w^+ ; $H\{PD2-3\}$, *Curly*.

To maintain putative male recombinants, $H\{P\Delta 2-3\}$ was selected against in F3 males by selecting only straight winged flies. The 10 putative male recombinants isolated in this screen were named $mr\#$, where mr represent male recombinant, and $\#$ is a serial identifier.

There are additional ways to produce a non-ebony, orange-eyed fly using this crossing scheme. First, rare reversion of e^1 , and second, mobilization and re-insertion of $P\{wA\}4-4$ into the $P\{PZ\}G45$ chromosome. The $P\{wA\}4-4$ P-element is inserted near the telomere, causing a variegated eye color phenotype in a w background. This variegated eye color was selected in the non-ebony orange-eyed putative male recombinants to enrich the isolation of chromosomes with $P\{wA\}4-4$ at its original position.

2.10 Characterization of the terminal phenotype of lethal *hephaestus* alleles

Each *heph* allele tested was balanced over $TM3$, $P\{Act-GFP\}$, Ser . Females of the appropriate genotype were allowed to lay embryos for 6hr on apple juice-agar plates supplemented with moistened Fleischmann's Active Dry Yeast. Homozygous mutant embryos and larvae were selected by screening for lack of green fluorescence under an epifluorescence-dissecting microscope. Because the egg's chorion is green auto-fluorescent, embryos were manually dechorionated before fluorescent screening. Selected embryos or larvae were incubated at 25°C on fresh apple juice-agar plates with yeast and their development was observed several times a day until the lethal phase was reached.

Apple juice-agar medium was made in 2 parts. First, 40g agar (4%) was dissolved in 500mL of water by boiling. Second, 50g sucrose (5%) was dissolved in 250mL of water and 250mL apple juice (Sunripe) by boiling. The two solutions were allowed to cool to ~60°C before mixing them together and adding 1g of the antifungal agent Nipagin M (Sigma-Aldrich, Inc.).

2.11 Targeted mis-expression of PTB

Expression of any cloned gene of interest—an effector gene—can be driven in *Drosophila* in the same expression pattern as a GAL4 enhancer trap insertion—a driver (Brand et al., 1994; Brand and Perrimon, 1993). The GAL4 transcription factor activates transcription of an effector gene under the control of a GAL4 upstream activation sequence (UAS). The level of expression of the effector gene is directly related to temperature and to promotor-dependent expression of GAL4 by the driver. Expression of *PTB* cDNA CST01 was driven from an *UAS-PTB* transgene (a gift from C. Schulz, unpublished) using *ap-GAL4*, *C96-GAL4*, and *omb-GAL4* drivers at various temperatures. Why these drivers were chosen is presented in the results section.

2.12 Rescue of the ectopic margin phenotype in *hephaestus* genetic mosaics

The ability of *PTB* cDNA CST01 expression to rescue the ectopic margin phenotype of *heph*⁰³⁴²⁹ was tested. Expression of *PTB* cDNA CST01 was driven from an *UAS-PTB* transgene (C.Schulz, unpublished) with the dorsal specific *ap-GAL4* driver. If dorsal *PTB* expression rescued the *heph* ectopic margin genetic mosaic phenotype, ventral but not dorsal ectopic margin was expected in target class flies. Since the *ap-GAL4* / *UAS-PTB* combination is lethal at 25°C and results in loss of most of the wing margin at RT, these crosses were designed using *P{GAL80}*, encoding a GAL4 repressor, so that *ap-GAL4* can induce expression of *PTB* only in *heph* mutant cells. This is an adaptation of the MARCM system (for mosaic analysis with a repressible cell marker) where mutant cells are the only cells labeled (Lee and Luo, 1999). In this case, the mutant cells are the only cells that express *PTB*.

Generating *heph* genetic mosaic wing discs that express *PTB* from a *UAS-PTB* transgene was a multi-step process. First, *UAS-PTB* and *P{neoFRT}82B P{tubP-GAL80}* were combined in a balanced stock (Stock II, Fig. 14). *UAS-PTB* was isolated in F1 males over the dominant marker *Sp* (Fig. 14A). When these males were crossed to F1 *CyO* females from the cross in Fig. 14B, *UAS-PTB* / *CyO* was selected in the F2 by selecting against *Sp* and for Curly wings.

P{neoFRT}82B P{tubP-GAL80} was selected on the basis of orange eyes caused by the *P{tubP-GAL80}* transgene. *P{neoFRT}82B P{tubP-GAL80}* was balanced over *TM6B* by selecting Humoral F2 flies.

Second, *ap-GAL4* and *P{neoFRT}82B P{πM} Sb heph*⁰³⁴²⁹ were combined in a balanced stock with a *P{hsFLP}* source on the X-chromosome (Stock III, Fig. 15). Both *P{neoFRT}82B P{πM} Sb heph*⁰³⁴²⁹ and *ap-GAL4* were selected using their *w*⁺ (orange eyes) transgenes. The combination of the *w*⁺ markers on these two chromosomes produced darker orange eyes than either marker alone.

Finally, males from Stock II were crossed to females from Stock III (Fig. 16). Mitotic recombination producing clones of *heph*⁰³⁴²⁹ that lack *P{tubP-GAL80}* were generated during the second larval instar with a 1hr 37°C heat treatment. Only non-Humoral F1 flies were scored to ensure both *P{neoFRT}82B P{tubP-GAL80}* and *P{neoFRT}82B P{πM} Sb heph*⁰³⁴²⁹ were present. Straight winged flies that inherited both *ap-GAL4* and *UAS-PTB* were compared to Curly winged flies that inherited *ap-GAL4* or *UAS-PTB* (but not both). Since *ap-GAL4* produces GAL4 only in dorsal cells of the wing disc, and GAL80 inhibits GAL4 activity, *PTB* should only be expressed from the *UAS-PTB* transgene only in dorsal *heph*⁰³⁴²⁹ homozygous mutant cells.

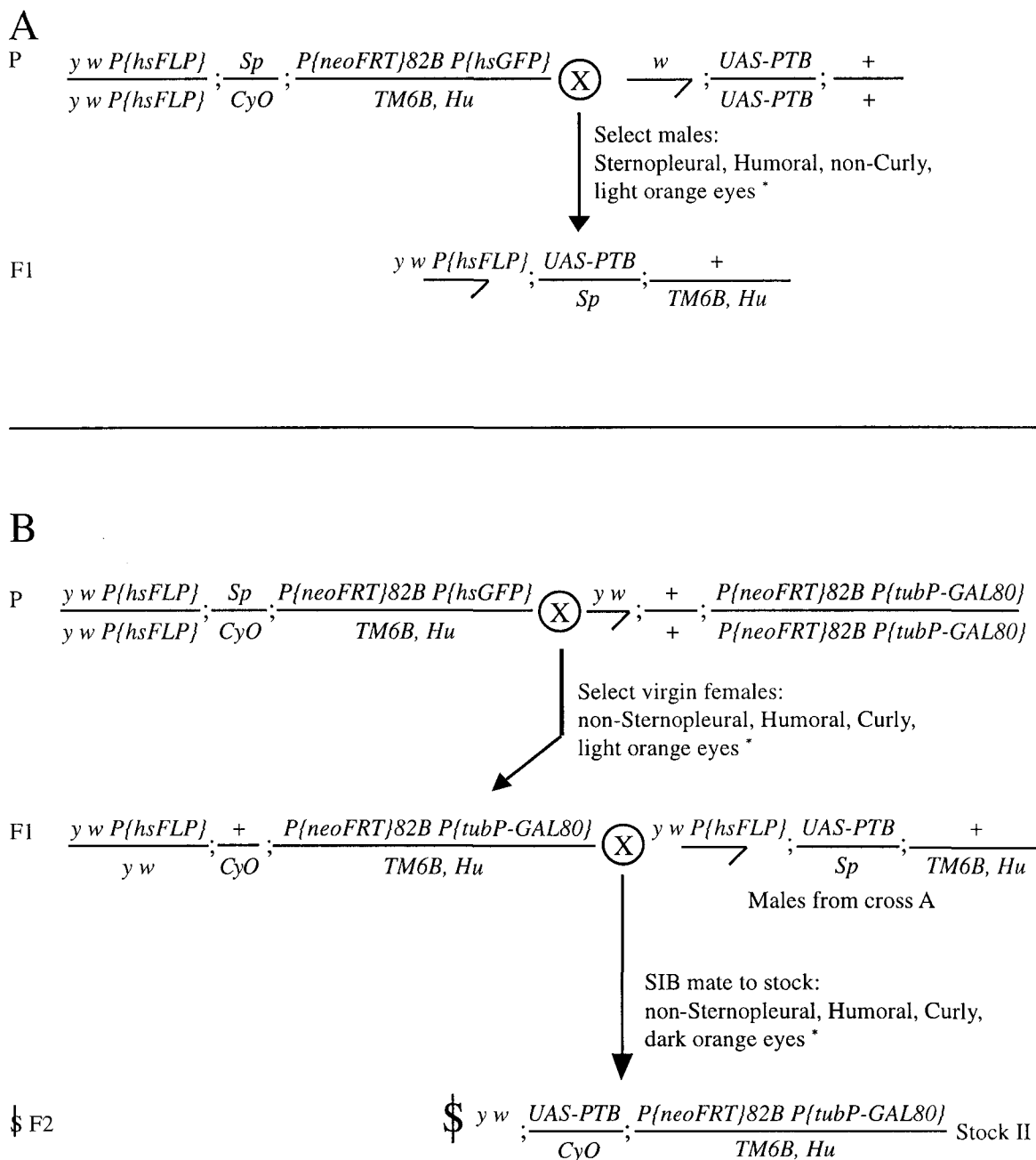


Figure 14. Crossing scheme used to generate Stock II (*heph* rescue).

F1 males from the cross in A were crossed to F1 females from the cross in B.

* Note that *UAS-PTB* and *tubP-GAL80* are P-element insertions marked with *w*⁺ (see Table 1).

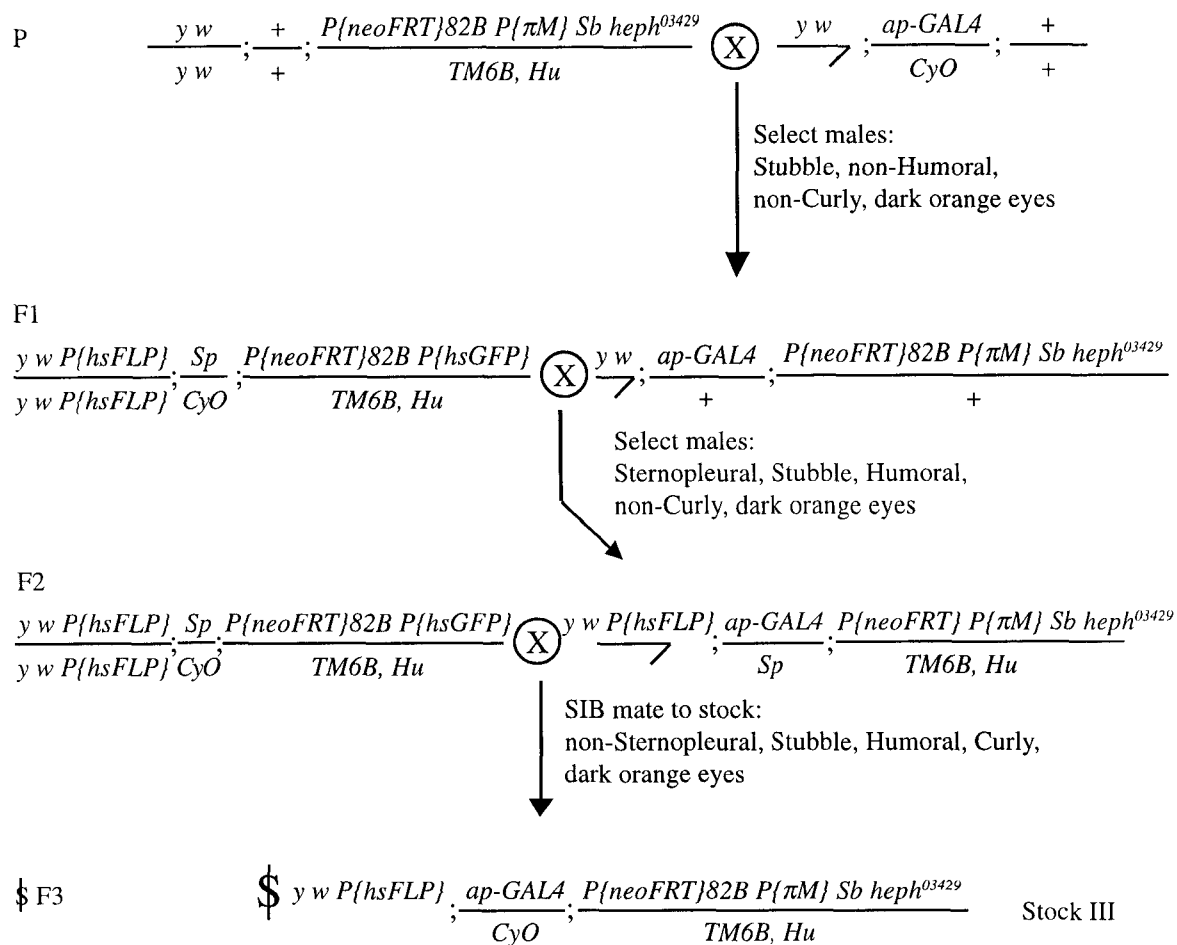


Figure 15. Crossing scheme used to generate Stock III (*heph* rescue).

F1 males from the cross in A were crossed to F1 females from the cross in B.

* Note that *ap-GAL4* is a *P{GawB}* insertion carrying *w*⁺; *P{pM}* also carries *w*⁺, giving dark orange eyes when both are present (see Table 1).

P

$$\frac{y\ w\ P\{hsFLP\}}{y\ w\ P\{hsFLP\}}; \frac{ap-GAL4}{CyO}; \frac{P\{neoFRT\}82B\ P\{\pi M\}\ Sb\ heph^{03429}}{TM6B,\ Hu}$$

Stock III

⊗

$$\frac{y\ w}{7}; \frac{UAS-PTB}{CyO}; \frac{P\{neoFRT\}82B\ P\{tubP-GAL80\}}{TM6B,\ Hu}$$

Stock II

2nd instar heat treatment: 1hr @ 37°C

F1

COMPARE:

$$\frac{y\ w\ P\{hsFLP\}}{y\ w\ P\{hsFLP\}}; \frac{ap-GAL4}{UAS-PTB}; \frac{P\{neoFRT\}82B\ P\{\pi M\}\ Sb\ heph^{03429}}{P\{neoFRT\}82B\ P\{tubP-GAL80\}}$$
Target class:
non-Curly, non-Humoral, Stubble

TO:

$$\frac{y\ w\ P\{hsFLP\}}{y\ w\ P\{hsFLP\}}; \frac{ap-GAL4}{CyO}; \frac{P\{neoFRT\}82B\ P\{\pi M\}\ Sb\ heph^{03429}}{P\{neoFRT\}82B\ P\{tubP-GAL80\}}$$

$$\frac{y\ w\ P\{hsFLP\}}{y\ w\ P\{hsFLP\}}; \frac{UAS-PTB}{CyO}; \frac{P\{neoFRT\}82B\ P\{\pi M\}\ Sb\ heph^{03429}}{P\{neoFRT\}82B\ P\{tubP-GAL80\}}$$
Control class:
Curly wings, non-Humoral, Stubble

Figure 16. Crossing scheme to rescue the ectopic margin phenotype of *hephaestus* in genetic mosaics.

2.13 Molecular techniques and DNA manipulation

Unless otherwise specified, routine molecular biology procedures of restriction enzyme digestion, ligation, plasmid preparation, and Southern transfer and hybridization were performed according to standard protocols (Sambrook et al., 1989). DNA clones were obtained from several sources as indicated in Table 2.

2.13.1 Cosmid and P1 DNA isolation

Cosmid and P1 DNA was isolated using a plasmid "midi-prep kit" (Qiagen, Inc.). Cosmid-containing bacteria were streaked from frozen stocks onto TYE plates (16g tryptone, 10g yeast extract, 5g NaCl, 15g agar/L) + 25µg/mL Kanamycin (Kan), then grown at 37°C overnight. A single colony was used to inoculate an overnight 5mL culture in 2xYT (10g tryptone, 5g yeast extract, 8g NaCl/L) + 50µg/mL Kan. The next day, 2.5mL of this culture was used to inoculate 250mL of 2xYT + 50µg/mL Kan. After 20hr of shaking at 37°C, cosmid DNA was isolated using the Qiagen tip 100 and Qiagen Plasmid Midi Kit protocol. An identical protocol was used to isolate P1 clone DNA except 25µg/mL Tetracycline was used as a selective agent.

2.13.2 Radioactive labeling of DNA

DNA fragments for use as Southern hybridization probes were labeled with α -³²P, dCTP (ICN, Inc.) with an "Oligo-labeling kit" (Pharmacia Technologies, Inc.). Reactions were performed in a 30µL total volume with 50-150ng heat denatured DNA and 30µCi of labeled nucleotide. Unincorporated α -³²P was removed with a sephadex-50 (Pharmacia Biotechnology, Inc.) spin column as described in Sambrook, et al. (1989). Generally, the entire labeling reaction was added to the hybridization solution.

2.13.3 Determining P-element insertion points with inverse PCR

Inverse PCR was used to confirm the insertion point of *P{PZ}heph⁰³⁴²⁹* and to map the insertion point of *P{LacW}heph^{j11B9}*. The full protocol can be downloaded from the BDGP website (<http://www.fruitfly.org>). Briefly, genomic DNA isolated from 30 flies using a standard fly miniprep procedure was resuspended in 150µL of TE. 10µL of resuspended DNA was restricted with *Sau3A* in a total volume of 20µL. After heat-inactivating *Sau3A*, 10µL of the digested genomic DNA was incubated with 2U DNA ligase in DNA ligase buffer overnight at 4°C. Ligated DNA was ethanol precipitated on ice for 10min and pellets were air dried, then resuspended in 150µL TE. PCR reactions were catalyzed with Pry1 (5'-CAA TCA TAT CGC TGT CTC ACT CA-3') and Pry2 (5'-CTT GCC GAC GGG ACC ACC TTA TGT TAT T-3') primers to allow sequencing off the 3' end of the P-element. The following PCR parameters were used:

1x: 5min at 95°C;

35x: 30sec at 95°C / 60sec at 61.5°C / 2min at 68°C;

1x: 10min at 72°C.

PCR reactions were passed through a PCR purification column (Qiagen, Inc.) to remove primers before sequencing with primer IR (5'-ACC TGT TAT TTC ATC AT-3'), a gift from T. Heslip, University of Calgary.

2.13.4 Identification, sequencing and mapping of *hephaestus* cDNAs

Sequence tagged sites (STS) from the *heph*² (AQ026438), *heph*⁰³⁴²⁹ (G00761) and *heph*^{11B9} (AF373596) P-element insertions were mapped to *Drosophila* genomic DNA using BLAST. DNA sequence information was retrieved from BDGP pages and was analyzed using MacVector 6.5 software (Oxford Molecular, Ltd.) and NCBI BLAST (www.ncbi.nlm.nih.gov/BLAST/; Madden et al. 1996; Altschul et al. 1997) searches of the GenBank database (Benson et al., 2000).

Expressed sequence tags (ESTs; Rubin et al. 2000) were identified by sequence homology to genomic DNA surrounding the *heph*², *heph*⁰³⁴²⁹ and *heph*^{11B9} P-elements insertions using BLAST. Full-length cDNA clones GH17441 (adult head cDNA library) and LD04329 (0-22hr embryonic cDNA library) were purchased from Research Genetics (Inc.). Clone CST01 was isolated in a low-stringency screen of a testis cDNA library for a *stem cell tumor* cDNA (C. Schulz, unpublished). Further studies showed that *stem cell tumor* is not synonymous with *PTB*.

Plasmid DNA from a small scale preparation using a plasmid "mini-prep kit" (Pharmacia Biotechnology, Inc.) was of sufficient quality for sequencing. T7 and T3 primers were used to sequence the 5' and 3' end of each cDNA. After the identity of the clone was confirmed from these sequences, a set of internal primers was used to complete the sequence. The sequence of PCR primers used to sequence CST01 (C. Schulz, unpublished), GH17441, and LD04329 are presented in Table 4. Oligonucleotides were synthesized by the GIBCO-BRL Supply Center or were gifts from C. Schulz (unpublished). DNA sequencing was performed by the University of Calgary Core DNA & Protein Services, DNA Sequencing Laboratory, University of Calgary.

Table 3. PCR primers used for DNA sequencing.

Primer	Sequence 5' => 3'	Orientation and approximate position
PTB2	cggttgtttgtctcctatgg	cDNA GH17441 560bp +
PTB3	cggactgatgaacaccaatg	cDNA GH17441 1850bp -
0	cgcttgcttaccgttttg	cDNA CST01 0 bp +
320	cgaggcagatgtgattgc	cDNA CST01 320bp +
360	ccagcacgttggtcacac	cDNA CST01 360bp -
460	gtgattcgactcggagagc	cDNA CST01 1850bp -
470	cacaagcgccgtcaatgcg	cDNA CST01 680bp +
570	gaggtgaaagcttctttgatg	cDNA CST01 1710bp -
780	gaagatctggtgcagtatg	cDNA CST01 780bp -
1000	cgcgcgacttcactaacc	cDNA CST01 1000bp +
1020	gttcaccaggtggcagag	cDNA CST01 1020bp -
1340	gagatggtcacgcctgatg	cDNA CST01 1340bp +
1370	cacatcgccgtatacacc	cDNA CST01 1370bp -
1650	gcactgcttcaactgttg	cDNA CST01 1770bp +
1900	tgaacctgactaggtacc	cDNA CST01 1900bp +
2270	ctttatcaattcagtaag	cDNA CST01 2270bp -
3fw	aagctacctcactgtcaacgtcg	genomic 5' of GH17441 exon 3
3rv	acccaagatcatgccttgc	genomic 3' of GH17441 exon 3
EM1fw	tgcctaaaatgtttcgcccc	genomic 5' of <i>PTB</i> exon 1
EM1rv	gcattccttacaaccgctcg	genomic 3' of <i>PTB</i> exon 1
EM2fw	tggctcctgtgttcattgatttc	genomic 5' of <i>PTB</i> exon 2
EM2rv	gcagcagcaacagattcattcc	genomic 3' of <i>PTB</i> exon 2
7fw	tgaaactgctcccgcac	genomic 5' of GH17441 exon 7
7rv	agacaaaaggaaaggcaagg	genomic 3' of GH17441 exon 7
8fw	aagcggaagtgcagacagc	genomic 5' of GH17441 exon 8
8rv	tggaattactgctggaagtttg	genomic 3' of GH17441 exon 8
9-12fw	cccgccttgtaaattgactc	genomic 5' of GH17441 exons 9-12
9-12rv	acagccatcctctagcttgg	genomic 3' of GH17441 exons 9-12
13fw	ccattcgtgcggaatac	genomic 5' of GH17441 exon 13
13rv	cacaaccacaccaacagc	genomic 3' of GH17441 exon 13
14-16fw	tggcaatgttctttctgagattc	genomic 5' of GH17441 exons 14-16
14-16rv	ttgtttgtgtctttcccactaag	genomic 3' of GH17441 exons 14-16

2.13.5 PCR-based sequencing of EMS-derived *hephaestus* alleles

Homozygous *heph^{e1}* and *heph^{e2}* larvae were selected by lack of a *P{Act-GFP}* marked balancer as previously described. PCR primers (Table 3) were designed by M. Lunke using MacVector software to amplify each *heph* exon or set of closely spaced exons from genomic DNA of homozygous mutant *heph* larvae. To minimize the possibility of contamination with genomic DNA from heterozygous or balancer animals, single first instar larvae that did not express GFP were selected for sequencing. PCR reactions and DNA sequencing was performed by M. Lunke. Sequence from the mutants was compared to sequence using the same primers from the original non-mutagenized *P{neoFRT}82B* line.

2.14 Histology and light microscopy

Adult cuticle was stored and dissected in SH (30% glycerol, 70% ethanol). Before mounting heads, thoraces or legs, the tissue was cleared in 1N NaOH overnight at 37°C. Cuticle was removed from the fly with microscissors and Dumont #5 forceps, washed in 70% ethanol, then mounted on a slide in Gurr's Aquamount (BDH Laboratory Supplies, Inc.). Wings were mounted between 2 coverslips to allow observation of both dorsal and ventral surfaces.

All photomicroscopy was carried out on a Leica DMRE photomicroscope using Kodak Elite-Chrome 400 A.S.A. slide film. Slides were scanned using a Polaroid Sprintscan 4000 slide scanner at 1200 dpi using Adobe Photoshop. Brightness, contrast and mid-tone levels of scanned images were adjusted automatically (auto-levels). Final resolution was adjusted to 150-200 dpi.

2.15 Antibody staining and laser scanning microscopy

Imaginal discs were stained essentially as in Pattatucci and Kaufman (1991) with some modifications. The anterior half of each larva was inverted in ice-cold PBS (140mM NaCl, 7mM Na₂HPO₄, 3mM KH₂PO₄) and stored in 2mL micro-centrifuge tubes on ice no longer than 30min. Incubations in methanol were omitted because it destroys GFP activity. Inverted heads were fixed in freshly mixed ice-cold 4% EM-grade (methanol-free) formaldehyde (Polysciences, Inc.) in PBS for 20min at RT. The heads were then washed three times for 10min each in BBX250 (250mM NaCl, 7mM Na₂HPO₄, 3mM KH₂PO₄, 0.1% w/v BSA, 0.2% w/v triton-X100). The primary antibody was added to a final volume of 100μL BBX250 and the tissue was gently rocked overnight at RT. Primary antibody dilutions were as recommended by the antibody's supplier (Table 4).

Unbound primary antibody was removed with five rinses in BBX250 over a period of 90min, and the tissue was blocked 2 x 30min in 500 μ L BBX250 + 20 μ L normal goat serum (NGS). Inverted heads were incubated with the appropriate secondary antibody in fresh BBX250 + NGS for 90min. Molecular Probes (Inc.) goat α -mouse Alexafluor^{594nm} secondary antibodies were diluted 1/10 in PBT (140mM NaCl, 7mM Na₂HPO₄, 3mM KH₂PO₄, 0.1% w/v Tween-20), pre-absorbed on dechorionated, fixed, devitellinized embryos, and used at a final concentration of 1/500. Jackson Immunoresearch (Inc.) goat α -rat Cy3 was not pre-absorbed and was used at a final concentration of 1/400. The secondary antibody was washed off with 6 changes of BBX250 over the period of 1hr. Wing discs were dissected, mounted and stored in 80% glycerol : 20% PBS (by volume) with 4% w/v *n*-propyl gallate (Sigma-Aldrich, Inc.) as an anti-fade reagent.

Laser scanning microscopy of all fluorescently labeled tissue was carried out on a Zeiss Axiovert100M laser-scanning microscope (Joint Injury Research Group, Department of Biochemistry and Molecular Biology, University of Calgary). Images were acquired and exported in TIFF format using Zeiss "Let's See More!" LSM510 software. Brightness, contrast and tone levels were manually adjusted using Adobe Photoshop.

Table 4. Primary antibodies

Primary antibodies	Type/Lot number	Working conc.	Source
mouse α -AC	monoclonal	1/25	J. Skeath * (Skeath and Carroll, 1991)
mouse α -CT	Mab 2B10	1/100	G. Rubin * (Blochlinger et al., 1990)
mouse α -DL	Mab 202.9B	1/25	M. Muskavitch, Boston College, US (Kooh et al., 1993)
mouse α -DLL	monoclonal	1/100	W. Brook, University of Calgary, CA (Diaz-Benjumea et al., 1994)
mouse α -E(SPL) [†]	MAB 323	1/3	S. Bray, University of Cambridge, UK (Jennings et al., 1994)
mouse α -NICD [‡]	MAB C17.9C6	1/10	S. Artavanis-Tsakonas * (Fehon et al., 1990)
mouse α -NECD [§]	MAB C458.2H	1/10	S. Artavanis-Tsakonas * (Diederich et al., 1994)
mouse α -NUB	monoclonal	1/10	S. Cohen, EMBL, DE (Averof and Cohen, 1997)
rat α -SER	polyclonal 2	1/5	K. Irvine, Rutgers, NJ State University, US (Papayannopoulos et al., 1998)
mouse α -WG	MAB 4D4	1/10	W. Brook, University of Calgary, CA (Brook and Cohen, 1996)

* These monoclonal antibodies were obtained from the Developmental Studies Hybridoma Bank developed under the auspices of the NICHD and maintained by the University of Iowa, Department of Biological Sciences, Iowa City, IA 552242.

[†] MAB 323 recognizes at least 5 of the bHLH E(SPL) proteins (de Celis et al., 1996a). All incubations and washes were carried out at 40C.

[‡] ICD = Intracellular domain of Notch, amino-acids 1791-2504

[§] ECD = Extracellular domain of Notch, EGF repeats 12-20

3 RESULTS

3.1 Summary of genetic and molecular analysis of the *hephaestus* locus

Mitotic clones of *Df(3R)G45* in the wing blade can induce the formation of ectopic wing margin bristles (Finkielsztejn, 1997). An analysis of this phenotype will be presented in detail in section 3.2. A simple genetic hypothesis drawn from this phenotype is that *Df(3R)G45* disrupts a gene that is required to repress the wing margin fate. Because of its phenotype in genetic mosaics, this hypothetical gene has been provisionally named *ectopic margin (ema)*. By definition, *ema* alleles are able to induce ectopic margin in genetic mosaics (the "*ema* phenotype").

In order to identify the locus responsible for the *ema* phenotype, it was necessary to identify the genes that are disrupted by *Df(3R)G45*. EMS-induced mutations and P-element excision derivatives were isolated, and extant P-element insertion mutations and deficiencies were identified, through complementation tests to *Df(3R)G45*. To identify which of these alleles might cause the *ema* phenotype, each was tested for the ability to induce ectopic margin in genetic mosaics. In addition to the original *Df(3R)G45* allele, *ema* is disrupted by 6 excision derivatives isolated in this work from P-elements that map to 100E-F. A single lethal complementation group corresponding to *ema* is defined by one lethal EMS-derived allele isolated in this work (*e2*) and two previously isolated but not characterized lethal P-element alleles (*l(3)03429* and *l(3)j11B9*). These *ema* alleles (*e2*, *l(3)03429* and *l(3)j11B9*) are part of a complex complementation group including a second EMS-derived lethal allele isolated in this work (*e1*) that is not able to induce ectopic margin in genetic mosaics, and the extant male sterile mutation *hephaestus (ms(3)heph²)*, Castrillon et al. 1993). Once alleles of a single locus corresponding to *ema* were identified, they were molecularly mapped to the *Drosophila* genome to identify the affected transcription unit. All five alleles map to a single transcription unit named *polypyrimidine tract binding protein (PTB)*, identified by similarity to its vertebrate counterpart (Davis et al., 2002). The name *hephaestus* takes precedence because it was coined before *ectopic margin* and *PTB*. EMS-induced lethal alleles *e1* and *e2* have been renamed *heph^{e1}* and *heph^{e2}*, and P-element induced lethal alleles *l(3)03429* and *l(3)j11B9* have been renamed *heph⁰³⁴²⁹* and *heph^{j11B9}*.

3.1.1 Mobilization of viable P-insertions mapping to polytene region 100E-F by hybrid dysgenesis.

Df(3R)G45 was isolated in a screen for lethal excision derivatives of *P{PZ}G45* that failed to complement *Df(3R)faf-BP* (Brook, 1994). Later, *Df(3R)G45* was shown to cause the *ema* clonal phenotype (Finkielsztein, 1997). Since *Df(3R)G45* was derived from *P{PZ}G45*, it was possible that the *ema* mutation was present on the original *P{PZ}G45* chromosome and was unrelated to *Df(3R)G45*. To rule out this possibility, I tested the ability of *P{PZ}G45* to induce ectopic margin in genetic mosaics using the FLP/FRT mitotic clone induction method and *y* as a mutant cell marker. *P{PZ}G45* is not associated with ectopic margin in genetic mosaics, is homozygous viable, and has no visible adult phenotype.

The insertion point of *P{PZ}G45* was mapped to polytene band 100E by *in situ* hybridization of a labeled P-element probe to the polytene chromosomes of *P{PZ}G45* larvae (Brook, 1994). Since the *P{PZ}G45* insertion maps to 100E, and the lethality of *Df(3R)G45* map between 100D1-3 and 100E-F (the interval deleted by *Df(3R)faf-BP*), the lethality of *Df(3R)G45* and the *ema* phenotype might both be caused by an imprecise excision of *P{PZ}G45*. Based on this hypothesis, I screened for new deletions induced by imprecise excision of the *P{PZ}G45* P-element, and expected a high frequency of *ema* alleles among the new excisions. In addition, with the goal of genetic deletion interval mapping of *ema* within the 100E-F region, I isolated imprecise excisions from two other viable P-elements that map to 100E-F, *P{lacW}L1022* and *P{wA}4-4*. Since deletions are often created by imprecise excisions in either direction from a P-element, these three P-elements (*P{PZ}G45[100E]*, *P{lacW}L1022[100F1-2]* and *P{wA}4-4[3R telomere]*) might be used to divide the 100E-F region into sections (for a map, see Fig. 19B).

Excisions of *P{PZ}G45* were isolated by screening for loss of the *rosy* rescuing transgene carried by *P{PZ}* (Fig. 11). To screen for imprecise excisions, only those lines that also failed to complement the lethality of *Df(3R)faf-BP* were studied. Of 110 independently isolated excisions of *P{PZ}G45*, five lines failed to complement *Df(3R)faf-BP*. Excisions of *P{LacW}L1022* and *P{wA}4-4* were isolated by screening for loss of the *white* rescuing transgene carried by *P{LacW}* and *P{wA}* (Fig. 12). To screen for imprecise excisions, only those lines that failed to complement the lethality of *Df(3R)G45* were studied. Of 160 independently isolated excisions of *P{LacW}L1022* and 112 independently isolated excisions of *P{wA}4-4*, seven lines failed to complement *Df(3R)G45*. These lines were named *l(3)P-#* where *P* refers to the original P-element insertion, and # is a serial identifier. To identify any alleles that disrupt *ema*, each excision was combined with a *P{neoFRT}82B*-bearing chromosome and recombination was induced using the FLP/FRT method and *y* as a clone marker. Since *y* only marks bristles, only those mutant clones associated with wing margin bristles could be identified. This means that a negative result (no ectopic margin) may be due to lack of mutant clones or because the allele being tested does not disrupt *ema*. To help limit the

possibility of a false negative, at least two independently isolated $P\{neoFRT\}82B\ l(3)P\#$ recombinants were tested for each allele.

Three of the five lethal excisions of $P\{PZ\}G45$ ($l(3)G45-11$, 66 and 73), two of the six lethal derivatives of $P\{LacW\}L1022$ ($l(3)L1022-47$ and 162) and the single lethal derivative of $P\{wA\}4-4$ ($l(3)A4-4-74$) are associated with the *ema* phenotype in genetic mosaics. The high frequency of *ema* alleles isolated in excision derivatives of P-elements mapping to 100E-F support a model where *ema* maps close to or within 100E-F.

To narrow down the interval to which *ema* maps, complementation tests were carried out between each of the lethal P-element excisions, and to $Df(3R)faf-BP$, $Df(3R)G45$, and $Df(3R)awd-KRB$ —which deletes the 100D-E region. The results of these complementation tests are summarized, with others, in Table 5 and Fig. 17.

All of the lethal P-element excisions fail to complement the lethality of $Df(3R)faf-BP$ and complement the lethality of $Df(3R)awd-KRB$. The lethality associated with the new deletions thus maps between 100D4-E1 and 100E-F, the interval deleted by $Df(3R)faf-BP$ that is not disrupted by $Df(3R)awd-KRB$. With only one exception, each of the lethal excision derivatives fails to complement each of the other excision derivatives and fails to complement $Df(3R)G45$. The exception, $l(3)G45-5$, complements each of the other excision derivatives and $Df(3R)G45$, and does not disrupt *ema*. Of the 11 alleles that fail to complement $Df(3R)G45$, 6 are associated with ectopic margin in genetic mosaics. These results suggest that the lethality of $Df(3R)G45$ is closely linked to *ema* but that $Df(3R)G45$ may disrupt multiple complementation groups.

3.1.2 EMS-induced mutations that fail to complement $Df(3R)G45$

To see if new point-mutant alleles of *ema* could be isolated, I screened for EMS-induced lethal alleles that fail to complement $Df(3R)G45$ (Fig. 10). The success of this method relied on the assumption that *ema* is an essential gene. Since its genetic mosaic phenotype suggests that *ema* is involved in cell communication and pattern formation, this seemed like a reasonable assumption.

I isolated 5 independent EMS-induced lethal mutations that fail to complement $Df(3R)G45$ from 9622 EMS mutagenized chromosomes. Each mutation was given a serial identifier (#) in the form $l(3)\#$. The allelism of these mutations was tested using complementation tests for lethality. Three mutations fall into one lethal complementation group ($l(3)1360$, $l(3)3570$, and $l(3)5D1$) and the other two alleles fall into a second complementation group ($l(3)2M2$ and $l(3)15M3$). To identify any alleles that disrupt *ema*, each allele was combined with a $P\{neoFRT\}82B$ -bearing chromosome and recombination was induced using the FLP-FRT method and *y* as a clone marker. Again, to help limit the possibility of a false negative, at least two independently isolated $P\{neoFRT\}82B\ l(3)\#$ recombinants were tested for each allele (in the case of $l(3)2M2$,

four lines were tested). In genetic mosaics of the first complementation group (*l(3)1360*, *l(3)3570*, and *l(3)5D1*), no ectopic margin was observed. In the second lethal complementation group, one allele (*l(3)2M2*, hereafter referred to as *e1*) does not induce ectopic margin in genetic mosaics, while a second allele (*l(3)15M3*, hereafter referred to as *ema^{e2}*) causes the *ema* phenotype in clones. Since *e1* fails to complement the lethality of *ema^{e2}*, but does not induce ectopic margin in genetic mosaics, these two alleles might share a second site lethal mutation unrelated to *ema*. Alternative explanations include the possibilities that *e1* and *ema^{e2}* both disrupt *ema* but that *e1* is a weak allele or that it does not affect the function of *ema* in the wing.

3.1.3 P-element insertions that fail to complement *Df(3R)G45*

To identify mutations affecting *ema* that already existed in public *Drosophila* allele collections, I first identified mutations listed in the Flybase database that map to 100E-F. From these, the mutations that failed to complement the lethality of *Df(3R)G45* were tested for the *ema* phenotype in genetic mosaics.

Deletions, P-element induced lethal alleles and alleles of characterized genes that map to 100E-F were obtained from *Drosophila* stock centers and from private collections. These alleles were tested for allelism to *Df(3R)G45*, *Df(3R)faf-BP* and *Df(3R)04661=Df(3R)100D2-100F5* (Table 6). Each complementation test was repeated at least twice and the lack of a non-balancer class in at least 100 flies (often several hundred) was scored as "failure to complement". The presence of an approximately equal proportion of balancer and non-balancer flies was often scored as "complement" in less than 100 flies. For male sterile (*ms*) alleles, complementation tests were first carried out with 5 males and approximately 10 females per vial. However, since *ms(3)heph²* is a male semi-sterile mutation, complementation tests with *heph²* were re-done using 10 single males in separate vials with 5 females each. Lack of progeny from most or all of these single crosses was scored as failure to complement the male sterility of *heph²*. To ensure that non-virgin females were not responsible for any progeny, females of genotype *y w ; TM3, Sb e / TM6, Hu e* were used and progeny were scored for the absence this genotype.

Many alleles mapping to 100E-F that were listed as lethal alleles complement the lethality of *Df(3R)faf-BP* and *Df(3R)04661*, both of which delete the entire 100E-F region. The lethality of these alleles likely does not map to 100E-F, or they are semi-lethal alleles. Several lethal alleles fail to complement *Df(3R)faf-BP* but complement *Df(3R)G45*. These were not studied further because lethal *ema* alleles were expected to fail to complement *Df(3R)G45*. Three previously uncharacterized P-element induced lethal mutations (*l(3)03429*, *l(3)j11B9*, and *l(3)s095214*) and a small deletion disrupting *mod* (*Df(3R)mod-L8*) fail to complement the lethality of *Df(3R)G45*, *Df(3R)faf-BP*, and *Df(3R)04661*. Additionally, the male-sterility of *ms(3)heph²* and *ms(3)07570* is not complemented by *Df(3R)G45*. While *ms(3)07570* is a "true *ms*" allele, *ms(3)heph²* is a

semi-male-sterile allele. 7/8 crosses between single *Df(3R)G45 / ms(3)heph²* males and balancer females produced no progeny, and 8/10 homozygous *ms(3)heph²* males produced no progeny.

To identify any alleles that disrupt *ema*, each lethal allele was combined with a *P{neoFRT}82B*-bearing chromosome and recombination was induced using the FLP-FRT method and *y* as a clone marker. *ms* alleles were not tested for the *ema* phenotype because they were homozygous viable and appeared normal. The phenotype of *Df(3R)mod-L8* clones had been previously published (small clones with short, slender bristles (Perrin et al., 1998), and this was not repeated. While *l(3)s095214* is not associated with ectopic margin in genetic mosaics, *l(3)03429* and *l(3)j11B9* can induce ectopic wing margin in genetic mosaics, so these will be referred to as *ema⁰³⁴²⁹* and *ema^{j11B9}*.

The lethal and male sterile mutations that fail to complement *Df(3R)G45* were tested for allelism to the 5 EMS induced *Df(3R)G45* alleles (Table 7 and Fig. 15). All of these alleles belong to one of two complementation groups disrupted by *Df(3R)G45*: *modulo* or *ema*. *l(3)s095214* fails to complement each of *l(3)5D1*, *l(3)1360* and *l(3)3570*. These four alleles fail to complement the lethality of the previously characterized null *modulo* allele *Df(3R)mod-L8* (Garzino et al., 1992) and are thus alleles of *modulo*. These alleles have been renamed *mod^{s095214}*, *mod^{e1}*, *mod^{e2}*, and *mod^{e3}*, respectively (Table 8). In addition, *Df(3R)mod-L8* fails to complement the male sterility of *ms(3)07570*, thus *ms(3)07570* is a *ms modulo* allele.

In the second complementation group, both *ema⁰³⁴²⁹* and *ema^{j11B9}* fail to complement the lethality of *ema^{e2}* and lethal allele *e1*. *ema⁰³⁴²⁹*, *ema^{j11B9}*, *ema^{e2}* and *e1* each fail to complement the male sterility of *ms(3)heph²*, indicating that the lethal *ema* alleles, *e1* and *ms(3)heph²* are different alleles of a single locus. Since the name *hephaestus* takes precedence, all alleles of this complementation group have been renamed as *heph* alleles (Table 8). These complementation results fit a model in which the *heph* complementation group is complex, with a *ms* allele (*heph²*), three lethal alleles that cause the *ema* phenotype (*heph⁰³⁴²⁹*, *heph^{j11B9}*, and *heph^{e2}*), and a lethal allele that does not cause the *ema* phenotype (*heph^{e1}*).

Table 5. Complementation test results between lethal P-element excisions and alleles mapping to 100F.

	<i>ectopic margin</i>	<i>Df(3R)awd-KRB</i>	<i>Df(3R)faf-BP</i>	<i>Df(3R)G45</i>	<i>l(3)03429</i>	<i>Df(3R)mod-L8</i>
<i>P{PZ}G45 excisions</i>						
<i>l(3)G45-5</i>	no	☺	☹	☺	☺	☺
<i>l(3)G45-11</i>	yes	☺	☹	☹	☹	☹
<i>l(3)G45-24</i>	no	☺	☹	☹	☹	☹
<i>l(3)G45-66</i>	yes	☺	☹	☹	☹	☹
<i>l(3)G45-73</i>	yes	☺	☹	☹	☹	☹
<i>P{LacW}L1022 excisions</i>						
<i>l(3)L1022-37</i>	no	☺	☹	☹	☺	☹
<i>l(3)L1022-47</i>	yes	☺	☹	☹	☺	☹
<i>l(3)L1022-84</i>	no	☺	☹	☹	☺	☹
<i>l(3)L1022-145</i>	no	☺	☹	☹	☺	☹
<i>l(3)L1022-146</i>	no	☺	☹	☹	☺	☹
<i>l(3)L1022-162</i>	yes	☺	☹	☹	☹	☹
<i>P{wA}4-4 excision</i>						
<i>l(3)A4-4-74</i>	yes	☺	☹	☹	☹	☹

Legend: ☺ complement
☹ fail to complement

Table 6. Complementation test results between alleles mapping to 100E-F.

Cytology	Allele name	<i>Df(3R)G45</i>	<i>Df(3R)faf-BP</i>	<i>Df(3R)04661</i>
100F5	<i>l(3)06497</i>	☺	☺	☺
100F5	<i>Df(3R)mod-L8</i>	☹	☹	☹
100F4-5	<i>l(3)095214</i>	☹	☹	☹
100F4-5	<i>l(3)06886</i>	☺	☺	☺
100F4-5	<i>l(3)rH304</i>	☺	☺	☺
100F1-2	<i>l(3)L7321</i>	☺	☺	☺
100F1-5; 74D3-5	<i>l(3)j11B9</i>	☹	☹	☹
100F1-2	<i>l(3)03429</i>	☹	☹	☹
100E-F	<i>l(3)008224</i>	☺	☹	nd
100E-F	<i>l(3)128104</i>	☺	☹	nd
100E-F	<i>l(3)s118416</i>	☺	☹	☹
100E-F	<i>l(3)041303</i>	☺	☺	nd
100E-F	<i>ms(3)07570</i>	ms	ms	nd
100E1-3	<i>ms(3)heph²</i>	ms	ms	ms
100E1-2	<i>faf^{F08}</i>	☺	faf	nd
100E1-2	<i>l(3)j2A4</i>	☺	☹	nd
100E1-2	<i>awd^{L8700}</i>	☺	☹	nd
100E1-2	<i>l(3)s1921</i>	☺	☹	☹
100E	<i>l(3)nuhl²</i>	☺	☺	nd
100D3-4	<i>l(3)s125015</i>	☺	☹	nd
100D1	<i>Med⁵</i>	☺	☺	☺
Legend:	☺	complement		
	☹	fail to complement		
	nd	not determined		
	ms	male sterile		
	faf	fat facets		

Table 7. Complementation test results between alleles that fail to complement *Df(3R)G45*.

	ectopic WM	<i>l(3)heph⁰³⁴²⁹</i>	<i>l(3)heph^{e1}</i>	<i>ms(3)heph²</i>	<i>Df(3R)G45</i>	<i>l(3)L1022-162</i>	<i>l(3)L1022-47</i>	<i>l(3)L1022-84</i>	<i>Df(3R)mod-L8</i>	<i>Df(3R)faf-BP</i>
<i>l(3)heph⁰³⁴²⁹*</i>	yes	☒								
<i>l(3)heph^{e1}</i>	no	☒	☒							
<i>ms(3)heph²</i>	nd	ms	ms	ms						
<i>Df(3R)G45*</i>	yes	☒	☒	ms	☒					
<i>l(3)L1022-162</i>	yes	☒	~☒	nd	☒	☒				
<i>l(3)L1022-47[†]</i>	yes	☺	☺	nd	☒	☒	☒			
<i>l(3)L1022-84*</i>	no	☺	☺	nd	☒	☒	☒	☒		
<i>Df(3R)mod-L8*</i>	no	☺	☺	mf	☒	☒	☒	☒	☒	
<i>Df(3R)faf-BP</i>	no [‡]	☒	☒	ms	☒	☒	☒	☒	☒	☒

Legend: ☺ complement
☒ fail to complement
~☒ rare escaper
nd not determined
ms male sterile
mf male fertile

* Several groups of alleles had identical complementation patterns. To simplify this table, the following alleles have been grouped together: *l(3)heph⁰³⁴²⁹* with *l(3)heph^{11B9}* and *l(3)heph^{e2}*; *Df(3R)G45* with *l(3)G45-11*, *l(3)G45-66* and *l(3)G45-73*; *l(3)L1022-84* with *l(3)L1022-37* and *l(3)L1022-145*; *Df(3R)mod-L8* with *l(3)s095214*.

[†] *l(3)L1022-47* may be exhibiting inter-allelic complementation with other alleles of *heph*.

[‡] Some patches of necrotic tissue were present in flies expected to have *Df(3R)faf-BP* clones, suggesting that *Df(3R)faf-BP* is cell lethal.

Table 8. Summary of allele names and synonyms

Allele name	Synonyms
<i>Df(3R)G45</i>	<i>G45Δ53</i>
<i>heph²</i>	<i>P{PZ}ms(3)heph²</i>
<i>heph^{e1}</i>	<i>l(3)2M2, e1</i>
<i>heph^{e2}</i>	<i>l(3)15M3, e2, emd^{e2}</i>
<i>heph⁰³⁴²⁹</i>	<i>P{PZ}l(3)03429, emd⁰³⁴²⁹</i>
<i>heph^{j11B9}</i>	<i>P{LacW}l(3)j11B9, emd^{j11B9}</i>
<i>mod^{e1}</i>	<i>l(3)5D1</i>
<i>mod^{e2}</i>	<i>l(3)1360</i>
<i>mod^{e3}</i>	<i>l(3)3570</i>
<i>mod^{s095214}</i>	<i>P{LacW}l(3)s095214</i>
<i>mod⁰⁷⁵⁷⁰</i>	<i>P{PZ}ms(3)07570</i>

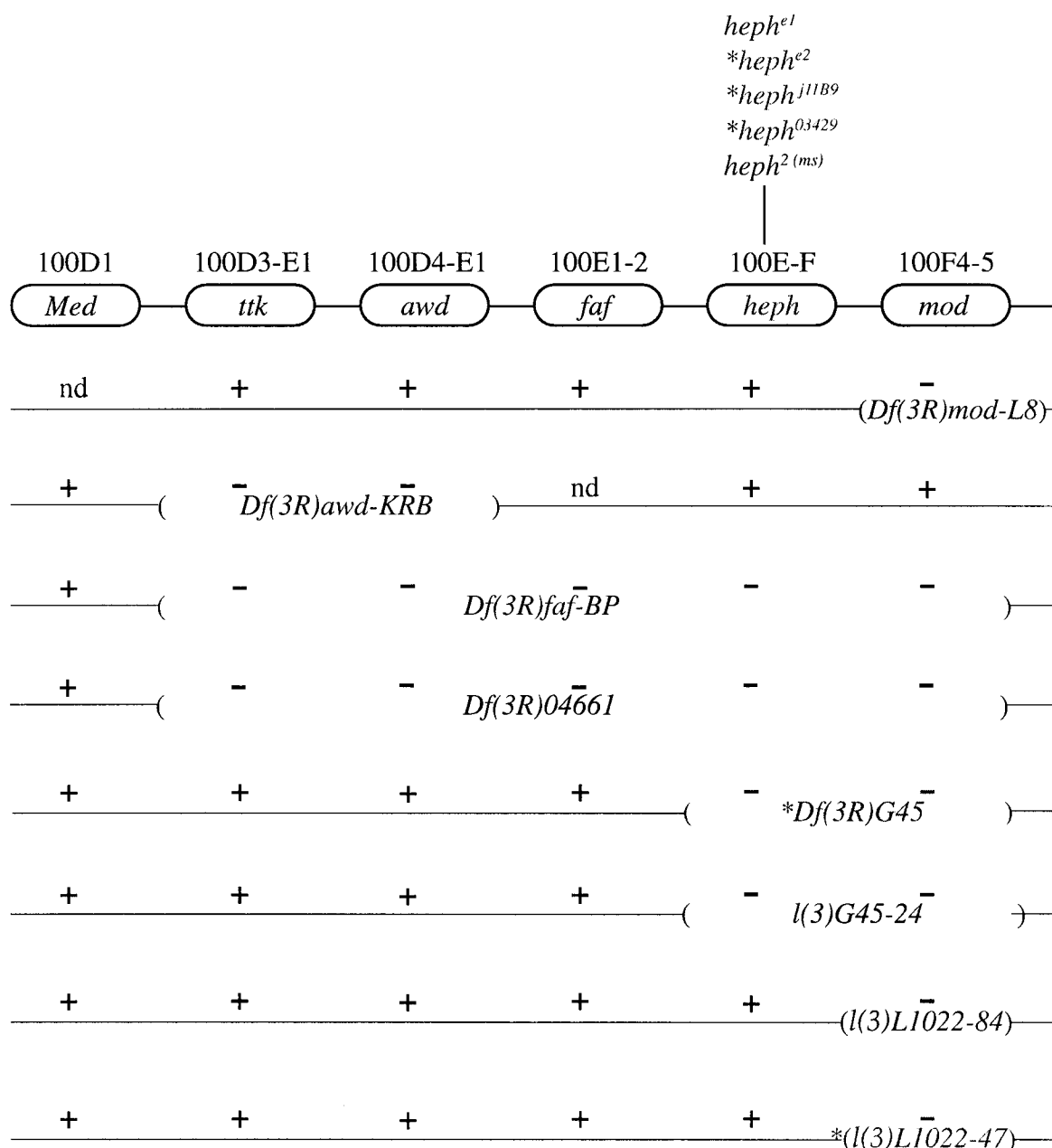


Figure 17. Diagrammatic summary of the genetic analysis of *hephaestus*.

The deficiencies and alleles that can induce ectopic margin in genetic mosaics are represented in blue and are marked with an asterisk (*). For simplicity, *Df(3R)G45* has been grouped with *l(3)G45-11*, *l(3)G45-66*, *l(3)G45-L73*, *l(3)L1022-162*, and *l(3)A4-4-74*; while *l(3)L1022-84* has been grouped with *l(3)L1022-37*, *l(3)L1022-145* and *l(3)L1022-146* due to their identical complementation patterns.

3.1.4 Complexities in the *hephaestus* complementation pattern

Alleles of *heph* and *mod* were tested for allelism to the lethal P-element excision derivatives of $P\{PZ\}G45$, $P\{LacW\}L1022$ and $P\{wA\}4-4$ (Table 5 and Fig. 17). Surprisingly, a complete correlation between the lethality of *heph* alleles and the ectopic margin genetic mosaic phenotype was not observed. First, although $l(3)G45-24$ fails to complement each of the four *heph* lethal alleles, no ectopic margin was observed when mitotic clones of $l(3)G45-24$ were made using the FLP/FRT system and *y* as a clone marker. This experiment was repeated with several different $P\{neoFRT\}82B$ $l(3)G45-24$ recombinants but the cell marker used does not allow the identification of mutant tissue that is not associated with margin bristles. As was done for all recombinants, the presence of the $P\{neoFRT\}$ transgene was selected using its neomycin resistance selectable marker and the presence of $l(3)G45-24$ was tested through complementation with $Df(3R)G45$. However, because *yellow* only marks bristles, the presence of $l(3)G45-24$ mutant clones in the wing blade could not be verified. Second, although $l(3)L1022-47$ complements the lethality each of the four *heph* alleles, it is able to induce ectopic margin in mitotic clones. These results raised the possibility that the lethality of *heph* alleles was not directly related to the ectopic margin genetic mosaic phenotype. It was also possible that loss of a combination of loci disrupted by $Df(3R)G45$ was required to elicit the ectopic margin phenotype. However, several lines of evidence suggest that neither of these are likely.

Prior to this study, *modulo* was the only lethal complementation group mapped to this region, and $Df(3R)G45$ fails to complement the *mod* lethality. *mod* is a characterized suppressor of position effect variegation and is the most distal lethal complementation group on 3R (Garzino et al., 1992). *Microtubule-associated protein 205* (*Map205*), a non-essential gene overlapping the *mod* transcription unit (Pereira et al., 1992) and *kurtz* (*krz*), a β -Arrestin ortholog (Roman et al., 2000), map very close to *mod* and may also be deleted by $Df(3R)G45$.

Mitotic clones of $Df(3R)mod-L8$, mutant for *mod*, *krz* and *Map205*, differentiate short, slender thoracic bristles and a Minute phenotype in the wing blade, but ectopic wing margin was not observed (Garzino et al., 1992; Pereira et al. 1992, J. Pradel, personal communication). As previously indicated, $mod^{s095214}$ is not associated with ectopic margin in genetic mosaics using the FLP/FRT method and *y* as a clone marker. $mod^{s095214}$ disrupts *mod* and also disrupts *kurtz-arrestin* (*krz*; Roman et al. 2000). These results indicate that loss of *modulo*, *Map205*, or *krz* is not sufficient to explain the ectopic margin phenotype of $Df(3R)G45$ clones.

To test whether loss of *mod* or *krz* was necessary to elicit the *ema* phenotype, $Df(3R)G45$ mitotic clones were induced in a $mod^+ krz^+$ genetic background (for details of method used, see Fig. 7 and section 2.6). In this experiment, $Df(3R)G45$ mutant tissue was marked with the bristle marker Sb^{63b} . $Df(3R)G45$ clones in $mod^+ krz^+$ flies still induce

ectopic margin (36 patches of ectopic margin in 140 wings). This is slightly higher than the frequency of ectopic margin observed in control flies from the same experiment (Curly wings, no *mod*⁺*krz*⁺ transgene; 23 patches of ectopic margin in 116 wings). Another difference also suggests that *Df(3R)G45* mitotic clones have a growth defect due to loss of *mod* and/or *krz*. In control Curly winged flies, only four homozygous mutant *Sb*^{63b} macrochaetae were observed (70 thoraces), while in straight winged *mod*⁺*krz*⁺ flies, 39 homozygous mutant *Sb*^{63b} macrochaetae were observed (58 thoraces). The presence of ectopic thoracic macrochaetae was also higher in *mod*⁺*krz*⁺ flies, which had 19 duplicated macrochaetae compared to 3 in control flies. These data suggest that *Df(3R)G45* clones have a growth defect due to loss of *mod* and/or *krz* that is rescued by the *mod*⁺*krz*⁺ transgene. It seems likely that a growth defect of *Df(3R)G45* mutant tissue would be due to loss of *mod*, which has a Minute-like phenotype in clones (Garzino et al., 1992). Additionally, the presence of ectopic margin in *Df(3R)G45* genetic mosaic wings with a *mod*⁺*krz*⁺ transgene indicate that loss of *mod* or *krz* is not required to elicit the ectopic margin phenotype. Since alleles of *mod*, *MAP205*, and *krz* do not cause the *ema* phenotype, and loss of *mod* or *krz* is not required to elicit it, alleles associated with the *ema* phenotype probably disrupt a previously uncharacterized transcription unit.

Since *l(3)L1022-47* complements the lethality of *heph* alleles, but is able to induce ectopic margin in genetic mosaics, it seems to separate the lethality of *heph* alleles from the *ema* phenotype. Except for *l(3)L1022-47*, complementation results support a model in which the *ema* phenotype is caused by loss of *heph*. If this were true, *l(3)L1022-47* might be complementing the lethality of *heph* alleles through inter-allelic complementation. The alternative explanation is that *l(3)L1022-47* disrupts *ema* but not *heph*, and that each of the *heph* alleles associated with the *ema* phenotype has two mutations: one lethal *heph* mutation and a second non-lethal *ema* mutation. The presence of multiple allelic mutations on each of *heph*^{e2}, *heph*⁰³⁴²⁹ and *heph*^{11B9} seems remote because each is an independently isolated lethal allele. However, it is formally possible that these alleles disrupt multiple (possibly overlapping) transcription units.

3.1.5 Identification of the *hephaestus* transcription unit

First, I will describe the work of Brook (1994) and Finkielstein (1997) that was carried out to identify transcripts near the *P{PZ}G45* insertion. The enhancer trap screen of Brook (1994) was designed to identify genes expressed during pattern regeneration in imaginal discs. Because *P{PZ}G45* was isolated in this screen, it was possible that sequences flanking the insertion could include sequences from a gene reported by *P{PZ}G45* during regeneration.

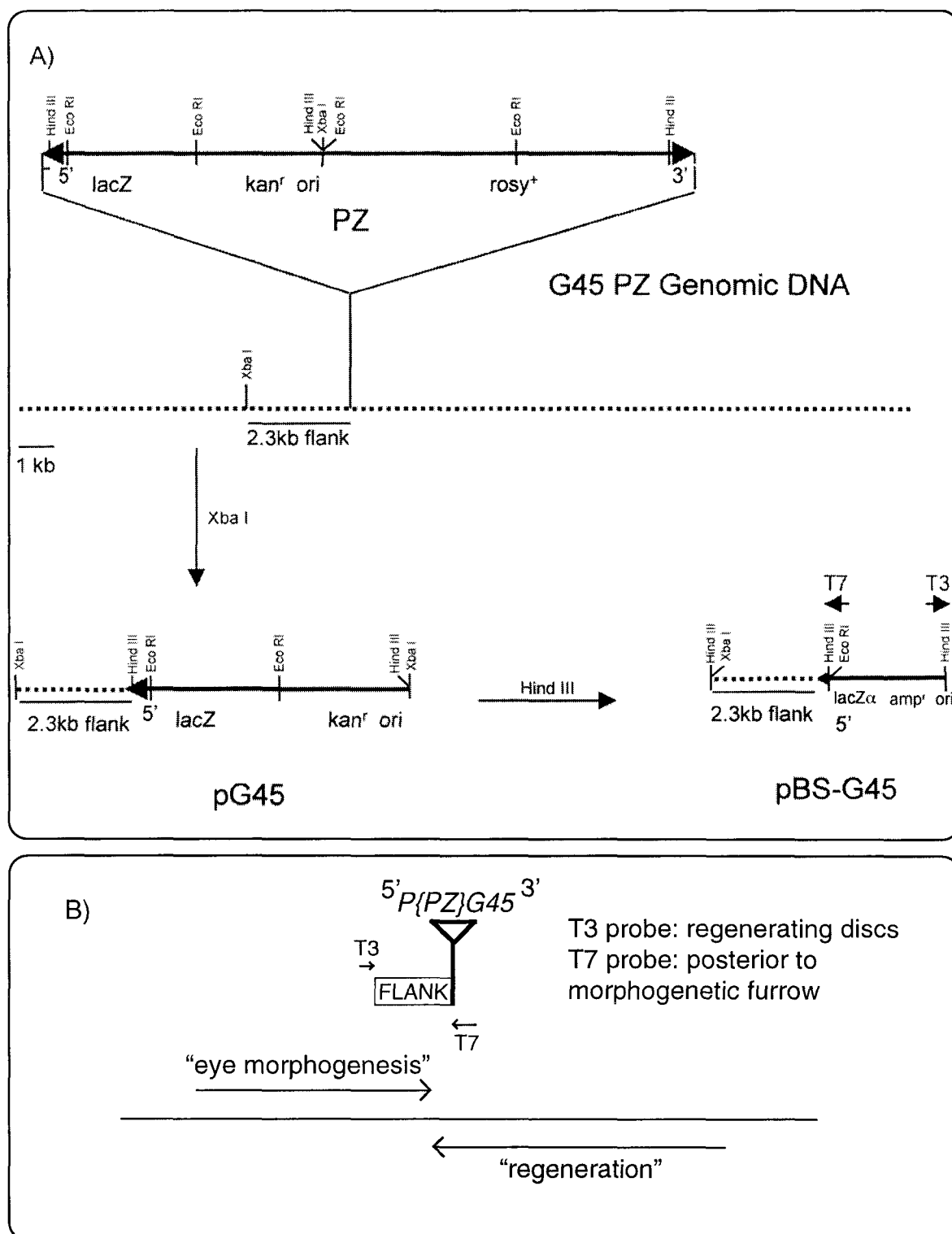
An approximately 2.3kb segment of genomic DNA flanking the *P{PZ}G45* insertion was isolated by plasmid rescue and was subcloned into the pBluescript vector (pBS) by Brook (1994) to produce pBS-G45 (Fig. 17A). To identify any transcript included in pBS-G45 expressed during disc regeneration, digoxigenin (DIG) labeled T3 or T7 transcript from pBS-G45 were hybridized to control and regenerating (*su(f)*¹² heat-treated) discs (Brook, 1994). Staining using the T3 probe suggested a generally transcribed gene expressed in regenerating discs but not in control discs. The T7 probe labeled cells behind the morphogenetic furrow in control eye discs and its staining was not affected by heat treatment. These staining patterns can be explained if genomic DNA flanking *P{PZ}G45* includes parts of two transcripts, one involved in regeneration—complementary to the T3 probe—and one involved in eye morphogenesis—complementary to the T7 probe (Brook, 1994).

To systematically search for transcripts near the *P{PZ}G45* insertion, I used the G45 flanking DNA as a probe to identify genomic DNA clones previously mapped to 100E-F that included the *P{PZ}G45* insertion. Genomic DNA flanking *P{PZ}G45* hybridizes to members of a cosmid contig (Siden-Kiamos et al., 1990) and P1 contig (Kimmerly et al., 1996) at 100E-F that span *heph*⁰³⁴²⁹ and *mod* (Fig. 19). A restriction map of cosmid 12C5 was made by analyzing restriction fragment patterns (Fig. 22A) and each *Hind*III fragment of cosmid 12C5 was subcloned for use as a probe for mapping *heph* alleles (described below).

As I will describe next, the *Drosophila* genome sequence (Adams et al., 2000; Myers et al., 2000) is a powerful tool that, together with the use of P-elements, has simplified gene mapping in *Drosophila*.

Figure 18. Model of transcripts complementary to the $P\{PZ\}G45$ genomic flanking DNA.

(A) Representation of the method used to isolate genomic DNA flanking the G45 P-element. First, genomic DNA was restricted with *Xba*I, ligated, and pG45 was isolated by selecting transformants for kanamycin resistance. The *Hind*III fragment of pG45 was subcloned into the pBluescript vector to create pBS-G45. Notice that the genomic flanking DNA was isolated from the 5' end of the P-element. Also notice the orientation of the T3 and T7 promoters of pBS-G45 relative to the orientation of the G45 P-element. (B) A model to account for the *in situ* staining pattern using the T7 and T3 probes from pBS-G45. In this model, the T7 probe recognizes a gene expressed posterior to the morphogenetic furrow of the eye disc, and the T3 probe recognizes a gene expressed in regenerating imaginal discs.



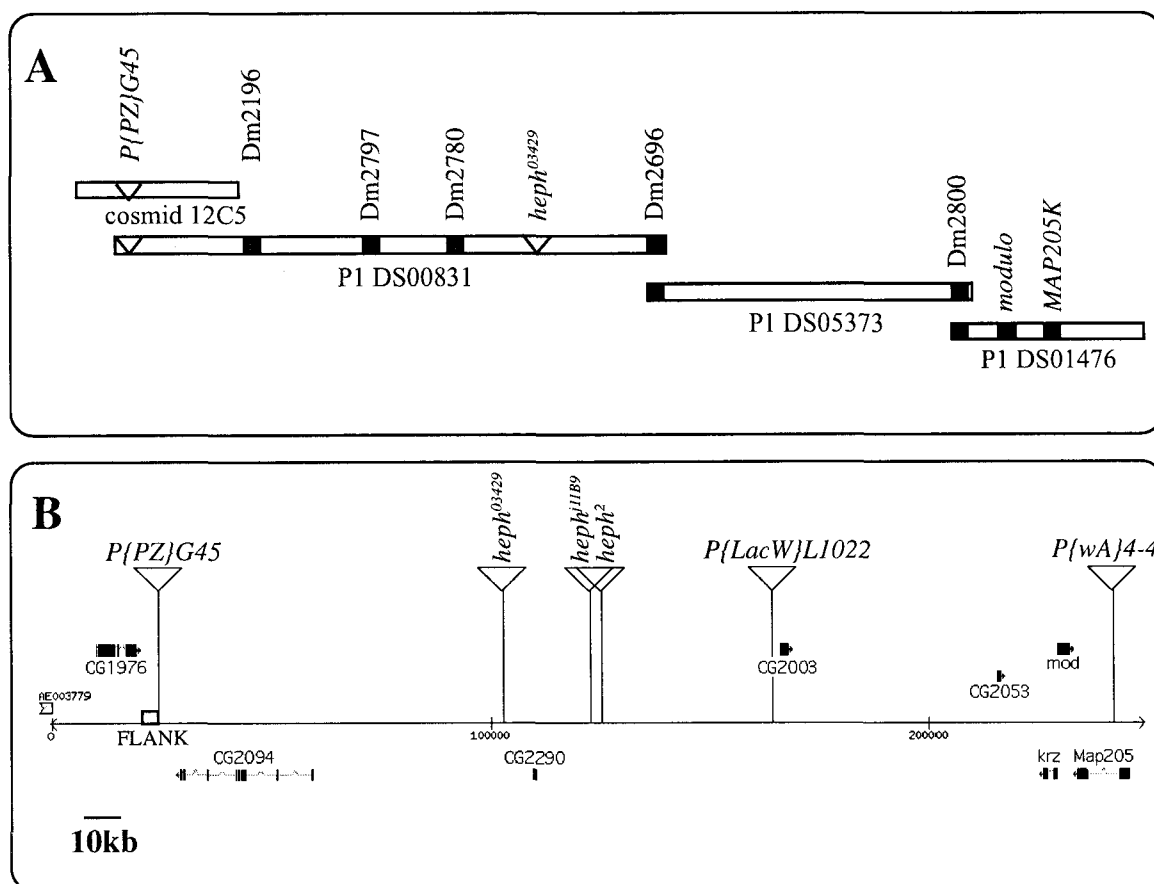


Figure 19. Schematic representation of overlapping Cosmid and P1 clones including sequences from *P{PZ}G45*, *heph* and *mod*.

(A) Genomic DNA flanking the *P{PZ}G45* insertion site hybridizes to cosmid 12C5 [100E-F], and to P1 clone DS00831 [100F1-2]. P1 clone DS00831 is part of a large P1 contig that covers most or all of 100F, including *P{PZ}G45* and *heph*⁰³⁴²⁹ insertion points and *mod*. This information suggests that *Df(3R)G45* may delete up to 180kb of genomic DNA (the length of 3 average P1 clones). Each filled box represents an STS used by BGD members to construct this P1 contig (Kimmerly, et al. 1996). Triangles represent P-element insertions. (B) A representation of predicted genes mapping to 100F (AE003780) adapted from the Flybase genome annotation illustrates the relation of *heph* mutations and viable P-element insertions used for excision mutagenesis to predicted genes in the region (3R telomere, right).

Including *Df(3R)G45*, all 7 of the *P{PZ}G45*, *P{LacW}L1022* and *P{wA}4-4* lethal excision derivatives that are associated with ectopic margin in genetic mosaics disrupt *mod*. Although loss of *mod* is not required for the ectopic margin phenotype, it is likely that the gene responsible for the *ema* phenotype maps close to *mod* and to the *P{PZ}G45*, *P{LacW}L1022*, *P{wA}4-4*, and *heph* P-elements. These P-element insertions and *mod* were mapped through sequence analysis to help identify the transcription unit responsible for the *ema* phenotype.

Genomic DNA sequences adjacent to a P-element insertion can be easily obtained using inverse PCR. To summarize this method: genomic DNA isolated from an insertion strain is digested with a restriction enzyme known to recognize internal P-element sequences. The digested genomic DNA is ligated to create many small circular genomic DNA molecules used as PCR templates. Primers have been designed by BDGP members for each P-element that face outward from the P-end so that genomic DNA next to the P-element in a circular ligated molecule is amplified. The products of the PCR reaction are then sequenced, producing a sequence tag site (STS) for that particular P-element insertion. STSs are available for many P-elements available from the public stock centers. For this project, available STSs include *P{PZ}heph⁰³⁴²⁹*, *P{PZ}heph²*, and *P{LacW}L1022*. An STS for *P{LacW}heph^{11B9}* was obtained, and that of *P{PZ}heph⁰³⁴²⁹* was confirmed, through inverse PCR. The *P{PZ}G45* STS was obtained by sequencing plasmid rescued genomic DNA by Finkielstein (1997). An STS is not available for *P{wA}4-4* but it has been mapped by Southern analysis to the 3R telomere (Garzino et al., 1992). The following results are summarized in Fig. 19B.

By sequence comparison using BLAST, the *P{PZ}G45* STS (AF436843) maps to genomic scaffold section 105/105 at 100F (AE003780). *mod*, *Map205* and *krz* are ~200kb away from the *P{PZ}G45* insertion point. Between *mod* and *P{PZ}G45* are four predicted genes: *CG2094*, predicted to encode an RNA binding protein similar to human polypyrimidine tract binding protein (PTB); *CG2290*, predicted to encode a novel protein; *CG2003*, predicted to encode an inorganic phosphate transporter; and *CG2053*, predicted to encode a novel protein. Telomere proximal to the *P{PZ}G45* insertion point is *CG1976*, predicted to encode a GTPase activator protein. There are no characterized alleles of *CG1976*, *CG2003* or *CG2053* so the correlation between their disruption and the *ema* phenotype could not be tested. In addition, there is currently a ~9kb gap in the genomic DNA sequence near *CG2094*, which is large enough to encode another gene. It is possible that *Df(3R)G45* disrupts (at least) these 8 genes.

Notice the relation between the model presented in Fig. 18B and the predicted genes illustrated in Fig. 19B. *CG2094* and *CG1976* are both close to *P{PZ}G45* and could provide the enhancer(s) reported by *P{PZ}G45* in regenerating discs. It is possible that *CG1976* is expressed in the eye disc as cDNA sequences from *CG1976* are included in the *P{PZ}G45* flanking DNA in the opposite orientation to the T7 promoter. Since *CG2094* is transcribed in the opposite orientation to the T3 promoter, which reports

expression in regenerating discs, it is tempting to speculate that *CG2094* expressed during regeneration. However, there are no known cDNA sequences from *CG2094* which map to the *P{PZ}G45* flanking DNA. See Fig. 22A for an alignment of cDNA sequences in the region to the flanking DNA. Since *CG2094* is a complex transcription unit (see below) it is possible that uncharacterized parts of the gene map to the flanking DNA. It would be interesting to characterize the *CG2094* expression pattern in regenerating discs.

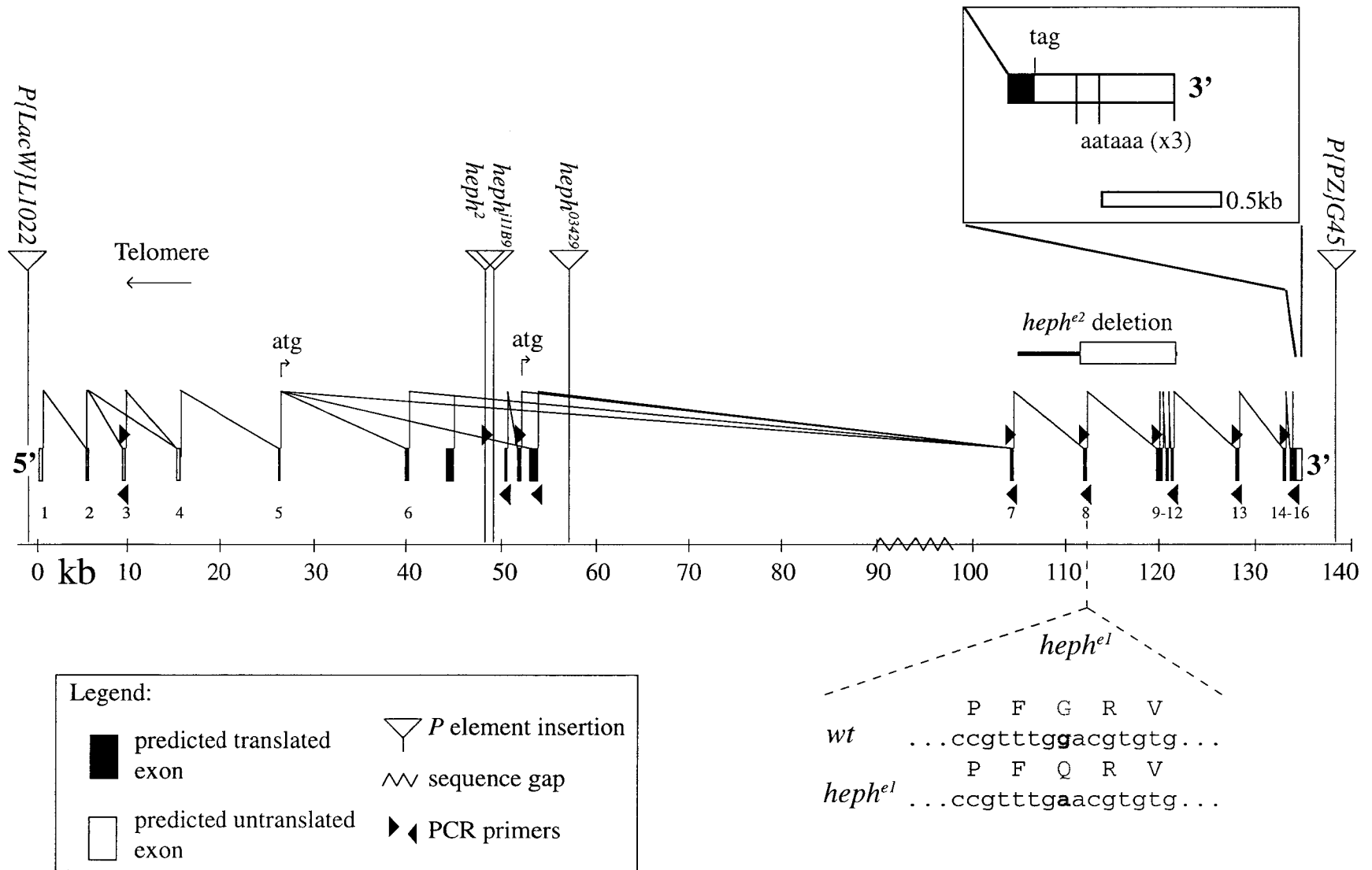
To map *heph* alleles to a transcription unit, DNA sequence flanking the *heph*² (AQ026438), *heph*⁰³⁴²⁹ (G00761), and *heph*^{j11B9} (AF373596) insertion points were mapped to genomic DNA. These three P-elements map within a ~10kb interval, ~90kb away from *P{PZ}G45*. Within this 10kb interval lies *CG2290*, predicted to encode a novel protein, and a single 5' EST from cDNA clone HL05832. HL05832 was sequenced and was not studied further because it appears to be a ~4kb fragment of genomic DNA unrelated to *CG2290* spanning the *heph*^{j11B9} insertion point. No additional genes were predicted within 50kb of genomic DNA spanning the *heph* P-element insertions by the gene prediction programs Genie (http://www.fruitfly.org/seq_tools/genie.html), Genscan (<http://genes.mit.edu/GENSCAN.html>) or Grail (<http://compbio.ornl.gov/Grail-1.3/>).

The 200kb of genomic DNA around the *heph* P-element insertions was compared to an EST database using BLAST. This search revealed a large set of 5' and 3' ESTs that suggest a ~145kb transcription unit including *CG2290* and *CG2094* sequences. From this group of ESTs, two different cDNAs, LD04329 (0-22hr embryo, AY052367) and GH17441 (adult head, AF436844), were selected for sequencing. GH17441 was selected because in addition to a 5'EST similar to many of the other ESTs, its 3'EST was available and it mapped very close to *P{PZ}G45*. LD04329 was selected because it had the only 5'EST including sequences from *CG2290*. For details of the sequencing method, see section 2.13.4. The full-length sequence of these cDNAs and two others (CST01 from C. Schulz and *PTB* from D. Standiford) have been used to construct a transcription map by sequence comparison using BLAST. This transcription unit is alternatively spliced and alternatively poly-adenylated (Fig. 20). All four cDNAs share the predicted coding exons of *CG2094*. Only LD04329 includes sequences of *CG2290*. CST01 and *PTB* are shorter than LD04329 and GH17441 and may not be full-length clones or may be produced by alternative promoters. The proteins predicted from *in silico* translation of each of the transcripts include a core sequence of 4 RNA recognition motifs (RRMs) with different N-terminal sequences depending on alternative splicing patterns. The N-terminal region predicted from LD04329 includes a poly-glutamine tract not included in the other proteins. Although the significance of this difference is not known, it may relate to the complex *heph* complementation pattern.

Figure 20. Physical map of the *hephaestus* transcription unit.

The 4 sequenced *heph* cDNAs (LD04329, AY052367; GH17441, AF436844; CST01, unpublished; *PTB*, AF211191) were aligned with genomic DNA to construct this map of the exon/intron boundaries of *heph* (5' and telomere are left). The viable P-element insertions *P{LacW}L1022* and *P{PZ}G45* map outside of the predicted *heph* transcription unit. The lethal P-element insertion alleles *heph*⁰³⁴²⁹ and *heph*^{11B9}, and the male sterile P-element insertion *heph*² map to *heph* introns. The lethal EMS-induced *heph*^{e2} mutation deletes exons 8-12, and the lethal EMS-induced *heph*^{e1} mutation is a g:c to a:t transition that changes a glycine (G) residue to a glutamine (Q) residue in the predicted *heph* protein. Primer pairs that were used to sequence the *heph*^{e1} and *heph*^{e2} mutations are represented by black arrowheads.

Inset: 3 different poly-A signals are present in the genomic DNA corresponding to the position of 3 different poly-A tails from these 4 cDNAs. This suggests that each cDNA is complete at its 3' end and that the 3'UTR differs between these transcripts.



The first published *mRNA* sequence from this transcription unit was isolated by sequence similarity to human *polypyrimidine tract binding protein* (*PTB*; AF211191 and D. Standiford, personal communication). Until I present evidence that *heph* is synonymous with *PTB*, I will refer to this transcription unit as *PTB*.

3.1.6 Male recombination-induced mutations at polytene region 100E-F

Although the *heph* P-element alleles all map to *PTB*, they map to introns ranging in size from ~8kb to ~50kb, and it is possible that there are uncharacterized, unpredicted genes in these introns. In order to correlate loss of *PTB* exons with the lethality of *heph* alleles, and possibly the *ema* phenotype, I used male recombination to try to engineer deletions of 3' *PTB* exons.

There is normally no recombination in *Drosophila* males. However, with the addition of a *P-transposase* source, recombination can be induced at the position of P-element insertions. This male recombination at P-elements has been used to isolate "designer deletions" with a breakpoint at one end of the P-element (Preston and Engels, 1996; Preston et al., 1996). The P-element is often left intact allowing the precise mapping of the resulting mutations with inverse PCR from known P-element sequences.

The crossing scheme used to isolate male-recombinants is described in Fig. 13 and section 2.9.3. In short, non-ebony orange-eyed flies were selected from the progeny of a *e P{w⁺} / P{PZ}G45* male carrying a P-transposase source. It was expected that any deletions isolated in this screen might be molecularly mapped by inverse PCR from *P{PZ}G45* to identify a possible deletion of *PTB* exons. 10 putative male-recombinants were isolated, all are viable and complement *Df(3R)G45*. One interesting male recombinant, *mr55*, is completely penetrant for a detached posterior crossvein phenotype that is not associated with either of the parent chromosomes (Fig. 21). However, no reliable sequence has been obtained by inverse PCR from *P{PZ}G45* sequences to molecularly map the distal breakpoints of a putative *mr55* deletion. The *PTB* transcription unit appears to be intact in *mr55* homozygotes since even the most 3' *PTB* exons can be amplified by PCR using the same primers designed for EMS allele sequencing (see below). By Southern analysis, different restriction fragment patterns exist both telomere proximal and distal to the *P{PZ}G45* insertion in *mr55* homozygotes compared to the original *P{PZ}G45* line (data not shown). *mr55* can not be explained in terms of a simple deletion and there is insufficient evidence to define a more complex rearrangement, so it is only possible that *mr55* disrupts the *PTB* transcription unit.

The detached posterior crossvein phenotype of *mr55* homozygotes warrants a closer examination. Most *heph* alleles are homozygous lethal, and fail to complement one another, with one exception. Flies of genotype *heph^{el} / 1(3)L1022-162* survived to

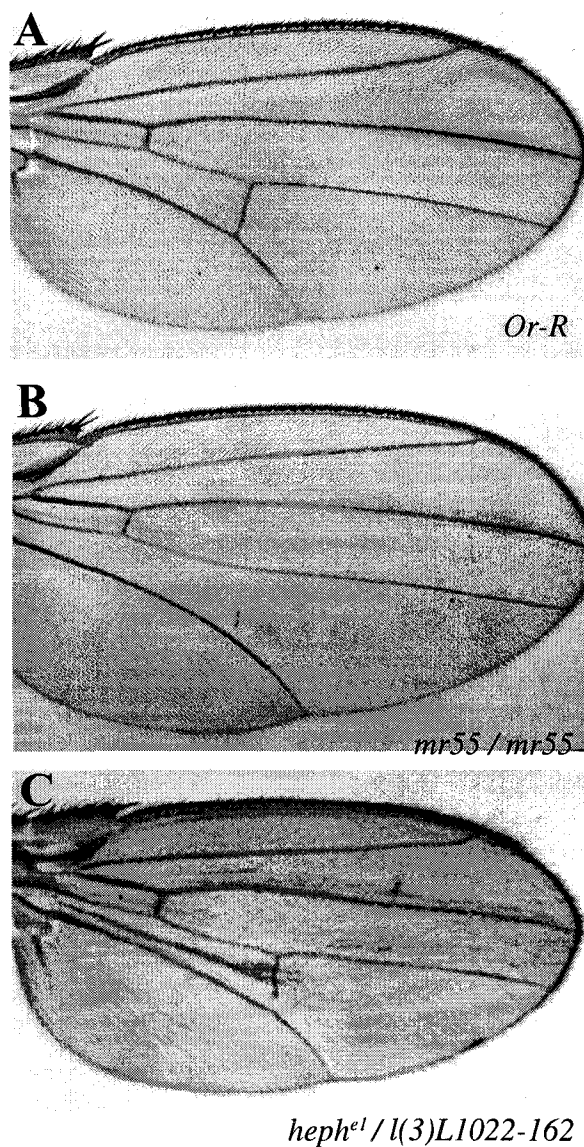


Figure 21. Examples of detached posterior crossveins from *mr55* and *hephaestus* mutant flies.

(A) An example of a wildtype wing. (B) An example of a wing from an *mr55* homozygous fly with a detached posterior crossvein. About half of *mr55* homozygotes are this severe, while the remaining half are only detached at one end. (C) An example of a wing from a rare *heph^{el} / l(3)L1022-162* escaper. This wing is typical, with only one end of the posterior crossvein detached. What appears to be extra vein material are folds in the wing. The detached crossvein phenotype was never observed for the anterior crossvein.

adulthood at a very low frequency, and these survivors had detached posterior crossveins (Fig. 21). In addition, *mr55* in *trans* with *Df(3R)G45* (19/158), *heph*⁰³⁴²⁹ (73/186) or *heph*^{11B9} (9/86)—but not with *Or-R* (0/100)—have the same detached crossvein phenotype, albeit at a lower penetrance than *mr55* homozygotes. These results suggest that the detached phenotype is related to *heph* and hint at a role for *heph* in attaching crossveins to the longitudinal veins. This will be discussed as it relates to Notch signalling.

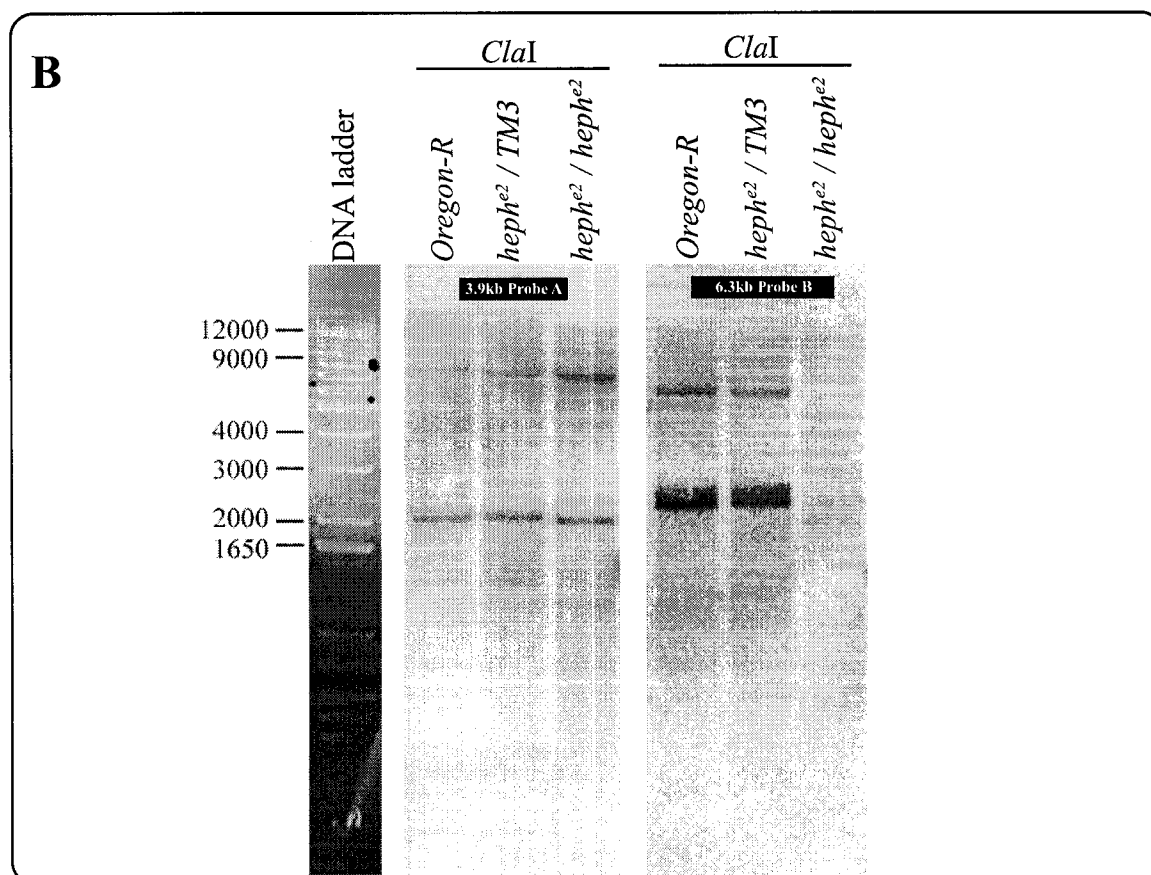
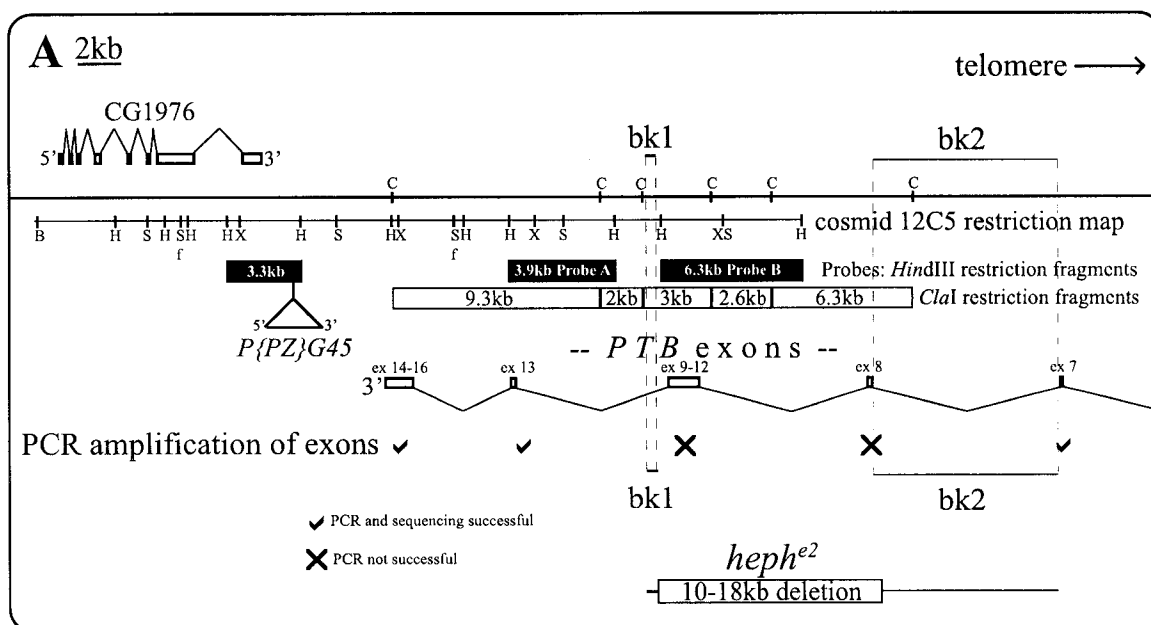
3.1.7 Sequencing EMS-induced alleles of *hephaestus*

Since *PTB* is the transcription unit most likely disrupted by the *heph* P-elements, PCR primers were designed to amplify and sequence the exons and intron/exon boundaries of *PTB* from *heph* mutant larvae. To study the terminal phenotype of *heph*, each *heph* lethal allele was balanced over *TM3*, *P{Act-GFP}*, *Ser*. This balancer carries a transgene expressing GFP under the control of an *Actin* promoter. Dechorionated embryos after stage 11 and any larvae expressing GFP from this transgene can be easily identified with a fluorescent dissecting microscope by their green fluorescence. Similar results were obtained from each of the four *heph* alleles: ~1/4 of the embryos expressed GFP and did not hatch; these were likely homozygous *TM3* embryos. ~1/2 of the embryos hatched into GFP expressing larvae, which were likely heterozygous animals. ~1/4 of the embryos hatched and did not express GFP. These were likely homozygous *heph* mutant larvae and were easily separated from their GFP-expressing sibs. The homozygous mutant *heph* larvae moved and grew slowly compared to their heterozygous sibs. At 25°C, homozygous mutant *heph* larvae die during the first larval instar. Cuticle preparations of homozygous first instar larvae were normal (data not shown). In contrast to other *heph* alleles, *heph*^{e1} homozygotes exhibit a multi-phasic lethal phenotype at 18°C. Of 50 *heph*^{e1} homozygous larvae that were grown at 18°C, 12 died during L1, 22 during L2, 4 during L3 and 12 died as apparently normal pharate adults.

At 18°C, *heph*^{e1} homozygotes survive longer than at 25°C, indicating that *heph*^{e1} is a temperature-sensitive *heph* allele. This might explain its inability to induce ectopic margin in genetic mosaics. That *heph*^{e1} is a weak *heph* allele is also supported by sequence data. *heph*^{e1} is a G:C to A:T transition causing a missense mutation in *PTB*. This mutation changes a conserved polar but uncharged Glycine (G) residue to another polar but uncharged Glutamine (Q) residue in RRM1 of *PTB* (Fig. 45). When several *PTB* exons could not be amplified by PCR from homozygous *heph*^{e2} DNA, Southern analysis was used to test the possibility that those exons were deleted by the *heph*^{e2} mutation. Using two different *HindIII* fragments from cosmid 12C5 as probes, it is clear that *heph*^{e2} genomic DNA contains a deletion of several exons of *PTB* (Fig. 22). These exons include the coding region for RRM1, RRM2 and part of RRM3. Because of the severity of this mutation, it may be a null allele of *PTB*. On the strength of this sequence data, and the insertion of 3 P-element induced *heph* alleles to *PTB* introns, it appears that all five *heph* alleles disrupt *PTB*, indicating that *heph* is synonymous with *PTB*.

Figure 22. Breakpoint map of the *heph^{e2}* deletion.

(A) The 3.3kb shaded *Hind*III fragment was used as a probe to make this restriction map of cosmid 12C5. *Cla*I restriction sites (C) were predicted using DNA Strider software and are shown on a line representing genomic DNA at 100E-F. Cosmid 12C5 has been aligned with genomic DNA sequences by comparing the *P{PZ}G45* STS (AF436843) and this restriction map to the genomic DNA. The 3.9 and 6.3kb shaded *Hind*III fragments of cosmid 12C5 were used to map the *heph^{e2}* deletion. Below the restriction map is a representation of several 3' exons of *PTB*, aligned by comparing *PTB* cDNA sequences to the genomic DNA. (B) Southern hybridization results used to map the breakpoints of the *heph^{e2}* deletion. Scale numbers (in bp) are interpretations of the 1kb Plus DNA Ladder (Gibco-BRL, Inc.) size markers. Using the 6.3kb probe, *heph^{e2}* homozygotes are missing 3 bands corresponding to the 3kb, 2.6kb and 6.3kb *Cla*I fragments of cosmid 12C5. The 3.9kb probe was used on the same blot to control for consistent loading and restriction digestion of genomic DNA and to map more precisely *heph^{e2}* breakpoint 1 (bk1). Restriction enzymes: H *Hind*III, S *Sal*I, Sf *Sfi*I, X *Xba*I, C *Cla*I, B *Bam*HI.



3.1.8 Rescue of the *hephaestus* genetic mosaic phenotype

If *heph* is synonymous with *PTB*, over-expression of *PTB* in the wing disc might induce gain-of-function phenotypes complementary to the *heph* loss-of-function phenotype of ectopic wing margin. The GAL4/UAS system of Brand and Perrimon (Brand and Perrimon, 1993) was used to express a *PTB* cDNA (CST01) driven from a *UAS-PTB* transgene (C.Schulz, unpublished) using *ap-GAL4*, *C96-GAL4* and *omb-GAL4*. These GAL4-expressing transgenes were chosen for their unique patterns of GAL4 expression in wing discs. The *ap-GAL4* transgene drives GFP expression in the *apterous* expression domain, i.e. in all dorsal wing disc cells (O'Keefe et al., 1998). *C96-GAL4* drives GFP expression in cells spanning the D/V boundary (Gustafson and Boulianne, 1996). *omb-GAL4* drives GFP expression in the *optomotor blind** expression domain, i.e. in a wide band of cells spanning the A/P boundary and crossing the central portion of the D/V boundary (Lecuit et al., 1996). These expression domains were confirmed by crossing each line to a stock carrying a *P{UAS-GFP}* transgene and observing green epifluorescence in wing discs from F1 roaming third instar larvae (data not shown).

UAS-PTB and *C96-GAL4* are homozygous viable transgene insertions with no visible adult phenotype. However, flies transheterozygous for *UAS-PTB* and *C96-GAL4* typically have some wing margin loss, although the phenotype is variable (Fig. 23B). *ap-GAL4* induces a strong *ap* hypomorphic mutation, but appears normal when heterozygous with a *CyO* balancer or with a wildtype chromosome (data not shown). Flies transheterozygous for *UAS-PTB* and *ap-GAL4* die at 25°C, lose most of their wing margin at RT, and look nearly normal except for a thick vein phenotype at 18°C (Fig. 23C,D). The change in phenotypic severity at different temperatures could be due to temperature-dependent changes in expression from the *UAS-PTB* transgene, since the GAL4/UAS combination causes more severe overexpression phenotypes at higher temperatures (Speicher et al., 1994). *omb-GAL4* induces a homozygous viable *omb* hypomorphic mutation, and causes a distal wing nicking phenotype in homozygous females and hemizygous males. Hemizygous males from a cross between *omb-GAL4* and *Or-R* were compared to males from a cross between *omb-GAL4* and *UAS-PTB* (hemizygous *omb-GAL4*, with one copy of *UAS-PTB*). Compared to the control, *omb-GAL4 UAS-PTB* flies have a more severe distal margin loss phenotype (Fig. 23E, F). This could be due to an enhancement of the *omb* phenotype, or due to expression of *PTB* in the *omb* expression domain. These data support a model where over-expression of *PTB* causes wings margin loss, which is opposite to the ectopic margin phenotype and is consistent with *heph* alleles disrupting *PTB*. The thick vein phenotype is also significant (see below).

* Also named *bifid*.

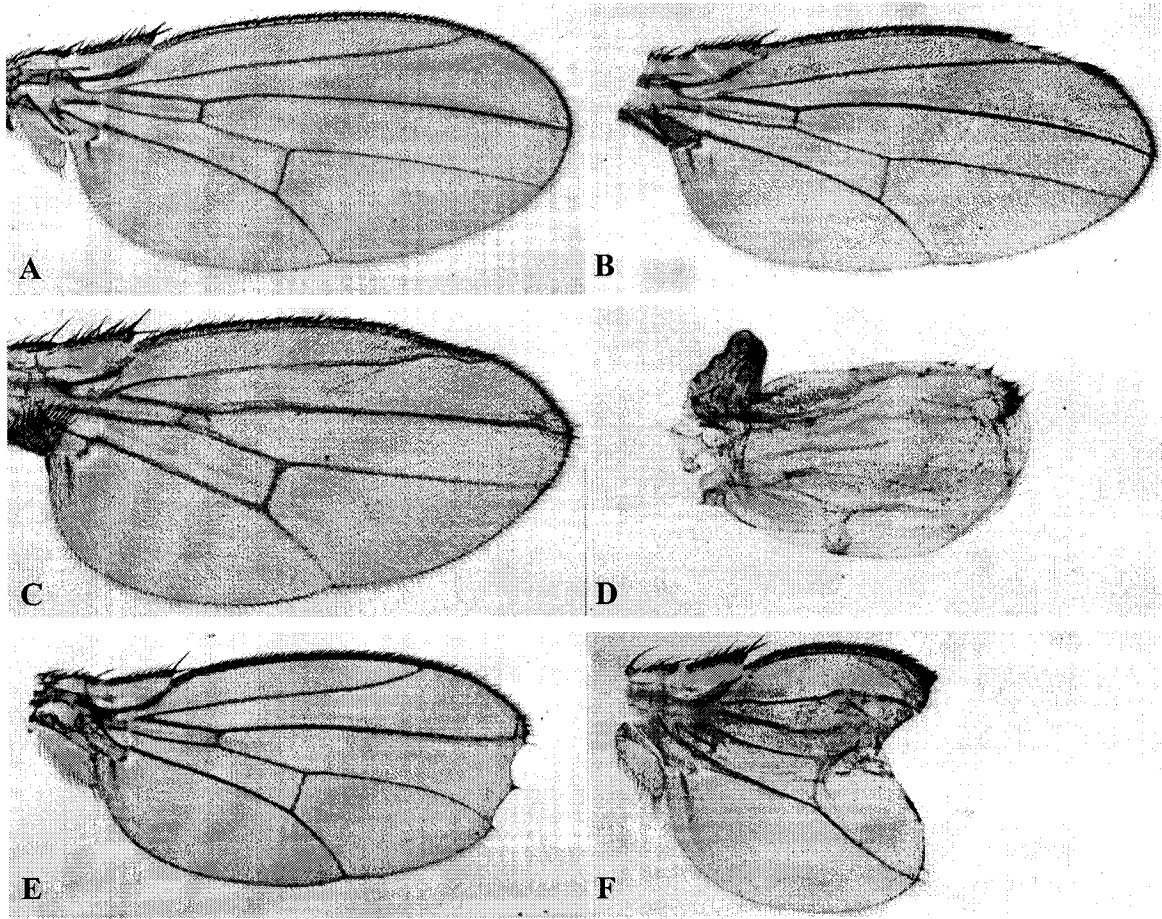


Figure 23. Ectopic expression of *PTB* is associated with wing margin loss.

(A) Wildtype wing. (B) *C96-GAL4/UAS-PTB* at 25°C. *C96-GAL4* drives expression in a band of cells that spans the D/V boundary. Notice the wing margin (WM) nick. (C) *ap-GAL4/UAS-PTB* at 18°C. *ap-GAL4* drives expression in all dorsal cells of the wing. The most noticeable defect at this temperature is wide veins. (D) *ap-GAL4/UAS-PTB* at room temperature. Most of the wing margin is missing. The *ap-GAL4/UAS-PTB* combination at 25°C is lethal. (E) *omb-GAL4/+* at 25°C. The *omb-GAL4* insertion is an *omb* allele and causes distal WM nicks. (F) *omb-GAL4/UAS-PTB* at 25°C. The distal WM nicks are more severe than *omb-GAL4* alone. *omb-GAL4* drives expression in a wide swath along the A/P axis, including the distal portion of the WM. All wings are typical examples of the phenotypes observed in male flies.

If the ectopic margin genetic mosaic phenotype of *heph* alleles is due to disruption of *PTB* expression, ectopic expression of *PTB* should suppress the formation of ectopic margin in *heph*⁰³⁴²⁹ genetic mosaics. Expression of a *PTB* cDNA (CST01) was again driven from a *UAS-PTB* transgene (C. Schulz, unpublished) with the dorsal specific *ap-GAL4* driver. Since *ap-GAL4* induces *PTB* expression only in dorsal wing disc cells, if *PTB* expression rescued the ectopic margin clonal phenotype, ventral but not dorsal ectopic margin would be expected in target class flies. Since the *ap-GAL4* / *UAS-PTB* combination is lethal at 25°C and results in loss of most of the wing margin at RT, this rescue experiment was carried out at 18°C. Flies of genotype *y w P{hsFLP} ; ap-GAL4 / UAS-PTB ; P{neoFRT}82B P{πM} Sb heph*⁰³⁴²⁹ / *P{neoFRT}82B P{hsGFP}* that were grown at 18°C and heat treated (1hr at 37°C) during second larval instar had both dorsal and ventral ectopic margin. Under these conditions, expression of *PTB* does not rescue the *ema* genetic mosaic phenotype of *heph*⁰³⁴²⁹. However, it is possible that the *ap-GAL4* / *UAS-PTB* combination does not express sufficient *PTB* to rescue *heph*⁰³⁴²⁹ at 18°C, since GAL4/UAS-dependent expression is directly related to temperature.

Therefore, the experiment was redesigned using *P{tubP-GAL80}*, which expresses a GAL4 repressor, in *trans* to *heph*⁰³⁴²⁹ so that *apGAL4* could induce expression of *PTB* only in *heph* clones (for method see Fig. 16 and section 2.12). Target class flies of genotype *y w P{hsFLP} ; ap-GAL4 / UAS-PTB ; P{neoFRT}82B P{πM} Sb heph*⁰³⁴²⁹ / *P{neoFRT}82B P{tubP-GAL80}* that were grown at RT and had been heat treated (1hr at 37°C) during second larval instar were compared to control class flies of genotype *y w P{hsFLP} ; (ap-GAL4 OR UAS-PTB) / CyO ; P{neoFRT}82B P{πM} Sb heph*⁰³⁴²⁹ / *P{neoFRT}82B P{hsGFP}* from the same vials. Results are presented in Table 9.

The proportion of target class flies with ventral ectopic margin (25/200) is roughly equivalent to that of control class flies (19/250), indicating similar wing clone induction frequencies between the control and target classes. As a second indicator of clone induction frequency, the presence of *Sb/Sb* or *Sb*⁺ marked thoracic macrochaetae was scored. Again, similar frequencies were observed in target class flies (64/100) and control class flies (71/125). The presence of ventral ectopic margin in the target class wings (25/200) indicates that *heph* clones were induced in the wings of target class flies. Because target class flies had no dorsal ectopic margin (0-1/200), while control class flies do (27/250), it appears under these conditions that *PTB* expression rescues the *ema* genetic mosaic phenotype of *heph*⁰³⁴²⁹. Additionally, the frequency of wing margin nicks is lower in rescued flies (9/200) compared to control flies (20/250). Since either a dorsal or ventral *heph* mutant clones can cause a wing margin nick (Fig. 29C,D), this result is consistent with dorsal *heph* rescue.

Table 9. Summary of the effects of *PTB* expression on the *hephaestus* ectopic margin phenotype.

	Rescue target class		Control class	
	Dorsal	Ventral	Dorsal	Ventral
Total number of flies	100		125	
Flies with <i>Sb/Sb</i> (clone) or <i>Sb</i> ⁺ (twin) thoracic macrochaetae	64		71	
Flies with <i>Sb/Sb</i> (clone) thoracic macrochaetae	36		42	
Total number of wings	200		250	
Number of wings with margin nicks	9		20	
Wing surface	Dorsal	Ventral	Dorsal	Ventral
Number of wings with ectopic margin	1 *	25	27	19

* This wing has two mTR bristles in the normal position of two dTR bristles and can be interpreted as an mTR to dTR fate transformation rather than ectopic wing margin.

However, high expression levels of *PTB* in dorsal *heph* mutant cells may simply kill the clone. If dorsal clones died, they might not induce ectopic margin. Without a marker for *heph* mutant cells in the adult wing, the presence of dorsal clones in the wings of target class flies is not certain. Since *ap-GAL4* is active in the presumptive thorax as well as presumptive dorsal wing, I scored the thoraces of target and control class flies for the presence of homozygous marked *Sb^{63b}* macrochaetae originating in a *heph* mutant clone. The frequency of *Sb^{63b} heph* clones in the thorax of target class flies is roughly equivalent to that in control class flies (Table 8). The presence of homozygous *heph* clones marked by *Sb^{63b}* in the thorax of target class flies shows at least that *PTB* expression does not kill all dorsal *heph* mutant cells, and suggests the presence of dorsal *heph* wing clones.

There is a near perfect correlation between lethality at the *heph* locus and the ectopic margin phenotype. All five molecularly mapped *heph* alleles map to a single complex transcription unit (*PTB*), indicating that the wing and male-sterile phenotypes are all due to loss of function in the same gene. The results of the rescue experiment suggest that *PTB* expression can rescue the ectopic margin phenotype of *heph* in genetic mosaics. Taken together, these results support the model that *heph* alleles disrupt expression of the *PTB* transcription unit. In this model, the multiple phenotypes and complex complementation pattern of the *heph* alleles may be related to the multiple spliced forms of the *PTB* transcripts. Although a recent report refers to this gene as *PTB* (Davis et al., 2002), there is precedence for the name *hephaestus* (Castrillon et al., 1993), which has been used here in accordance with *Drosophila* gene nomenclature.

3.2 Analysis of *hephaestus* in genetic mosaics

Analysis of genetic mosaics is useful for the study of genes with pleiotropic early lethal effects. This method allows heterozygous animals to survive past early developmental stages, after which small patches of mutant tissue of clonal origin (mitotic clones) can be induced within an otherwise wildtype animal at any developmental stage. However, in order to draw any conclusions about the effect of mutant clones on patterning, the position and extent of the mutant tissue must be known. Using a cell marker for mutant tissue, analysis of a mutation in genetic mosaics can provide useful information about the position and nature of a gene's function.

In this thesis, I have relied heavily on genetic mosaic analysis of the adult wing and thorax to study the role in development of *hephaestus* (*heph*). The innocuous cell markers *yellow*, which affects bristles, and *forked*, *bald*, and *pawn*, which affect both bristles and trichomes, were used to mark *Df(3R)G45* or *heph* mutant cells in genetic mosaics. These markers are discussed in more detail in the Materials and Methods (2.5) and in the accompanying Figure legends of this section.

3.2.1 *Df(3R)G45* mitotic clones marked with *yellow*

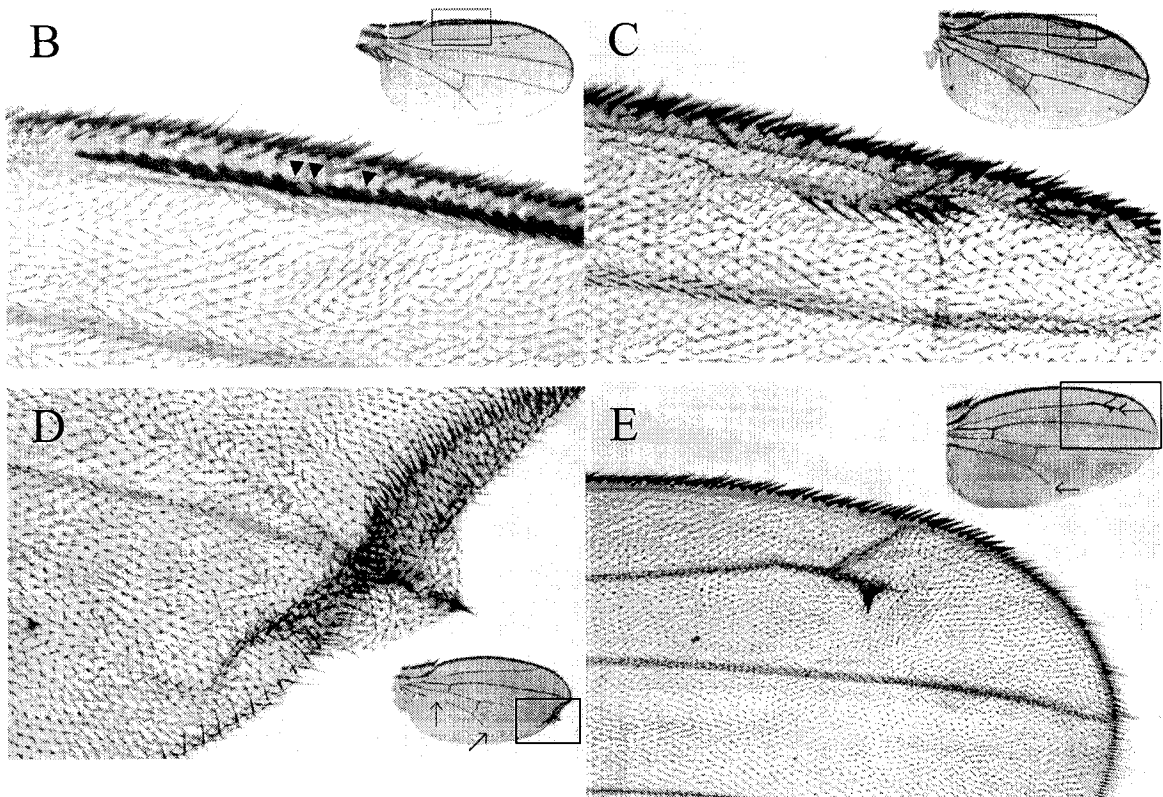
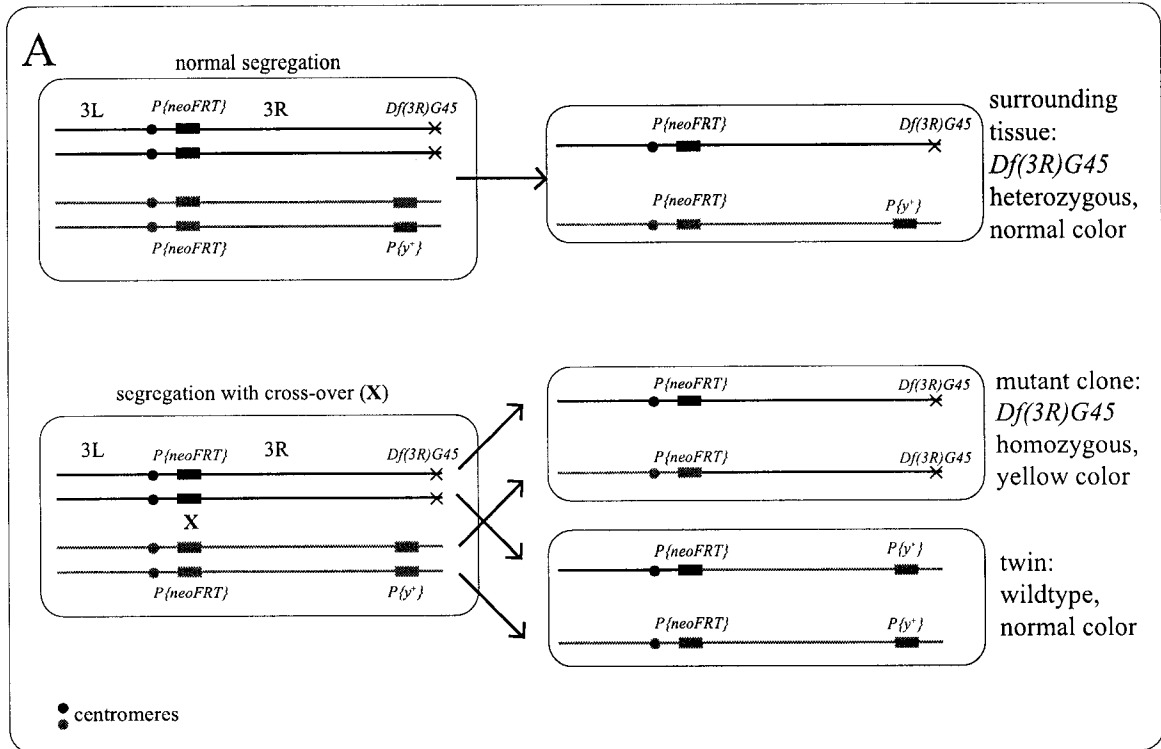
The FLP/FRT method of Xu and Rubin (1993) was used to induce mitotic clones of *Df(3R)G45* using *y* as a clone marker (Fig. 24A). Expression of the *Flip-recombinase* enzyme from a *P{hsFLP}* transgene was induced by heat treatment during the second larval instar. Cells that express the yeast *Flip-recombinase* may recombine their chromosomes between two *P{neoFRT}* transgenes at homologous chromosomal sites (in this case, 82B). Any mutations and markers located distal to the *P{neoFRT}* transgenes are subject to aberrant segregation. This allows unambiguous assignment of mutant genotype to cells that secrete marked cuticle.

300 wings from flies of genotype *y w P{hsFLP} ; P{neoFRT}82B Df(3R)G45 / P{neoFRT}82B P{y⁺}96E* that were heat treated during the second larval instar were mounted and analyzed. From these 300 wings, 129 patches of ectopic margin were observed only within a region close to the normal margin (Fig. 26A). Only a fraction of the ectopic patches of bristles included *Df(3R)G45*, *y* marked ectopic bristles (12/58 patches, all from the anterior compartment where *y* can be reliably scored). These 58 patches all included unmarked ectopic bristles from wildtype tissue. Patches of ectopic margin containing mostly wildtype tissue were found in the dorsal, ventral, anterior and posterior compartments of the wing (Fig. 24). The ectopic bristles, both from within and outside of the clone, differentiate bristle types corresponding to their normal compartmental identities. Ectopic bristles found near the A/P boundary were associated with outgrowths of the wing causing a blistered appearance. Similar results were obtained by Finkielsztejn (1997). Although many patches of ectopic margin were not associated with marked *Df(3R)G45* tissue, he found that marked bristles were significantly more frequent among the ectopic margin bristles than among bristles at the normal margin of the same wings. This supports a clonal origin of the ectopic margin phenotype.

However, better evidence in favor of a genetic mosaic origin for the *ema* phenotype was needed. These experiments also left unanswered questions related to the size and position of *Df(3R)G45* mitotic clones since *y* marks bristles but not trichomes. Thus, any clones that did not induce ectopic margin bristles could not be scored using *y* as a clone marker. Although wing vein defects were observed (Fig. 24D,E), without an appropriate marker to identify *Df(3R)G45* mitotic clones in untransformed parts of the wing blade, the presence of a mutant clone could only be assessed indirectly based on the ectopic margin phenotype close to the endogenous margin. It is possible that *Df(3R)G45* mitotic clones in the middle of the wing blade do not affect cell fate or that *Df(3R)G45* mutant cells farther from the margin die or do not produce cuticle.

Figure 24. Examples of mitotic clones of *Df(3R)G45* marked by *yellow*.

(A) With a cross-over at the *P{neoFRT}82B* transgenes, the *Df(3R)G45* mutant clone does not inherit a *P{y⁺}* transgene and produces yellow cuticle in a *y* mutant background (X-chromosome, not shown). The twin, with two copies of *P{y⁺}* produces wildtype colored cuticle indistinguishable from the heterozygous surrounding tissue with one *P{y⁺}* transgene. *yellow* is of limited utility as a clone marker in the wing. While it marks bristles and hairs, it does not mark trichomes in the wing blade. Because of this, while there is an association between *Df(3R)G45*, *y* clones and ectopic margin, the position and extent of the clone is not known. (B) An example of a dorsal *Df(3R)G45* clone (yellow ectopic bristles, arrowheads) associated with dorsal ectopic margin. The ectopic margin is composed almost completely of mTR bristles from wt tissue. (C) An example of a ventral *Df(3R)G45* clone associated with ventral ectopic margin. Yellow vTR bristles are present but are difficult to see in this picture. (D) This ventral patch of ectopic margin induced along the A/P boundary is associated with a wing blade outgrowth. (E) A dorsal patch of ectopic margin associated with a branch in vein L2. Notice the common disruptions in vein pattern (arrows in D and E).



3.2.2 *Df(3R)G45* mitotic clones marked with *forked*

The bristle and trichome markers *bald* (*bld*) and *forked* (*f*) were used to directly correlate the presence and position of unambiguously marked *Df(3R)G45* mitotic clones in the wing blade with the occurrence of the ectopic wing margin phenotype (Fig. 25A). In this experiment, homozygous mutant *Df(3R)G45* cells are *f*, and the adjacent twin from the same recombination event is marked by *bld*. Both of these markers can be scored in untransformed wing blade tissue as well as in bristles. Unfortunately, there was no method available to apply the efficient FLP/FRT method of inducing recombination to the *bld* and *f* cell markers. An alternative method of inducing recombination uses γ -rays to cause random chromosome breaks. Since γ -rays induce recombination at a low frequency, each wing has rarely more than one mitotic clone and any effect on pattern that is associated with marked tissue can be assigned to a single mitotic clone. The crossovers induced by γ -rays occur at random positions along the chromosome arm. Since *Df(3R)G45* is distal to both *bld* and *P{f⁺}*, *f*-marked tissue should always be *Df(3R)G45* mutant in the absence of very rare double crossovers. It should be noted that *Df(3R)G45* mitotic clones will not always be marked, and a few unmarked patches of ectopic margin might be expected. Another drawback to the use of γ -rays is that the dose used to induce somatic crossing over also causes some cell death. With this in mind, the significance of changes in pattern that involve the deletion of pattern elements (e.g. wing margin nicks) is debatable.

Mitotic clones were induced in second instar larvae of genotype *f^{36a} ; bld^l P{f⁺}96E / ry Df(3R)G45* using γ -rays. Twenty patches of ectopic margin bristles were found in 687 wings that were mounted and analyzed; 16 of these contained *f* bristles or were adjacent to *bld* or *f* trichomes (Fig. 26C). This is a strong correlation between the ectopic margin phenotype and *Df(3R)G45* mutant tissue. Patches of ectopic wing margin not associated with *f* cells could be due to death of the mitotic clone, or a crossover event distal to *P{f⁺}* that created an unmarked *Df(3R)G45* mitotic clone.

An example of a marked mitotic clone and its twin that are associated with ectopic margin is shown in Fig. 25B,C. Like most other twin/clone pairs observed (Fig. 26B,C), this *bld* twin is much larger than the associated *Df(3R)G45*, *f* mitotic clone suggesting a growth disadvantage or death of the *Df(3R)G45* mutant tissue. This difference in size is true of mitotic clone/twin pairs regardless of position in the wing blade. The non-autonomous effect of *Df(3R)G45* mitotic clones is nicely illustrated in Fig. 25C where about half of the ectopic bristles are marked with *bld* and thus come from otherwise wildtype tissue from within the twin. Only those *f* cells contained within a competent region close to the normal margin produce and induce margin bristles, while outside of this region, mutant cells secrete only *f* trichomes.

Figure 25. An example of a *Df(3R)G45* mitotic clone marked by *forked*.

(A) A single γ -ray induced cross-over between the centromere and the *bld* locus produces a *Df(3R)G45* mutant clone marked by *f* (in a *f^{36a}* mutant background, X-chromosome, not shown). The twin-clone from the same recombination event is *f⁺* (along with the surrounding tissue) and is marked by loss of cuticle color (*bld*). Both *f* and *bld* can be scored in untransformed wing blade tissue as well as in bristles. *bld* trichomes, hairs and bristles are almost entirely transparent. *f* trichomes are bent or hooked rather than relatively straight when compared to wildtype. *f* dTR hairs are bent and *f* mTR bristles are short and stout. (B) This anterior dorsal *Df(3R)G45* clone differentiates ectopic *f* bristles or *f* trichomes (red arrowheads) and induces the formation of ectopic mTR and dTR bristles in adjacent *bld* tissue (blue outline). Only when the *Df(3R)G45*, *f* mutant tissue is close to the normal margin is ectopic margin induced. Away from the wing margin, the mutant clone differentiates trichomes. Notice the small number of *Df(3R)G45*, *f* mutant trichomes adjacent to the *bld* twin. (C) A higher magnification view of the patch of ectopic margin in (B) illustrates the non-autonomous effect of *Df(3R)G45* clones. Ectopic bristles are *f* (red arrowheads), *bld* (blue arrows) or wildtype (unmarked).

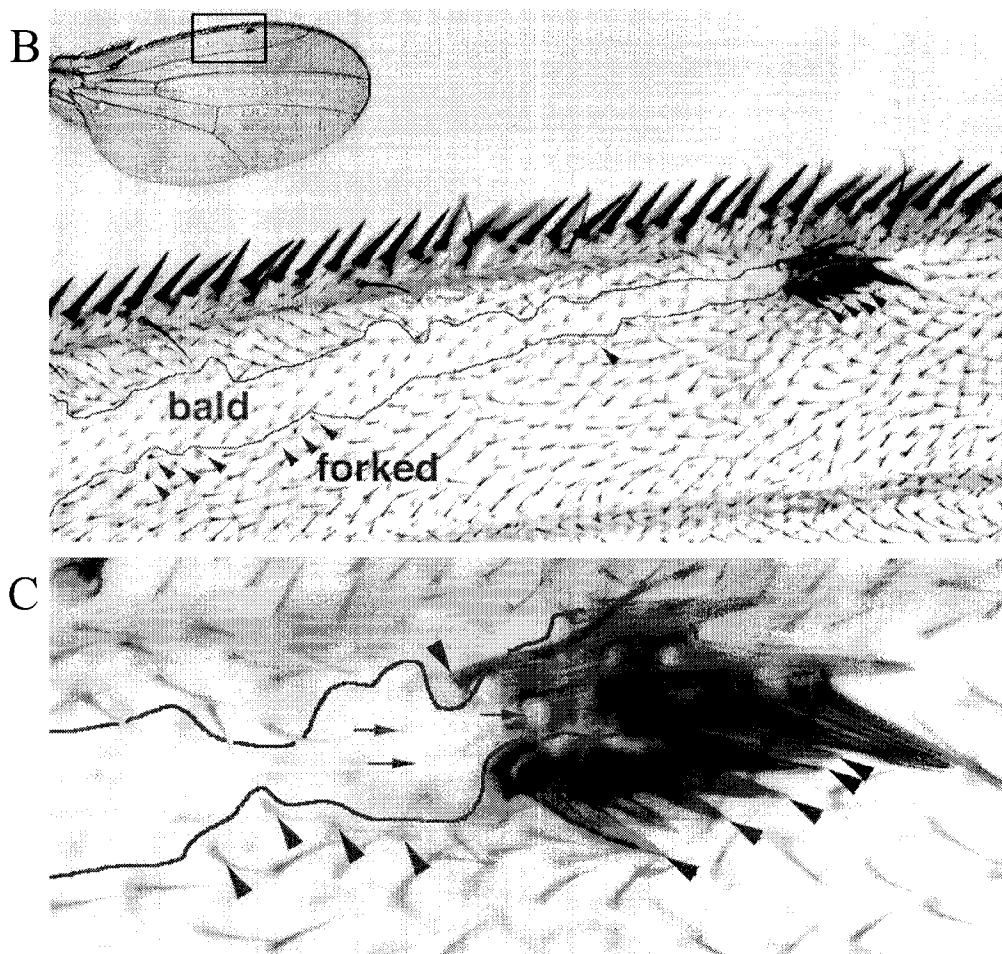
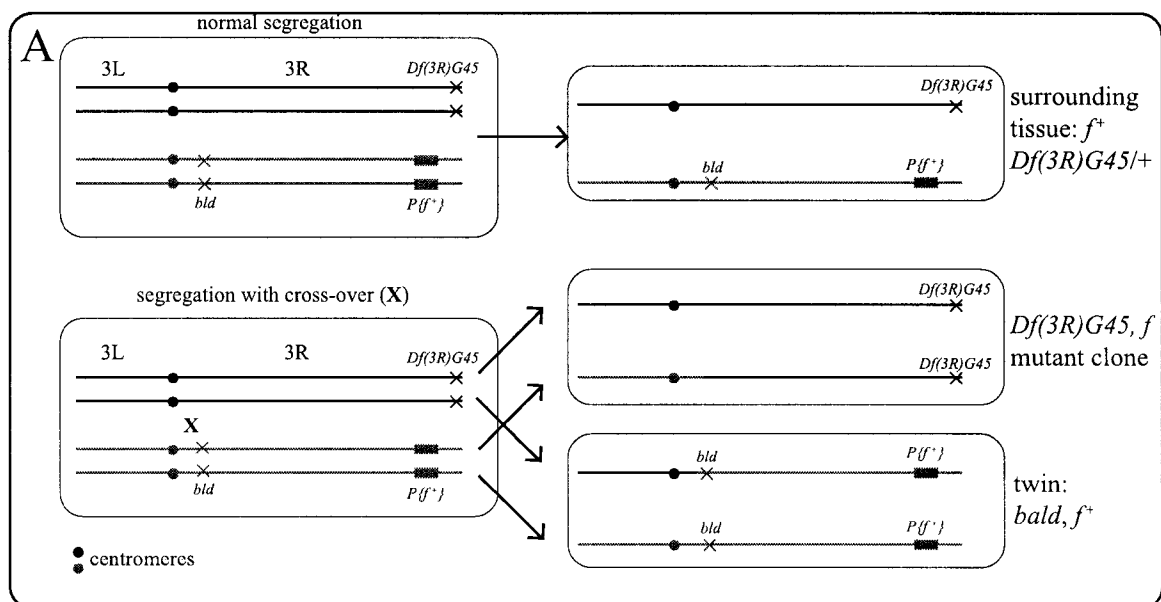
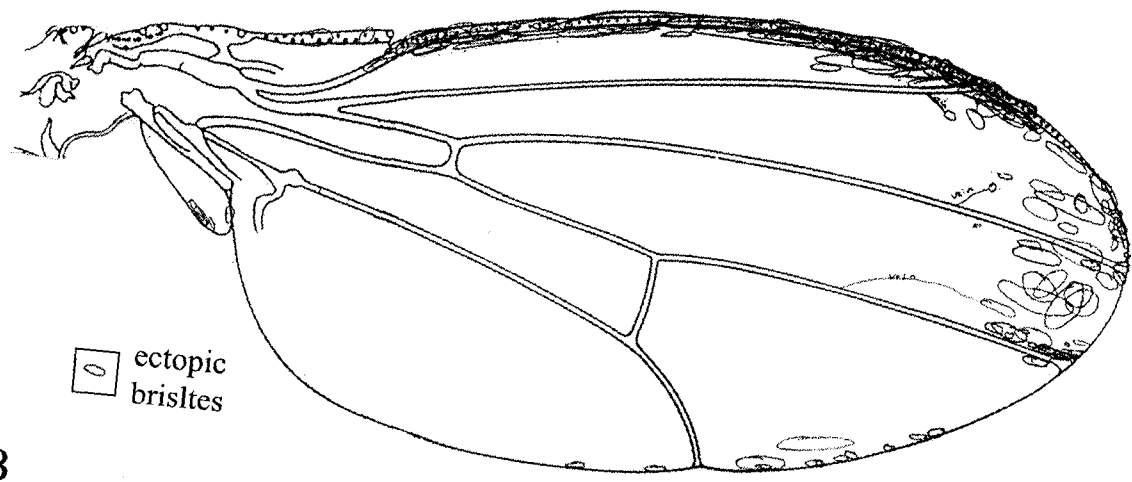


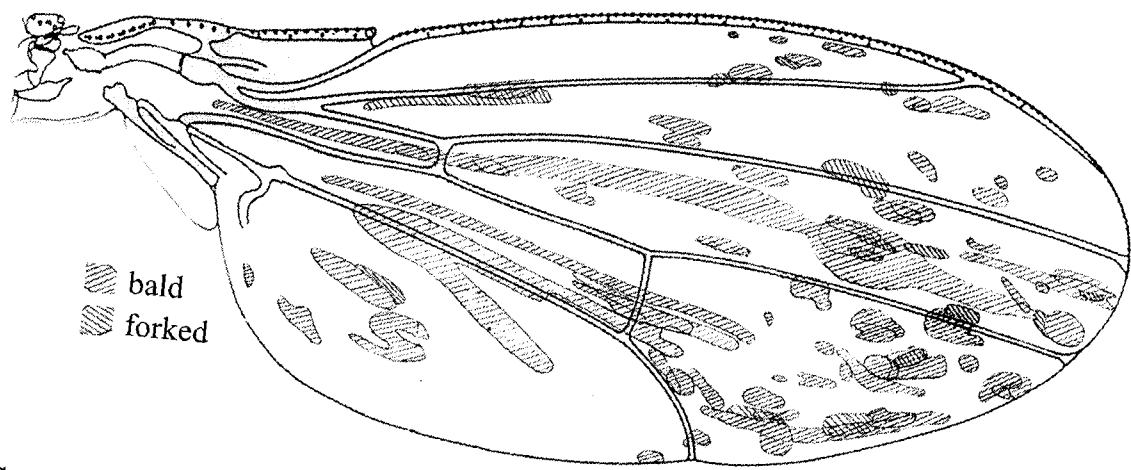
Figure 26. Summary of *Df(3R)G45* genetic mosaic analyses.

(A) *Df(3R)G45*, *y* clones produced 129 patches of ectopic margin within a competent region close to the normal margin. (B) The position of *Df(3R)G45*, *f* clones that were not associated with ectopic margin were studied in 145 wings: 43 *f* clones that did not induce ectopic margin bristles were found throughout the wing blade. (C) The correlation between *Df(3R)G45*, *f* clones and the ectopic WM phenotype was studied in 687 wings. All 20 patches of ectopic margin examined fell within a short distance of the normal margin. 16 of these contained *f* bristles or were closely associated with *bld* or *f* trichomes. One patch of ectopic margin was associated with a large outgrowth or blister of the wing blade (circle).

A



B



C

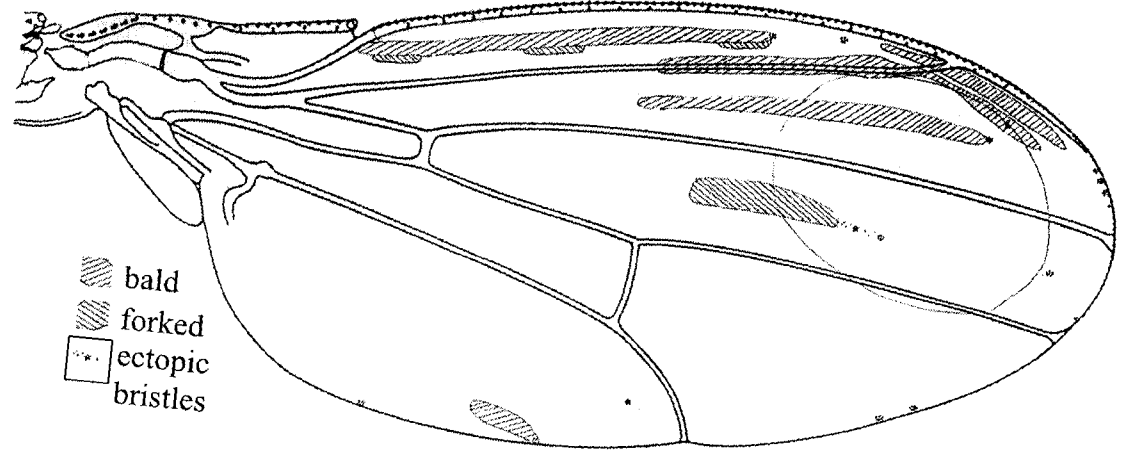
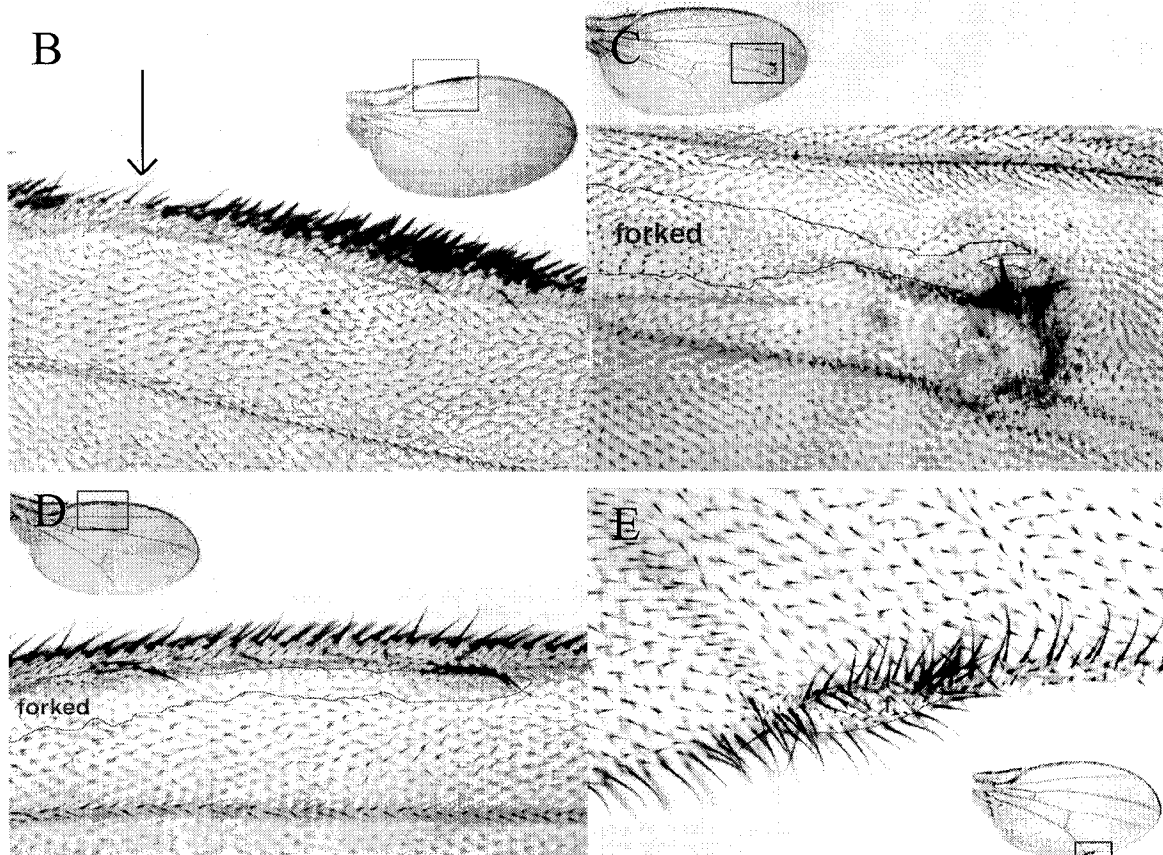
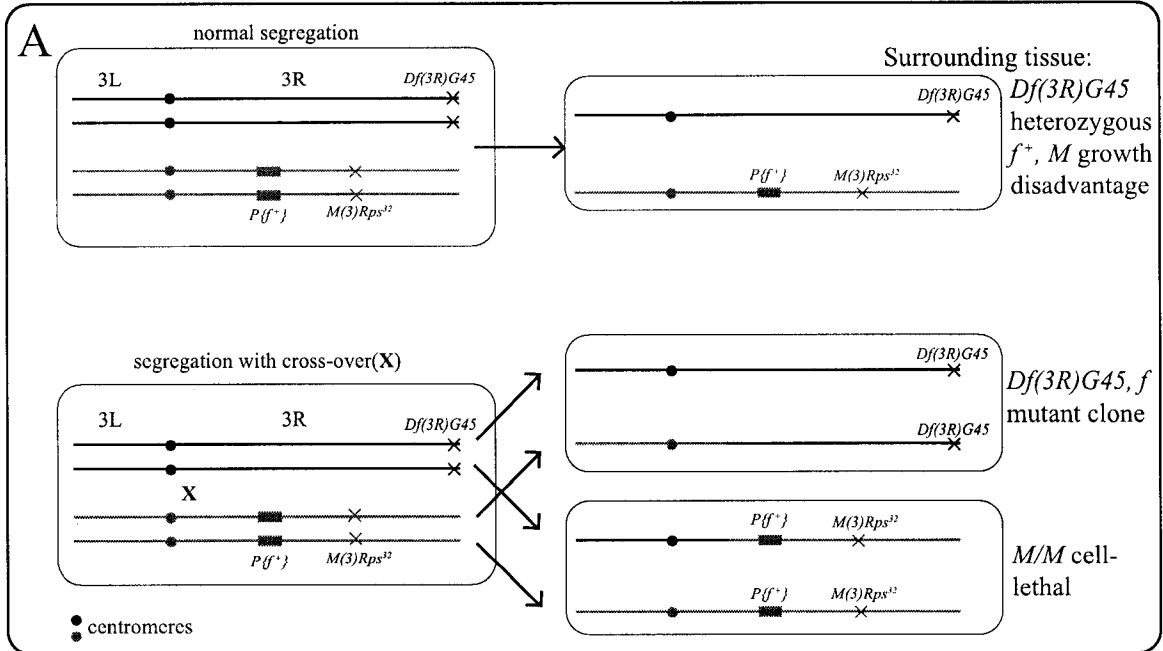


Figure 27. Examples of *Minute*⁺ mitotic clones of *Df(3R)G45* marked by *forked*.

(A) A dominant *Minute* mutation (*M(3)Rps*³²) has been used to give the *Df(3R)G45* mutant tissue a growth advantage relative to the *M* twin and surrounding tissue. With a single cross-over between the centromere and the *P{f⁺}* transgene, the homozygous *Df(3R)G45* clone will not inherit a chromosome carrying a *P{f⁺}* transgene or a *M(3)Rps*³² allele. The *Df(3R)G45, f M⁺* clone will produce forked trichomes, bristles and hairs in a *f*^{36a} mutant background (X-chromosome, not shown). (B) An example of a dorsal *Df(3R)G45* clone associated with a patch of ectopic mTR bristles (including some ectopic *f* mTR bristles). Notice that a section of the normal dorsal margin is missing (arrow) while the ventral margin is intact. (C) A large *Df(3R)G45, f M⁺* clone near the A/P boundary of the wing. At the distal tip of the clone (which is closest to the normal margin), ectopic bristles are associated with a wing blade outgrowth. (D) An example of a ventral *Df(3R)G45, f M⁺* clone associated with ectopic vTR bristles. (E) An example of a posterior *Df(3R)G45, f M⁺* clone associated with ectopic PR bristles. Notice that the ectopic margin in C, D and E is present along the edge of each clone. Mutant tissue marked with *f* is outlined in red.



From the same experiment, 145 wings were analyzed for the presence of clones that were not associated with ectopic margin. These wings contained 43 *f* mitotic clones and/or *bld* twins in the wing blade that were not associated with margin bristles (Fig. 26B). Some patches of *f* trichomes within the competent region were not associated with ectopic wing margin. These mitotic clones may not be homozygous *Df(3R)G45* due to a second recombination event distal to the $P\{f^+\}$ transgene. Alternatively, some *Df(3R)G45* mitotic clones within the competent region may not induce ectopic margin.

3.2.3 *Minute*⁺ *Df(3R)G45* mitotic clones marked with *forked*

To rescue the hypothesized growth defect of *Df(3R)G45* mutant tissue, a dominant *Minute* mutation was used to give the *Df(3R)G45* mitotic clone a growth advantage (Fig. 27A). If the *Df(3R)G45* mitotic clones are growing slowly, the *M*⁺ mitotic clones should be much larger and may produce a more severe ectopic margin phenotype. Mitotic clones were induced in second instar larvae of genotype $f^{36a}; P\{f^+\}87D M(3)Rps^{32}/ry Df(3R)G45$ using γ -rays. Wings with ectopic margin were selected with a dissecting microscope and were mounted and analyzed. The size of both the marked *Df(3R)G45*, *f* *M*⁺ mitotic clones and the associated patches of ectopic margin are much larger than in the previous experiment. Ectopic margin was induced almost exclusively from wt cells along the boundary between mutant and wt tissue, when that boundary was within a competent region (Fig. 27D,E).

Df(3R)G45 mitotic clones induced near the A/P boundary are associated with distal outgrowths of the wing causing a blistered phenotype (Fig. 27C). A dorsal or ventral mitotic clone associated with a blister always contains ectopic socketed (DR) and unsocketed (PR) bristles characteristic of the wing margin at the intersection of the A/P and D/V boundaries. No wing blade outgrowths were observed that were not associated with ectopic margin bristles suggesting that the wing blade outgrowths are an indirect effect of the induction of ectopic wing margin near the A/P boundary.

3.2.4 *hephaestus* mitotic clones disrupt the pattern of the wing margin, wing veins, and ommatidia.

The preceding analysis of *Df(3R)G45* clones was necessary to show a direct relationship between unambiguously marked *Df(3R)G45* mitotic clones and the ectopic wing margin phenotype. Once this was established, I isolated EMS and P-element derived alleles of *heph* that fail to complement *Df(3R)G45* and are associated with ectopic wing margin in genetic mosaics. Since *Df(3R)G45* disrupts several genes, an analysis of *heph* alleles in genetic mosaics was undertaken to ensure that: 1) phenotypes associated with *Df(3R)G45* mitotic clones were also associated with *heph* mitotic clones, and 2) phenotypes associated with *heph* mitotic clones were not masked by other genes disrupted by *Df(3R)G45*. Before the severity of the *heph*^{e2} lesion was molecularly characterized,

*heph*⁰³⁴²⁹ was selected for the following analysis because genetically, *heph*⁰³⁴²⁹, *heph*^{11B9}, and *heph*^{e2} are identical, i.e. they have identical complementation patterns and genetic mosaic phenotypes.

To characterize the phenotype of *heph* in genetic mosaics, I studied the range of adult phenotypes elicited by clone induction at various times after a 12hr egg lay (AEL). Larvae of genotype *y w P{hsFLP} ; P{neoFRT}82B P{πM} Sb heph⁰³⁴²⁹ / P{neoFRT}82B P{y⁺}* were heat treated for 1hr at 37°C at 10 different intervals (Fig. 28A). Before the larvae were heat treated, they were observed under the dissecting microscope and were staged as belonging to 4 classes: late embryos, first, second or third instar larvae. Phenotypes subsequently observed in the adults included the presence of ectopic wing margin bristles, wing margin nicks, disrupted crossveins, rough eyes and marked, missing or ectopic thoracic macrochaetae (data is presented in Table 10). *heph* loss does not affect leg joint formation (data not shown). The percentage of flies for each time of heat treatment with marked thoracic macrochaetae (either *Sb*^{63b} / *Sb*^{63b} or *Sb*⁺ / *Sb*⁺) was used as an estimate of the clone induction frequency. Clone induction frequency was very high in all cases but one, ranging from 60% to 100% except in the earliest AEL clone induction class (Fig. 28B). This may be due to the small number of cells making up the wing disc at this early stage that are targets for recombination.

As was observed with *Df(3R)G45* mitotic clones, *heph*⁰³⁴²⁹ clones non-autonomously induce ectopic wing margin bristles in both the dorsal and ventral surfaces of the wing within the competent region (Table 10 and Fig. 28A,B). This phenotype is consistent with ectopic Notch activation or ectopic *wg* expression in *heph* mutant tissue (among others-see discussion).

Several other phenotypes were common in *heph* genetic mosaic wing discs. First, a high frequency of wing margin nicks was observed that dropped sharply between the 66hr AEL and 78hr AEL heat treatment classes (e.g. 30 nicks in 144 wings, heat treated at 66hr AEL; 3 nicks in 92 wings, heat treated 78hr AEL, see Table 10 and Fig. 28). During this interval, the estimated clone induction frequency and the frequency of other phenotypes remained high. This has important implications when developing a hypothesis as to the role of *heph* in wing patterning. In previous experiments, nicks in the normal wing margin were occasionally associated with *Df(3R)G45, f* mitotic clones induced with γ -rays (Fig. 27B). Since the frequency and total number of wing margin nicks was low, and not all of them were associated with marked *f* cells, they may have been caused by γ -ray induced cell death. However, since the frequency of WM nicks was so high in *heph*⁰³⁴²⁹ genetic mosaic wings, the effect of *heph* clones on the differentiation of the normal wing margin was studied using *pwn* as a clone marker. WM nicks are associated with both dorsal and ventral *heph* clones that meet the margin (Fig. 29C,D). Surprisingly, this phenotype is consistent with loss of Notch activation along the D/V boundary of the disc (see discussion).

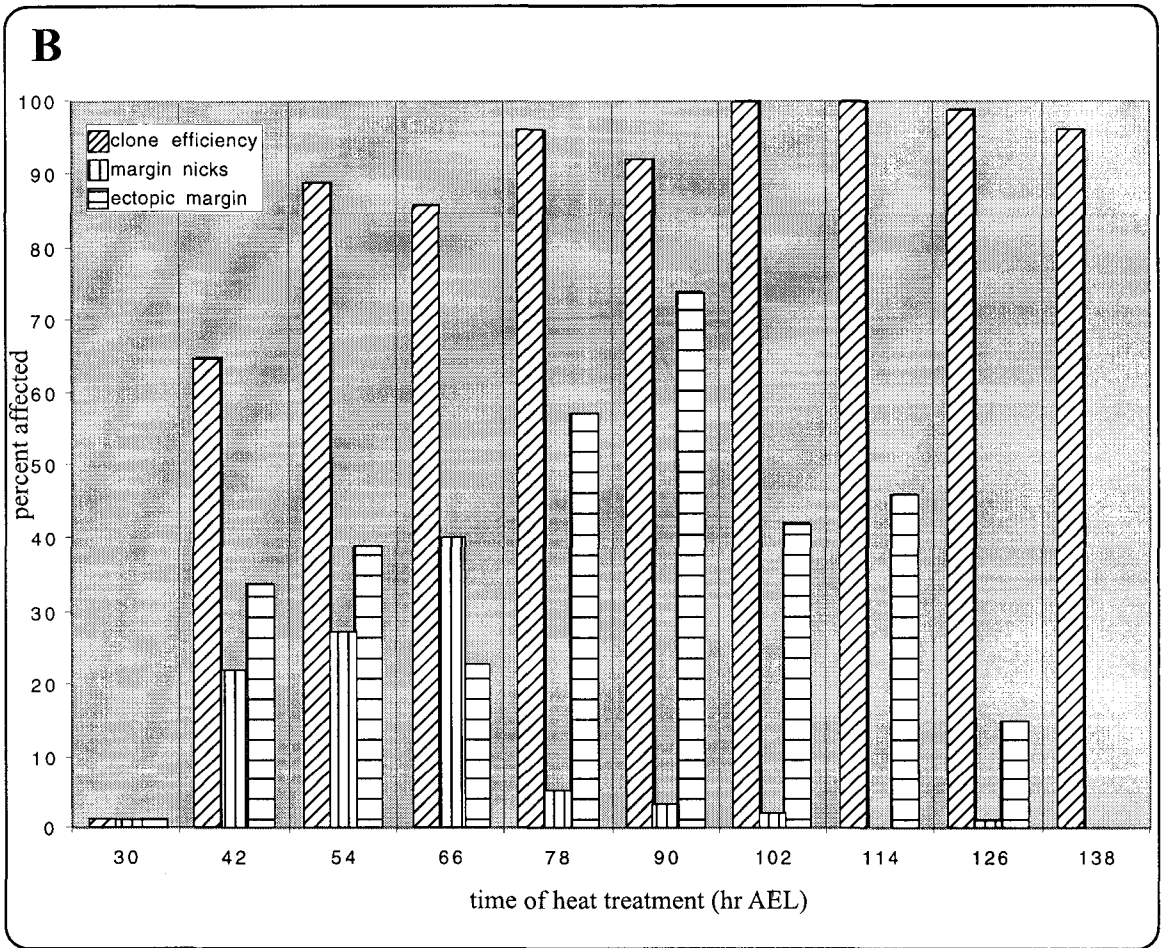
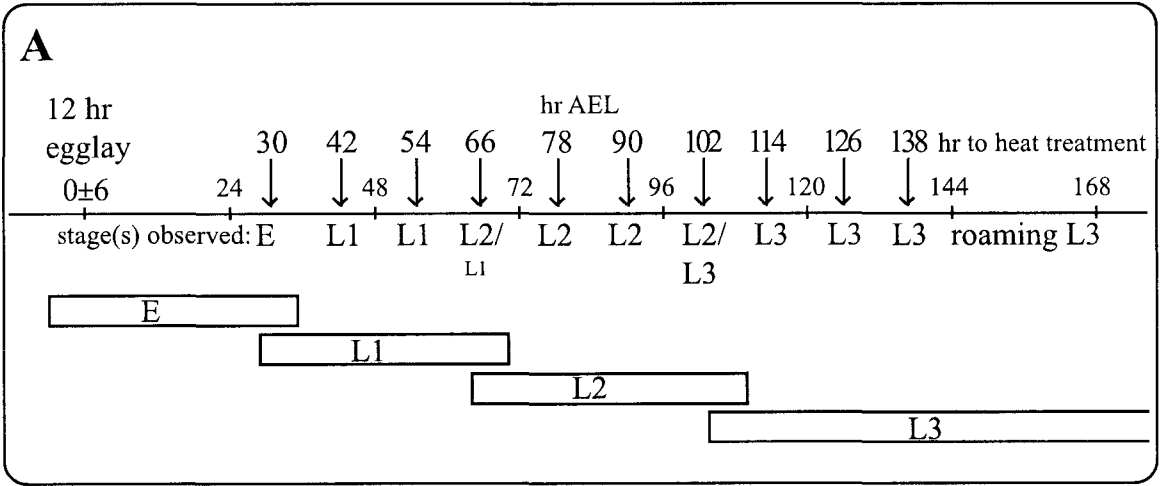
Table 10. The effect of timing of *heph*⁰³⁴²⁹ clone induction on the range of adult phenotypes observed.

time of heat treatment (hr AEL)	number of flies scored (n)	% of n with ectopic wing margin*	% of n with wing margin nicks	% of n with disrupted crossveins	% of n with marked thoracic clones	% of n with missing thoracic macrochaetae	% of n with ectopic thoracic macrochaetae	% of n with rough eyes
30	100	1	1	2	1	0	1	0
42	112	34	22	22	65	22	33	10
54	66	39	27	34	89	10	51	51
66	72	23	40	44	86	8	82	52
78	46	57	5	59	96	11	68	57
90	63	74	3	29	92	12	45	40
102	60	42	2	17	100	5	75	47
114	65	46	0	15	100	2	65	17
126	72	15	1	7	99	8	15	0
138	89	0	0	0	96	0	0	0

* Each number represents the percent of flies with at least one patch of ectopic wing margin, wing margin nick, disrupted crossvein, marked thoracic clone (i.e. *Sb*^{63b} / *Sb*^{63b} or *Sb*⁺), missing or ectopic macrochaetae, or with at least one rough eye.

Figure 28. The timing of *heph*⁰³⁴²⁹ clone induction affects the ratio of WM nicks to ectopic margin.

(A) Clones of *heph*⁰³⁴²⁹ were induced at different times after the midpoint of a 12hr egg-lay (AEL) by varying the time of heat treatment. Since this experiment was done at RT, the life cycle stages that were observed at the time of heat treatment are noted under the timeline. An interpretation of these observations as they relate to the life cycle is presented in boxes under the time line. All times are \pm 6hr. Second instar larvae were observed between 66hr and 102hr AEL; the middle of the second instar can be estimated at between 78hr and 90hr AEL. (B) A comparison of the estimated clone induction efficiency to the percentage of flies with WM nicks and the percentage of flies with ectopic wing margin. The clone efficiency has been estimated using the percentage of flies with marked clones or twins on their thorax. Notice the decrease in the percentage of flies with WM nicks between the 66hr and 78hr AEL heat treatments. The raw data used to make this graph is presented in Appendix I. Stages: E, embryonic; L1-3, larval instar 1-3.



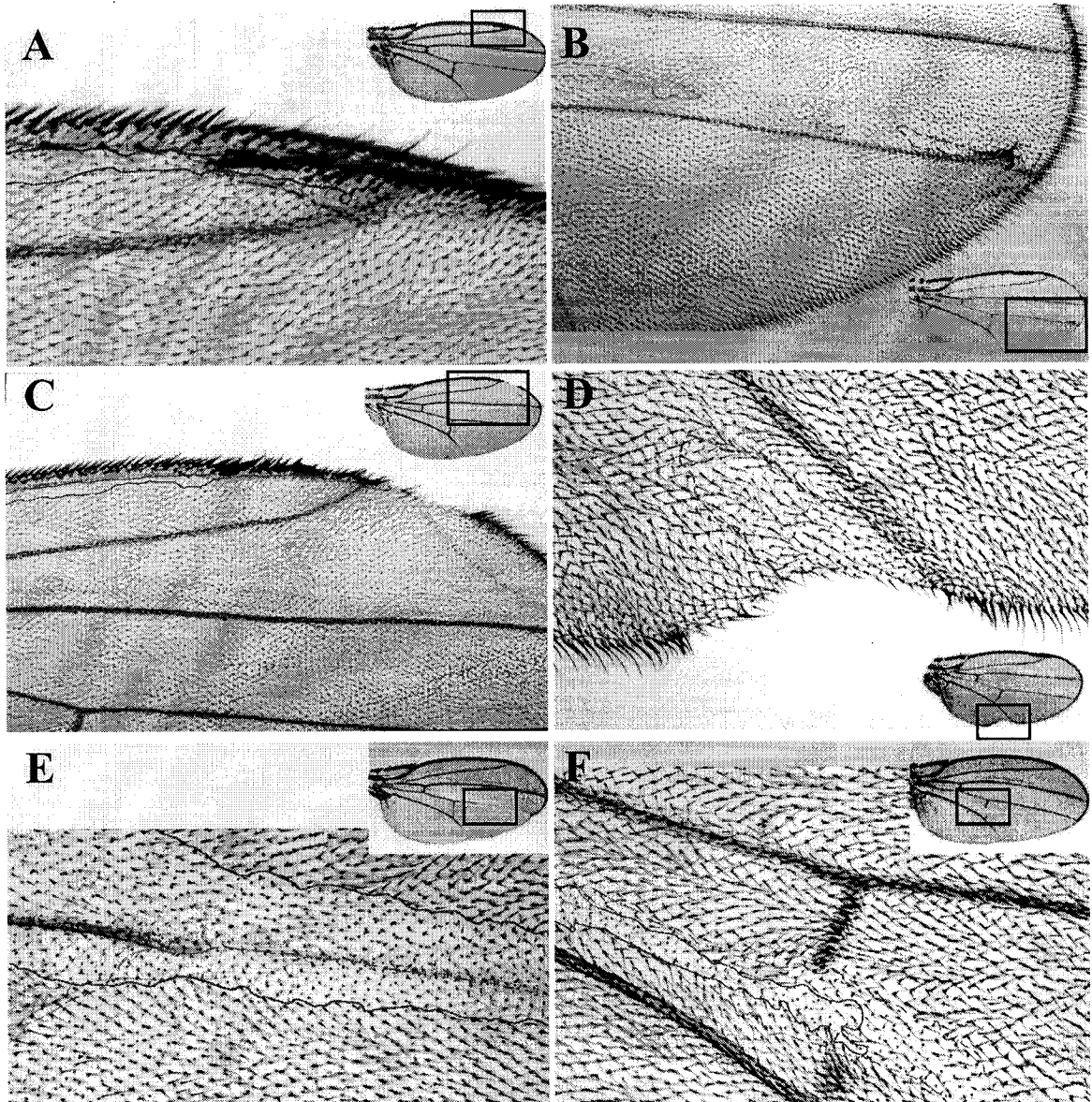


Figure 29. *hephaestus* genetic mosaic wing phenotypes.

Marked *pwn* clones have been outlined with a red (dorsal) or broken blue line (ventral). Examples of dorsal (A) and ventral (B) *heph*⁰³⁴²⁹, *pwn* clones associated with ectopic wing margin bristles. Examples of dorsal (C) and ventral (D) *heph*⁰³⁴²⁹, *pwn* clones closely associated with WM nicks. (E) An example of a wing with two *heph*⁰³⁴²⁹, *pwn* clones, one dorsal and one ventral, with autonomous loss of the dorsal aspect of vein L4 and the portion of the ventral aspect of L4 included in the ventral clone. (F) An example of two *heph*⁰³⁴²⁹, *pwn* clones, one dorsal and one ventral, that overlap and disrupt differentiation of the pCV.

Since the frequency of crossvein disruptions was so high in *heph* genetic mosaic wings (Table 10), the effect of *heph*⁰³⁴²⁹ clones on the differentiation of veins was also studied using *pwn* as a cell marker. *heph* mitotic clones autonomously disrupt vein differentiation. For example, a dorsal *heph*⁰³⁴²⁹ clone that covers the position of a vein is missing the dorsal aspect of that vein within the entire clone (Fig. 29E). Only if both dorsal and ventral clones coincide does a vein appear to be completely missing (Fig. 29F). This phenotype matches that of mitotic clones of *Hairless* (*H*), a canonical Notch repressor (Bang et al., 1995; Bang and Posakony, 1992; Maier et al., 1992; Schweisguth and Lecourtois, 1998), and thus is consistent with ectopic Notch activation in *heph* clones.

Many *heph*⁰³⁴²⁹ mosaic flies had a rough eye appearance (e.g. 37/72 flies (~52%) heat treated at 66hr AEL, see Table 10) associated with *w*⁺ mosaicism of *P{πM}* carried on the *heph*⁰³⁴²⁹ chromosome. Using a light microscope, I found that *y* marks the interommatidial bristles of the eye and in 6/6 clones studied in this way, fused and misshapen ommatidia are adjacent to these marked bristles (Fig. 30). The best way to study the clonal origin and autonomy of a rough eye phenotype is to fix, imbed, and section (~1μm sections) mosaic eyes. Ideally, clones would be marked by loss of a *w*⁺ marker, which is visible in a stained section using a light microscope. This would allow a cell by cell analysis of the autonomy and cellular basis of the rough eye phenotype. This analysis has not been completed.

3.2.5 Thoracic bristle pattern in *hephaestus* genetic mosaics.

Notch-mediated lateral inhibition affects thoracic microchaete placement. Since the *heph* mutant wing phenotypes suggest Notch activation (see discussion), the effect of *heph* loss on thoracic microchaete placement was studied.

A high frequency of extra thoracic macrochaetae that were almost exclusively scutellar and postalar was observed (e.g. 59/72 flies (~82%) heat treated 66hr AEL had one or more ectopic, marked *heph*⁰³⁴²⁹ macrochaetae, see Table 10). A low frequency of thoraces with missing macrochaetae (mostly dorsocentral, DC) were also observed (e.g. 5/72 flies (~8%) heat treated at 66hr AEL had one missing DC macrochaete, see table 10). These phenotypes were studied in more detail as follows.

From flies of genotype *y w P{hsFLP} ; P{neoFRT}82B P{πM} Sb heph⁰³⁴²⁹ / P{neoFRT}82B P{y⁺}* that were heat treated during second larval instar (1hr at 37°C), thoraces including a total of 43 large clones marked by *Sb^{63b}/Sb^{63b}* were analyzed. *Sb^{63b}* marks both microchaetae and macrochaetae of the thorax but not the intervening epidermal hairs. As observed using only *Sb^{63b}* as a cell marker, among 16 *heph* mutant clones that included the scutellar bristles, 18 *heph* mutant ectopic scutellar bristles were observed (Fig. 31A,B). In this and additional tests, the extra macrochaetae were invariably *heph* mutant (marked with *Sb^{63b}* or *pwn*). Among the 43 thoraces scored, 9

were missing a DC macrochaetae, and 8 of these had Sb^{63b}/Sb^{63b} marked (*heph* mutant) clones spanning the normal position of the missing macrochaetae (Fig. 31C). Among the remaining 34 thoraces that were not missing DC macrochaetae, 35 (of a possible 136) DC bristles were adjacent to one or more Sb^{63b}/Sb^{63b} (*heph* mutant) microchaete (Fig. 31D). In only 9 of these 35 cases (~26%) was the DC bristle of mutant genotype (*heph* mutant). This suggests a bias for bristle differentiation on the wildtype side of a *heph* clone border similar to that observed for clones of *Dl* hypomorphic alleles (Heitzler and Simpson, 1991).

In order to characterize this possible bias, I scored the frequency of *heph* mutant, marked microchaetae that differentiate adjacent to wildtype cells (unmarked epidermal hairs-see Fig. 31E,F). 18 *heph* mutant clones marked with both *pwn* and Sb^{63b} were selected from flies of genotype $pr\ pwn\ P\{hsFLP\}38 / pr\ pwn ; P\{neoFRT\}82B\ P\{\pi M\}\ Sb\ heph^{03429} / P\{neoFRT\}82B\ kar\ ry\ bx^{34e}\ Dp(2;3)P32=pwn^+$ that were heat treated during second larval instar (1hr at 37°C). Together, *pwn* and Sb mark macrochaetae, microchaetae, and the intervening epidermal hairs. In these clones, ~41% (n=97) of the microchaetae that differentiated along a *heph* clone border were of mutant genotype (*heph* mutant, marked with *pwn* and Sb^{63b}).

As a control, of the microchaetae that differentiated along the borders of otherwise wildtype clones (marked with *pwn* and Sb^{63b}), ~48% (n=90) differentiated within the clone. This agrees with the expected random choice of microchaetae fate along a wildtype clone border (Heitzler and Simpson, 1991).

I would like to compare this result to those previously reported by Heitzler and Simpson (1991) for *Notch* and *Dl*:

- Differentiation of bristles along the border of an otherwise wildtype clone (marked with *pwn*) microchaetae differentiation is random (51% within the clone, n=160).
- At the border of clones with decreased *Notch* gene dose compared to surrounding tissue, microchaetae usually differentiate from marked cells within the clone (99%, n=90 and 100%, n=78).
- At the border of clones with increased *Dl* gene dose compared to surrounding tissue, microchaete differentiation is biased to within the clone (74%, n=80).
- When *Notch* activity is decreased in a marked N^{ts} clone at the restrictive temperature, microchaetae usually differentiate within the clone (98%, n=121).
- When *Dl* activity is decreased in a marked *Dl(lf)* clone, microchaete differentiation is biased to adjacent cells outside of the clone (13% within the clone, n=114 and 12%, n=56).

Figure 30. *hephaestus* mitotic clones disrupt ommatidial pattern.

heph mitotic clones in the eye disrupt the pattern of ommatidial bristles and the pattern of ommatidia. Light microscopic images of the inter-ommatidial bristles of a heat treated balancer control fly (A,B), and an eye with a *heph*⁰³⁴²⁹ clone marked with *y* (D,E) illustrate the disruption of bristle pattern in the clone. (C,F) Phase contrast images at the same positions as in B and E illustrate the normal ommatidial pattern (C) and the fused and misshapen ommatidia within the *heph* mitotic clone (F).

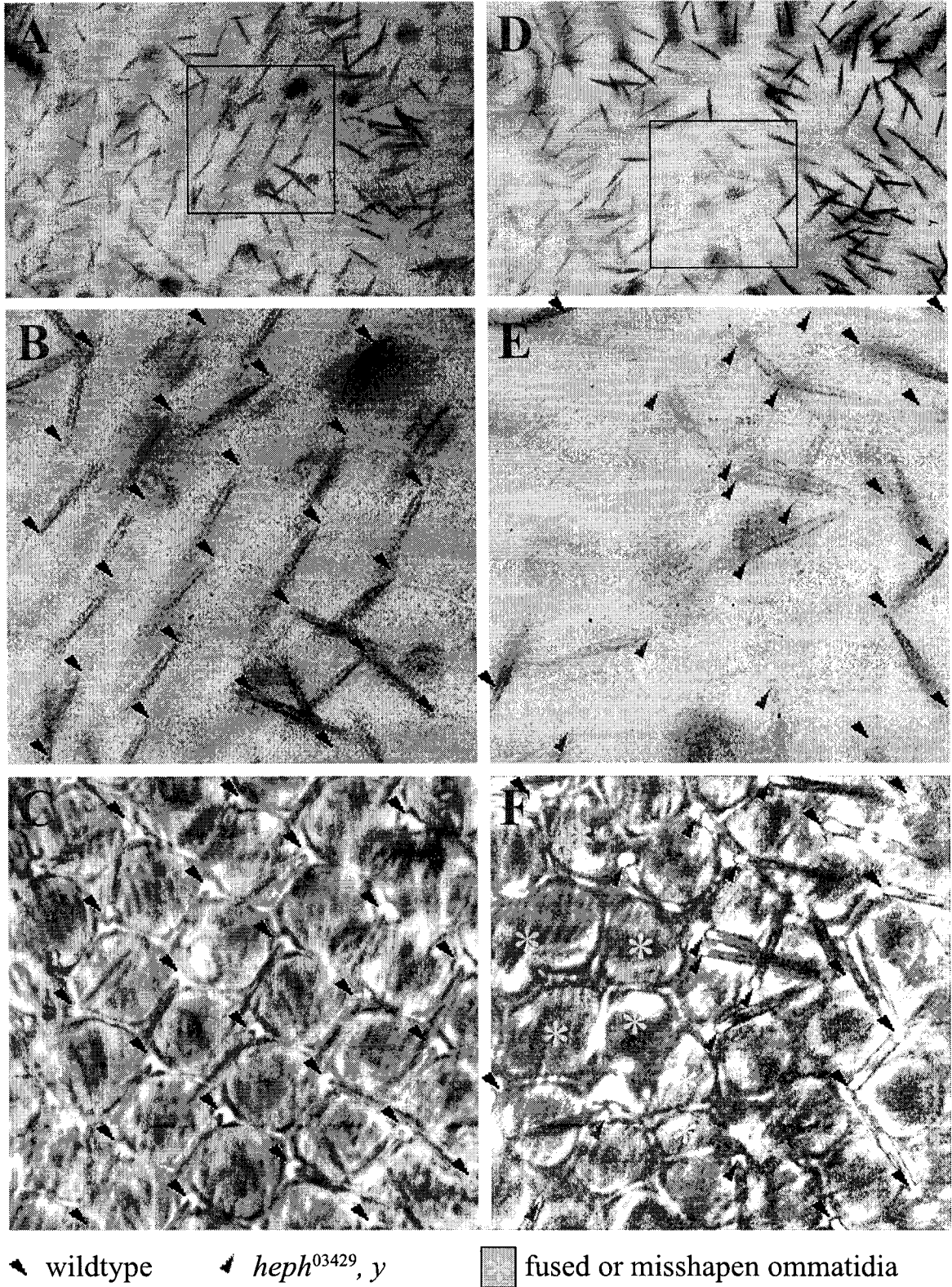
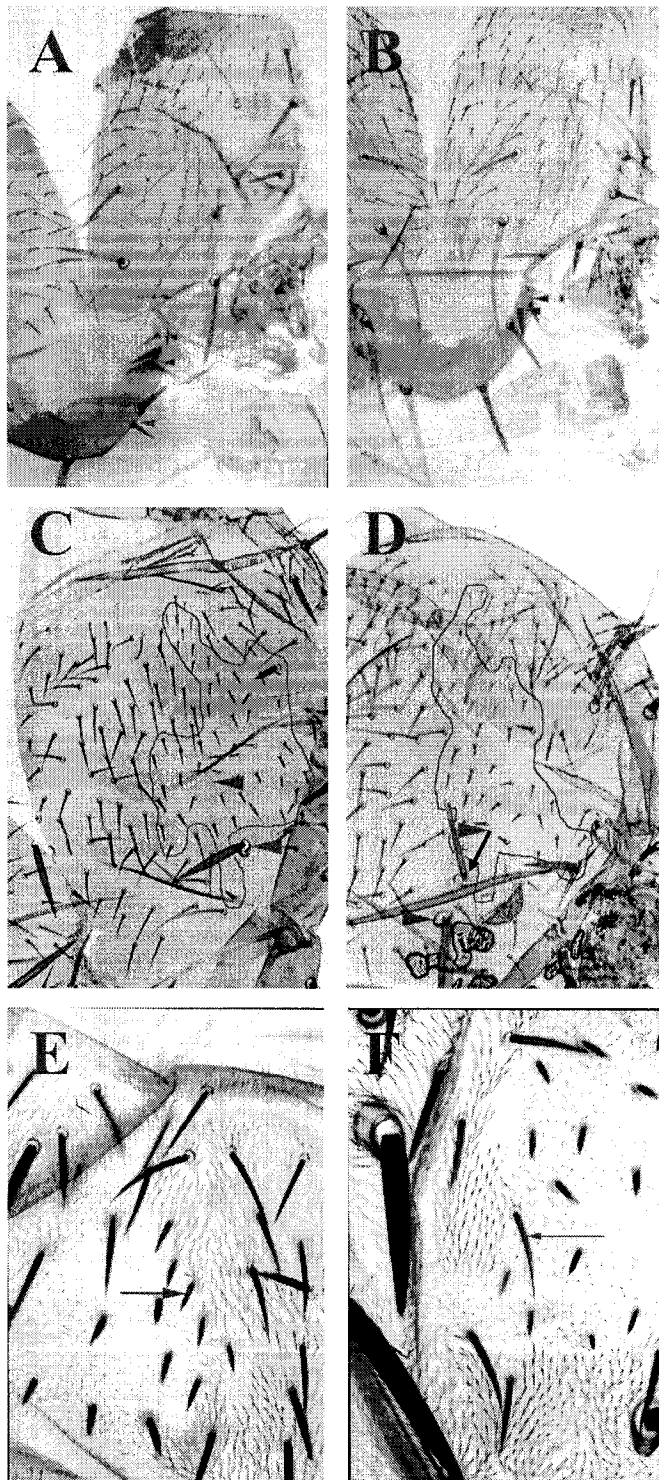


Figure 31. Thoracic phenotypes of *hephaestus* genetic mosaics.

(A,B) A high frequency of ectopic thoracic macrochaetae are associated with *Sb/Sb* marked *heph* mitotic clones. These typical examples have several *heph* mutant ectopic scutellar macrochaetae (arrowheads). (C,D) At a low frequency, *Sb/Sb* marked *heph* mitotic clones in the thorax are associated with a missing thoracic macrochaete. The normal positions of the two DC macrochaetae are marked (arrowheads). (C) This is an example of a missing anterior DC macrochaete (arrowhead) within a large, marked *heph* clone (outlined). (D) In thoraces without missing DC macrochaetae, tissue next to the *heph* mutant clone often differentiate a DC macrochaetae. In this example, the anterior DC (black arrow) appears to "move" out of the clone (red arrowhead - normal DC site). (E,F) Examples of microchaetae that differentiate along the *heph* mutant (marked by *pwn* and *Sb*) clone borders. Marked *heph* mutant microchaetae can differentiate beside unmarked epidermal hairs (E), or unmarked (*heph*⁺) microchaetae can differentiate beside *heph* mutant epidermal hairs (F). These thoraces are oriented anterior to the top of the page.



The difference between these results and those obtained along the marked *heph* clone boundary (41% within the clone, n=97) suggests that neither *Notch* nor *Dl* expression is appreciably increased, and that neither *Notch* nor *Dl* activity is severely decreased in *heph* mutant cells in the thorax.

In addition to the microchaete differentiation bias, Heitzler and Simpson (1991) found that there are fewer epidermal hairs between microchaetae within *N^{ts}* or *Dl(lf)* clones. Some microchaetae pairs appear closer than normal in *heph* mutant clones. However, on average within *heph* mutant clones, microchaetae spacing did not deviate significantly from normal ($4.8^{\pm}1.4$ epidermal hairs between any two microchaetae, n=34) when compared to *pwn* marked controls ($5.0^{\pm}0.9$ epidermal hairs between any two microchaetae, n=42). The apparent difference in microchaetae spacing may be the result of small cell size in *heph* clones marked with *Sb* and *pwn*.

Heitzler and Simpson (1991) interpreted their results in a model of cell fate specification where *Dl* and *Notch* function in a lateral inhibition feedback loop required to space bristle precursors in the thorax. My results suggest that this mechanism is not severely disrupted in *heph* mutant clones. However, the slight bias for microchaetae differentiation outside *heph* clones, and the common occurrence of ectopic scutellar macrochaetae, might indicate a reduction in *Dl* expression and/or an increase in Notch activation in *heph* clones. This does not explain why DC macrochaetae fail to differentiate inside some *heph* clones. Instead, this phenotype is commonly associated with *Ax* alleles of *Notch*, which disrupt proneural cluster specification (Brennan et al., 1999).

3.3 Epistasis

3.3.1 Genetic epistasis between *Delta* and *hephaestus*

Several of the *heph* phenotypes may be explained via effects on the Notch intercellular signalling pathway (see discussion). Notch signalling is involved in a number of patterning processes including the determination of wing vein width. *Notch* encodes a transmembrane receptor and one of its ligands is encoded by the *Dl* gene. During wing vein differentiation, activation of Notch in the lateral provein cells by DL is required to inhibit vein differentiation in the Notch activated lateral provein cells. Thus, loss of *Dl* function causes a wide vein phenotype because without *Dl*, Notch is not activated in the lateral provein cells and the vein fate is not laterally restricted. Extra vein differentiation in *Dl* genetic mosaics is both cell-autonomous and non-autonomous, since cells in a *Dl* mutant clone cannot activate Notch in neighboring cells. In contrast, veins do not differentiate within *heph* mutant tissue. This may be explained in terms of Notch signalling if Notch were ectopically active and able to inhibit vein differentiation cell-autonomously within *heph* mutant clones.

The opposite effects of *Dl* and *heph* mitotic clones on the phenotype of wing veins allowed the determination of the epistatic relation between *Dl* and *heph*. When two genes act in the same linear pathway, a mutation of the gene acting further downstream in the pathway will be epistatic to a mutation affecting the gene acting upstream, in the double mutant. To observe this interaction, it is necessary that the two mutations have different phenotypes, for example, a gain-of-function (*gf*) allele and a loss-of-function (*lf*) allele in two genes that are required for activation of a function. Although the *Dl* and *heph* alleles used here are both *lf* alleles, they have opposite phenotypic effects on vein differentiation that can be interpreted as opposite effects of the two wt gene activities on Notch activity. A *Dl(lf)* mutation is similar to a *Notch(lf)* mutation, and a *heph(lf)* mutation is similar to a *Notch(gf)* mutation in their effects on wing veins.

To investigate the order in which *Dl* and *heph* act in the pathway promoting vein differentiation, the phenotypes of *Dl* clones and *heph* clones were compared to that of *Dl heph* double mutant clones. Mitotic clones of cells mutant for both *Dl* and *heph* differentiate wider vein than normal because of extra autonomous and non-autonomous vein differentiation, and thus clearly resemble *Dl* mitotic clones rather than *heph* clones (Fig. 32). Since the *Dl* genetic mosaic vein phenotype is due to a non-autonomous loss of Notch activation, and since the *heph* genetic mosaic phenotype can be explained as a gain of Notch function, *Dl* is epistatic to *heph*. A simple interpretation of this kind of epistatic interaction would be that the function of *heph* is mediated at the veins through *Dl*. In order to explain the opposite loss-of-function vein phenotypes of *heph* and *Dl*, *heph* would normally function in opposition to *Dl* function. However, this interpretation is not consistent with gene expression data (presented below) so this topic will be revisited in the discussion.

3.3.2 *heph*⁰³⁴²⁹ partially rescues the *fng*^{D4} margin loss phenotype

To study the possible role of *heph* in the wing margin pathway, I tested the ability of *Df(3R)G45* or *heph*⁰³⁴²⁹ to modify visible dominant adult phenotypes of mutations in characterized wing patterning genes. Possible transheterozygous genetic interactions were screened by comparing the phenotype of the visible allele in the F1 of a cross to *Oregon-R*, and to *Df(3R)G45* and *heph*⁰³⁴²⁹. Recessive visible alleles on the X-chromosome (e.g. *ct⁶*) were scored in hemizygous males. The genes that I have screened for interactions include members of the *Notch*, *wg*, *dpp* and *Egfr* signalling pathways, each of which is necessary for wing patterning. The results of this screen are presented in Table 11 but, with the exception of *fng*^{D4}, are negative results and will not be discussed here. Negative results may be due to low sensitivity of a genetic interaction assay possibly due to an inability to quantify mild interactions or minor effects after changing *heph* gene dose. The lack of dominant interactions with other elements in the *Notch* signalling pathway does not exclude a role for *heph* in the *Notch* pathway, rather it may indicate that one dose of *heph* is sufficient except in highly sensitive genetic backgrounds.

Figure 32. *Delta* is epistatic to *hephaestus*.

Marked *pwn* clones have been outlined with a red line (dorsal clone) or a broken blue line (ventral clone). (A, B) Typical examples of *heph*⁰³⁴²⁹ mitotic clones marked with *pwn* that cross a territory where a vein is normally differentiated. Vein differentiation is autonomously inhibited within the *heph* clones. (C, D) Typical examples of *DI*^{rev10} mitotic clones marked with *pwn* that include vein territories. Loss of *DI* causes an autonomous wide vein phenotype and non-autonomous vein differentiation in neighboring tissue. (E, F) Typical examples of mitotic clones marked with *pwn* that are doubly mutant for *DI*^{rev10} and *heph*⁰³⁴²⁹. Like *DI* clones, these clones cause an autonomous wide vein phenotype and are associated with non-autonomous vein differentiation in neighboring tissue.

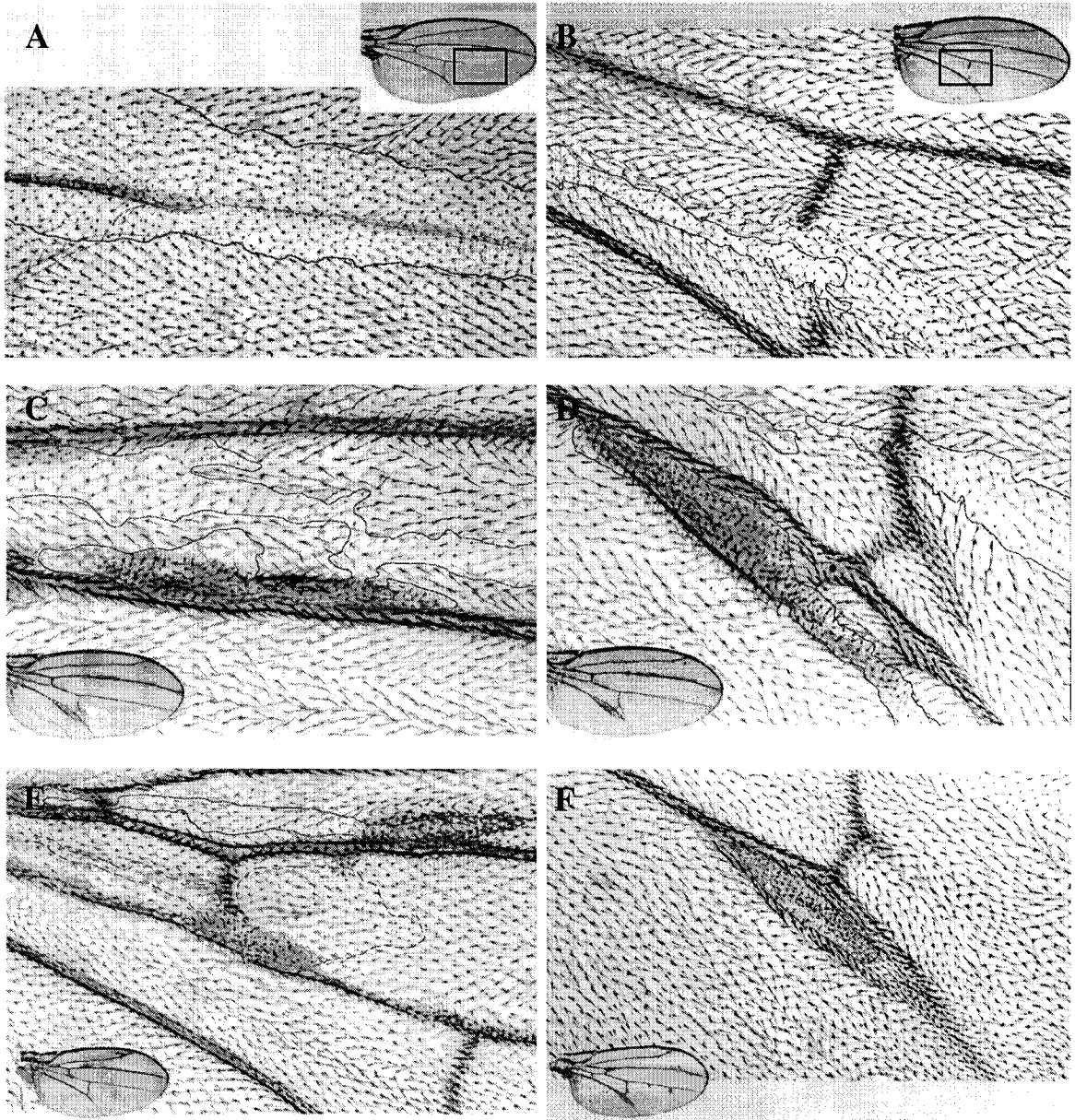


Table 11. Summary of genetic interactions.

Allele name	Allele class	<i>Df(3R)G45</i>	<i>heph</i> ⁰⁴³²⁹
<i>Bx</i> ¹	hypermorph	no effect	nd
<i>ct</i> ⁶	hypomorph	no effect	nd
<i>Dl</i> ³	loss of function	no effect	nd
<i>dx</i> sm	visible dominant	nd	no effect
<i>Egfr</i> ^{E1}	hypermorph	no effect	nd
<i>fng</i> ² / <i>fng</i> ⁵²	hypomorphs	Suppressed	no effect
<i>fng</i> ^{D4}	gain of function	Suppressed *	Suppressed *
<i>H</i> ¹	hypomorph	no effect	nd
<i>N</i> ^{Ax-1}	gain of function	Enhanced †	no effect
<i>N</i> ^{spl-1}	gain of function	no effect	nd
<i>N</i> ^{nd-1}	hypomorph	no effect	no effect
<i>N</i> ^{Co}	antimorph	no effect	nd
<i>Ser</i> ^D	gain of function	no effect	no effect
<i>Ser</i> ^{Bd-3}	antimorph	no effect	nd
<i>Sno</i> ^{E1}	gain of function	nd	no effect
<i>P</i> { <i>sev-N</i> ^{act} }	Synthetic <i>N(gf)</i>	nd	no effect

* Both *Df(3R)G45* and *heph*⁰³⁴²⁹ suppress the *fng*^{D4} margin loss phenotype.

† *Df(3R)G45* but not *heph*⁰³⁴²⁹ enhance the *N*^{Ax} vein loss phenotype. *l(3)s095214*, which disrupts both *mod* and *krz* also enhances the *N*^{Ax} vein loss phenotype, suggesting that the effect of *Df(3R)G45* on *N*^{Ax} is due to loss of *mod* or *krz*.

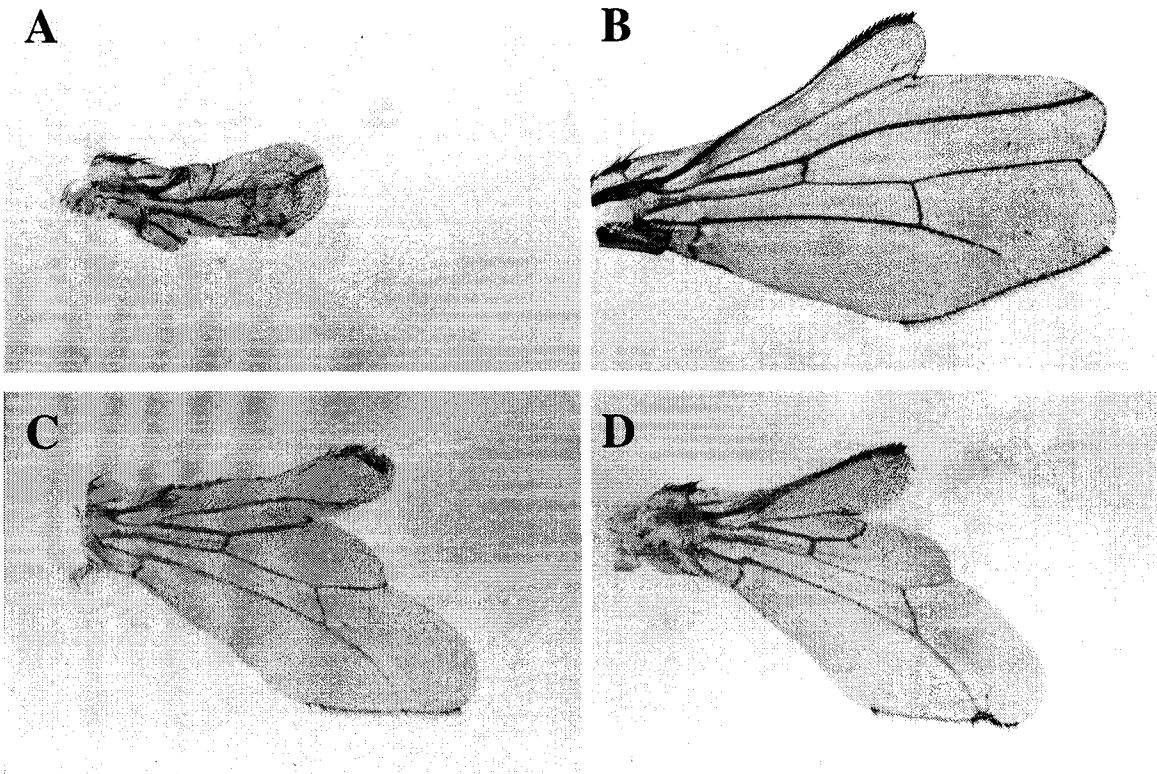


Figure 33. *heph*⁰³⁴²⁹ partially rescues the *fng*^{D4} margin loss phenotype.

(A) An example of a wing from *fng*^{D4} / + male flies. Most or all of the wing margin is missing. (B) An example of a wing from a *N^{Ax-1}* / + ; *fng*^{D4} / + transheterozygous female. This partial rescue of the *fng*^{D4} phenotype is similar to that of *fng*^{D4} / *Df(3R)G45* (C) and *fng*^{D4} / *heph*⁰³⁴²⁹ (D) in transheterozygous male flies. All flies were cultured at 25°C. Since the *fng*^{D4} phenotype is variable, these images are representatives of the most common (median) phenotype observed in flies of a given genotype.

As previously described, FNG facilitates the activation of Notch by DL and inhibits the activation of Notch by SER (Panin et al. 1997). Because of its central role in wing margin specification, the phenotype of a dominant gain of function *fng* allele (*fng^{D4}*), was tested for interaction with *heph⁰³⁴²⁹*. In *fng^{D4}* mutants, *fng* expression is initially restricted to the dorsal half of the wing disc as in normal development. However, broad ventral mis-expression appears later in development during the third instar (Irvine and Wieschaus, 1994). Genetic mosaic analysis of loss of function *fng* mutants illustrated the importance of a *fng* expression boundary in the establishment of the wing margin. In *fng^{D4}* wing discs, the initially normal *fng* expression boundary breaks down causing loss of wing margin and wing blade tissue, consistent with loss of Notch activation at the D/V boundary (de Celis and Bray, 2000). Wings from *fng^{D4} / heph⁰³⁴²⁹* transheterozygotes have larger wings with more margin than the wings of *fng^{D4}* flies (Fig. 33). The partial rescue of *fng^{D4}* by *heph⁰³⁴²⁹* is similar to the rescue of *fng^{D4}* by *N^{4x-1}* in females (Fig. 33; de Celis and Bray 2000) and is consistent with a role for *heph* as an inhibitor of Notch activation.

3.3.3 wingless protein expression in *hephaestus* genetic mosaic wing discs

The position of *heph* relative to other genes in the *Notch* and *wg* pathways were studied in *heph* genetic mosaic wing discs using antibodies specific for WG, CUT, AC, DL, SER, DLL, and NICD. Mitotic clones were induced in flies of genotype *y w P{hsFLP}1 ; P{neoFRT}82B P{πM} Sb^{63b} heph⁰³⁴²⁹ / P{neoFRT}82B P{GFP}*, where *P{GFP}* is either *P{hsGFP}* or *P{Ubi-GFP}* as noted in the figure legends. Flies were allowed to lay eggs for 24hr, then larvae were heat treated (1hr at 37°C) after two days at RT. Thus, clones were induced between 48hr and 72hr AEL, during the stage that produces frequent ectopic margin, margin nicks, and vein disruptions. All discs were dissected from roaming third instar larvae.

Autonomous activation of the WG pathway (Rulifson et al. 1996; Micchelli et al. 1997) or ectopic expression of the WG signal (Diaz-Benjumea and Cohen, 1995) are sufficient to induce marginal bristle fate in cells of the wing blade. The *heph* phenotype of mostly non-autonomous induction of wing margin bristles surrounding the mutant tissue strongly suggests that *heph* mitotic clones near the D/V boundary express *wg*. Using an antibody that recognizes the WG protein, I examined *wg* expression in *heph* genetic mosaic imaginal discs. Homozygous *heph* mitotic clones were marked by the absence of a Green Fluorescent Protein (GFP) cell marker (Fig. 34).

Ectopic expression of *wg* is associated with *heph* mutant clones (Fig. 35). In accordance with the distribution of mitotic clones that cause ectopic margin, ectopic WG only seems to be induced at detectable levels in *heph* clones situated near the endogenous margin. Ectopic WG is not found in all cells in the *heph* mitotic clones but tends to be expressed by the cells of the clone that are closest to the margin stripe of WG.

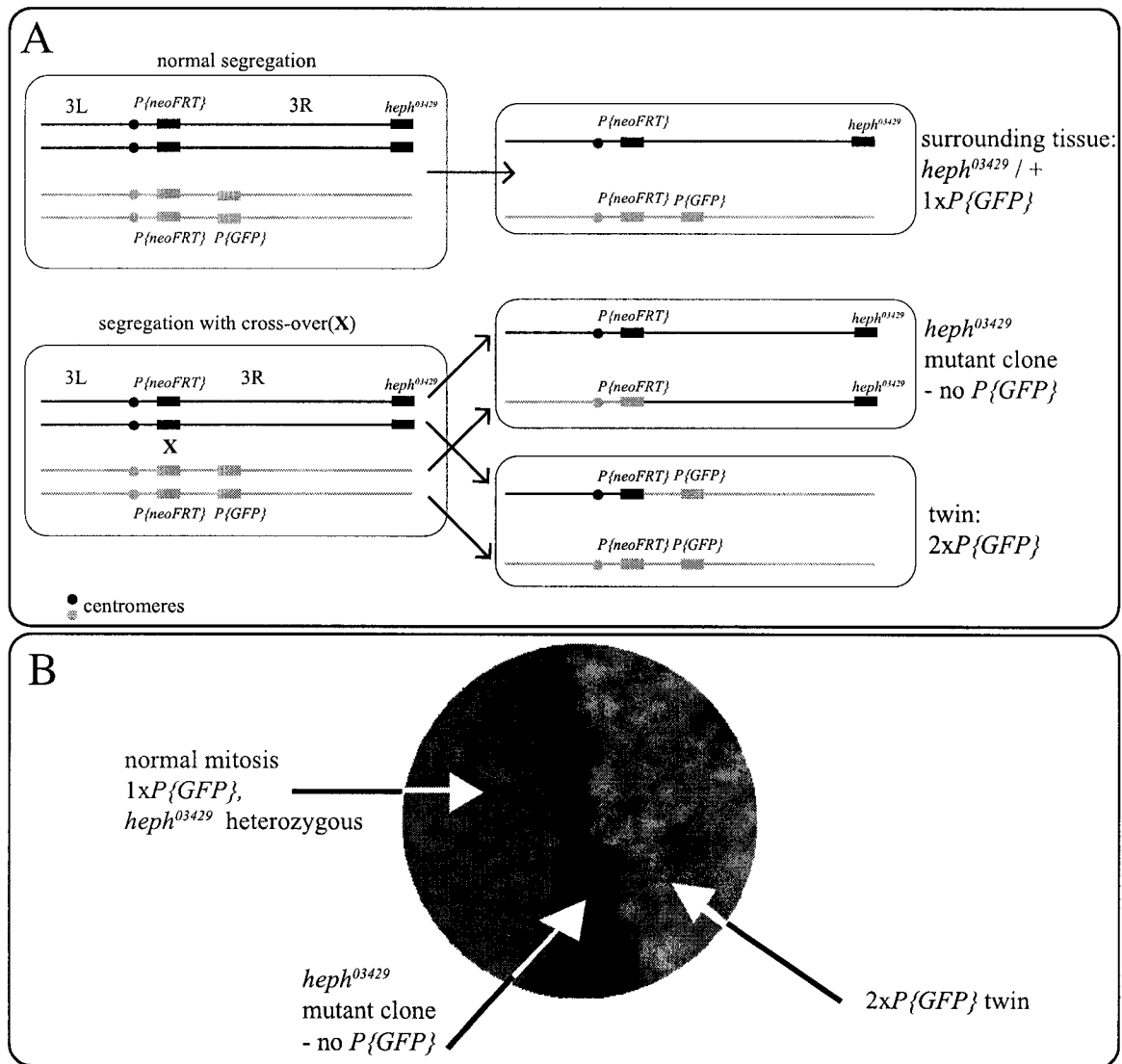


Figure 34. GFP as a cell marker for analysis of genetic mosaic discs.

(A) Segregation of post S-phase mitotic chromosomes with or without mitotic recombination at the *P{neoFRT}*82*B* insertion sites. Normal mitosis yields heterozygous *heph*⁰³⁴²⁹ / + daughter cells with one copy of the *P{GFP}* transgene. With recombination at the *P{neoFRT}* transgenes, mitosis yields a homozygous *heph*⁰³⁴²⁹ mutant clone and a wildtype twin with two copies of *P{GFP}*. (B) An example of a laser scanning fluorescent image of a *heph*⁰³⁴²⁹ clone (black), its twin (bright green) and the surrounding, heterozygous tissue (light green). The size difference between the clone and twin suggests a growth defect of *heph* mutant cells.

Figure 35. Ectopic *wingless* expression is induced autonomously in *hephaestus* mitotic clones.

Laser scanning fluorescent images of WG (middle panel and red) visualized with a mouse anti-WG primary antibody and an anti-mouse Alexa-fluor^{594nm} secondary antibody, and GFP (left panel and green), expressed from a *P{hsGFP}* transgene that is not present in cells mutant for *heph*⁰³⁴²⁹. (A, B) An example of wildtype *wg* protein expression in a typical wing disc from heterozygous *heph*⁰³⁴²⁹ / *TM6B*, *Tb* third instar larvae. (C-E) Examples of *heph* mosaic wing discs with ectopic *wg* expression (arrowheads) within *heph*⁰³⁴²⁹, *GFP*⁻ mitotic clones that are close to the normal *wg*-expressing cells.

(A, C, E) bar, 100 μ M.

(B, D) bar, 25 μ M.

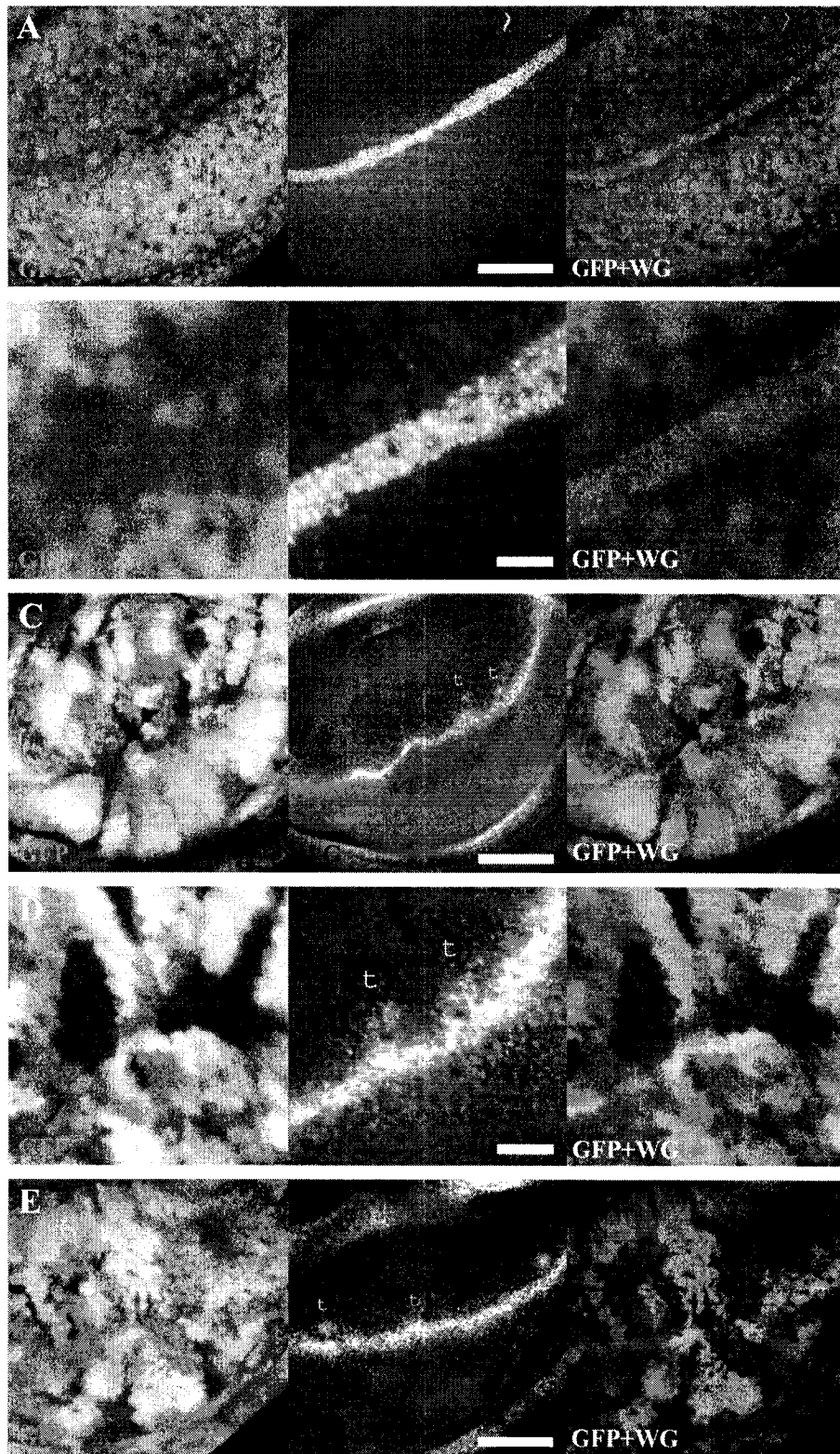


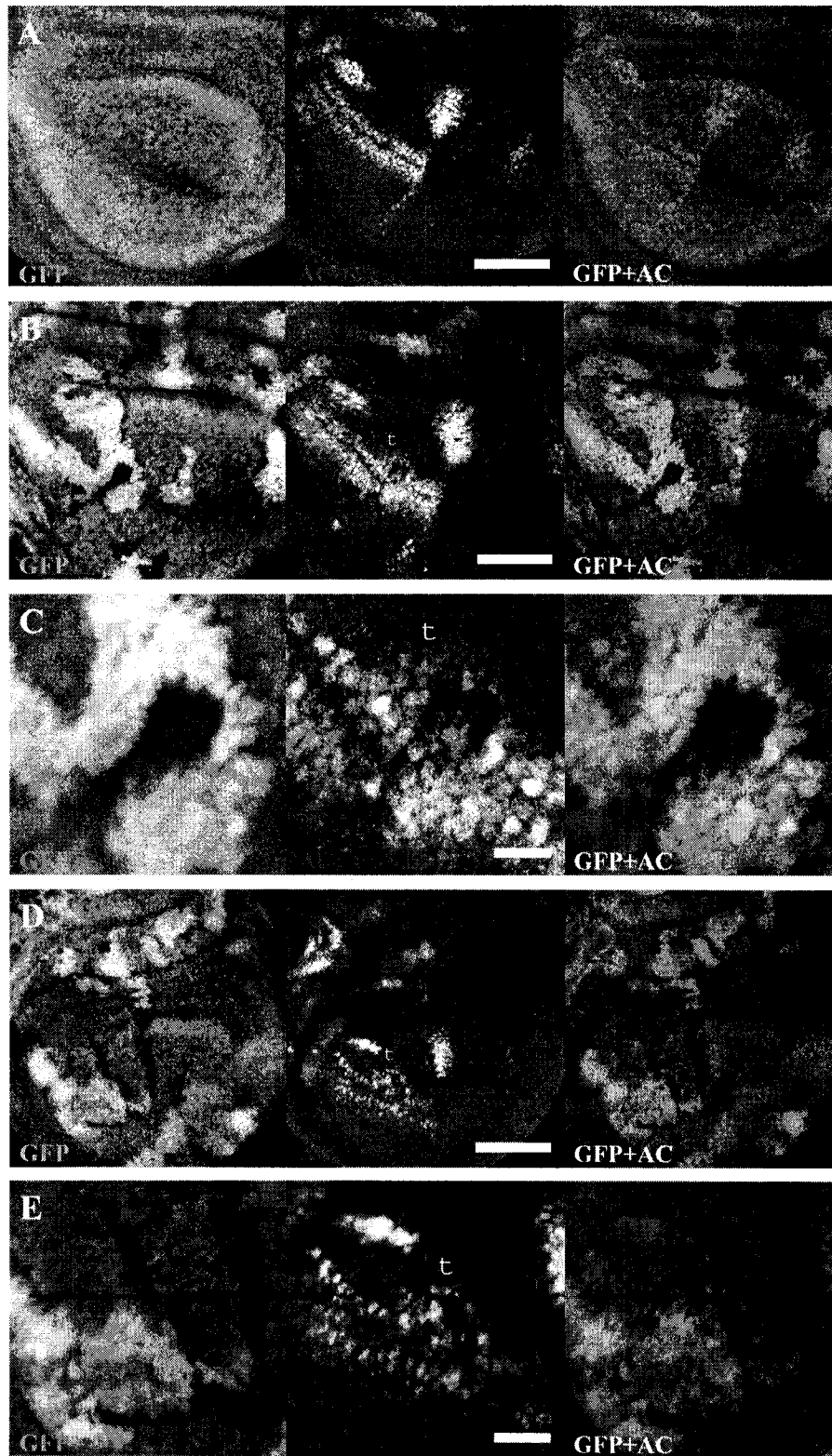
Figure 36. Ectopic *achaete* expression is induced non-autonomously around *hephaestus* clones.

Laser scanning fluorescent images of AC (middle panel and red) visualized with a mouse anti-AC primary antibody and an anti-mouse Alexa-fluor^{594nm} secondary antibody, and GFP (left panel and green), expressed from a *P{hsGFP}* transgene that is not present in cells mutant for *heph*⁰³⁴²⁹. (A) An example of wildtype *ac* protein expression in a typical wing disc from heterozygous *heph*⁰³⁴²⁹ / *TM6B, Tb* third instar larvae. (B-E) Examples of *heph* mosaic wing discs with ectopic *ac* expression in cells adjacent to *heph*⁰³⁴²⁹ clones that are close to the normal D/V boundary (marked by the normal gap between domains of *ac* expression). Notice in C and E that some of the *heph*⁰³⁴²⁹ mutant cells express low levels of *ac*.

(A, B, D) bar, 100 μ M.

(C) bar, 25 μ M.

(E) bar, 50 μ M.



3.3.4 *achaete* protein expression in *hephaestus* genetic mosaic wing discs

WG normally diffuses from the boundary cells in the anterior compartment and defines a proneural zone that will give rise to the sensory bristles of the anterior wing margin (Blair, 1993; Couso et al., 1994; Diaz-Benjumea and Cohen, 1995; Phillips and Whittle, 1993). The induction of anterior wing margin bristles by WG depends on non-autonomous activation of target genes such as the proneural bHLH gene *achaete* (*ac*). Thus, there is a strong prediction that anterior *heph* mitotic clones should non-autonomously induce *ac* expression. The expression of *ac* was studied in *heph* genetic mosaic wing discs using an antibody to the AC protein. As was the case for bristles induced by *heph* mitotic clones in the adult wing, most of the ectopic AC expression associated with *heph* mitotic clones in the wing disc is induced surrounding the clones (Fig. 36). As seen in the adult, where occasional marked cells within the mitotic clone differentiate bristles, some AC expression was also seen in the *heph* clones.

Taken together, the association of ectopic *wg* and *ac* expression in and surrounding *heph* mutant tissue suggests that, following ectopic induction of *wg* expression, ectopic margin is induced around *heph* mitotic clones by a mechanism similar to that used during normal wing development. This raises the question of how *wg* expression becomes activated in *heph* mitotic clones. One explanation for the ectopic *wg* expression and wing margin nicks caused by *heph* mitotic clones is that *heph* may be required for WG signal transduction. In this model, the *heph* mutant flanking cells would not respond to the WG signal emanating from the boundary cells. It has been previously demonstrated with *disheveled* mitotic clones that WG signal reception is required to repress *wg* expression in the boundary cells and to induce WM formation (Couso et al. 1994; Micchelli et al. 1997). In order to test this hypothesis, expression of the WG target genes (*Dl*, *Ser* and *Distal-less* (*Dll*)) was examined in *heph* mosaic wing discs using antibodies against the DL, SER and DLL proteins.

3.3.5 *Delta*, *Serrate* and *Distal-less* protein expression in *hephaestus* genetic mosaic wing discs.

Both *Dl* and *Ser* are expressed in flanking cells along the D/V boundary in response to WG signal reception (Micchelli et al., 1997). The levels of both DL and SER are low in *heph* mutant tissue both in the flanking cells and throughout the wing disc (Fig. 37 and 38). However, the expression of *Dll* is unaltered in *heph* mitotic clones (Fig. 39). *Dll* expression in the wing pouch, and elevated *Dl* and *Ser* expression along the wing margin are dependent on WG signal transduction but, unlike *Dl* and *Ser*, *Dll* is not also a target of the Notch pathway. This suggests that *heph* mutant cells are able to receive and respond normally to the WG signal. This interpretation is also supported by the ability of *heph* mutant cells to express *ac*, another WG target (Fig. 36). Since *heph* mutant cells are able to transduce the WG signal, another explanation for the reduction of DL and SER expression must be found. One possibility is that there is an autonomous increase in

Notch activation in *heph* cells leading to the observed reduction in *Dl* and *Ser* expression and increase in *wg* expression. An alternative is that the loss of *heph* directly affects the expression of *Dl* and *Ser*. If so, this might secondarily allow increased Notch activation.

An important aspect of the *heph* genetic mosaic phenotype supports the latter alternative: mitotic clones of *heph*⁰³⁴²⁹ are associated with WM nicks (Fig. 28, 29). These nicks are especially frequent when mitotic clones are induced before mid-second instar, when DL and SER first activate Notch along the D/V boundary to initiate wing margin determination. Loss of *Dl* and *Ser* expression in *heph* mitotic clones can explain the association of *heph* clones with WM nicks, but can it explain ectopic margin genetic mosaic phenotype of *heph*?

High levels of DL and SER flanking the *wg*-expressing boundary cells are required to inactivate Notch signal transduction through an autonomous inhibition for which there is no defined mechanism (see discussion). This serves to restrict the Notch-dependent boundary expression of *wg*. Thus, loss of *Dl* and *Ser* expression beside the boundary cells could lead to cell autonomous ectopic Notch activation, and ectopic *wg* expression, leading to ectopic wing margin induction in neighboring cells. Therefore, the ectopic margin and wing margin nicks induced by *heph* mitotic clones can be explained by loss of *Dl* and *Ser* expression (see discussion).

3.3.6 *cut* protein expression in *hephaestus* genetic mosaic wing discs

Mitotic clones doubly mutant for *Dl* and *Ser* located adjacent to the normal D/V boundary have an ectopic margin phenotype similar to those induced by *heph* (see discussion). In both of these cases, ectopic margin is induced only near the endogenous margin and the margin markers WG and CUT are detected only within a competent region close to the D/V boundary (Rulifson et al., 1996). In both *Dl Ser* double mutant clones (Rulifson et al. 1996) and *heph* mutant clones (Fig. 40), ectopic CUT is only observed just inside the clone boundary. Together with ectopic *wg* expression, the ectopic expression of *cut* in *heph* clones suggests that Notch is active in these cells, since WG and Notch activation normally cooperate to activate *cut* expression (Neumann and Cohen, 1996).

cut is expressed in *heph* mutant cells adjacent to wild type cells near the D/V boundary. Because adjacent cells in this region presumably express SER and DL, this result suggests that the *heph* mutant *cut*-expressing cells have the highest levels of Notch activation in the *heph* clone. This is consistent with the observation that boundary *cut* expression is activated later in development than *wg*, after higher levels of DL and SER in the flanking cells are thought to induce higher levels of Notch-activation in the boundary cells (Micchelli et al. 1997; de Celis and Bray 1997).

Figure 37. *Delta* expression is low in *hephaestus* mutant tissue.

Laser scanning fluorescent images of DL (middle panel and red) visualized with a mouse anti-DL primary antibody and an anti-mouse Alexa-fluor^{594nm} secondary antibody, and GFP (left panel and green), expressed from a *P{Ubi-GFP}* transgene that is not present in cells mutant for *heph*⁰³⁴²⁹. (A) An example of *Dl* protein expression typical of wing discs from heterozygous *heph*⁰³⁴²⁹ / *TM6B, Tb* roaming third instar larvae. (B-E) Examples of *heph* mosaic wing discs stained for *Dl* protein expression. The wildtype level of *Dl* expression is lost within *heph*⁰³⁴²⁹ clones. Although it does not depend on proximity to the normal margin, this effect on *Dl* expression can be observed most clearly in cells flanking the boundary cells, where *Dl* expression is high.

(A, B, E) bar, 100 μ M.

(C, D) bar, 25 μ M.

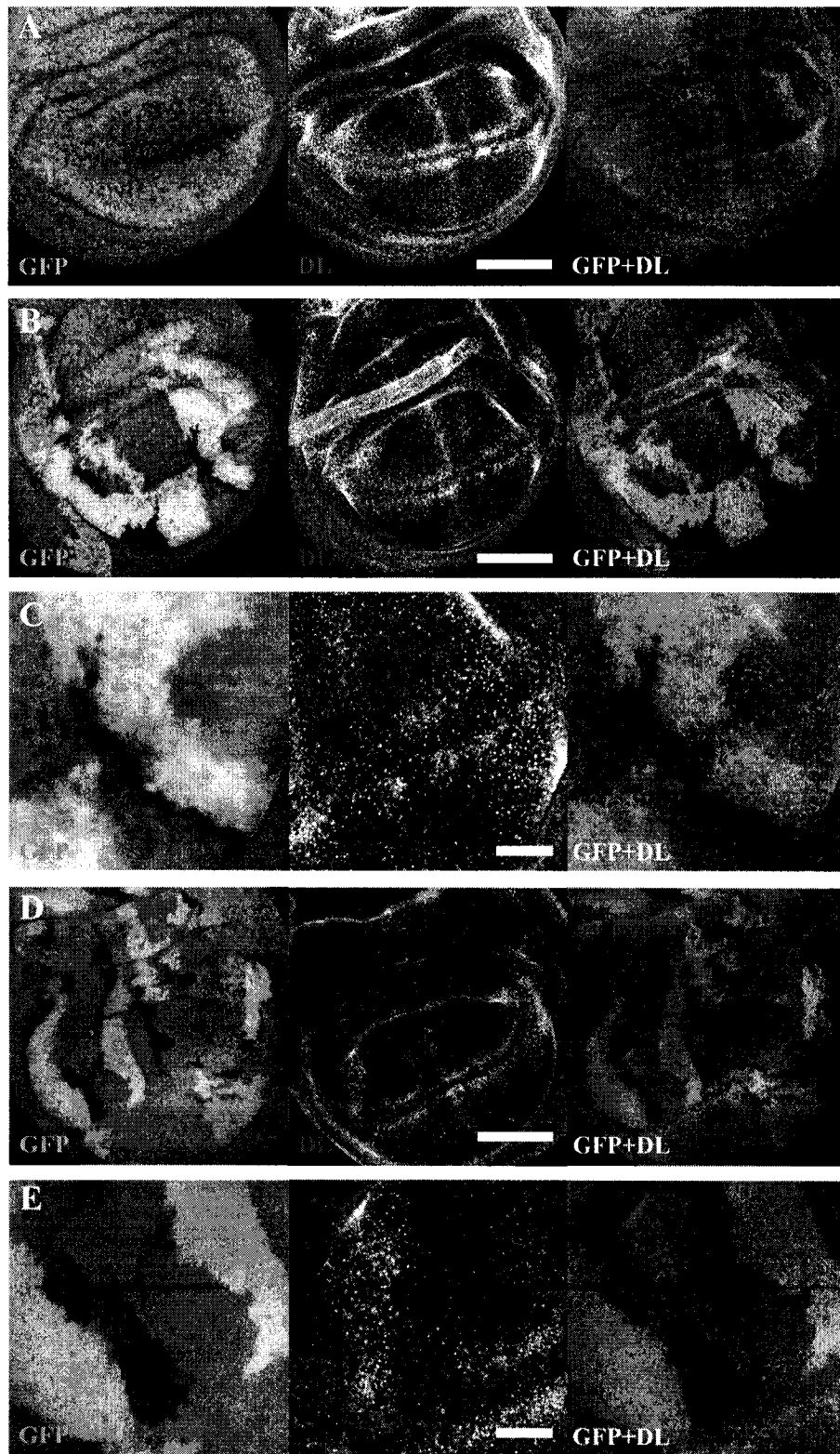


Figure 38. *Serrate* expression is low in *hephaestus* mutant tissue.

Laser scanning fluorescent images of SER (middle panel and red) visualized with a rat anti-SER primary antibody and an anti-rat Cy3 secondary antibody, and GFP (left panel and green), expressed from a *P{Ubi-GFP}* transgene that is not present in cells mutant for *heph*⁰³⁴²⁹. (A) An example of wildtype *Ser* protein expression typical of wing discs from heterozygous *heph*⁰³⁴²⁹ / *TM6B*, *Tb* roaming third instar larvae. (C-E) An example of a *heph* mosaic wing disc stained for *Ser* protein expression. *Ser* expression is lost within *heph*⁰³⁴²⁹ clones. Although it does not depend on proximity to the normal margin, this effect on *Ser* expression can be observed most clearly in cells flanking the boundary cells, where *Ser* expression is high.

(A, C) bar, 100 μ M.

(B, D, E) bar, 25 μ M.

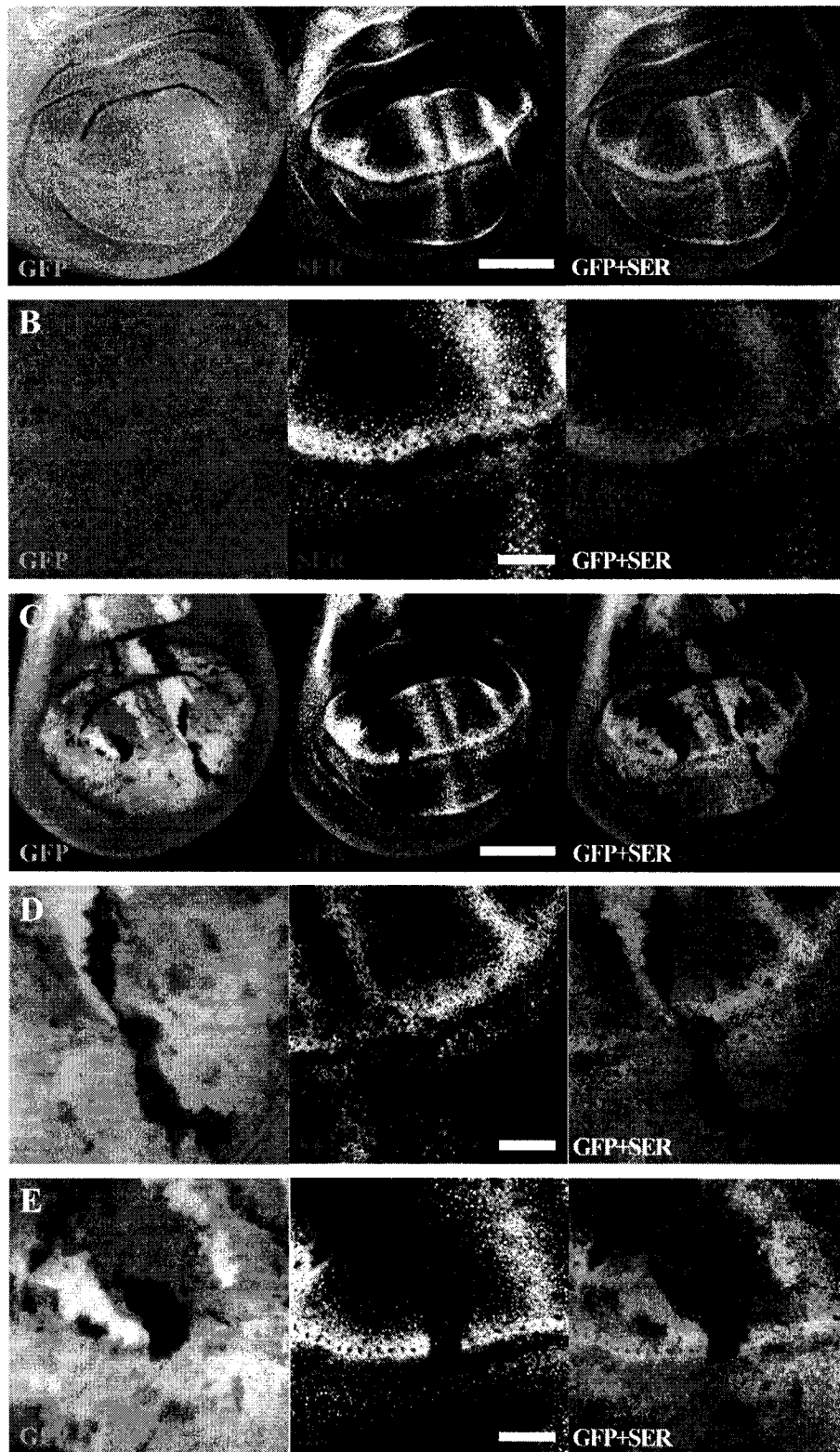


Figure 39. Expression of *Distal-less* is not altered by loss of *hephaestus*.

Laser scanning fluorescent images of DLL (middle panel and red) visualized with a mouse anti-DLL primary antibody and an anti-mouse Alexa-fluor^{594nm} secondary antibody, and GFP (left panel and green), expressed from a $P\{hsGFP\}$ transgene that is not present in cells mutant for $heph^{03429}$. (A) Wildtype *Dll* protein expression a typical wing disc from heterozygous $heph^{03429} / TM6B, Tb$ third instar larvae. (B-E) Examples of normal *Dll* protein expression in *heph* mosaic wing discs suggest that WG signal transduction is normal in $heph^{03429}$ mutant tissue.

(A-E) bar, 100 μ M.

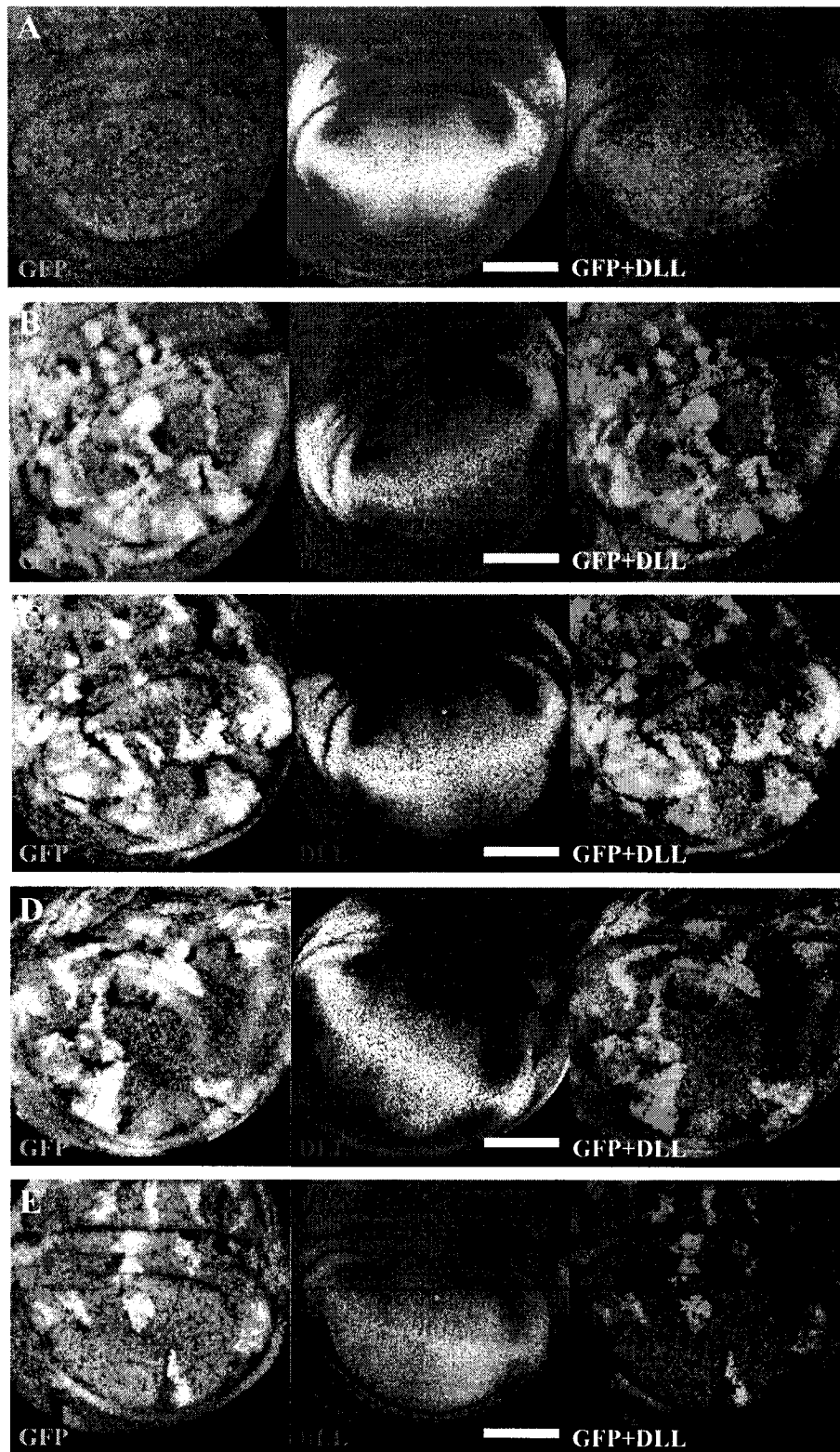
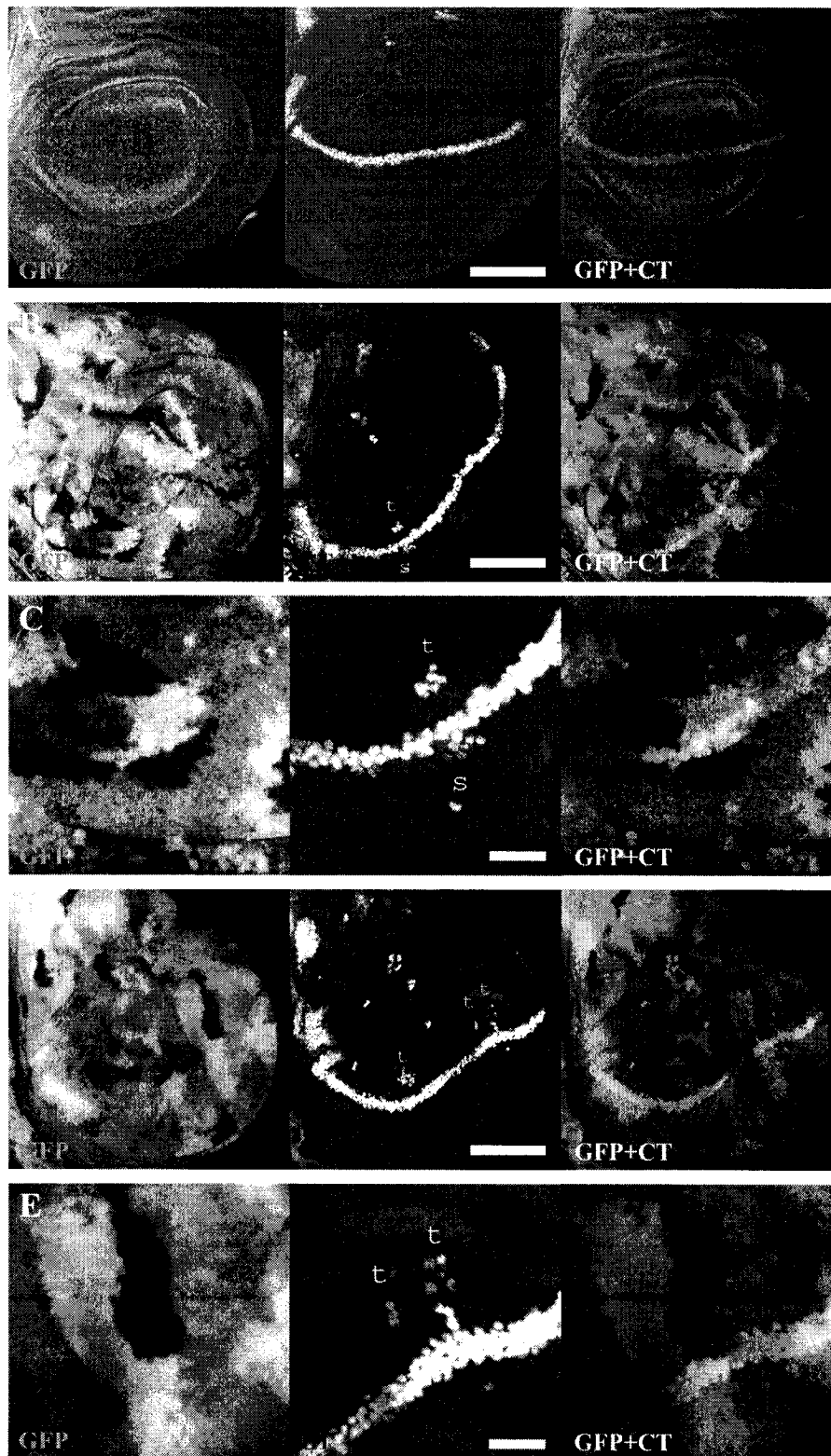


Figure 40. Ectopic *cut* expression is induced within *hephaestus* mitotic clones that are near the D/V boundary.

Laser scanning fluorescent images of CT (middle panel and red) visualized with a mouse anti-CT primary antibody and an anti-mouse Alexa-fluor^{594nm} secondary antibody, and GFP (left panel and green), expressed from a *P{Ubi-GFP}* transgene that is not present in cells mutant for *heph*⁰³⁴²⁹. (A) An example of wildtype *ct* protein expression from a typical heterozygous *heph*⁰³⁴²⁹ / *TM6B, Tb* third instar wing disc. (B-E) Examples of *ct* protein expression in *heph* mosaic wing discs. Both dorsal and ventral ectopic *ct* expression (arrowheads) within *heph*⁰³⁴²⁹, GFP- mitotic clones that are close to the normal *ct*-expressing boundary cells.

(A, B, D) bar, 100 μ M.

(C, E) bar, 25 μ M.



3.3.7 Molecular nature of Notch signalling

In order to identify possible points of regulation in the Notch signal transduction pathway, an introduction to the mechanism of Notch signalling is required. Notch and its ligands, DL and SER are cell-surface tethered transmembrane proteins. In its extracellular domain, Notch has 36 epidermal growth factor (EGF) repeats and 3 LIN-12/Notch repeats (LNR) required for association with its ligands. The Notch intracellular domain (NICD) includes 6 Ankyrin repeats that are required for signal transduction, and a PEST* domain thought to limit protein stability.

Notch activation involves a series of proteolytic steps that are required for the eventual release of the Notch ICD in response to ligand binding. Notch proteins can be cleaved in the extracellular domain (S1 cleavage) before export to the cell surface to produce a disulfide-bonded heterodimer (Blaumueller et al., 1997). Upon ligand binding to the extracellular domain of Notch, a second cleavage (S2) releases the extracellular domain of Notch (NECD) (Brou et al., 2000; Mumm et al., 2000). This cleavage can be catalyzed by the metalloprotease TACE (ADAM17) (Brou et al., 2000). The extracellular domain of Notch is *trans*-endocytosed into ligand expressing cells at least when Notch is activated during pupal wing vein and R-cell development in the eye disc (Parks et al., 2000). The extracellularly truncated Notch receptor (NEXT) is now a good substrate for intracellular S3 cleavage resulting in the release of NICD (Mumm et al., 2000), which requires the γ -secretase activity of Presenilin (PSN; De Strooper et al. 1999; Struhl and Greenwald 1999; Ye et al. 1999).

Truncated forms of Notch that lack the extracellular domain are constitutively active (they make good Presenilin targets) and localize predominately to the nucleus (Lieber et al. 1993; Struhl and Greenwald 1999). This suggests a direct mechanism of Notch signal transduction in which NICD is transported to the nucleus where it regulates gene expression. However, endogenous Notch nuclear fragments have not been convincingly detected in normal cells by immunofluorescent methods. Evidence that NICD accesses the nucleus *in vivo* is drawn from indirect methods designed to detect the nuclear access of chimeric transcription factors. For example, full length Notch expressed as a fusion protein with the GAL4 DNA binding domain and the viral VP16 transcriptional activation domain (GV) can activate transcription from a *UAS-lacZ* transgene (Struhl and Adachi, 1998). The reporter construct was activated only when the GV domains were inserted into the intracellular portion of Notch, and only in response to Notch ligands. As is the case for Notch, the GAL4 DNA binding domain localized predominately to the cell periphery, but appears to have access to the nucleus in response to ligand.

In the nucleus, NICD appears to interact with the DNA binding protein encoded by *Su(H)* to activate target gene expression (Jarriault et al., 1995; Kao et al., 1998; Klein et al.,

* Rich in proline (P), glutamic acid (E), serine (S) and threonine (T).

2000). Key targets and the major effectors of Notch signal transduction are genes of the *E(spl)-C*. They are direct targets for binding by SU(H) and are transcriptionally activated in response to Notch signalling (Bailey and Posakony, 1995; Fortini and Artavanis-Tsakonas, 1994; Lecourtois and Schweisguth, 1995). Although a direct role has not been shown for *Su(H)* in *wg* and *cut* transcriptional activation, *Notch* and *Su(H)* are required for *wg* and *cut* expression at the D/V boundary and ectopic Notch activation is sufficient to induce their expression (de Celis and Bray, 1997; Klein et al., 2000; Neumann and Cohen, 1996). Fusion proteins between SU(H) and the ankyrin repeats of Notch or the viral VP16 activation domain can produce Notch activated phenotypes (Klein et al., 2000). When NICD is expressed at high levels, the intracellular localization of endogenous SU(H) changes to become more nuclear (Gho et al., 1996), suggesting that Notch and SU(H) access the nucleus together. As a nuclear complex, NICD probably acts as the transactivation domain and SU(H) as the DNA-binding domain, supported by the activity of fusion proteins of Notch given a DNA binding domain, and fusion proteins of SU(H) given a transactivation domain (Klein et al., 2000; Struhl and Adachi, 1998).

3.3.8 NICD protein expression in *hephaestus* genetic mosaic wing discs.

The distribution of the intra-cellular domain of Notch (NICD) was examined in *heph* mosaic wing discs using an antibody that recognizes NICD and the intracellular portion of full-length Notch (FLN). In XY confocal micrographs, the level of NICD staining in *heph* mutant cells appears higher compared to surrounding wild-type cells (Fig. 41). This increase occurs in all cells independent of position within the imaginal wing disc. In XZ sections, reconstructed from series of optical sections through *heph* mosaic wing discs, the increased NICD staining appears to be localized away from the apical cell membrane and into the cytoplasm or nucleus of the cell (Fig. 40, 41). This apparent change in NICD localization and levels in *heph* mutant cells is similar to that seen in wildtype boundary cells where Notch target genes are highly expressed. This result suggests that *heph* has an autonomous effect on Notch, and that Notch is activated in *heph* mutant cells.

Figure 41. The amount of NICD may be higher in *hephaestus* clones relative to normal surrounding tissue.

XY Projections of 20 Laser scanning fluorescent images (spanning a 30 μM total thickness) of GFP from a $P\{Ubi-GFP\}$ transgene (left panel and green) and mouse anti-NICD primary antibody labeled with an anti-mouse Alexa-fluor^{594nm} secondary antibody (middle panel and red). XZ sections through the stack of images is shown below B and D (black arrowheads along the Y axis mark the position of the section). For each XZ section, the apical surface of the disc is up. (A, B) An example of NICD staining in a wing disc from heterozygous *heph*⁰³⁴²⁹/*TM6B, Tb* roaming third instar larvae. This disc has been rotated so the XZ section would bisect the D/V boundary. In this way, the localization of NICD in a section of tissue known to have highly activated N signalling can be observed. The position of the D/V boundary can be seen in A (arrowhead). (C, D) A typical example of *heph*⁰³⁴²⁹ mosaic wing discs with elevated levels of NICD staining corresponding to the position of *heph* clones. D is a higher magnification view of the disc in C, with an XZ section through a *heph* clone.

(A, C) bar, 100 μM .

(B, D) bar, 25 μM .

NICD, intracellular domain of Notch

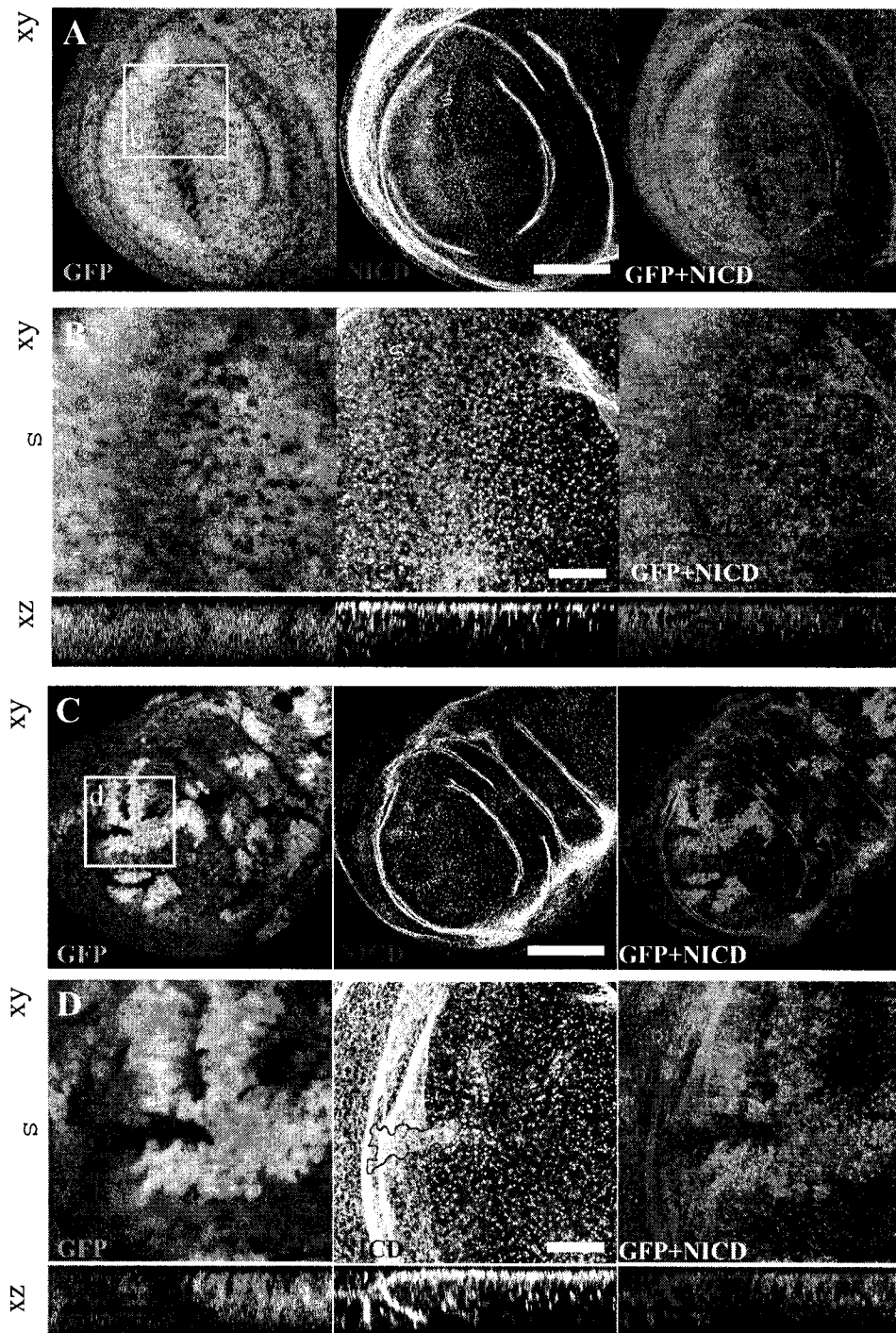


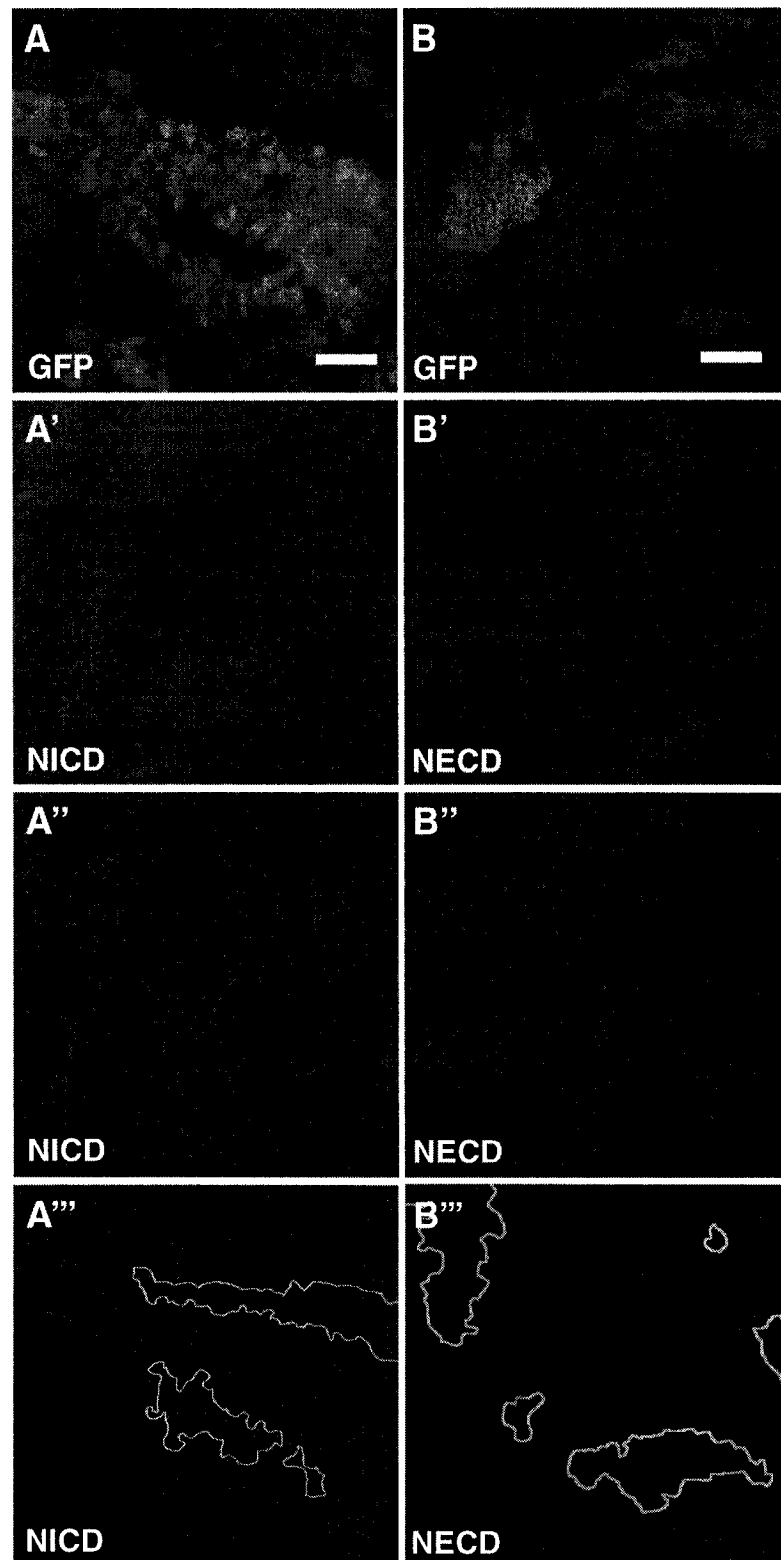
Figure 42. The intracellular localization of NICD is altered in *hephaestus* clones.

Laser scanning fluorescent images of a mouse anti-NICD primary antibody (A'-A''') or a mouse anti-NECD primary antibody (B'-B''') labeled with anti-mouse Alexa-fluor^{594nm} secondary antibodies. Loss of *heph* is marked by loss of GFP from a *P{Ubi-GFP}* transgene (A,B top). Each NICD or NECD image is an XY projection representing one of three 10 μ M apical (A',B') to basal (A''',B''') sections through the disc. The increased relative amount of NICD staining in *heph*⁰³⁴²⁹ clones appears to be inside of the mutant cells, not bound to the apical membrane. No corresponding increase is apparent using the NECD antibody.

bar, 25 μ M.

NICD, intracellular domain of Notch

NECD, extracellular domain of Notch



3.3.9 *Delta* and NICD protein expression in *Su(H)* mutant *hephaestus* genetic mosaic wing discs.

In order to test whether activation of Notch might lead to the observed decrease in SER and DL staining, the effects of *heph* mitotic clones on *Dl* protein staining were observed in imaginal discs mutant for *Su(H)* (for method, see Fig. 9). Since SU(H) is required to mediate the activating effects of Notch (Bailey and Posakony, 1995; Fortini and Artavanis-Tsakonas, 1994; Klein et al., 2000; Lecourtois and Schweisguth, 1995), if *heph* affects the expression of *Dl* through Notch activation, removing *Su(H)* might block the effects that loss of *heph* has on *Dl* protein expression. If on the other hand, *heph* directly affects DL levels, DL should still be reduced in cells doubly mutant for *heph* and *Su(H)*.

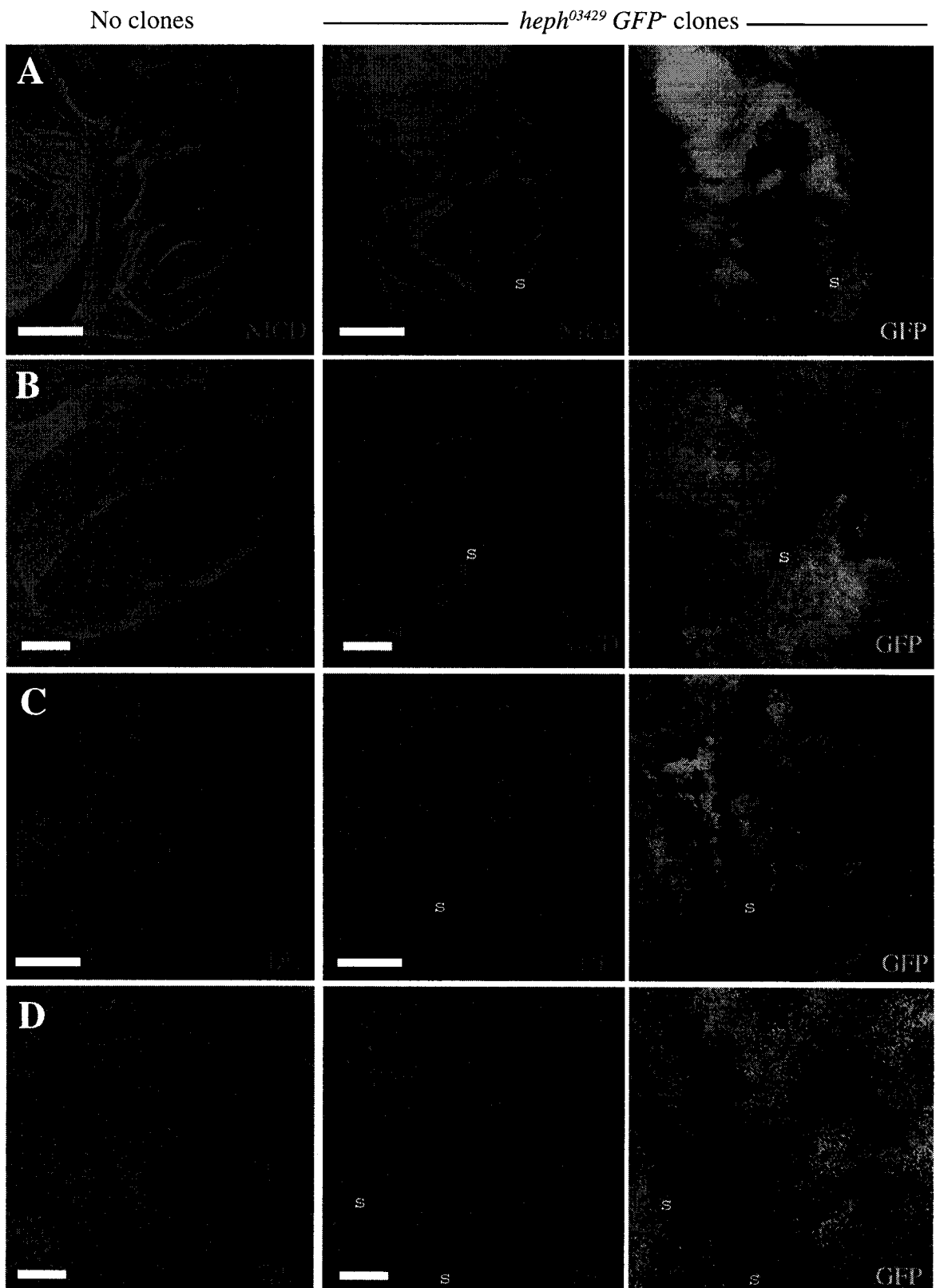
heph mutant clones induced in $Su(H)^2 / Su(H)^8$ mutant wing discs are not associated with a reduction of DL compared to surrounding wild-type tissue (Fig. 43). This is consistent with a reduction in DL due to Notch activation in *heph* mitotic clones. The staining pattern of NICD was also observed in *heph* mitotic clones induced in $Su(H)^2 / Su(H)^8$ mutant discs. Surprisingly however, no accumulation of NICD was observed in these clones (Fig. 43).

Figure 43. The effects of *heph* clones on DL and NICD depend on *Su(H)*.

Laser scanning fluorescent images of GFP expressed from a $P\{hsGFP\}$ transgene (right panel and green) and mouse anti-NICD primary antibodies (A, B) or a mouse anti-DL primary antibodies (C, D) labeled with anti-mouse Alexa-fluor^{594nm} secondary antibodies (red). The left column are images of $Su(H)^8 / Su(H)^2$ wing discs from *TM6B, Tb* larvae (no clones). The center column are images of NICD (A, B) or DL (C, D) expression from a $Su(H)^8 / Su(H)^2$ wing discs with *heph*⁰³⁴²⁹ clones. The *heph* clones in these discs lack green fluorescence (left panel). Notice that staining for NICD and DL is comparable between *heph*⁰³⁴²⁹ mutant and wildtype tissue within mosaic wing discs and when compared to non-mosaic discs. Arrowheads indicate the position of *heph* mutant clones.

(A, C) bar, 100 μ M.

(B, D) bar, 25 μ M.



4 DISCUSSION

4.1 Logic identifying *ectopic margin* with *hephaestus*

There is a near-perfect correlation between lethality at the *heph* locus and the *ema* phenotype. *Df(3R)G45*, *l(3)G45-11*, *l(3)G45-66*, *l(3)G45-73*, *l(3)L1022-162* and *l(3)A4-4-74* fail to complement the lethality of *heph* and cause the *ema* phenotype in clones. *l(3)G45-5*, *l(3)L1022-84*, *l(3)L1022-145* and *l(3)L1022-146* complement the lethality of *heph* and are not associated with ectopic margin in genetic mosaics. However, *l(3)G45-24* fails to complement the *heph* lethality but does not induce ectopic margin in clones. Mitotic clones of *l(3)G45-24* in the wing were not positively identified, so this could be a false negative result. *l(3)L1022-47* complements the lethality of *heph* and does induce ectopic margin in genetic mosaics. *l(3)L1022-47* may be a *heph* enhancer mutant exhibiting inter-allelic complementation other *heph* alleles.

*heph*⁰³⁴²⁹, *heph*^{j11B9}, and *heph*^{e2} are loss of function *heph* alleles that likely disrupt expression of *PTB*, leading to the *ema* phenotype. These three alleles are lethal, fail to complement one another, and are associated with ectopic margin in genetic mosaics. *heph*⁰³⁴²⁹, *heph*^{j11B9} are P-element induced alleles both with a P-element mapping to an intron of the *PTB* transcription unit. *heph*^{e2}, an EMS- derived allele, deletes several coding exons of *PTB*, including the coding region for RNA recognition motif 1 (RRM1), RRM2 and part of RRM3.

heph^{e1} is a temperature sensitive EMS-induced lethal allele and thus appears to be a weak allele compared to the *heph* alleles that cause the *ema* phenotype in clones. *heph*^{e1} fails to complement the lethality of *heph*⁰³⁴²⁹, *heph*^{j11B9}, and *heph*^{e2}, and fails to complement the male sterility of *heph*² as do each of the other lethal *heph* alleles. In genetic mosaics, *heph*^{e1} causes crossvein disruptions as do each of the lethal *heph* alleles, but it does not induce ectopic margin. Genomic DNA from *heph*^{e1} mutant larvae contains a missense mutation (G:C to A:T) that changes a conserved glycine (G) residue to a glutamine (Q) residue in the first predicted RRM of *PTB* (Fig. 20,46).

*heph*² is a P-element induced male sterile mutation that produces apparently normal homozygous adults, and complements the lethality of lethal *heph* alleles. However, flies trans-heterozygous for *heph*² and any one of the lethal *heph* alleles are male sterile.

Therefore, lethal and male sterile mutations of *heph* belong to one complementation group. In addition, molecular analysis has indicated that each of the five *heph* alleles map to a single transcription unit. The *heph* transcription unit is complex, with multiple alternatively spliced 5'UTRs, several polyadenylation sites, and the possibility of multiple promoters (Fig. 20). *heph*² may disrupt a subset of these transcripts, e.g. a testis-specific splice variant or promoter use, leading to a relatively mild phenotype. An alternate explanation is that *heph*² may be a hypomorph and male fertility is very sensitive to *heph* loss.

mr55 is a male-recombination induced mutation that causes a recessive detached posterior crossvein (pCV) phenotype and may be a weak *heph* allele due to the observed genomic DNA restriction fragment length polymorphism 3' to the *PTB* transcription unit. Rare escapers from a cross between *heph*^{el} and *l(3)L1022-162* also have detached pCVs, and may survive because of interallelic complementation within *heph*. The occurrence of the detached pCV phenotype in both these genotypes of different origin, and the loss of vein differentiation in mitotic clones of lethal *heph* alleles suggests that the detached pCV phenotype is related to loss of *heph*.

4.2 The *hephaestus* ectopic margin clonal phenotype is consistent with ectopic *wingless* expression

The non-autonomous margin-inducing effect of *heph* mitotic clones implies that wildtype tissue adjacent to the mitotic clone is responding to a signal produced by the *heph* mutant tissue. The response to this putative signal is to adopt the wing margin fate, suggesting that cells at the *heph* mitotic clone boundary may be recapitulating part of the cell signalling responsible for patterning the normal wing margin. Comparison of the *heph* ectopic margin phenotype to the genetic mosaic phenotypes of other genes known to act in wing margin signalling is instructive. For example, while both dorsal and ventral mitotic clones of *heph* are associated with ectopic wing margin bristles, mitotic clones of *fringe* (*fng*) mutations are associated with ectopic margin only when the mutant clone is within the dorsal compartment. Likewise, the margin-inducing effects of *apterous* (*ap*) mitotic clones or of *Serrate* (*Ser*) or *Delta* (*Dl*) over-expressing clones are compartment-specific unlike *heph* mutant clones. Thus, the phenotype of *heph* clones can not be explained conveniently through changes in expression of these genes. In addition, the non-autonomous effect of *heph* mitotic clones suggests *heph* likely does not encode a repressor of Wingless (WG) signal transduction or a repressor of WG target gene transcription. Mutants that mimic the reception of a WG signal (e.g. *shaggy* clones) express *wg* target genes and become neural in a cell-autonomous manner (Blair 1994 and references therein).

The phenotype caused by ectopic expression of *wg* closely matches the ectopic margin phenotype of *heph* mitotic clones. Ectopic *wg* expression is sufficient to non-autonomously induce ectopic wing margin and wing blade outgrowths from both dorsal and ventral compartments without affecting the compartmental identity of those cells (Diaz-Benjumea and Cohen, 1995). Therefore, the *heph* mutant phenotype is likely due to the ectopic *wg* expression that I observed in *heph* mutant cells close to the D/V boundary (Fig. 35)

Consistent with the role of *wg* in margin induction, I find that *heph* clones near the D/V boundary are surrounded by ectopic expression of *achaete (ac)*, a proneural marker for the anterior wing margin (Fig. 36). WG normally activates proneural gene expression (including *ac*) in cells flanking the anterior boundary cells. A subset of the *ac* expressing cells will give rise to the sensory bristles of the anterior wing margin (Blair, 1993; Couso et al., 1994; Diaz-Benjumea and Cohen, 1995; Phillips and Whittle, 1993). Further support for this ectopic *wg* expression hypothesis may be the outgrowths formed when ectopic margin induced by *heph* clones is near the A/P boundary. These outgrowths suggest that proteins present in or next to *heph* mitotic clones are interacting with proteins normally expressed along the A/P boundary to induce growth in surrounding tissue. This is reminiscent of the ectopic distal outgrowths formed by the coincident expression of *dpp* and *wg* (Campbell et al., 1993). Although ectopic *wg* expression can explain the ectopic margin and outgrowth phenotypes of *heph* in genetic mosaics, there are several observations indicating that ectopic *wg* is not the only consequence of *heph* loss.

Firstly, in addition to non-autonomously inducing margin differentiation, *wg* over-expressing cells in the wing blade often form margin bristles from within the clone (Diaz-Benjumea and Cohen, 1995). This might be because the ectopic *wg*-expressing cells do not express *cut* (Micchelli et al., 1997). Normally, the *wg* and *cut*-expressing cells at the presumptive margin do not form bristles (Couso et al., 1994). NICD expressing clones do express *cut*, and they induce only non-autonomous ectopic margin (Diaz-Benjumea and Cohen 1995; Micchelli et al. 1997). Ectopic *cut* expression is sufficient to inhibit *ac* expression, and *ac* is ectopically expressed within the boundary cell domain in discs from *cut* mutant larvae (Couso et al., 1994; Micchelli et al., 1997; Neumann and Cohen, 1996). These results suggest that *cut* inhibits wing margin formation in Notch activated cells. Ectopic *cut* expression is restricted to a subset of *heph* mutant cells (Fig. 40), and this might explain the partial loss of *ac* expression in *heph* clones, and the presence of some autonomous bristle differentiation from *heph* mutant tissue. Ectopic *cut* expression in *heph* mutant tissue also suggests that Notch is active in these cells and is responsible for both the ectopic *wg* and *cut* expression.

Secondly, ectopic *wg* expression does not account for the *heph* WM nick or vein disruption phenotypes. WM nicks closely match the phenotype caused by loss of *wg* expression at the D/V boundary and *wg* plays only a peripheral role in the formation of

crossveins (CVs; unpublished data cited in Conley et al. 2000). *wg* mutant clones including cells of either the dorsal or ventral compartment do not cause nicking but early *wg* clones that cross the boundary cause extensive non-autonomous loss of margin (de Celis and Garcia-Bellido, 1994b). Therefore, the *heph* margin loss phenotype (Fig. 29) might be explained by loss of *wg* expression along the D/V boundary possibly due to loss of *Notch* activation. Early clones often include both dorsal and ventral structures, and this may explain why the frequency of wing margin nicks is higher in *heph* genetic mosaics induced prior to formation of the D/V lineage restriction. The wing margin nicks that are observed in *heph* genetic mosaic wings are difficult to explain satisfactorily, so this topic will be revisited.

4.3 The *hephaestus* ectopic margin and vein loss phenotypes suggest ectopic Notch activation

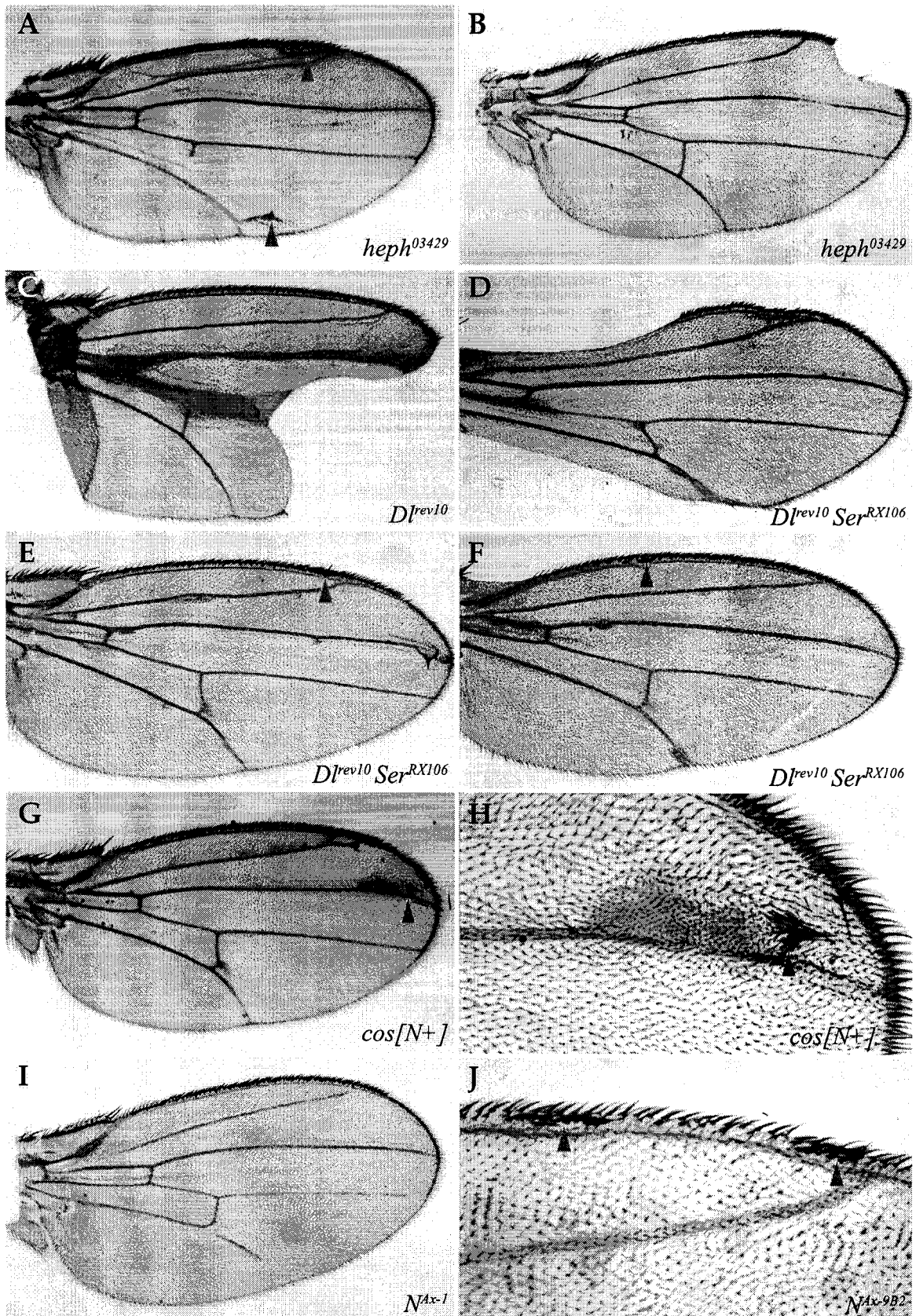
Several other genetic manipulations lead to an ectopic wing margin phenotype similar to that of *heph*. These include *disheveled* (*dsh*) mutant clones, increasing the dosage of full length *Notch*, ectopic expression of the active, intracellular domain of Notch (NICD), loss of *Dl* and *Ser* in double mutant clones, or changes in *Notch* function due to *Abruptex* (*Ax*) mutations. Of these, the one that most closely matches the *heph* genetic mosaic phenotype is that of *Ax* alleles of *Notch* (*N^{Ax}*).

Firstly, reducing the ability to receive the *wg* signal (in *dsh* mutant clones close to the D/V boundary) leads to autonomous ectopic *wg* expression and non-autonomous ectopic wing margin formation (Rulifson et al., 1996). The ectopic *wg* expression in *dsh* mutant clones closely resembles that observed in *heph* mutant clones (Fig. 35). In addition, *ac* expression is autonomously lost in *dsh* mutant clones and ectopic *ac* expression is induced outside of *dsh* mutant clones (Rulifson et al., 1996). Again, this is similar to the effects on *ac* expression observed in *heph* genetic mosaics (Fig. 36). These similarities lead to the hypothesis that WG signal transduction is compromised in *heph* mutant cells, leading to a failure to resolve the *wg* expression domain along the D/V boundary. However, expression of the WG target genes *ac* and *Dll* within *heph* mutant clones (Fig. 36, 39) indicates that *heph* mutant cells are able to respond normally to the WG signal.

Secondly, an increase in *Notch* gene dose ("extra-*Notch*") in clones causes ectopic wing margin from both dorsal and ventral compartments similar to the *heph* mutant phenotype (Fig. 44G,H and Doherty et al. 1996; de Celis and Bray 1997). However, unlike *heph* mitotic clones that autonomously disrupt the differentiation of veins, extra-*Notch* clones cause a wide vein phenotype similar to that caused by loss of *Dl* expression (Fig. 44). This phenotype suggests that Notch is able to inhibit the normal function of DL, perhaps by an autonomous inhibitory interaction. This is consistent with the observed phenotypic sensitivity of the ratio of *Dl* and *Notch* gene dose (see below).

Figure 44. Comparison of genetic mosaic phenotypes among *heph*, *Dl*, *Ser*, N^+ , and N^{Ax} .

(A,B) The *heph* genetic mosaic phenotype includes ectopic wing margin (arrowheads), vein loss, and wing margin nicks. (C) Loss of *Dl* causes wing margin nicks and the differentiation of wider veins. Loss of *Dl* and *Ser* in clones causes wing margin nicks (D), ectopic wing margin (arrowheads in E and F), and differentiation of wide veins (D-F). Changing the *Notch* gene dose in clones of a *cos[N⁺]* transgene causes ectopic margin and the differentiation of wide veins (G,H). N^{Ax} alleles (*Ax-1* is shown here) disrupt the differentiation of veins in hemizygotes (I). N^{Ax-9B2} hemizygous males differentiate ectopic wing margin bristles close to the endogenous margin (J).



If *Notch* expression were increased in *heph* mutant cells, a wide vein phenotype should result from the change in the relative levels of DL and Notch. In addition, I did not observe increased Notch immunostaining in *heph* mutant cells compared to surrounding wildtype cells when *heph* genetic mosaic wing discs were stained with an antibody recognizing the extracellular domain of Notch (Fig. 42). Thus, it is unlikely that *heph* mitotic clones have increased levels of full-length Notch.

Thirdly, ectopic Notch activation in clones that continuously over-express the intracellular domain of Notch is sufficient to induce ectopic *wg* expression and ectopic wing margin (Diaz-Benjumea and Cohen, 1995). However, these NICD-expressing clones are able to induce *wg* expression and ectopic margin outside of the *heph* competent region. One interpretation is that continuously over-expressing NICD creates a very high level of Notch activation sufficient to induce the boundary cell fate, i.e. "boundary levels" of Notch activation. This indicates that cells away from the normal margin are wing margin competent and suggests that Notch may be activated at boundary levels in *heph* mitotic clones only within a short distance of the normal margin. Within this domain, cells normally expressing high levels of *Dl* and *Ser* would be present directly beside *heph* mitotic clone borders. High levels of Notch ligands in adjacent tissue might therefore be inducing boundary levels of Notch activation along the *heph* mitotic clone border. In support of this idea, ectopic expression of *cut*, which requires high levels of Notch activation (Micchelli et al., 1997), was observed in mutant cells along *heph* clone borders close to the normal margin (Fig. 40).

Ectopic Notch activation can also explain the loss of vein differentiation in *heph* mitotic clones. Vein loss is a characteristic phenotype of ectopic activation of the Notch signalling pathway, accomplished in various ways. A pulse of general NICD over-expression driven with a heat shock promoter during pupal development is associated with loss of all veins (Huppert et al., 1997). *Abruptex* (*Ax*) alleles of *Notch* lead to ectopic Notch activation (de Celis and Bray, 2000; de Celis et al., 1996b) and result in autonomous loss of vein differentiation in genetic mosaics (de Celis and Garcia-Bellido, 1994a; de Celis and Garcia-Bellido, 1994b). Loss of the Notch repressor *Hairless* (*H*) in mitotic clones also causes autonomous loss of vein differentiation (de Celis et al., 1997; Schweisguth and Lecourtois, 1998). Major targets of the Notch signalling pathway in the wing disc include members of the *Enhancer of split Complex* (*E(spl)-C*). Over-expression of single members of this gene complex in the wing disc is sufficient to inhibit vein differentiation (de Celis, 1998; de Celis et al., 1996a). The autonomous loss of wing vein differentiation in *heph* mitotic clones can therefore be explained in terms of ectopic Notch activation in *heph* mutant cells, since Notch activation is sufficient to inhibit the vein fate.

Fourthly, loss of *Dl* and *Ser* in double mutant clones allows the differentiation of ectopic margin near the normal margin. After the initial activation of Notch at the D/V boundary, a genetic circuit comes into play to restrict the domain of Notch activation to a

2-3 cell wide stripe of boundary cells. This feedback circuit (Fig. 45D) is based on autonomous inhibition and lateral activation between the *wg*-expressing boundary cells and the flanking cells (Rulifson et al. 1996; Micchelli et al. 1997; de Celis and Bray 1997; Neumann and Cohen 1996). Boundary *wg* expression, induced during the second instar by DL and SER, is required to activate high levels of DL and SER in the flanking cells, some of which will ultimately give rise to the wing margin. The high levels of DL and SER in the presumptive D and V margin serve two roles. First, they are required to inactivate Notch signalling through an autonomous inhibition for which there is currently no defined mechanism. This serves to restrict the Notch-dependent boundary expression of *wg* (and explains the requirement for *dsh* to refine D/V boundary *wg* expression). Flanking domains of DL and SER also serve to induce high levels of Notch activation in adjacent boundary cells to maintain the expression of *wg* and induce the expression of the homeobox gene *cut* (*ct*). Notch activation in boundary cells serves to repress the WG targets *ac*, *Dl* and *Ser* in a manner that depends at least partially on CT. The result of this signalling loop is a band of cells expressing *wg* and *ct* where Notch is activated (the boundary cells) spanned on each side by stripes of *Ser* and *Dl* expressing cells where Notch activation is repressed (the flanking cells). This feedback loop therefore maintains the polarity of signalling and the separation of boundary cells from the flanking cells.

In *Dl Ser* double mutant clones occurring in the flanking cell domain, this feedback loop would break down, allowing ectopic Notch activation and ectopic *wg* expression in the disc, and ectopic wing margin in the adult. My results show that *heph* mutant clones have reduced levels of *Dl* and *Ser* in the flanking cells (Fig. 37,38). These observations might be sufficient to explain the observed ectopic *wg* expression and ectopic wing margin only close to the normal margin. The competent region for ectopic wing margin induction in *heph* genetic mosaics is likely the flanking cell domain where *Dl* and *Ser* expression is normally high and required to inhibit Notch activation. The role of *Dl* and *Ser* expression in the flanking cells is to autonomously inhibit Notch activation and to maintain Notch activation in the neighboring boundary cells. In a *heph* mitotic clone, *Dl* and *Ser* expression is low, and their autonomous inhibition of Notch activation must also be low. This might allow boundary levels of Notch activation in *heph* mutant cells that are adjacent to *Dl* and *Ser* expressing cells.

Although loss of *Dl* and *Ser* in *heph* mutant clones is sufficient to account for the ectopic wing margin phenotype, it does not explain the vein loss phenotype of *heph* mutant clones. Unlike *heph* mutant cells, which autonomously disrupt vein differentiation, mitotic clones of cells mutant for *Dl* and *Ser* cause a wide vein phenotype (Fig. 44E,F). This is presumably due to loss of *Dl*, because loss of *Ser* in genetic mosaics does not affect vein differentiation (Diaz-Benjumea and Cohen, 1995). Although *heph* clones express only low levels of *Dl* and *Ser*, the difference in effect between *heph* and *Dl Ser* clones on vein differentiation implies that the decrease of *Dl* and *Ser* expression in *heph* clones is indirect. I have shown that the decrease in *Dl* expression in *heph* clones does not occur in the absence of *Su(H)* (Fig. 43). *Su(H)* encodes a DNA binding

transcriptional co-factor that mediates the effects of activated Notch on target cells. If *heph* were directly required for *Dl* expression, DL antibody staining should still be lower in *heph Su(H)* double mutant clones, and *heph* clones should cause wide veins, not loss of veins. These results therefore support the alternative model that Notch activation causes the observed reduction of ligand expression in *heph* mutant cells.

This hypothesis is also supported by a general increase in the intracellular levels of NICD in *heph* clones similar in intracellular localization and level to that along the D/V boundary where Notch is highly activated (Figs. 41,42). Although the phenotypic consequences resembling those of Notch activation are spatially restricted within the wing, the effect of *heph* loss on NICD immunostaining is position independent. To explain this increase in NICD immunostaining, I suggest that *heph* has as its primary effect an autonomous increase in the intracellular levels of NICD and that the effects on DL and SER are secondary consequences of ectopic Notch signalling.

Unexpectedly, an increase in NICD staining was not observed in *heph* mutant clones in the $Su(H)^2 / Su(H)^8$ background. One explanation for this result may be that the observed increase in NICD staining in *heph* clones depends on the decrease in *Dl* and *Ser* expression. An alternative explanation is that *Su(H)* is required for the observed increase in NICD staining, possibly related to its proposed role in helping NICD access the nucleus (Kidd et al., 1998). Unfortunately, the morphology of the wing disc is severely affected by loss of *Su(H)*, as are the mechanisms responsible for inducing patterned expression of *Dl* and *Ser*. To gain supporting evidence that ligand levels drop in *heph* clones as a result of Notch activation, DL, SER and NICD expression should be studied in *heph Df(3R)E(spl)-C* double mutant clones. Loss of the *E(spl)-C* should suppress the reduction in ligand expression if it is a response to Notch activation.

Finally, mitotic clones of *Ax* alleles of *Notch* are associated with ectopic wing margin close to the endogenous margin (de Celis and Garcia-Bellido, 1994a; de Celis et al., 1996b). *Ax* alleles of *Notch* are characterized by wing veins that do not reach the WM (Fig. 27I), probably due to the ectopic expression of *Notch* target genes away from the D/V boundary of *Ax* discs (de Celis and Bray, 2000; de Celis et al., 1996b). Clones of lethal *Ax* alleles cause cell autonomous loss of vein differentiation (de Celis and Garcia-Bellido, 1994a; de Celis and Garcia-Bellido, 1994b) and complete vein loss when the *Ax* clone covers both the dorsal and ventral vein surfaces. In addition, ectopic WM close to the normal margin similar to that associated with *Dl Ser* or *heph* mitotic clones can be found in N^{Ax-9B2} males (Fig. 27J). The *Ax* phenotype likely results from an inability to repress Notch activation (de Celis and Bray, 2000; de Celis et al., 1996b). One explanation that accounts for the *Ax* phenotype is that *Ax* mutations disrupt autonomous inhibition of Notch by its ligands (de Celis and Bray, 2000). The similar partial rescue of the dominant gain-of-function *fng* allele, *fng^{D4}*, by *heph⁰³⁴²⁹* and N^{Ax-1} suggests that *heph⁰³⁴²⁹* might cause unregulated Notch signalling similar to that caused by the *Ax* alleles of *Notch* or loss of *Dl* and *Ser* expression in the flanking cells. In other words, the

partial rescue of *fng*^{D4} by *heph*⁰³⁴²⁹ can be explained if *heph* is autonomously required to repress Notch signalling.

4.4 *Delta hephaestus* epistasis

Since *Dl* and *Ser* expression levels drop in *heph* mutant cells, and this could be used to explain the ectopic margin phenotype of *heph*, it was possible that *heph* is normally required for high levels of *Dl* and *Ser* expression. However, this hypothesis is not supported by the opposite genetic mosaic phenotypes of *heph* and *Dl* in veins and the observation that *Dl* is epistatic to *heph*.

If *heph* were required for *Dl* expression or activity, loss of *heph* should cause the same phenotype as loss of *Dl*. However, loss of *Dl* leads to a loss of *Notch* activation and vein fate refinement, leading to the differentiation of wider veins. In contrast, loss of *heph* causes autonomous loss of vein differentiation similar to ectopic *Notch* activation.

The apparent opposite effects of *Dl* and *heph* on *Notch* activity in vein differentiation allowed the determination that *Dl* is epistatic to *heph* in double mutant clones (Fig. 32). With the assumption that *Dl* and *heph* act in the same linear pathway, the standard interpretation of the epistatic relationship between *Dl* and *heph* would be that *heph* acts upstream of and in opposition to *Dl*. A prediction of this interpretation is that *Dl* expression or activity should increase in *heph* clones, yet its expression drops. There are several alternative explanations for this discrepancy. First, *heph* and *Dl* may not act in a simple linear pathway. Since available evidence supports a role for *heph* in the *Notch* signalling pathway, these results may be explained better using a non-linear view of the *Notch* pathway (see below). Using this model, cells that normally escape *Notch* activation (cells flanking the D/V boundary and presumptive vein cells) no longer do so.

If *heph* has an autonomous effect on *Notch* signalling, how can the epistatic relationship between *Dl* and *heph* now be explained? In the absence of *Dl*, vein differentiation is no longer laterally restricted due to a loss of *Notch* activation in lateral provein cells. Loss of *heph* causes vein loss, consistent with ectopic *Notch* activation in central provein cells. In a *Dl heph* double mutant, the ectopic *Notch* activation phenotype of *heph* is masked by the *Dl(lf)* loss of *Notch* activation phenotype. This can be explained if *Notch* activation in a *heph* mutant cell is still dependent on a *Notch* ligand, and thus *heph* is only required after *Notch* is activated. This would imply, in other words, that *heph* may normally function as a repressor of activated *Notch*.

4.5 *hephaestus* is required where *Notch* activity must be reduced

The *heph* ectopic margin and vein loss phenotypes in genetic mosaics illustrate that *heph* is required only in those areas of the wing where Notch activation would otherwise occur, and must be prevented to form a normal pattern. Firstly, *heph* is required in cells flanking the boundary cells where earlier Notch activation is restricted to allow the induction of the wing margin fate, and to limit production of the *wg* signal to the restricted domain of boundary cells. In *heph* mitotic clones, the boundary fate is no longer inhibited in the flanking cells, allowing ectopic induction of the WM fate. This is likely due to loss of high levels of *Dl* and *Ser* expression, which would be expected to allow boundary levels of N activation where DL and SER are available from adjacent cells. This restricted boundary-level activation of Notch in *heph* mutant cells in the flanking domain would then lead to ectopic expression of *wg* and *cut*, and ectopic margin in neighboring cells. Thus, the ectopic margin-competent region is likely defined by the presence of high DL and SER levels adjacent to *heph* mutant tissue when the clone is within the flanking cell domain.

heph is also required within the presumptive vein where Notch activation must be prevented to allow vein differentiation. Within the presumptive vein of a pupating wing disc, DL activates Notch in lateral provein cells, and activated Notch represses *rhomboid* (*rho*) expression. Since *rho* promotes expression of *Dl*, expression of *rho* and *Dl* are restricted to the vein. That *Dl* expression is low in *heph* clones can be explained since *rho*-dependent activation of *Dl* expression is inhibited by Notch activation. If in *heph* mutant pro-vein cells activated Notch is not inhibited, then *rho* expression should be repressed, leading to loss of vein differentiation. In the absence of *Dl* in a *heph Dl* double mutant clone, Notch would not be activated in the clone, *rhomboid* expression would not be repressed, and the provein would be allowed to differentiate as vein (i.e. *Dl* epistatic to *heph* as observed). In the preceding discussion, the level of Notch activation in *heph* mutant cells is presumed to be sufficient to inhibit *rhomboid* expression and the vein fate, but insufficient to activate *wg* and *cut* expression. The boundary levels of Notch activation are only induced close to the normal margin, where high levels of DL and SER normally induce high levels of Notch activation in adjacent cells.

The *mr55* (and *heph*^{el} / *l(3)L1022-162*) recessive detached posterior crossvein phenotype (Fig. 21) suggests that *heph* may be most stringently required at the connection between the posterior crossvein (pCV) and longitudinal veins (LV). The only vein defect in *mr55* homozygotes is that differentiation of the pCV is not continuous with the LVs. Proveins for the LVs and the anterior CV are patterned before that of the pCV (Conley et al., 2000). Notch is already highly expressed and activated along the length of the LVs in lateral provein cells when the CVs are patterned, so the CVs must form within territory that has already been specified as intervein (de Celis et al. 1997; Huppert et al. 1997; Conley et al. 2000). When the pCV is patterned, the existence of a mechanism to prevent continued Notch activation at the LV/CV intersection seems probable, in order to allow

continuous vein differentiation. Since Notch activation and expression is high along the LV lateral vein cells before CV patterning and decreases after, the LV/CV boundary is a good candidate for an area of high sensitivity to a gain in Notch function.

4.6 Model of Notch-Ligand interactions

Notch activation can explain the *heph* ectopic wing margin and vein loss phenotypes, but does not seem to be sufficient to explain the wing margin nicking phenotype. How can this discrepancy be explained? One possibility is that *heph* regulates multiple genes in the wing disc, and that the WM nicks are unrelated to the ectopic wing margin. Alternatively, we might be able to explain these nicks in terms of the following non-standard model for Notch-ligand interactions, which is supported by a series of observations that cannot easily be explained using the simple model that *Dl* acts solely as a ligand that activates the Notch receptor.

The haploinsufficient loss of function phenotypes of *Dl* and *Notch* are similar in that they both cause differentiation of wider veins (de Celis and Bray, 2000; Lindsley and Zimm, 1992; Vässin et al., 1985). Therefore, the *Notch(lf)* wide vein phenotype can be explained in the same way as a deficiency in the function of *Dl* that activates *Notch*. In addition, while *Notch(lf)* alleles cause wide veins, *Notch(gf)* *Abruptex* alleles cause loss of veins (de Celis and Garcia-Bellido, 1994b; Foster, 1975; Welshons, 1971). As previously presented, these phenotypes are consistent with a role for DL-Notch signalling in restricting vein width. The following exceptions to this model argue for the presence of autonomous inhibitory interactions between *Notch* and its ligands.

Firstly, flies doubly heterozygous for both *Dl* and *Notch* loss-of-function mutations differentiate veins of normal width (de Celis and Bray, 2000; Vässin et al., 1985). If *Dl* and *Notch* were only involved in interactions resulting in activation of *Notch*, a reduction of both *Notch* and *Dl* should cause a more abnormal phenotype than a reduction in either *Dl* or *Notch* alone.

Secondly, the *Dl(lf)* wing phenotype is indistinguishable from the wide vein phenotype caused by extra doses of *Notch*⁺ (de Celis and Bray, 2000). Additionally, extra doses of *Dl*⁺ cancel the wide vein phenotype of extra doses of *Notch*⁺ (de Celis and Garcia-Bellido, 1994a), while increasing *Notch*⁺ gene dose enhances the *Dl(lf)* vein widening phenotype (de Celis and Bray, 2000). The same *Notch* duplication can rescue the *Notch(lf)* neurogenic phenotype (de la Concha et al., 1988), and can correct phenotypes caused by *Ser* deficiency (Thomas et al., 1991). These results indicate that the phenotype displayed depends on the relative levels of *Dl* and *Notch* function.

Thirdly, mitotic clones of a *Notch*⁺ duplication can induce neighboring wildtype cells to differentiate as veins (de Celis and Garcia-Bellido, 1994b). In this study, the marker used

(*shavenoid*) did not allow the identification of vein histotype within the clone. Using a *Notch*⁺ rescuing transgene on 3R and *pwn* as a clone marker, I have observed autonomous and non-autonomous vein differentiation associated with clones with added *Notch*⁺ gene dose (Fig. 44H). These observations suggest that *Notch* can negatively regulate *Dl* function.

Fourthly, a *Dl*⁺ duplication enhances the neurogenic phenotype of a *Notch* hypomorphic allele (de la Concha et al., 1988; Vässin et al., 1985). If the only role for *Dl* were to non-autonomously activate *Notch*, increasing the *Dl*⁺ gene dose would be expected to compensate, in part, for a decrease in *Notch* expression. In fact, over-expressing either *Ser*⁺ or *Dl*⁺ in the wing disc with the GAL4/UAS system can autonomously cause wing margin nicks and the differentiation of wide veins, while they induce Notch activation only non-autonomously (de Celis and Bray, 1997). This apparent dominant-negative interaction of *Dl* or *Ser* inhibiting *Notch* can be rescued by co-(over)-expressing either ligand with *Notch* (Doherty et al., 1996; Klein and Arias, 1998). These results suggest that excess ligand expression by a cell prevents activation of Notch expressed in the same cell. Normally, there must be a finely-tuned balance between the protein levels of Notch and its ligands, since altering the relative *Notch*⁺ and *Dl*⁺ gene dosage produces dominant phenotypes.

Finally, small *Dl(lf)* clones have elevated and ectopic *wg* expression adjacent to the normal *wg*-expressing cells, especially extending ventrally (Doherty et al., 1996). Since *wg* expression depends on *Notch* activation, this result indicates that one role for *Dl* is to inhibit *Notch* activation cell autonomously. This observation has been recently explained by the characterization of a cell-autonomous inhibitory mechanism between DL, SER and Notch (Fig. 45A; de Celis et al. 1996b; Rulifson et al. 1996; de Celis and Bray 1997; Micchelli et al. 1997). Boundary *wg* expression, induced during the second instar by ventral DL and dorsal SER, is required to activate high levels of both DL and SER in the dorsal and ventral flanking cells. Here, DL and SER are required to autonomously inactivate Notch signalling and to induce and maintain high levels of Notch activation in adjacent boundary cells. Notch activation in the boundary cells activates *wg* expression and represses WG target genes including *Dl* and *Ser*. A similar feedback loop may operate along the pupal vein primordia (Fig. 45B). Activation of Notch indirectly inhibits *Dl* expression in the lateral provein cells and restricts high levels of *Dl* expression to the presumptive vein. It is possible that high *Dl* expression in the vein cells allows these cells to escape inhibition by Notch.

Figure 45. Schematic representation of Notch feedback mechanisms in the wing disc.

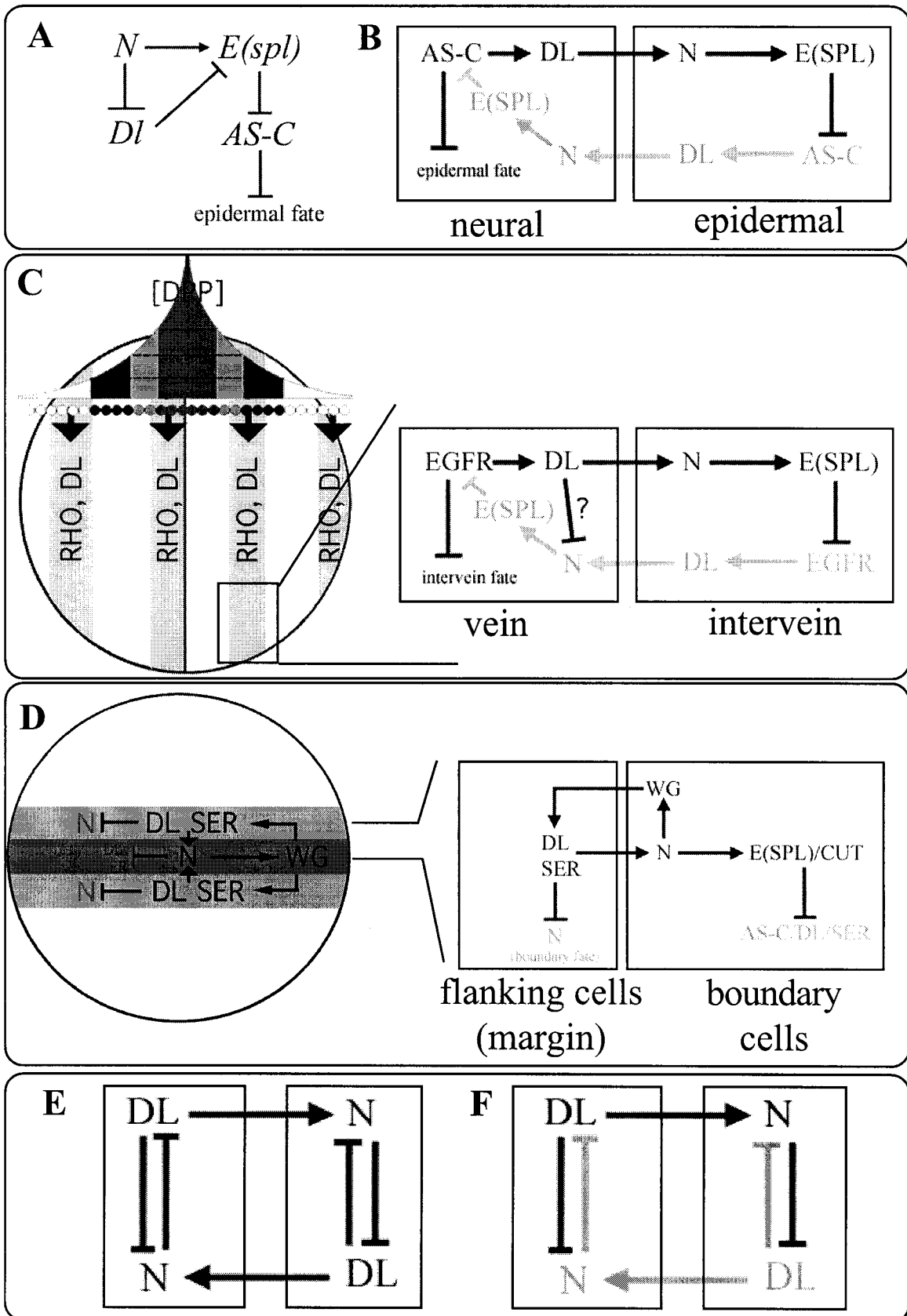
(A) Formal genetic pathway summarizing dosage interactions between *Notch*, *Delta*, *E(spl)* and *AS-C* during embryonic neurogenesis (de la Concha et al. 1988).

(B) Model of protein interactions regulating the choice between neural and epidermal fate in the developing thorax (Heitzler and Simpson 1991, 1993, 1996a). Each box represents a single cell of a proneural cluster.

(C) A model representing the DPP morphogen gradient inducing bands of vein competent cells by inducing *rhomboid* (*rho*) expression. During pupal development, a feedback loop illustrated to the right refines *rho* expression therefore refining EGFR activation and vein differentiation to a subset of the vein competent cells (de Celis et al. 1997). Each box represents a single provein cell. Notice the similarity between the models in B and C.

(D) A model representing asymmetric intercellular communication along the D/V boundary during the third larval instar (Micchelli et al. 1997). The circle represents the wing disc, the red domain represents Notch activated boundary cells, and the purple domains represent the flanking cell domain where Notch is repressed. The feedback loop represented here restricts and maintains Notch activation in the boundary cells through autonomous inhibition and non-autonomous activation. Each box to the right represents a single cell along the border between the flanking cell domains and the boundary cell domain.

(E,F) General model of the interactions between Delta and Notch in the above situations that may account for the exceptions noted in the text. (E) represents two early cells, with a balance between autonomous inhibition and non-autonomous activation while (F) represents the same cells after asymmetric signalling has been established. A mechanism that converts cells from balanced to asymmetric Notch signalling is not defined and may rely on external positional asymmetries.



The DL-Notch feedback loop operating at the wing margin and vein primordia can be represented as a simple non-linear Notch pathway (Fig. 45C,D). In this model, DL non-autonomously activates Notch, while it also autonomously inhibits activation of Notch. Notch activation inhibits *Dl* (and *Ser*) expression autonomously, while also activating *Dl* (and *Ser*) expression non-autonomously (and indirectly). It is with this model that I can most easily explain the *hephaestus* genetic mosaic phenotype. To state a hypothesis which might explain the *heph* genetic mosaic phenotype:

- 1) The principal effect of *heph* loss is excess *Notch* signalling due to an inability to reduce or turn off Notch signalling once Notch has been activated by its ligands.
- 2) It is known that ectopic *Notch* signalling is sufficient to inhibit *rhomboid* (*rho*) expression and vein differentiation. It can be inferred that *heph* is required within the presumptive vein to reduce *Notch* signalling and thus permit *rho* expression and promote the vein fate.
- 3) Genetic evidence indicates that *Notch* can act in opposition to *Dl*. Evidence presented here suggests that excess *Notch* signalling causes the decrease in *Dl* and *Ser* expression observed in *heph* mutant cells. Loss of Notch ligand expression in *heph* mutant clones is expected to have several different consequences. Firstly, loss of the *Dl* and *Ser* function that induces and/or maintains boundary levels of Notch activation along the D/V boundary would be expected to cause wing margin nicks. Secondly, loss of the *Dl* and *Ser* function that autonomously inhibits *Notch* activation would be expected to cause a failure to restrict margin Notch activation and *wg* expression, allowing the induction of ectopic margin. This effect seems to depend on Notch ligand expression in neighboring wildtype cells in the flanking cell domain, which would be expected to activate and/or maintain Notch signalling at boundary levels along the *heph* clone borders.

4.7 NICD degradation

The vein loss, ectopic margin and wing margin nicks associated with *heph* mutant clones can all be explained as excess *Notch* signalling in *heph* mutant cells. Therefore, it can be inferred that *heph* normally represses *Notch* signalling. Genetic epistasis indicates that excess *Notch* signalling in *heph* mutant vein cells still depends on *Delta*. This suggests that Notch is trafficked to the membrane properly, and any regulatory mechanisms that maintain ligand dependence of NICD release and target gene expression are still functioning normally. Any inhibitory regulation by receptor endocytosis seems to be working normally because defects here would leave more full-length Notch on the cell surface, which is expected to cause wide veins. Notch target genes are expressed in *heph* clones, indicating that nuclear access of NICD and its ability to activate gene expression are not inhibited by loss of *heph*. Where, then, might the *heph* Notch(gf) phenotype come from? Since the *heph* genetic mosaic phenotype identifies regions of the wing

where Notch signalling must be inhibited to form a normal pattern, *heph* may be required to limit NICD protein stability. Recent evidence indicates that degradation of NICD regulates its activity. The possibility that *heph* is required for NICD degradation is attractive because it would be a ligand-dependent requirement (*Dl* epistatic to *heph*) and can explain the increase in intracellular levels of NICD observed in *heph* mutant cells.

The PEST domain of NICD and ubiquitin-proteasome pathway have been implicated in regulating the activity of Notch through its regulated degradation. A rapid turnover of the nuclear form of Notch may explain the observation that endogenous Notch nuclear fragments have not been convincingly detected in normal cells by immunofluorescence methods. NICD expressed from a transgene is quickly degraded (Lieber et al., 1993), consistent with wildtype NICD molecules having short half-lives. NICD includes a PEST domain, a characteristic of proteins with very short half-lives (Rogers et al., 1986). Mutations of *Notch* that delete the PEST domain are associated with Notch(gf) phenotypes (Romain et al., 2001), suggesting the PEST domain is required for NICD degradation.

The proteasome is the predominant nuclear and cytoplasmic non-lysosomal proteolytic mechanism. By expressing a dominant negative proteasome subunit, Schweisguth (1999) has shown that the proteasome is required for NICD degradation in the *Drosophila* wing disc, and that a wildtype level of proteasome activity is required for alternative cell fate decisions during sense organ development. In addition, treatment of cells with chemical proteasome inhibitors allows the detection of nuclear NICD (De Strooper et al., 1999). These findings indicate that targeting the active form of Notch for proteasome mediated degradation may normally limit Notch signalling. Two different proteins have been implicated in ubiquitin-proteasome degradation of Notch, *Drosophila* Suppressor of deltex (Su(dx)) and its mammalian counterpart ITCH, and the *C. elegans* and mammalian SEL-10 proteins.

Sel-10 was isolated in *C. elegans* as a suppressor of the *lin-12(lf)* egg laying defect (Hubbard et al., 1997). *lin-12* encodes a protein similar to Notch. *Sel-10* encodes a protein with a HECT (Homologous to E6-AP C-Terminus) domain and 7 WD40 repeats, suggesting it is an E3 ubiquitin ligase. An E3 ubiquitin ligase specifically binds to a substrate, and ubiquitin is attached to the substrate by an E2 ubiquitin transfer enzyme. Ubiquitination targets the substrate for degradation by the proteasome. In worms, SEL-10 interacts with LIN-12, ubiquitinates it, and negatively regulates its activity (Hubbard et al., 1997). Mammalian SEL-10 binds to Notch1, and inhibits its transcriptional activity possibly through ubiquitination (Gupta-Rossi et al. 2001; Oberg et al. 2001). The Sel-10:Notch interaction is restricted to the nuclear compartment and depends on the phosphorylation of NICD (Gupta-Rossi et al., 2001). These results suggest that NICD is phosphorylated during its transport to the nucleus, creating a suitable substrate for ubiquitin-proteasome degradation in the nucleus. In *Drosophila*, the protein with highest sequence identity with human SEL-10 (78%) is encoded by *archipelago (ago)*. However,

a stabilization of Cyclin E but not of NICD was observed in genetic mosaics of *ago*. It should be noted that the *ago* alleles used were isolated in a screen for mutations with a growth advantage in genetic mosaics, so these alleles may specifically disrupt the SEL-10:Cyclin E interaction. It is possible that *heph* is required for expression or activity of *archipelago* or some other gene in this NICD degradation pathway.

Genetically, *Su(dx)* is a negative regulator of *Notch* because it rescues *Notch(lf)* wing margin loss. It also suppresses the wing margin loss of *dx*, a positive Notch regulator, enhances *N^{dx}* and *H* vein loss and suppresses the *Dl* wide vein phenotype (Fostier et al., 1998). The mammalian protein ITCH is similar to SU(DX) and can bind to the intracellular domain of Notch and promote its ubiquitination (Qiu et al., 2000). However, Gupta-Rossi et al. (2001) point out that ITCH does not need the PEST domain to bind Notch, and that ITCH may be able to bind a membrane attached form of Notch. They suggest that there are two different mechanisms that control the stability of Notch, one that acts in the nucleus (SEL-10) and one in the cytoplasm (SU(DX)).

4.8 Future directions: Targets of *hephaestus*, molecular and genetic approaches

heph is predicted to encode a protein with four RNA recognition motifs (RRM1-4). RRM1s are found in a variety of RNA binding proteins, including various heterogenous ribonucleoproteins (hnRNP), and protein components of small nuclear ribonucleoproteins (snRNP). The RRM motifs encoded by *heph* are probably diagnostic of an RNA binding protein. The most closely related proteins (by a.a. sequence comparison) are vertebrate PTB, and *Xenopus* Vg1RBP60, which is required for vegetal localization of *vg1* mRNA (Cote et al., 1999). PTB was identified in vertebrates as a heterogenous ribonucleoprotein (hnRNP I) that binds to RNA polypyrimidine-tracts. This binding was later shown with iterative *in vitro* target selection to be sequence specific (Singh et al., 1995). PTB is required for the control of alternative exon selection, internal ribosome entry site (IRES) use, and translational control (for a review, see (Valcarcel and Gebauer 1997, and references in Conte et al. 2000). *in vitro* deletion mutagenesis has been used to map important PTB domains (Oh et al., 1998; Perez et al., 1997). PTB can homo-dimerize and this requires RRM2. Interactions between PTB and hnRNPK requires RRM1, which may be compromised by the *heph^{el}* mutation. The strongest determinants of RNA binding specificity have been mapped by deletion mutagenesis to RRM3 and RRM4.

Surprisingly, a recent paper on the control of mammalian *High mobility group a (Hmga)* gene expression implicates PTB as a transcription factor (Rustighi et al., 2002). Rustighi et al identify a nuclease-sensitive element in the TATA-less *Hmga2* promoter region that is centered within a 60bp polypyrimidine tract which is essential for gene activity. This study reports that the ppy-tract can adopt a single-stranded conformation *in vitro* and that PTB is one of the nuclear factors that can bind to the ppy-tract.

A comparison between the predicted *D. melanogaster heph* protein (AF211191), *X. laevis* 60 kDa Vg1 mRNA binding protein (VgRBP60; AF091370), and *H. sapiens* (heterogenous nuclear RiboNucleoProtein I, hnRNP I / PTB; XM_055185) is presented in Fig. 46. The apparent sequence conservation between these proteins from divergent species suggests that they are functionally related. The direct targets of PTB in vertebrates are thus good candidates for direct targets of HEPH in *Drosophila*. Known targets of PTB are summarized in Table 12.

In addition to these known targets in mammalian cells, *heph* could be required for the expression (transcription) or activity (alternative splicing, mRNA stability, translation or localization) of characterized (or uncharacterized) repressors of Notch signalling.

A yeast 3-hybrid system can be used to analyze interactions between RNA and proteins (reviewed in Zhang et al. 1999). To summarize the method, yeast carrying a reporter transgene dependent on the GAL4 activation domain is transformed with three plasmids. The first encodes a DNA binding domain (e.g. LEX2, with a LEX2 binding domain upstream of the reporter transgene) conjugated to a known RNA binding protein (e.g. MS2). The second encodes a fusion between the GAL4 activation domain and an RNA binding domain of interest (e.g. HEPH RRM). In order to activate reporter transgene expression, the third plasmid would express a fusion RNA between the MS2 binding site and the HEPH binding site. This RNA would link the DNA binding domain and the transcriptional activation domain at the reporter gene promoter. To find targets of HEPH, the fusion RNA could be a library of short cDNA or genomic DNA fragments inserted upstream of the MS2 RNA target. Since a minimal binding site is preferential, an RNA target under 150nt is recommended (Zhang et al., 1999a).

An alternative method for isolating targets of HEPH is to immunoprecipitate HEPH from wing discs (for example), then isolate the co-immunoprecipitated RNA. However, since HEPH is predicted to encode an hnRNP, and hnRNPs were identified based on their co-immunoprecipitation, this might not be a very discerning experiment. The same argument can be applied against a yeast 2-hybrid screen for protein-protein interactions. Many expected protein targets of HEPH are other hnRNPs and a host of splicing factors.

PTB has been implicated in the repression of IRES dependent translation of both cellular and viral RNAs (Kim et al., 2000). Interestingly, there is evidence of truncated Notch protein expression from an IRES in the *Notch* RNA. Human tumor cells that have deletions of the 5' coding region of the *Notch* gene are able to produce a truncated Notch protein from an IRES (Lauring and Overbaugh, 2000). This IRES has been mapped to the coding region of the transmembrane domain. The truncated protein initiates at a methionine residue that is conserved among all Notch proteins. This raises the possibility that HEPH plays a role in the repression of *Notch* IRES use. If this were true, HEPH

Figure 46. Comparison among *D. melanogaster* HEPH, *X. laevis* VgRBP60 and *H. sapiens* PTB1.

ClustalW formatted alignment of the predicted a.a. sequences of *H. sapiens* PTB1, *D. melanogaster* HEPH and *X. laevis* VgRBP60. The position of a putative bipartite nuclear localization signal (NLS) and each of the 4 conserved RNA Recognition Motifs (RRM1-4) are noted. Identical a.a. are black, similar a.a. are shaded. The position and predicted effect of the *heph^{el}* mutation in RRM1 is marked. These possible orthologs of PTB were identified through a psi-BLAST search of GenBank nt database.

Table 12. Characterized targets of PTB/hnRNPI

Target	Mode of action	Reference
<i>α-actinin</i>	alternative splicing	(Southby et al., 1999)
<i>α-tropomyosin</i>	alternative splicing	(Lin and Patton, 1995)
<i>β-tropomyosin</i>	alternative splicing	(Mulligan et al., 1992)
<i>BiP (human immunoglobulin heavy chain binding protein=Hsp70)</i>	IRES repression	(Kim et al., 2000)
<i>c-src</i>	alternative splicing	(Chan and Black, 1997)
<i>Calcitonin/CGRP</i>	alternative splicing	(Lou et al., 1999)
<i>caspase-2</i>	alternative splicing	(Cote et al., 2001)
<i>Clathrin light chain</i>	alternative splicing	(Zhang et al., 1999b)
<i>fibroblast growth factor receptor 2</i>	alternative splicing	(Carstens et al., 2000)
<i>fibronectin</i>	alternative splicing	(Norton, 1994)
<i>GABA_A γ2 subunit</i>	alternative splicing	(Zhang et al., 1999b)
<i>Hepatitis C (viral)</i>	translation repression	(Ito and Lai, 1999)
<i>Hmga2 promoter</i>	possible transcription factor	(Rustighi et al., 2002)
<i>insulin</i>	mRNA stability	(Tillmar et al., 2002)
<i>N-methyl-D-aspartate receptor NR1 subunit</i>	alternative splicing	(Zhang et al., 1999b)
<i>TMEV (viral)</i>	IRES repression	(Pilipenko et al., 2000)
<i>Vgl mRNA</i>	mRNA localization	(Cote et al., 1999)

might bind directly to *Notch* mRNA, and a change in the ratio of Notch isoforms, or the presence of a novel Notch isoform, might be observed in *heph* mutant tissue. However, a prediction of the "IRES hypothesis" is that the *heph* phenotype should not depend on activation of Notch by DL or SER because the *heph* cells would be expressing an intracellular, truncated (and active) Notch isoform.

In mammals, PTB regulates the alternative splicing of α -tropomyosin and α -actinin. Both genes produce muscle-specific isoforms that are repressed by PTB. α -tropomyosin and α -actinin are actin bundling proteins that regulate the structure of the filamentous (F-actin) cytoskeleton. It is possible that HEPH represses muscle-specific splicing of one (or both) of these proteins and that NICD builds up in *heph* mitotic clones because of a cytoskeletal defect.

This is supported by the role of the actin cytoskeleton in trafficking of receptor proteins and by the suggested role of *sanpodo* (*spdo*) in Notch regulated alternative cell fate decisions in *Drosophila* (Dye et al., 1998). *spdo* encodes a ortholog of tropomodulin, an actin/tropomyosin associated protein. In mammals, there are isoform-specific interactions between tropomyosin and tropomodulin (Babcock and Fowler, 1994). Loss of *spdo* in *Drosophila* causes aberrant F-actin distribution and leads to a phenotype similar to loss of Notch function. Additionally, genetic studies showed that *spdo* is epistatic to *numb* (an inhibitor of *Notch*), suggesting that an actin based process is involved in Notch signalling.

Fluorescently labeled phalloidin was used to visualize a possible defect in the distribution of F-actin in wing discs with *heph* mitotic clones. There is no apparent difference in the F-actin levels or distribution between *heph* mutant cells and wildtype cells (data not shown). This experiment does not disprove the possibility that *heph* regulates the isoform ratios of the actin bundling proteins α -tropomyosin and α -actinin. However, if the alternative splicing of these genes is regulated by *heph*, loss of this regulation has no detectable effect on F-actin distribution.

Two other characterized inhibitors of Notch function should be mentioned. First, *nubbin* is thought to repress Notch activation below a hypothetical threshold in the wing disc (i.e. away from the D/V boundary; Neumann and Cohen 1998). I did not observe a change in the expression of *nubbin* in *heph* genetic mosaic wing discs using an antibody specific to the *nubbin* protein (data not shown). Second, several members of the *E(spl)*-Complex negatively regulate the Notch pathway (Lai et al., 2000). Expression of these Notch repressors might be reduced in *heph* mutant cells.

Finally, several members of the *E(spl)-C* that act as positive effectors of Notch activation are repressed post-transcriptionally (Lai et al., 1998; Lai and Posakony, 1997; Nellesen et al., 1999). This regulation depends on 3'UTR negative regulatory elements that are sufficient to decrease β -galactosidase activity expressed from a *LacZ* transgene including an *E(spl)m8* 3'UTR (*LacZ-m8-3'UTR*). Preliminary evidence (not shown) suggests that *heph* is required for negative regulation of the *LacZ-m8-3'UTR* transgene. This evidence implies that HEPH has the ability to regulate *E(spl)* RNA stability or translation by interacting with conserved 3'UTR elements. The possibility that HEPH normally inhibits the Notch signalling pathway by directly regulating *E(spl)-C* transcript stability or translation should be an interesting avenue to pursue.

4.9 Summary

Geneticists are sometimes tempted to classify genes as belonging to an interesting, developmentally important regulatory class or a non-interesting "housekeeping" class. The regulatory class includes transcription factors, and transmembrane or secreted signalling molecules to name a few. The housekeeping class, properly defined as those essential genes required in all (or most) kinds of cells, include structural components of the cell, or enzymes involved in RNA metabolism. Obviously, the separation of genes into housekeeping and regulatory classes is simplistic. As may be the case for many genes in the putative housekeeping class, PTB has some very specific functions that may mediate regulative processes. For example, PTB binds to the 3'UTR of the human insulin mRNA and increases its stability. In *Xenopus*, VgRBP60 is required for localization of *Vgl* mRNA to the vegetal pole of the oocyte. This early step in the polarization of the oocyte is required for *Xenopus* primary axis specification. In *Drosophila*, data presented here supports a role for HEPH as a negative regulator in the Notch signalling pathway. Intermediary events between transcription and protein function (RNA processing and localization, protein modification and sorting, etc.) may be equally as important as the transcriptional regulation that are often thought to underly development. Further analysis of the potential RNA and protein partners of HEPH/PTB may reveal other important roles for HEPH/PTB during development, and might molecularly define the role of *heph* in the Notch pathway. To this end, a genetic screen in *Drosophila* may be helpful. Genetic screens for Suppressors of the lethality of *heph^{el}* might produce interesting results, as might a screen for genetic modifiers of the *mr55* detached crossvein phenotype.

5 BIBLIOGRAPHY

- Abbott, L. C., Karpen, G. H. and Schubiger, G.** (1981). Compartmental restrictions and blastema formation during pattern regulation in *Drosophila* imaginal leg discs. *Dev. Biol.* **87**, 64-75.
- Adams, M. D., al., e., Smith, H. O., Gibbs, R. A., Myers, E. W., Rubin, G. M. and Venter, J. C.** (2000). The genome sequence of *Drosophila melanogaster*. *Science* **287**, 2185-2195.
- Altschul, S. F., Madden, T. L., Schaffer, A. A., Zhang, J., Zhang, Z., Miller, W. and Lipman, D. J.** (1997). Gapped BLAST and PSI-BLAST: a new generation of protein database search programs. *Nucleic Acids Res.* **25**, 3389-3402.
- Artavanis-Tsakonas, S., Matsuno, K. and Fortini, M. E.** (1995). Notch signaling. *Science* **268**, 225-232.
- Ashburner, M.** (1989). *Drosophila: a Laboratory Manual*. Cold Spring Harbor, New York: CSH Laboratory Press.
- Babcock, G. G. and Fowler, V. M.** (1994). Isoform-specific interaction of tropomodulin with skeletal muscle and erythrocyte tropomyosins. *J. Biol. Chem.* **269**, 27510-27518.
- Bailey, A. M. and Posakony, J. W.** (1995). Suppressor of Hairless directly activates transcription of *Enhancer of split Complex* genes in response to Notch receptor activity. *Genes Dev.* **9**, 2609-2622.
- Bang, A. G., Bailey, A. M. and Posakony, J. W.** (1995). Hairless promotes stable commitment to the sensory organ precursor cell fate by negatively regulating the activity of the Notch signaling pathway. *Dev. Biol.* **172**, 479-494.
- Bang, A. G. and Posakony, J. W.** (1992). The *Drosophila* gene *Hairless* encodes a novel basic protein that controls alternative cell fates in adult sensory organ development. *Genes Dev.* **6**, 1752-1769.
- Benson, D. A., Karsch-Mizrachi, I., Lipman, D. J., Ostell, J., Rapp, B. A. and Wheeler, D. L.** (2000). GenBank. *Nucleic Acids Res.* **28**, 15-18.

Blair, S. S. (1993). Mechanisms of compartment formation: evidence that non-proliferating cells do not play a critical role in defining the D/V lineage restriction in the developing wing of *Drosophila*. *Development* **119**, 339-351.

Blair, S. S. (1994). A role for the segment polarity gene *shaggy-zeste white 3* in the specification of regional identity in the developing wing of *Drosophila*. *Dev. Biol.* **162**, 229-244.

Blair, S. S. (1995). Compartments and appendage development in *Drosophila*. *BioEssays* **17**, 299-309.

Blair, S. S., Brower, D. L., Thomas, J. B. and Zavortink, M. (1994). The role of *apterous* in the control of dorsoventral compartmentalization and *PS integrin* gene expression in the developing wing of *Drosophila*. *Development* **120**, 1805-1815.

Blaumueller, C. M., Qi, H., Zagouras, P. and Artavanis-Tsakonas, S. (1997). Intracellular cleavage of Notch leads to a heterodimeric receptor on the plasma membrane. *Cell* **90**, 281-291.

Bodenstein, D. (1994). The postembryonic development of *Drosophila*. In *Biology of Drosophila*, (ed. M. Demerek), pp. 275-367. Cold Spring Harbor, New York: CSH Laboratory Press.

Brand, A. H., Manoukian, A. S. and Perrimon, N. (1994). Ectopic expression in *Drosophila*. *Methods Cell Biol.* **44**, 635-654.

Brand, A. H. and Perrimon, N. (1993). Targeted gene expression as a means of altering cell fates and generating dominant phenotypes. *Development* **118**, 401-415.

Brand, M. and Campos-Ortega, J. A. (1988). Two groups of interrelated genes regulate early neurogenesis in *Drosophila melanogaster*. *Roux's Archives of Developmental Biology* **197**, 457-470.

Bray, S. J. (1997). Expression and function of Enhancer of split bHLH proteins during *Drosophila* neurogenesis. *Perspect Dev and Neurobiol* **4**, 313-323.

Brennan, K., Tateson, R., Lewis, K. and Arias, A. M. (1997). A functional analysis of *Notch* mutations in *Drosophila*. *Genetics* **147**, 177-188.

Brennan, K., Tateson, R., Lieber, T., Couso, J. P., Zecchini, V. and Arias, A. M. (1999). The *Abruptex* mutations of *Notch* disrupt the establishment of proneural clusters in *Drosophila*. *Dev. Biol.* **216**, 230-242.

- Brook, W. J.** (1994). Gene expression in regenerating imaginal discs of *Drosophila melanogaster*, Ph.D. Thesis, University of Alberta.
- Brook, W. J., Diaz-Benjumea, F. J. and Cohen, S. M.** (1996). Organizing spatial pattern in limb development. *Annu Rev Cell Dev Biol* **12**, 161-180.
- Brou, C., Logeat, F., Gupta, N., Bessia, C., LeBail, O., Doedens, J. R., Cumano, A., Roux, P., Black, R. A. and Israel, A.** (2000). A novel proteolytic cleavage involved in Notch signaling: the role of the disintegrin-metalloprotease TACE. *Molecular Cell* **5**, 207-216.
- Bruckner, K., Perez, L., Clausen, H. and Cohen, S.** (2000). Glycosyltransferase activity of Fringe modulates Notch-Delta interactions. *Nature* **406**, 411-415.
- Bryant, P. J.** (1970). Cell lineage relationships in the imaginal wing disc of *Drosophila melanogaster*. *Dev. Biol.* **22**, 389-411.
- Bryant, P. J.** (1971). Regeneration and duplication following operations in situ on the imaginal discs of *Drosophila melanogaster*. *Dev. Biol.* **26**, 637-651.
- Bryant, P. J.** (1975). Pattern formation in the imaginal wing disc of *Drosophila melanogaster*: fate map, regeneration and duplication. *J. Exp. Zool.* **193**, 49-77.
- Cabrera, C. V.** (1990). Lateral inhibition and cell fate during neurogenesis in *Drosophila*: the interactions between *scute*, *Notch* and *Delta*. *Development* **110**, 733-742.
- Cabrera, C. V., Martinez-Arias, A. and Bate, M.** (1987). The expression of three members of the *achaete-scute* gene complex correlates with neuroblast segregation in *Drosophila*. *Cell* **50**, 425-433.
- Campbell, G., Weaver, T. and Tomlinson, A.** (1993). Axis specification in the developing *Drosophila* appendage: the role of *wingless*, *decapentaplegic*, and the homeobox gene *aristaless*. *Cell* **74**, 1113-1123.
- Campos-Ortega, J. A.** (1993). Early neurogenesis in *Drosophila melanogaster*. In *The Development of Drosophila melanogaster*, vol. II (ed. M. Bate and A. Martinez-Arias), pp. 1091-1130. Cold Spring Harbor: CSH Laboratory Press.
- Campuzano, S., Carramolino, L., Cabrera, C. V., Ruiz-Gomez, M., Villares, R., Boronat, A. and Modolell, J.** (1985). Molecular genetics of the *achaete-scute* gene complex of *D. melanogaster*. *Cell* **40**, 327-338.

Campuzano, S. and Modolell, J. (1992). Patterning of the *Drosophila* nervous system: the achaete-scute gene complex. *Trends Genet.* **8**, 202-208.

Capdevila, J. and Guerrero, I. (1994). Targeted expression of the signaling molecule Decapentaplegic induces pattern duplications and growth alterations in *Drosophila* wings. *EMBO J.* **13**, 4459-4468.

Carstens, R. P., Wagner, E. J. and Garcia-Blanco, M. A. (2000). An intronic splicing silencer causes skipping of the IIIb exon of *fibroblast growth factor receptor 2* through involvement of polypyrimidine tract binding protein. *Mol. Cell. Biol.* **20**, 7388-7400.

Castrillon, D. H., Gonczy, P., Alexander, S., Rawson, R., Eberhart, C. G., Viswanathan, S., DiNardo, S. and Wasserman, S. A. (1993). Toward a molecular genetic analysis of spermatogenesis in *Drosophila melanogaster*: characterization of male-sterile mutants generated by single P element mutagenesis. *Genetics* **135**, 489-505.

Chan, R. C. and Black, D. L. (1997). The polypyrimidine tract binding protein binds upstream of neural cell-specific *c-src* exon N1 to repress the splicing of the intron downstream. *Mol. Cell. Biol.* **17**, 4667-4676.

Cohen, B., McGuffin, M. E., Pfeifle, C., Segal, D. and Cohen, S. M. (1992). *apterous*, a gene required for imaginal disc development in *Drosophila* encodes a member of the LIM family of developmental regulatory proteins. *Genes Dev.* **6**, 715-729.

Cohen, S. M. (1993). Imaginal disc development. In *The Development of Drosophila melanogaster*, vol. II (ed. M. Bate and A. Martinez-Arias), pp. 747-842. Cold Spring Harbor: CSH Laboratory Press.

Conley, C. A., Silburn, R., Singer, M. A., Ralston, A., Rohwer-Nutter, D., Olson, D. J., Gelbart, W. and Blair, S. S. (2000). Crossveinless 2 contains cysteine-rich domains and is required for high levels of BMP-like activity during the formation of the cross veins in *Drosophila*. *Development* **127**, 3947-3959.

Conte, M. R., Grune, T., Ghuman, J., Kelly, G., Ladas, A., Matthews, S. and Curry, S. (2000). Structure of tandem RNA recognition motifs from polypyrimidine tract binding protein reveals novel features of the RRM fold. *EMBO J.* **19**, 3132-3141.

Cote, C. A., Gautreau, D., Denegre, J. M., Kress, T. L., Terry, N. A. and Mowry, K. L. (1999). A *Xenopus* protein related to hnRNP I has a role in cytoplasmic RNA localization. *Molecular Cell* **4**, 431-437.

Cote, J., Dupuis, S. and Wu, J. Y. (2001). Polypyrimidine track-binding protein binding downstream of *caspase-2* alternative exon 9 represses its inclusion. *J. Biol. Chem.* **276**, 8535-8543.

Couso, J. P., Bishop, S. A. and Martinez Arias, A. (1994). The *wingless* signalling pathway and the patterning of the wing margin in *Drosophila*. *Development* **120**, 621-636.

Crick, F. H. and Lawrence, P. A. (1975). Compartments and polyclones in insect development. *Science* **189**, 340-347.

Davis, M. B., Sun, W. and Standiford, D. M. (2002). Lineage-specific expression of polypyrimidine tract binding protein (*PTB*) in *Drosophila* embryos. *Mech. Dev.* **111**, 143-147.

de Celis, J. F. (1998). Positioning and differentiation of veins in the *Drosophila* wing. *Int. J. Dev. Biol.* **42**, 335-343.

de Celis, J. F., Barrio, R., del Arco, A. and Garcia-Bellido, A. (1993). Genetic and molecular characterization of a *Notch* mutation in its Delta- and Serrate-binding domain in *Drosophila*. *Proc Natl Acad Sci U S A* **90**, 4037-4041.

de Celis, J. F. and Bray, S. (1997). Feed-back mechanisms affecting Notch activation at the dorsoventral boundary in the *Drosophila* wing. *Development* **124**, 3241-3251.

de Celis, J. F., Bray, S. and Garcia-Bellido, A. (1997). Notch signalling regulates *veinlet* expression and establishes boundaries between veins and interveins in the *Drosophila* wing. *Development* **124**, 1919-1928.

de Celis, J. F. and Bray, S. J. (2000). The Abruptex domain of Notch regulates negative interactions between Notch, its ligands and Fringe. *Development* **127**, 1291-1302.

de Celis, J. F., de Celis, J., Ligoxygakis, P., Preiss, A., Delidakis, C. and Bray, S. (1996a). Functional relationships between *Notch*, *Su(H)* and the bHLH genes of the *E(spl)* complex: the *E(spl)* genes mediate only a subset of *Notch* activities during imaginal development. *Development* **122**, 2719-2728.

de Celis, J. F. and Garcia-Bellido, A. (1994a). Modifications of Notch function by *Abruptex* mutations in *Drosophila melanogaster*. *Genetics* **136**, 183-194.

de Celis, J. F. and Garcia-Bellido, A. (1994b). Roles of the *Notch* gene in *Drosophila* wing morphogenesis. *Mech. Dev.* **46**, 109-122.

de Celis, J. F., Garcia-Bellido, A. and Bray, S. J. (1996b). Activation and function of Notch at the dorsal-ventral boundary of the wing imaginal disc. *Development* **122**, 359-369.

de Celis, J. F., Mari-Beffa, M. and Garcia-Bellido, A. (1991). Cell-autonomous role of *Notch*, an epidermal growth factor homologue, in sensory organ differentiation in *Drosophila*. *Proc Natl Acad Sci U S A* **88**, 632-636.

de la Concha, A., Dietrich, D., Weigel, D. and Campos-Ortega, J. A. (1988). Functional interactions of neurogenic genes of *Drosophila melanogaster*. *Genetics* **118**, 499-508.

De Strooper, B., Annaert, W., Cupers, P., Saftig, P., Craessaerts, K., Mumm, J. S., Schroeter, E. H., Schrijvers, V., Wolfe, M. S., Ray, W. J. et al. (1999). A presenilin-1-dependent gamma-secretase-like protease mediates release of Notch intracellular domain. *Nature* **398**, 518-522.

Diaz-Benjumea, F. J. and Cohen, S. M. (1993). Interaction between dorsal and ventral cells in the imaginal disc directs wing development in *Drosophila*. *Cell* **75**, 741-752.

Diaz-Benjumea, F. J. and Cohen, S. M. (1995). Serrate signals through Notch to establish a Wingless-dependent organizer at the dorsal/ventral compartment boundary of the *Drosophila* wing. *Development* **121**, 4215-4225.

Diaz-Benjumea, F. J. and Garcia-Bellido, A. (1990). Behaviour of cells mutant for an EGF receptor homologue of *Drosophila* in genetic mosaics. *Proc. R. Soc. Lond. B. Biol. Sci.* **242**, 36-44.

Dobzhansky, T. (1929). The influence of the quantity and quality of the chromosomal material on the size of the cells of *Drosophila melanogaster*. *Wilhelm Roux's Archive Entwicklungsmech. Organismen* **115**, 363-379.

Doe, C. Q. and Goodman, C. S. (1985). Early events in insect neurogenesis. II. The role of cell interactions and cell lineage in the determination of neuronal precursor cells. *Dev. Biol.* **111**, 206-219.

Doherty, D., Feger, G., Younger-Shepherd, S., Jan, L. Y. and Jan, Y. N. (1996). Delta is a ventral to dorsal signal complementary to Serrate, another Notch ligand, in *Drosophila* wing formation. *Genes Dev.* **10**, 421-434.

Dye, C. A., Lee, J. K., Atkinson, R. C., Brewster, R., Han, P. L. and Bellen, H. J. (1998). The *Drosophila sanpodo* gene controls sibling cell fate and encodes a

tropomodulin homolog, an actin/tropomyosin-associated protein. *Development* **125**, 1845-1856.

Fehon, R. G., Johansen, K., Rebay, I. and Artavanis-Tsakonas, S. (1991). Complex cellular and subcellular regulation of *Notch* expression during embryonic and imaginal development of *Drosophila*: implications for *Notch* function. *J. Cell Biol.* **113**, 657-669.

Finkielsztein, A. (1997). A genetic study of a P-element insertion line expressed in imaginal discs of *Drosophila*, M.Sc. Thesis, University of Alberta.

Fischer-Vize, J. A., Rubin, G. M. and Lehmann, R. (1992). The *fat facets* gene is required for *Drosophila* eye and embryo development. *Development* **116**, 985-1000.

Fleming, R. J., Gu, Y. and Hukriede, N. A. (1997). Serrate-mediated activation of Notch is specifically blocked by the product of the gene *fringe* in the dorsal compartment of the *Drosophila* wing imaginal disc. *Development* **124**, 2973-2981.

FlyBase. (1999). The FlyBase database of the *Drosophila* genome projects and community literature. *Nucleic Acids Res.* **27**, 85-88.

Fortini, M. E. and Artavanis-Tsakonas, S. (1994). The Suppressor of Hairless protein participates in Notch receptor signaling. *Cell* **79**, 273-282.

Foster, G. G. (1975). Negative complementation at the *Notch* locus of *Drosophila melanogaster*. *Genetics* **81**, 99-120.

Fostier, M., Evans, D. A., Artavanis-Tsakonas, S. and Baron, M. (1998). Genetic characterization of the *Drosophila melanogaster* *Suppressor of deltex* gene: A regulator of Notch signaling. *Genetics* **150**, 1477-1485.

French, V., Bryant, P. J. and Bryant, S. V. (1976). Pattern regulation in epimorphic fields. *Science* **193**, 969-981.

Fristrom, D. and Fristrom, J. W. (1993). The metamorphic development of the adult epidermis. In *The Development of Drosophila melanogaster*, vol. II (ed. M. Bate and A. Martinez-Arias), pp. 843-898. Cold Spring Harbor, New York: CSH Laboratory Press.

Garcia-Bellido, A. (1975). Genetic control of wing disc development in *Drosophila*. In *Cell Patterning*, vol. 29 (ed. 161-182. Amsterdam: Ciba Foundation Symposium, Elsevier.

Garcia-Bellido, A. and de Celis, J. F. (1992). Developmental genetics of the venation pattern of *Drosophila*. *Annu. Rev. Genet.* **26**, 277-304.

Garcia-Bellido, A. and Merriam, J. R. (1971). Parameters of the wing imaginal disc development of *Drosophila melanogaster*. *Dev. Biol.* **24**, 61-87.

Garcia-Bellido, A., Ripoll, P. and Morata, G. (1973). Developmental compartmentalisation of the wing disk of *Drosophila*. *Nature New Biology* **245**, 251-253.

Garcia-Bellido, A. and Santamaria, P. (1972). Developmental analysis of the wing disc in the mutant *engrailed* of *Drosophila melanogaster*. *Genetics* **72**, 87-104.

Garzino, V., Pereira, A., Laurenti, P., Graba, Y., Levis, R. W., Le Parco, Y. and Pradel, J. (1992). Cell lineage-specific expression of *modulo*, a dose-dependent modifier of variegation in *Drosophila*. *EMBO J.* **11**, 4471-4479.

Gho, M., Lecourtois, M., Geraud, G., Posakony, J. W. and Schweisguth, F. (1996). Subcellular localization of Suppressor of Hairless in *Drosophila* sense organ cells during Notch signalling. *Development* **122**, 1673-1682.

Ghysen, A. and Dambly-Chaudiere, C. (1989). Genesis of the *Drosophila* peripheral nervous system. *Trends Genet.* **5**, 251-255.

Ghysen, A. and Dambly-Chaudiere, C. (1990). Early events in the development of *Drosophila* peripheral nervous system. *J. Physiol.* **84**, 11-20.

Golic, K. G. (1991). Site-specific recombination between homologous chromosomes in *Drosophila*. *Science* **252**, 958-961.

Golic, K. G. and Lindquist, S. (1989). The FLP recombinase of yeast catalyzes site-specific recombination in the *Drosophila* genome. *Cell* **59**, 499-509.

Gupta-Rossi, N., Le Bail, O., Gonen, H., Brou, C., Logeat, F., Six, E., Ciechanover, A. and Israel, A. (2001). Functional interaction between SEL-10, an F-box protein, and the nuclear form of activated Notch1 receptor. *J. Biol. Chem.* **276**, 34371-34378.

Gustafson, K. and Boulianne, G. L. (1996). Distinct expression patterns detected within individual tissues by the GAL4 enhancer trap technique. *Genome* **39**, 174-182.

Haynie, J. L. and Bryant, P. J. (1976). Intercalary regeneration in imaginal wing disk of *Drosophila melanogaster*. *Nature* **259**, 659-662.

Hazelrigg, T., Levis, R. and Rubin, G. M. (1984). Transformation of *white* locus DNA in *Drosophila*: dosage compensation, zeste interaction, and position effects. *Cell* **36**, 469-481.

- Heitzler, P., Bourouis, M., Ruel, L., Carteret, C. and Simpson, P.** (1996a). Genes of the *Enhancer of split* and *achaete-scute* complexes are required for a regulatory loop between *Notch* and *Delta* during lateral signalling in *Drosophila*. *Development* **122**, 161-171.
- Heitzler, P., Haenlin, M., Romain, P., Calleja, M. and Simpson, P.** (1996b). A genetic analysis of *pannier*, a gene necessary for viability of dorsal tissues and bristle positioning in *Drosophila*. *Genetics* **143**, 1271-1286.
- Heitzler, P. and Simpson, P.** (1991). The choice of cell fate in the epidermis of *Drosophila*. *Cell* **64**, 1083-1092.
- Heitzler, P. and Simpson, P.** (1993). Altered epidermal growth factor-like sequences provide evidence for a role of Notch as a receptor in cell fate decisions. *Development* **117**, 1113-1123.
- Hoppe, P. E. and Greenspan, R. J.** (1986). Local function of the *Notch* gene for embryonic ectodermal pathway choice in *Drosophila*. *Cell* **46**, 773-783.
- Horvitz, H. R. and Sternberg, P. W.** (1991). Multiple intercellular signalling systems control the development of the *Caenorhabditis elegans* vulva. *Nature* **351**, 535-541.
- Hubbard, E. J., Wu, G., Kitajewski, J. and Greenwald, I.** (1997). *sel-10*, a negative regulator of *lin-12* activity in *Caenorhabditis elegans*, encodes a member of the CDC4 family of proteins. *Genes Dev.* **11**, 3182-3193.
- Huppert, S. S., Jacobsen, T. L. and Muskavitch, M. A.** (1997). Feedback regulation is central to Delta-Notch signalling required for *Drosophila* wing vein morphogenesis. *Development* **124**, 3283-3291.
- Irvine, K. D. and Wieschaus, E.** (1994). Fringe, a Boundary-specific signaling molecule, mediates interactions between dorsal and ventral cells during *Drosophila* wing development. *Cell* **79**, 595-606.
- Ito, T. and Lai, M. M.** (1999). An internal polypyrimidine-tract-binding protein-binding site in the hepatitis C virus RNA attenuates translation, which is relieved by the 3'-untranslated sequence. *Virology* **254**, 288-296.
- Jarriault, S., Brou, C., Logeat, F., Schroeter, E. H., Kopan, R. and Israel, A.** (1995). Signalling downstream of activated mammalian Notch. *Nature* **377**, 355-358.

- Jennings, B., Preiss, A., Delidakis, C. and Bray, S.** (1994). The Notch signalling pathway is required for *Enhancer of split* bHLH protein expression during neurogenesis in the *Drosophila* embryo. *Development* **120**, 3537-3548.
- Ju, B. G., Jeong, S., Bae, E., Hyun, S., Carroll, S. B., Yim, J. and Kim, J.** (2000). Fringe forms a complex with Notch. *Nature* **405**, 191-195.
- Kao, H. Y., Ordentlich, P., Koyano-Nakagawa, N., Tang, Z., Downes, M., Kintner, C. R., Evans, R. M. and Kadesch, T.** (1998). A histone deacetylase corepressor complex regulates the Notch signal transduction pathway. *Genes Dev.* **12**, 2269-2277.
- Kidd, S., Kelley, M. R. and Young, M. W.** (1986). Sequence of the *Notch* locus of *Drosophila melanogaster*: relationship of the encoded protein to mammalian clotting and growth factors. *Mol. Cell. Biol.* **6**, 3094-3108.
- Kidd, S., Lieber, T. and Young, M. W.** (1998). Ligand-induced cleavage and regulation of nuclear entry of Notch in *Drosophila melanogaster* embryos. *Genes Dev.* **12**, 3728-3740.
- Kim, J., Irvine, K. D. and Carroll, S. B.** (1995). Cell recognition, signal induction, and symmetrical gene activation at the dorsal-ventral boundary of the developing *Drosophila* wing. *Cell* **82**, 795-802.
- Kim, Y. K., Hahm, B. and Jang, S. K.** (2000). Polypyrimidine tract-binding protein inhibits translation of *Bip* mRNA. *J. Mol. Biol.* **304**, 119-133.
- Kimmerly, W., Stultz, K., Lewis, S., Lewis, K., Lustre, V., Romero, R., Benke, J., Sun, D., Shirley, G., Martin, C. et al.** (1996). A P1-based physical map of the *Drosophila* euchromatic genome. *Genome Res.* **6**, 414-430.
- Klein, T. and Arias, A. M.** (1998). Interactions among Delta, Serrate and Fringe modulate Notch activity during *Drosophila* wing development. *Development* **125**, 2951-2962.
- Klein, T., Seugnet, L., Haenlin, M. and Martinez Arias, A.** (2000). Two different activities of *Suppressor of Hairless* during wing development in *Drosophila*. *Development* **127**, 3553-3566.
- Kooh, P. J., Fehon, R. G. and Muskavitch, M. A.** (1993). Implications of dynamic patterns of Delta and Notch expression for cellular interactions during *Drosophila* development. *Development* **117**, 493-507.

Kopczynski, C. C., Alton, A. K., Fachtel, K., Kooh, P. J. and Muskavitch, M. A. (1988). *Delta*, a *Drosophila* neurogenic gene, is transcriptionally complex and encodes a protein related to blood coagulation factors and epidermal growth factor of vertebrates. *Genes Dev.* **2**, 1723-1735.

Lai, E. C., Bodner, R., Kavalier, J., Freschi, G. and Posakony, J. W. (2000). Antagonism of *Notch* signaling activity by members of a novel protein family encoded by the *Bearded* and *Enhancer of split* gene complexes. *Development* **127**, 291-306.

Lai, E. C., Burks, C. and Posakony, J. W. (1998). The K box, a conserved 3' UTR sequence motif, negatively regulates accumulation of *Enhancer of split complex* transcripts. *Development* **125**, 4077-4088.

Lai, E. C. and Posakony, J. W. (1997). The Bearded box, a novel 3' UTR sequence motif, mediates negative post-transcriptional regulation of *Bearded* and *Enhancer of split Complex* gene expression. *Development* **124**, 4847-4856.

Lauring, S. A. and Overbaugh, J. (2000). Evidence that an IRES within the *Notch2* coding region can direct expression of a nuclear form of the protein. *Molecular Cell* **6**, 939-945.

Lecourtois, M. and Schweisguth, F. (1995). The neurogenic Suppressor of Hairless DNA-binding protein mediates the transcriptional activation of the *Enhancer of split complex* genes triggered by *Notch* signaling. *Genes Dev.* **9**, 2598-2608.

Lecuit, T., Brook, W. J., Ng, M., Calleja, M., Sun, H. and Cohen, S. M. (1996). Two distinct mechanisms for long-range patterning by Decapentaplegic in the *Drosophila* wing. *Nature* **381**, 387-393.

Lee, T. and Luo, L. (1999). Mosaic analysis with a repressible cell marker for studies of gene function in neuronal morphogenesis. *Neuron* **22**, 451-461.

Lehmann, R., Dietrich, U., Jiménez, F. and Campos-Ortega, J. A. (1981). Mutations of early neurogenesis in *Drosophila*. *Wilhelm Roux's Archives of Developmental Biology* **190**, 226-229.

Lehmann, R., Jiménez, F., Dietrich, U. and Campos-Ortega, J. A. (1983). On the phenotype and development of mutants of early neurogenesis in *Drosophila melanogaster*. *Wilhelm Roux's Archives of Developmental Biology* **192**, 62-74.

Lewis, E. B. and Bacher, F. (1968). Method of feeding ethyl methane sulfonate (EMS) to *Drosophila* males. *Drosophila Information Service: technical notes* **43**, 193.

- Lieber, T., Kidd, S., Alcamo, E., Corbin, V. and Young, M. W.** (1993). Antineurogenic phenotypes induced by truncated Notch proteins indicate a role in signal transduction and may point to a novel function for Notch in nuclei. *Genes Dev.* **7**, 1949-1965.
- Lin, C. H. and Patton, J. G.** (1995). Regulation of alternative 3' splice site selection by constitutive splicing factors. *RNA* **1**, 234-245.
- Lindsley, D. L. and Zimm, G. G.** (1992). *The genome of Drosophila melanogaster*. San Diego, USA: Academic Press.
- Lou, H., Helfman, D. M., Gagel, R. F. and Berget, S. M.** (1999). Polypyrimidine tract-binding protein positively regulates inclusion of an alternative 3'-terminal exon. *Mol. Cell. Biol.* **19**, 78-85.
- Madden, T. L., Tatusov, R. L. and Zhang, J.** (1996). Applications of network BLAST server. *Methods Enzymol.* **266**, 131-141.
- Maier, D., Stumm, G., Kuhn, K. and Preiss, A.** (1992). *Hairless*, a *Drosophila* gene involved in neural development, encodes a novel, serine rich protein. *Mech. Dev.* **38**, 143-156.
- Mann, R. S. and Morata, G.** (2000). The developmental and molecular biology of genes that subdivide the body of *Drosophila*. *Annu Rev Cell Dev Biol* **16**, 243-271.
- Micchelli, C. A. and Blair, S. S.** (1999). Dorsoventral lineage restriction in wing imaginal discs requires Notch. *Nature* **401**, 473-476.
- Micchelli, C. A., Rulifson, E. J. and Blair, S. S.** (1997). The function and regulation of *cut* expression on the wing margin of *Drosophila*: Notch, Wingless and a dominant negative role for Delta and Serrate. *Development* **124**, 1485-1495.
- Milan, M., Weihe, U., Perez, L. and Cohen, S. M.** (2001a). The LRR proteins Capricious and Tartan mediate cell interactions during DV boundary formation in the *Drosophila* wing. *Cell* **106**, 785-794.
- Milan, M., Weihe, U., Tiong, S., Bender, W. and Cohen, S. M.** (2001b). *msh* specifies dorsal cell fate in the *Drosophila* wing. *Development* **128**, 3263-3268.
- Moloney, D. J., Panin, V. M., Johnston, S. H., Chen, J., Shao, L., Wilson, R., Wang, Y., Stanley, P., Irvine, K. D., Haltiwanger, R. S. et al.** (2000). Fringe is a glycosyltransferase that modifies Notch. *Nature* **406**, 369-375.

- Morata, G. and Lawrence, P. A.** (1975). Control of compartment development by the *engrailed* gene in *Drosophila*. *Nature* **255**, 614-617.
- Mulligan, G. J., Guo, W., Wormsley, S. and Helfman, D. M.** (1992). Polypyrimidine tract binding protein interacts with sequences involved in alternative splicing of beta-tropomyosin pre-mRNA. *J. Biol. Chem.* **267**, 25480-25487.
- Mumm, J. S., Schroeter, E. H., Saxena, M. T., Griesemer, A., Tian, X., Pan, D. J., Ray, W. J. and Kopan, R.** (2000). A ligand-induced extracellular cleavage regulates gamma-secretase-like proteolytic activation of Notch1. *Molecular Cell* **5**, 197-206.
- Munro, S. and Freeman, M.** (2000). The notch signalling regulator fringe acts in the Golgi apparatus and requires the glycosyltransferase signature motif DXD. *Curr. Biol.* **10**, 813-820.
- Muskavitch, M. A.** (1994). Delta-Notch signaling and *Drosophila* cell fate choice. *Dev. Biol.* **166**, 415-430.
- Myers, E. W., Sutton, G. G., Delcher, A. L., Dew, I. M., Fasulo, D. P., Flanigan, M. J., Kravitz, S. A., Mobarry, C. M., Reinert, K. H., Remington, K. A. et al.** (2000). A whole-genome assembly of *Drosophila*. *Science* **287**, 2196-2204.
- Nellen, D., Burke, R., Struhl, G. and Basler, K.** (1996). Direct and long-range action of a DPP morphogen gradient. *Cell* **85**, 357-368.
- Nellesen, D. T., Lai, E. C. and Posakony, J. W.** (1999). Discrete enhancer elements mediate selective responsiveness of *Enhancer of split complex* genes to common transcriptional activators. *Dev. Biol.* **213**, 33-53.
- Neumann, C. J. and Cohen, S. M.** (1996). A hierarchy of cross-regulation involving *Notch*, *wingless*, *vestigial* and *cut* organizes the dorsal/ventral axis of the *Drosophila* wing. *Development* **122**, 3477-3485.
- Neumann, C. J. and Cohen, S. M.** (1997). Long-range action of Wingless organizes the dorsal-ventral axis of the *Drosophila* wing. *Development* **124**, 871-880.
- Neumann, C. J. and Cohen, S. M.** (1998). Boundary formation in *Drosophila* wing: *Notch* activity attenuated by the POU protein Nubbin. *Science* **281**, 409-413.
- Norton, P. A.** (1994). Polypyrimidine tract sequences direct selection of alternative branch sites and influence protein binding. *Nucleic Acids Res.* **22**, 3854-3860.

- O'Brochta, D. A. and Bryant, P. J.** (1987). Distribution of S-phase cells during the regeneration of *Drosophila* imaginal wing discs. *Dev. Biol.* **119**, 137-142.
- O'Keefe, D. D. and Thomas, J. B.** (2001). *Drosophila* wing development in the absence of dorsal identity. *Development* **128**, 703-710.
- O'Keefe, D. D., Thor, S. and Thomas, J. B.** (1998). Function and specificity of LIM domains in *Drosophila* nervous system and wing development. *Development* **125**, 3915-3923.
- Oberg, C., Li, J., Pauley, A., Wolf, E., Gurney, M. and Lendahl, U.** (2001). The Notch intracellular domain is ubiquitinated and negatively regulated by the mammalian *Sel-10* homolog. *J. Biol. Chem.* **276**, 35847-35853.
- Oh, Y. L., Hahm, B., Kim, Y. K., Lee, H. K., Lee, J. W., Song, O., Tsukiyama-Kohara, K., Kohara, M., Nomoto, A. and Jang, S. K.** (1998). Determination of functional domains in polypyrimidine-tract-binding protein. *Biochemistry Journal* **331**, 169-175.
- Palka, J., Schubiger, M. and Schwaninger, H.** (1990). Neurogenic and antineurogenic effects from modifications at the Notch locus. *Development* **109**, 167-175.
- Panin, V. M., Papayannopoulos, V., Wilson, R. and Irvine, K. D.** (1997). Fringe modulates Notch-ligand interactions. *Nature* **387**, 908-912.
- Parks, A. L., Klueg, K. M., Stout, J. R. and Muskavitch, M. A.** (2000). Ligand endocytosis drives receptor dissociation and activation in the Notch pathway. *Development* **127**, 1373-1385.
- Pattatucci, A. M. and Kaufman, T. C.** (1991). The homeotic gene *Sex combs reduced* of *Drosophila melanogaster* is differentially regulated in the embryonic and imaginal stages of development. *Genetics* **129**, 443-461.
- Pereira, A., Doshen, J., Tanaka, E. and Goldstein, L. S.** (1992). Genetic analysis of a *Drosophila* Microtubule-associated protein. *J. Cell Biol.* **116**, 377-383.
- Perez, I., McAfee, J. G. and Patton, J. G.** (1997). Multiple RRM domains contribute to RNA binding specificity and affinity for polypyrimidine tract binding protein. *Biochemistry* **36**, 11881-11890.
- Perrin, L., Demakova, O., Fanti, L., Kallenbach, S., Saingery, S., Mal'ceva, N. I., Pimpinelli, S., Zhimulev, I. and Pradel, J.** (1998). Dynamics of the sub-nuclear

distribution of Modulo and the regulation of position-effect variegation by nucleolus in *Drosophila*. *J. Cell Sci.* **111**, 2753-2761.

Phillips, R. G. and Whittle, J. R. (1993). *wingless* expression mediates determination of peripheral nervous system elements in late stages of *Drosophila* wing disc development. *Development* **118**, 427-438.

Pilipenko, E. V., Pestova, T. V., Kolupaeva, V. G., Khitrina, E. V., Poperechnaya, A. N., Agol, V. I. and Hellen, C. U. (2000). A cell cycle-dependent protein serves as a template-specific translation initiation factor. *Genes Dev.* **14**, 2028-2045.

Poole, S. J., Kauvar, L. M., Drees, B. and Kornberg, T. (1985). The *engrailed* locus of *Drosophila*: structural analysis of an embryonic transcript. *Cell* **40**, 37-43.

Preston, C. R. and Engels, W. R. (1996). P-element-induced male recombination and gene conversion in *Drosophila*. *Genetics* **144**, 1611-1622.

Preston, C. R., Sved, J. A. and Engels, W. R. (1996). Flanking duplications and deletions associated with P-induced male recombination in *Drosophila*. *Genetics* **144**, 1623-1638.

Qiu, L., Joazeiro, C., Fang, N., Wang, H. Y., Elly, C., Altman, Y., Fang, D., Hunter, T. and Liu, Y. C. (2000). Recognition and ubiquitination of Notch by Itch, a hect-type E3 ubiquitin ligase. *J. Biol. Chem.* **275**, 35734-35737.

Ramain, P., Khechumian, K., Seugnet, L., Arbogast, N., Ackermann, C. and Heitzler, P. (2001). Novel *Notch* alleles reveal a *Deltex*-dependent pathway repressing neural fate. *Curr. Biol.* **11**, 1729-1738.

Rauskolb, C., Correia, T. and Irvine, K. D. (1999). *fringe*-dependent separation of dorsal and ventral cells in the *Drosophila* wing. *Nature* **401**, 476-480.

Reinhardt, C. A., Hodgkin, N. M. and Bryant, P. J. (1977). Wound healing in the imaginal discs of *Drosophila*. I. Scanning electron microscopy of normal and healing wing discs. *Developmental Biology* **60**, 238-257.

Rogers, S., Wells, R. and Rechsteiner, M. (1986). Amino acid sequences common to rapidly degraded proteins: the PEST hypothesis. *Science* **234**, 364-368.

Roman, G., He, J. and Davis, R. L. (2000). *kurtz*, a novel nonvisual arrestin, is an essential neural gene in *Drosophila*. *Genetics* **155**, 1281-1295.

Rubin, G. M., Hong, L., Brokstein, P., Evans-Holm, M., Frise, E., Stapleton, M. and Harvey, D. A. (2000). A *Drosophila* complementary DNA resource. *Science* **287**, 2222-2224.

Ruiz-Gomez, M. and Ghysen, A. (1993). The expression and role of a proneural gene, *achaete*, in the development of the larval nervous system of *Drosophila*. *EMBO J.* **12**, 1121-1130.

Rulifson, E. J. and Blair, S. S. (1995). Notch regulates *wingless* expression and is not required for reception of the paracrine Wingless signal during wing margin neurogenesis in *Drosophila*. *Development* **121**, 2813-2824.

Rulifson, E. J., Micchelli, C. A., Axelrod, J. D., Perrimon, N. and Blair, S. S. (1996). *wingless* refines its own expression domain at the *Drosophila* wing margin. *Nature* **384**, 72-74.

Rustighi, A., Tessari, M. A., Vascotto, F., Sgarra, R., Giacotti, V. and Manfioletti, G. (2002). A Polypyrimidine/Polypurine Tract within the *Hmga2* Minimal Promoter: A Common Feature of Many Growth-Related Genes. *Biochemistry* **41**, 1229-1240.

Sambrook, J., Fritsch, E. F. and Maniatis, T. (1989). *Molecular Cloning: A Laboratory Manual*. Cold Spring Harbor, N.Y.: Cold Spring Harbor Laboratory.

Schubiger, G. (1968). Anlageplan, determinationszustand und transdeterminationsleistungen der männlichen vorderbeinscheibe von *Drosophila melanogaster*. *Wilhelm Roux's Arch. Entwicklungsmech. Organismen* **160**, 9-40.

Schubiger, G. (1971). Regeneration, duplication and transdetermination in fragments of the leg disc of *Drosophila melanogaster*. *Dev. Biol.* **26**, 277-295.

Schweisguth, F. (1999). Dominant-negative mutation in the beta2 and beta6 proteasome subunit genes affect alternative cell fate decisions in the *Drosophila* sense organ lineage. *Proc Natl Acad Sci U S A* **96**, 11382-11386.

Schweisguth, F. and Lecourtois, M. (1998). The activity of *Drosophila* *Hairless* is required in pupae but not in embryos to inhibit Notch signal transduction. *Development, Genes and Evolution* **208**, 19-27.

Seugnet, L., Simpson, P. and Haenlin, M. (1997). Transcriptional regulation of *Notch* and *Delta*: requirement for neuroblast segregation in *Drosophila*. *Development* **124**, 2015-2025.

- Siden-Kiamos, I., Saunders, R. D., Spanos, L., Majerus, T., Treanear, J., Savakis, C., Louis, C., Glover, D. M., Ashburner, M. and Kafatos, F. C.** (1990). Towards a physical map of the *Drosophila melanogaster* genome: mapping of cosmid clones within defined genomic divisions. *Nucleic Acids Res.* **18**, 6261-6270.
- Simpson, P.** (1990). Lateral inhibition and the development of the sensory bristles of the adult peripheral nervous system of *Drosophila*. *Development* **109**, 509-519.
- Singh, R., Valcarcel, J. and Green, M. R.** (1995). Distinct binding specificities and functions of higher eukaryotic polypyrimidine tract-binding proteins. *Science* **268**, 1173-1176.
- Skeath, J. B. and Carroll, S. B.** (1992). Regulation of proneural gene expression and cell fate during neuroblast segregation in the *Drosophila* embryo. *Development* **114**, 939-946.
- Southby, J., Gooding, C. and Smith, C. W.** (1999). Polypyrimidine tract binding protein functions as a repressor to regulate alternative splicing of *alpha-actinin* mutually exclusive exons. *Mol. Cell. Biol.* **19**, 2699-2711.
- Speicher, S. A., Thomas, U., Hinz, U. and Knust, E.** (1994). The *Serrate* locus of *Drosophila* and its role in morphogenesis of the wing imaginal discs: control of cell proliferation. *Development* **120**, 535-544.
- Spemann, H. and Mangold, H.** (1923). Induction of embryonic primordia by implantation of organizers from a different species. (2001). *Int. J. Dev. Biol.* **45**, 13-38.
- Spradling, A. C., Stern, D., Beaton, A., Rhem, E. J., Laverly, T., Mozden, N., Misra, S. and Rubin, G. M.** (1999). The Berkeley *Drosophila* genome project gene disruption project. Single P-element insertions mutating 25% of vital *Drosophila* genes. *Genetics* **153**, 135-177.
- Sternberg, P. W.** (1988). Lateral inhibition during vulval induction in *Caenorhabditis elegans*. *Nature* **335**, 551-554.
- Strigini, M. and Cohen, S. M.** (2000). Wingless gradient formation in the *Drosophila* wing. *Curr. Biol.* **10**, 293-300.
- Struhl, G. and Adachi, A.** (1998). Nuclear access and action of Notch in vivo. *Cell* **93**, 649-660.
- Struhl, G. and Basler, K.** (1993). Organizing activity of *wingless* protein in *Drosophila*. *Cell* **72**, 527-540.

Struhl, G., Fitzgerald, K. and Greenwald, I. (1993). Intrinsic activity of the Lin-12 and Notch intracellular domains *in vivo*. *Cell* **74**, 331-345.

Struhl, G. and Greenwald, I. (1999). Presenilin is required for activity and nuclear access of Notch in *Drosophila*. *Nature* **398**, 522-525.

Sturtevant, M. A., Roark, M. and Bier, E. (1993). The *Drosophila rhomboid* gene mediates the localized formation of wing veins and interacts genetically with components of the EGF-R signaling pathway. *Genes Dev.* **7**, 961-973.

Sun, X. and Artavanis-Tsakonas, S. (1997). Secreted forms of DELTA and SERRATE define antagonists of Notch signaling in *Drosophila*. *Development* **124**, 3439-3448.

Teleman, A. A. and Cohen, S. M. (2000). DPP gradient formation in the *Drosophila* wing imaginal disc. *Cell* **103**, 971-980.

Thomas, U., Speicher, S. A. and Knust, E. (1991). The *Drosophila* gene *Serrate* encodes an EGF-like transmembrane protein with a complex expression pattern in embryos and wing discs. *Development* **111**, 749-761.

Tillmar, L., Carlsson, C. and Welsh, N. (2002). Control of Insulin mRNA Stability in Rat Pancreatic Islets. Regulatory role of a 3'-untranslated region pyrimidine-rich sequence. *J. Biol. Chem.* **277**, 1099-1106.

Tiong, S. Y., Nash, D. and Bender, W. (1995). *Dorsal wing*, a locus that affects dorsoventral wing patterning in *Drosophila*. *Development* **121**, 1649-1656.

Valcarcel, J. and Gebauer, F. (1997). Post-transcriptional regulation: the dawn of PTB. *Curr. Biol.* **7**, R705-708.

Vässin, H., Bremer, K. A., Knust, E. and Campos-Ortega, J. A. (1987). The neurogenic *Delta* locus in *Drosophila* is expressed in neurogenic territories and encodes a putative transmembrane protein with EGF-like repeats. *EMBO J.* **6**, 3434-3440.

Vässin, H., Vielmetter, J. and Campos-Ortega, J. A. (1985). Genetic interactions in early neurogenesis of *Drosophila melanogaster*. *J. Neurogenet.* **2**, 291-308.

Waddington, C. H. (1941). The genetic control of wing development in *Drosophila*. *Journal of Genetics* **41**, 75-139.

Welshons, W. J. (1971). Genetic basis for two types of recessive lethality at the *Notch* locus of *Drosophila*. *Genetics* **68**, 259-268.

Wharton, K. A., Johansen, K. M., Xu, T. and Artavanis-Tsakonas, S. (1985). Nucleotide sequence from the neurogenic locus *Notch* implies a gene product that shares homology with proteins containing EGF-like repeats. *Cell* **43**, 567-581.

Wigglesworth, V. B. (1940). Local and general factors in the development of pattern in *Rhodnius prolixus* (Hemiptera). *J. Exp. Biol.* **36**, 180-200.

Williams, J. A., Paddock, S. W., Vorwerk, K. and Carroll, S. B. (1994). Organization of wing formation and induction of a wing-patterning gene at the dorsal/ventral compartment boundary. *Nature* **368**, 299-305.

Wolpert, L. (1969). Positional information and the spatial pattern of cellular differentiation. *J. Theor. Biol.* **25**, 1-47.

Xu, T. and Rubin, G. M. (1993). Analysis of genetic mosaics in developing and adult *Drosophila* tissues. *Development* **117**, 1223-1237.

Ye, Y., Lukinova, N. and Fortini, M. E. (1999). Neurogenic phenotypes and altered Notch processing in *Drosophila Presenilin* mutants. *Nature* **398**, 525-529.

Zecca, M., Basler, K. and Struhl, G. (1995). Sequential organizing activities of *engrailed*, *hedgehog* and *decapentaplegic* in the *Drosophila* wing. *Development* **121**, 2265-2278.

Zecca, M., Basler, K. and Struhl, G. (1996). Direct and long-range action of a *wingless* morphogen gradient. *Cell* **87**, 833-844.

Zhang, B., Kraemer, B., SenGupta, D., Fields, S. and Wickens, M. (1999a). Yeast three-hybrid system to detect and analyze interactions between RNA and protein. *Methods Enzymol.* **306**, 93-113.

Zhang, L., Liu, W. and Grabowski, P. J. (1999b). Coordinate repression of a trio of neuron-specific splicing events by the splicing regulator PTB. *RNA* **5**, 117-130.